

TE
662
.A3
no.
FHWA-
RD-
77-24

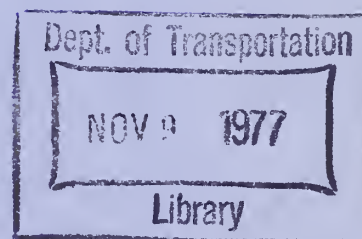
Report No. FHWA-RD-77-24

CLE-SAFE GRATE INLETS STUDY

Vol. 1. Hydraulic and Safety Characteristics of Selected Grate Inlets on Continuous Grades



June 1977
Final Report



Document is available to the public through
the National Technical Information Service,
Springfield, Virginia 22161

Prepared for
FEDERAL HIGHWAY ADMINISTRATION
Offices of Research & Development
Washington, D. C. 20590


Foreword

This report describes the structural analysis and bicycle-safe test of 11 selected grate designs, and the hydraulic and debris tests of 7 bicycle-safe grates. Three grates (the curved vane, the parallel bar with transverse rod, and the parallel bar with spacers) show better overall hydraulic performance for the conditions studied. For mild longitudinal slopes, other grates also perform well hydraulically. As the more efficient grates do not necessarily have the better debris passing characteristics, the user can choose the grate which best suits his special conditions.

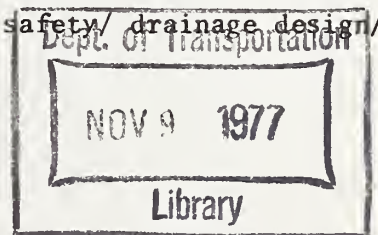
This research is being conducted by the Bureau of Reclamation's Engineering and Research Center for the Federal Highway Administration, Office of Research, Washington, D.C., under P.O. 5-3-0166. This report covers the results of tests on 2 ft. by 2 ft. (0.61 m by 0.61 m) and 2 ft. by 4 ft. (0.61 m by 1.22 m) size grates on continuous grades. Subsequent reports will cover the results of tests on the 3 selected grates for different widths on continuous grades and at the low point of a vertical curve.

The report is disseminated under the sponsorship of the Department of Transportation in the interest of information exchange. The United States Government assumes no liability for its contents or use thereof.

Sufficient copies of this report are being distributed to provide a minimum of two copies to each FHWA Regional Office, one copy to each Division Office, and two copies to each State highway agency. Direct distribution is being made to the Division Offices.

For 
Charles F. Scheffey
Director, Office of Research
Federal Highway Administration

1. REPORT NO. FHWA-RD-77-24	2. GOVERNMENT ACCESSION NO.	3. RECIPIENT'S CATALOG NO.
4. TITLE AND SUBTITLE Bicycle-safe Grate Inlets Study Volume 1 - Hydraulic and Safety Characteristics of Selected Grate Inlets on Continuous Grades		5. REPORT DATE June 1977
7. AUTHOR(S) P. H. Burgi and D. E. Gober		6. PERFORMING ORGANIZATION CODE
9. PERFORMING ORGANIZATION NAME AND ADDRESS U.S. Department of Interior Bureau of Reclamation Engineering and Research Center Denver, Colorado 80225		8. PERFORMING ORGANIZATION REPORT NO.
12. SPONSORING AGENCY NAME AND ADDRESS U.S. Department of Transportation Federal Highway Administration 2100 2nd Street, S.W. Washington, D.C. 20590		10. WORK UNIT NO.
		11. CONTRACT OR GRANT NO. PO-5-3-0166
		13. TYPE OF REPORT AND PERIOD COVERED Volume 1 of Final Report
		14. SPONSORING AGENCY CODE E0269
15. SUPPLEMENTARY NOTES Project Manager: D. C. Woo		
16. ABSTRACT Eleven drain inlet grates were tested to evaluate their safety characteristics for bicycle as well as pedestrian traffic. Four of the grates that rated highest in the safety tests were selected for hydraulic testing. Three other grates with designs and bar spacings similar to grates proven safe were also selected for hydraulic testing. A parallel bar grate was included in the hydraulic test program as a standard with which to compare the performance of the other test grates. Hydraulic and debris tests were performed on full-size grates in sizes of 2 ft by 4 ft (0.61 m by 1.22 m) and 2 ft by 2 ft (0.61 m by 0.61 m). The grates were tested at cross slopes of 1:48, 1:24, 1:16 and longitudinal slopes of 0.5, 1, 2, 4, 6, 9, and 13 percent with gutter flows up to 5.6 ft ³ /s (0.158 m ³ /s). Debris tests were run using 150 pieces of 3 in (76 mm) by 4 in (102 mm) paper debris. Test results show that two of the grate designs (a cast and a steel fabricated grate) are nearly as hydraulically efficient as the parallel bar grate and considerably more efficient than the other grate designs tested. One other design (a steel fabricated grate) shows high hydraulic efficiencies at longitudinal slopes up to 6 percent. These three grate designs are recommended for additional testing. A grate's ability to handle debris without clogging was shown to be most dependent on the spacing of its longitudinal bars. Grates with the widest longitudinal bar spacing tested consistently outperformed grates with narrower longitudinal bar spacings.		
17. KEY WORDS AND DOCUMENT ANALYSIS a. DESCRIPTORS-- / hydraulics/ grate inlets/ bicycle safety/ drainage design/ surface runoff b. IDENTIFIERS-- c. COSATI Field/Group COWRR:		
18. DISTRIBUTION STATEMENT Available from the National Technical Information Service, Operations Division, Springfield, Virginia 22161.		19. SECURITY CLASS (THIS REPORT) UNCLASSIFIED
		20. SECURITY CLASS (THIS PAGE) UNCLASSIFIED
		21. NO. OF PAGES 183
		22. PRICE



CONTENTS

	<u>Page</u>
Abstract	1
Acknowledgments	2
Notation	3
<u>Chapter</u>	
1 Introduction	1-1
2 Analysis of Structural Integrity	2-1
3 Analysis of Bicycle and Pedestrian Safety	3-1
4 Hydraulic Considerations	4-1
5 Test Facility and Experimental Approach	5-1
6 Hydraulic Efficiency and Debris Tests - Parallel Bar Grates	6-1
7 Hydraulic Efficiency and Debris Tests - Reticuline Grates	7-1
8 Hydraulic Efficiency and Debris Tests - 45° Tilt-bar Grates	8-1
9 Hydraulic Efficiency and Debris Tests - 30° Tilt-bar Grates	9-1
10 Hydraulic Efficiency and Debris Tests - Curved Vane Grates	10-1
11 Hydraulic Efficiency and Debris Tests - Parallel Bar with Transverse Rod Grates (P - 1-7/8 - 4)	11-1
12 Hydraulic Efficiency and Drbris Tests - Parallel Bar Grates with Spacers (P - 1-1/8)	12-1
13 Discussion of Results	13-1
14 Summary and Recommendations	14-1

LIST OF FIGURES

<u>Figure</u>		<u>Page</u>
2-1	Schematic Drawings For Three Fabricated Steel Grate Designs	2-2
2-2	Schematic Load Diagram	2-4
2-3	Typical Fabricated Grate	2-6
2-4	Tubular End Piece Design	2-7
2-5	Cross Sections of Bearing Bars - Cast Grates	2-12
2-6	STR5 Tubular Model	2-18
3-1	2 ft by 4 ft (0.61 m by 1.22 m) Test Grates	3-3
3-2	Bicycle Safety Test Site	3-5
3-3	Test site and Observation Team	3-7
3-4	Severe Tire Deformation on a Grate with 8 in (203 mm) Transverse Bar Spacing	3-14
3-5	Severe Skidding in Turn	3-15
4-1	Triangular Gutter Sections	4-2
4-2	Depth-discharge Relationships for a Gutter Section, T = 5 ft	4-4
4-3	Effect of Longitudinal and Cross Slope on Gutter Flow With Constant T = 5 ft	4-6
4-4	Definition Sketch of Gutter Flow Near an Open Hole	4-7
4-5	Hydraulic Efficiency of Frontal Flow vs. Width of Spread	4-8
4-6	Theoretical Hydraulic Efficiency vs. Gutter Flow, 2 ft by 4 ft (0.61 m by 1.22 m) Open Hole	4-10
4-7a	Typical Velocity Profiles, $S_0 = 0.5\%$ and 4%, Z = 24	4-11
4-7b	Typical Velocity Profiles, $S_0 = 6\%$ and 13%, Z = 24	4-12
4-8	Device Used to Measure Intercepted Frontal Flow, Q_F	4-14
5-1	Hydraulic Test Facility Elevation View (Schematic)	5-2
5-2	Hydraulic Test Facility Section A-A (Schematic)	5-3
5-3	Principal Components of Hydraulic Test Facility	5-5
5-4	Principal Components of Hydraulic Test Facility (continued)	5-6
5-5	Roadbed Surface Treatment	5-9
5-6	Hydrograph for Debris Tests	5-13
5-7	Sample Inlet Capacity Curve	5-15
6-1	2 ft by 4 ft (0.61 m by 1.22 m) Steel Fabricated Parallel Bar Grate	6-2
6-2	Hydraulic Efficiency vs. Gutter Flow, 2 ft by 4 ft (0.61 m by 1.22 m) Parallel Bar Grate	6-3

LIST OF FIGURES - Continued

<u>Figure</u>		<u>Page</u>
6-3	Hydraulic Efficiency vs. Gutter Flow, 2 ft by 2 ft (0.61 m by 0.61 m) Parallel Bar Grate	6-4
6-4	Parallel Bar Grates, $S_0 = 13\%$, $Z = 24$	6-6
6-5	View of 2 ft by 2 ft (0.61 m by 0.61 m) Parallel Bar Grate, $Z = 24$	6-7
6-6	Gutter Flow Patterns, Parallel Bar Grate, $E = 100\%$	6-8
6-7	Hydraulic Efficiency vs. Width of Spread, 2 ft by 4 ft (0.61 m by 1.22 m) Parallel Bar Grate, $Z = 24, 16$	6-9
6-8	Hydraulic Efficiency vs. Width of Spread, 2 ft by 4 ft (0.61 m by 1.22 m) Parallel Bar Grate, $Z = 96, 48$	6-10
6-9	Hydraulic Efficiency vs. Width of Spread, 2 ft by 2 ft (0.61 m by 0.61 m) Parallel Bar Grate, $Z = 24, 16$	6-11
6-10	Hydraulic Efficiency vs. Width of Spread, 2 ft by 2 ft (0.61 m by 0.61 m) Parallel Bar Grate, $Z = 96, 48$	6-12
6-11	Grate Inlet Capacity Curves, 2 ft by 4 ft (0.61 m by 1.22 m) Parallel Bar Grate, $Z = 16$	6-14
6-12	Grate Inlet Capacity Curves, 2 ft by 4 ft (0.61 m by 1.22 m) Parallel Bar Grate, $Z = 24$	6-15
6-13	Grate Inlet Capacity Curves, 2 ft by 4 ft (0.61 m by 1.22 m) Parallel Bar Grate, $Z = 48$	6-16
6-14	Grate Inlet Capacity Curves, 2 ft by 4 ft (0.61 m by 1.22 m) Parallel Bar Grate, $Z = 96$	6-17
6-15	Grate Inlet Capacity Curves, 2 ft by 2 ft (0.61 m by 0.61 m) Parallel Bar Grate, $Z = 16$	6-18
6-16	Grate Inlet Capacity Curves, 2 ft by 2 ft (0.61 m by 0.61 m) Parallel Bar Grate, $Z = 24$	6-19
6-17	Grate Inlet Capacity Curves, 2 ft by 2 ft (0.61 m by 0.61 m) Parallel Bar Grate, $Z = 48$	6-20
6-18	Grate Inlet Capacity Curves, 2 ft by 2 ft (0.61 m by 0.61 m) Parallel Bar Grate, $Z = 96$	6-21
6-19	Debris Test, 2 ft by 4 ft (0.61 m by 1.22 m) Parallel Bar Grate, $S_0 = 4\%$, $Z = 24$	6-22
7-1	2 ft by 4 ft (0.61 m by 1.22 m) Steel Fabricated Reticuline Grate	7-2
7-2	Hydraulic Efficiency vs. Gutter Flow, 2 ft by 4 ft (0.61 m by 1.22 m) Reticuline Grate	7-3
7-3	Hydraulic Efficiency vs. Gutter Flow, 2 ft by 2 ft (0.61 m by 0.61 m) Reticuline Grate	7-4

LIST OF FIGURES - Continued

<u>Figure</u>		<u>Page</u>
7-4	Development of Splash of 2 ft by 2 ft (0.61 m by 0.61 m) Reticuline Grate, Z = 48	7-5
7-5	Variation in Splash Height with Changing Grade for 2 ft by 4 ft (0.61 m by 1.22 m) Reticuline Grate, Z = 24	7-7
7-6	Hydraulic Efficiency vs. Width of Spread, 2 ft by 4 ft (0.61 m by 1.22 m) Reticuline Grate, Z = 24 and 16	7-8
7-6 (cont)	Hydraulic Efficiency vs. Width of Spread, 2 ft by 4 ft (0.61 m by 1.22 m) Reticuline Grate, Z = 48 and 96	7-9
7-7	Hydraulic Efficiency vs. Width of Spread, 2 ft by 2 ft (0.61 m by 0.61 m) Reticuline Grate, Z = 24 and 16	7-10
7-7 (cont)	Hydraulic Efficiency vs. Width of Spread, 2 ft by 2 ft (0.61 m by 0.61 m) Reticuline Grate, Z = 48 and 96	7-11
7-8	Grate Inlet Capacity Curves, 2 ft by 4 ft (0.61 m by 1.22 m) Reticuline Grate, Z = 16	7-12
7-9	Grate Inlet Capacity Curves, 2 ft by 4 ft (0.61 m by 1.22 m) Reticuline Grate, Z = 24	7-13
7-10	Grate Inlet Capacity Curves, 2 ft by 4 ft (0.61 m by 1.22 m) Reticuline Grate, Z = 48	7-14
7-11	Grate Inlet Capacity Curves, 2 ft by 4 ft (0.61 m by 1.22 m) Reticuline Grate, Z = 96	7-15
7-12	Grate Inlet Capacity Curves, 2 ft by 2 ft (0.61 m by 0.61 m) Reticuline Grate, Z = 16	7-16
7-13	Grate Inlet Capacity Curves, 2 ft by 2 ft (0.61 m by 0.61 m) Reticuline Grate, Z = 24	7-17
7-14	Grate Inlet Capacity Curves, 2 ft by 2 ft (0.61 m by 0.61 m) Reticuline Grate, Z = 48	7-18
7-15	Grate Inlet Capacity Curves, 2 ft by 2 ft (0.61 m by 0.61 m) Reticuline Grate, Z = 96	7-19
7-16	Debris Test, 2 ft by 4 ft (0.61 m by 1.22 m) Reticuline Grate, Z = 24, S ₀ = 4%	7-21
8-1	2 ft by 4 ft (0.61 m by 1.22 m) cast 45° Tilt-bar Grates	8-2
8-2	Hydraulic Efficiency vs. Gutter Flow 2 ft by 4 ft (0.61 m by 1.22 m) 45 - 2-1/4 - 4 Grate	8-3
8-3	Hydraulic Efficiency vs. Gutter Flow 2 ft by 2 ft (0.61 m by 0.61 m) 45 - 2-1/4 - 4 Grate	8-4
8-4	Hydraulic Efficiency vs. Gutter Flow 2 ft by 4 ft (0.61 m by 1.22 m) 45 - 3-1/4 - 4 Grate	8-5

LIST OF FIGURES - Continued

<u>Figure</u>		<u>Page</u>
8-5	Hydraulic Efficiency vs. Gutter Flow 2 ft by 2 ft (0.61 m by 0.61 m) 45 - 3-1/4 - 4 Grate	8-6
8-6	Splash Patterns at 13% Slope, Z = 48 2 ft by 2 ft (0.61 m by 0.61 m) 45° Tilt-bar Grates	8-9
8-7	Hydraulic Efficiency vs. Width of Spread 2 ft by 4 ft (0.61 m by 1.22 m) 45 - 2-1/4 - 4 Grate	8-10
8-8	Hydraulic Efficiency vs. Width of Spread 2 ft by 2 ft (0.61 m by 0.61 m) 45 - 2-1/4 - 4 Grate	8-11
8-9	Hydraulic Efficiency vs. Width of Spread 2 ft by 4 ft (0.61 m by 1.22 m) 45 - 3-1/4 - 4 Grate	8-12
8-10	Hydraulic Efficiency vs. Width of Spread 2 ft by 2 ft (0.61 m by 0.61 m) 45 - 3-1/4 - 4 Grate	8-13
8-11	Flow Carrying Completely Across the 2 ft by 4 ft (0.61 m by 1.22 m) 45 - 2-1/4 - 4 Grate, Z = 24	8-14
8-12	Flow Carrying Completely Across the 2 ft by 4 ft (0.61 m by 1.22 m) 45 - 3-1/4 - 4 Grate, Z = 24	8-15
8-13	Grate Inlet Capacity Curves, 2 ft by 4 ft (0.61 m by 1.22 m) 45 - 2-1/4 - 4 Grate, Z = 16	8-16
8-14	Grate Inlet Capacity Curves, 2 ft by 4 ft (0.61 m by 1.22 m) 45 - 2-1/4 - 4 Grate, Z = 24	8-17
8-15	Grate Inlet Capacity Curves, 2 ft by 4 ft (0.61 m by 1.22 m) 45 - 2-1/4 - 4 Grate, Z = 48	8-18
8-16	Grate Inlet Capacity Curves, 2 ft by 2 ft (0.61 m by 0.61 m) 45 - 2-1/4 - 4 Grate, Z = 16	8-19
8-17	Grate Inlet Capacity Curves, 2 ft by 2 ft (0.61 m by 0.61 m) 45 - 2-1/4 - 4 Grate, Z = 24	8-20
8-18	Grate Inlet Capacity Curves, 2 ft by 2 ft (0.61 m by 0.61 m) 45 - 2-1/4 - 4 Grate, Z = 48	8-21
8-19	Grate Inlet Capacity Curves, 2 ft by 4 ft (0.61 m by 1.22 m) 45 - 3-1/4 - 4 Grate, Z = 16	8-22

LIST OF FIGURES - Continued

<u>Figure</u>		<u>Page</u>
8-20	Grate Inlet Capacity Curves, 2 ft by 4 ft (0.61 m by 1.22 m) 45 - 3-1/4 - 4 Grate, Z = 24	8-23
8-21	Grate Inlet Capacity Curves, 2 ft by 4 ft (0.61 m by 1.22 m) 45 - 3-1/4 - 4 Grate, Z = 48	8-24
8-22	Grate Inlet Capacity Curves, 2 ft by 2 ft (0.61 m by 0.61 m) 45 - 3-1/4 - 4 Grate, Z = 16	8-25
8-23	Grate Inlet Capacity Curves, 2 ft by 2 ft (0.61 m by 0.61 m) 45 - 3-1/4 - 4 Grate, Z = 24	8-26
8-24	Grate Inlet Capacity Curves, 2 ft by 2 ft (0.61 m by 0.61 m) 45 - 3-1/4 - 4 Grate, Z = 48	8-27
8-25	Development of Splash on 2 ft by 2 ft (0.61 m by 0.61 m) 45 - 2-1/4 - 4 Grate, Z = 24	8-28
8-26	Development of Splash on 2 ft by 2 ft (0.61 m by 0.61 m) 45 - 3-1/4 - 4 Grate, Z = 24	8-29
8-27	Debris Test 2 ft by 4 ft (0.61 m by 1.22 m) 45 - 2-1/4 - 4 Grate, $S_0 = 4\%$, Z = 24	8-30
8-28	Debris Test 2 ft by 4 ft (0.61 m by 1.22 m) 45 - 3-1/4 - 4 Grate, $S_0 = 4\%$, Z = 24	8-31
9-1	2 ft by 4 ft (0.61 m by 1.22 m) Cast 30° Tilt-bar Grate	9-2
9-2	Hydraulic Efficiency vs. Gutter flow 2 ft by 4 ft (0.61 m by 1.22 m) 30° Tilt-bar Grate	9-3
9-3	Hydraulic Efficiency vs. Gutter Flow 2 ft by 2 ft (0.61 m by 0.61 m) 30° Tilt-bar Grate	9-4
9-4	Spray Pattern on 2 ft by 2 ft (0.61 m by 0.61 m) 30° Tilt-bar Grate, Z = 24	9-5
9-5	Development of Spray Pattern on 2 ft by 2 ft (0.61 m by 0.61 m) 30° Tilt-bar Grate, Z = 48	9-6
9-6	Hydraulic Efficiency vs. Width of Spread 2 ft by 4 ft (0.61 m by 1.22 m) 30° Tilt-bar Grate	9-8
9-7	Hydraulic Efficiency vs. Width of Spread 2 ft by 2 ft (0.61 m by 0.61 m) 30° Tilt-bar Grate	9-9

LIST OF FIGURES - Continued

<u>Figure</u>		<u>Page</u>
9-8	Grate Inlet Capacity Curves, 2 ft by 4 ft (0.61 m by 1.22 m) 30° Tilt-bar Grate, Z = 16	9-10
9-9	Grate Inlet Capacity Curves, 2 ft by 4 ft (0.61 m by 1.22 m) 30° Tilt-bar Grate, Z = 24	9-11
9-10	Grate Inlet Capacity Curves 2 ft by 4 ft (0.61 m by 1.22 m) 30° Tilt-bar Grate, Z = 48	9-12
9-11	Grate Inlet Capacity Curves 2 ft by 2 ft (0.61 m by 0.61 m) 30° Tilt-bar Grate, Z = 16	9-13
9-12	Grate Inlet Capacity Curves 2 ft by 2 ft (0.61 m by 0.61 m) 30° Tilt-bar Grate, Z = 24	9-14
9-13	Grate Inlet Capacity Curves 2 ft by 2 ft (0.61 m by 0.61 m) 30° Tilt-bar Grate, Z = 48	9-15
9-14	Debris Tests, 2 ft by 4 ft (0.61 m by 1.22 m) 30° Tilt-bar Grate	9-16
10-1	2 ft by 4 ft (0.61 m by 1.22 m) Curved Vane Grate	10-2
10-2	Hydraulic Efficiency vs. Gutter Flow 2 ft by 4 ft (0.61 m by 1.22 m) Curved Vane Grate	10-3
10-3	Hydraulic Efficiency vs. Gutter Flow 2 ft by 2 ft (0.61 m by 0.61 m) Curved Vane Grate	10-4
10-4	Flow Performance of the Curved Vane Grate at $S_0 = 13\%$, Z = 24	10-5
10-5	Development of Spray Pattern on the 2 ft by 2 ft (0.61 m by 0.61 m) Curved Vane Grate, Z = 24	10-6
10-6	Hydraulic Efficiency vs. Width of Spread 2 ft by 4 ft (0.61 m by 1.22 m) Curved Vane Grate	10-8
10-7	Hydraulic Efficiency vs. Width of Spread 2 ft by 2 ft (0.61 m by 0.61 m) Curved Vane Grate	10-9
10-8	Grate Inlet Capacity Curves 2 ft by 4 ft (0.61 m by 1.22 m) Curved Vane Grate, Z = 16	10-10
10-9	Grate Inlet Capacity Curves 2 ft by 4 ft (0.61 m by 1.22 m) Curved Vane Grate, Z = 24	10-11
10-10	Grate Inlet Capacity Curves 2 ft by 4 ft (0.61 m by 1.22 m) Curved Vane Grate, Z = 48	10-12

LIST OF FIGURES - Continued

<u>Figure</u>		<u>Page</u>
10-11	Grate Inlet Capacity Curves 2 ft by 2 ft (0.61 m by 0.61 m) Curved Vane Grate, Z = 16	10-13
10-12	Grate Inlet Capacity Curves 2 ft by 2 ft (0.61 m by 0.61 m) Curved Vane Grate, Z = 24	10-14
10-13	Grate Inlet Capacity Curves 2 ft by 2 ft (0.61 m by 0.61 m) Curved Vane Grate, Z = 48	10-15
10-14	Debris Tests, 2 ft by 4 ft (0.61 m by 1.22 m) Curved Vane Grate, $S_0 = 4\%$, Z = 24	10-16
11-1	2 ft by 4 ft (0.61 m by 1.22 m) Steel Fabricated P - 1-7/8 - 4 Grate	11-2
11-2	Hydraulic Efficiency vs. Gutter Flow, 2 ft by 4 ft (0.61 m by 1.22 m) P - 1-7/8 - 4 Grate	11-4
11-3	Hydraulic Efficiency vs. Gutter Flow, 2 ft by 2 ft (0.61 m by 0.61 m) P - 1-7/8 - 4 Grate	11-5
11-4	Flow Layer Effect, P - 1-7/8 - 4 Grate, Z = 24	11-6
11-5	Development of "flow layer" on 2 ft by 2 ft (0.61 m by 0.61 m) P - 1-7/8 - 4 Grate, Z = 48	11-7
11-6	Hydraulic Efficiency vs. Width of Spread, 2 ft by 4 ft (0.61 m by 1.22 m) P - 1-7/8 - 4 Grate	11-8
11-7	Hydraulic Efficiency vs. Width of Spread, 2 ft by 2 ft (0.61 m by 0.61 m) P - 1-7/8 - 4 Grate	11-9
11-8	Grate Inlet Capacity Curves 2 ft by 4 ft (0.61 m by 1.22 m) P - 1-7/8 - 4 Grate, Z = 16	11-11
11-9	Grate Inlet Capacity Curves 2 ft by 4 ft (0.61 m by 1.22 m) P - 1-7/8 - 4 Grate, Z = 24	11-12
11-10	Grate Inlet Capacity Curves 2 ft by 4 ft (0.61 m by 1.22 m) P - 1-7/8 - 4 Grate, Z = 48	11-13
11-11	Grate Inlet Capacity Curves 2 ft by 2 ft (0.61 m by 0.61 m) P - 1-7/8 - 4 Grate, Z = 16	11-14
11-12	Grate Inlet Capacity Curves 2 ft by 2 ft (0.61 m by 0.61 m) P - 1-7/8 - 4 Grate, Z = 24	11-15
11-13	Grate Inlet Capacity Curves 2 ft by 2 ft (0.61 m by 0.61 m) P - 1-7/8 - 4 Grate, Z = 48	11-16

LIST OF FIGURES - Continued

<u>Figure</u>		<u>Page</u>
11-14	Debris Tests, 2 ft by 4 ft (0.61 m by 1.22 m) P - 1-7/8 - 4 Grate, $S_0 = 4\%$, $Z = 24$	11-17
12-1	2 ft by 4 ft (0.61 m by 1.22 m) Steel Fabricated P - 1-1/8 Grate	12-2
12-2	Hydraulic Efficiency vs. Gutter Flow, 2 ft by 4 ft (0.61 m by 1.22 m) P - 1-1/8 Grate	12-3
12-3	Hydraulic Efficiency vs. Gutter Flow, 2 ft by 2 ft (0.61 m by 0.61 m) P - 1-1/8 Grate	12-4
12-4	Development of Splash From Pipe Spacers on 2 ft by 4 ft (0.61 m by 1.22 m) P - 1-1/8 Grate, $Z = 24$	12-6
12-5	Flow Deflected Out of the Inlet by the Cast Steel Spacer, 2 ft by 2 ft (0.61 m by 0.61 m) P - 1-1/8 Grate, $Z = 16$	12-7
12-6	Hydraulic Efficiency vs. Width of Spread, 2 ft by 4 ft (0.61 m by 1.22 m) P - 1-1/8 Grate	12-8
12-7	Hydraulic Efficiency vs. Width of Spread, 2 ft by 2 ft (0.61 m by 0.61 m) P - 1-1/8 Grate	12-9
12-8	Grate Inlet Capacity Curves 2 ft by 4 ft (0.61 m by 1.22 m) P - 1-1/8 Grate, $Z = 16$	12-10
12-9	Grate Inlet Capacity Curves 2 ft by 4 ft (0.61 m by 1.22 m) P - 1-1/8 Grate, $Z = 24$	12-11
12-10	Grate Inlet Capacity Curves 2 ft by 4 ft (0.61 m by 1.22 m) P - 1-1/8 Grate, $Z = 48$	12-12
12-11	Grate Inlet Capacity Curves 2 ft by 2 ft (0.61 m by 0.61 m) P - 1-1/8 Grate, $Z = 16$	12-13
12-12	Grate Inlet Capacity Curves 2 ft by 2 ft (0.61 m by 0.61 m) P - 1-1/8 Grate, $Z = 24$	12-14
12-13	Grate Inlet Capacity Curves 2 ft by 2 ft (0.61 m by 0.61 m) P - 1-1/8 Grate, $Z = 48$	12-15
12-14	Debris Test of 2 ft by 4 ft (0.61 m by 1.22 m) P - 1-1/8 Grate, $S_0 = 0.5\%$, $Z = 24$	12-17
12-15	Debris Test of 2 ft by 2 ft (0.61 m by 0.61 m) P - 1-1/8 Grate, $S_0 = 4.0\%$, $Z = 24$	12-18
13-1	Hydraulic Efficiency vs. Longitudinal Slope for a 2 ft by 4 ft (0.61 m by 1.22 m) Open Hole, $T = 5.0$ ft (1.52 m), $Z = 24$	13-3

LIST OF FIGURES - Continued

<u>Figure</u>		<u>Page</u>
13-2	Hydraulic Efficiency vs. Gutter Flow for the 2 ft by 4 ft (0.61 m by 1.22 m) Grates, $S_0 = 0.5\%$, $Z = 48$, 24, and 16	13-5
13-3	Hydraulic Efficiency vs. Gutter Flow for the 2 ft by 4 ft (0.61 m by 1.22 m) Grates, $S_0 = 1.0\%$, $Z = 48$, 24, and 16	13-6
13-4	Hydraulic Efficiency vs. Gutter Flow for the 2 ft by 4 ft (0.61 m by 1.22 m) Grates, $S_0 = 2.0\%$, $Z = 48$, 24, and 16	13-7
13-5	Hydraulic Efficiency vs. Gutter Flow for the 2 ft by 4 ft (0.61 m by 1.22 m) Grates, $S_0 = 4.0\%$, $Z = 48$, 24, and 16	13-8
13-6	Hydraulic Efficiency vs. Gutter Flow for the 2 ft by 4 ft (0.61 m by 1.22 m) Grates, $S_0 = 6.0\%$, $Z = 48$, 24, and 16	13-9
13-7	Hydraulic Efficiency vs. Gutter Flow for the 2 ft by 4 ft (0.61 m by 1.22 m) Grates, $S_0 = 9.0\%$, $Z = 48$, 24, and 16	13-10
13-8	Hydraulic Efficiency vs. Gutter Flow for the 2 ft by 4 ft (0.61 m by 1.22 m) Grates, $S_0 = 13.0\%$, $Z = 48$, 24, and 16	13-11
13-9	Hydraulic Efficiency vs. Gutter Flow for the 2 ft by 2 ft (0.61 m by 0.61 m) Grates, $S_0 = 0.5\%$, $Z = 48$, 24, and 16	13-12
13-10	Hydraulic Efficiency vs. Gutter Flow for the 2 ft by 2 ft (0.61 m by 0.61 m) Grates, $S_0 = 1.0\%$, $Z = 48$, 24, and 16	13-13
13-11	Hydraulic Efficiency vs. Gutter Flow for the 2 ft by 2 ft (0.61 m by 0.61 m) Grates, $S_0 = 2.0\%$, $Z = 48$, 24, and 16	13-14
13-12	Hydraulic Efficiency vs. Gutter Flow for the 2 ft by 2 ft (0.61 m by 0.61 m) Grates, $S_0 = 4.0\%$, $Z = 48$, 24, and 16	13-15
13-13	Hydraulic Efficiency vs. Gutter Flow for the 2 ft by 2 ft (0.61 m by 0.61 m) Grates, $S_0 = 6.0\%$, $Z = 48$, 24, and 16	13-16
13-14	Hydraulic Efficiency vs. Gutter Flow for the 2 ft by 2 ft (0.61 m by 0.61 m) Grates, $S_0 = 9.0\%$, $Z = 48$, 24, and 16	13-17
13-15	Hydraulic Efficiency vs. Gutter Flow for the 2 ft by 2 ft (0.61 m by 0.61 m) Grates, $S_0 = 13.0\%$, $Z = 48$, 24, and 16	13-18
13-16	Hydraulic Efficiency vs. Gutter Flow for the 2 ft by 4 ft (0.61 m by 1.22 m) Grates, $Z = 96$	13-19

LIST OF FIGURES - Continued

<u>Figure</u>		<u>Page</u>
13-17	Hydraulic Efficiency vs. Gutter Flow for the 2 ft by 2 ft (0.61 m by 0.61 m) Grates, Z = 96	13-20
13-18	Hydraulic Efficiency vs. Longitudinal Slope for a Constant Width of Spread, T' = 7.0 ft (2.13 m) 2 ft by 4 ft (0.61 m by 1.22 m) Grates, Z = 48	13-24
13-19	Hydraulic Efficiency vs. Longitudinal Slope for a Constant Width of Spread, T' = 5.5 ft (1.68 m) 2 ft by 4 ft (0.61 m by 1.22 m) Grates, Z = 24	13-25
13-20	Hydraulic Efficiency vs. Longitudinal Slope for a Constant Width of Spread, T' = 4.0 ft (1.22 m) 2 ft by 4 ft (0.61 m by 1.22 m) Grates, Z = 16	13-26
13-21	Hydraulic Efficiency vs. Longitudinal Slope for a Constant Width of Spread, T' = 7.0 ft (2.13 m) 2 ft by 2 ft (0.61 m by 0.61 m) Grates, Z = 48	13-27
13-22	Hydraulic Efficiency vs. Longitudinal Slopes for a Constant Width of Spread, T' = 5.5 ft (1.68 m) 2 ft by 2 ft (0.61 m by 0.61 m) Grates, Z = 24	13-28
13-23	Hydraulic Efficiency vs. Longitudinal Slopes for a Constant Width of Spread, T' = 4.0 ft (1.22 m) 2 ft by 2 ft (0.61 m by 0.61 m) Grates, Z = 16	13-29
14-1	Favorable and Unfavorable Gutter Flow Conditions	14-3

LIST

LIST OF TABLES

<u>Table</u>		<u>Page</u>
2-1	Required Depth of Bearing Bars	
	Parallel Bar Grates	2-5
2-2	Required Depth of Bearing Bars	
	Parallel Bar with Transverse Rod Grates	2-8
2-3	Required Depth of Bearing Bars	
	Parallel Bar with Transverse Spacer Grates	2-10
2-4	Required Depth of 45° Tilt Bearing Bars	2-13
2-5	Required Depth of 30° Tilt Bearing Bars	2-14
2-6	Curved Vane Bar Analysis	2-15
2-7	Results of 2 ft by 2 ft (0.61 m by 0.61 m)	
	Tubular Grate Analysis	2-19
2-8	Results of 2 ft by 4 ft (0.61 m by 1.22 m)	
	Tubular Grate Analysis	2-20
2-8	Moment Diagrams	2-21
(cont)		
3-1	Principal Grate Dimensions	3-2
3-2	Test Subjects - Physical Data	3-5
3-3	Tire Widths for Test Bicycles	3-6
3-4	Evaluation Criteria	3-9
3-5	Observer Evaluation	3-10
3-6	Bicyclist Evaluation	3-11
3-7	Composite Evaluation	3-12
4-1	Inlet Flow Measurements for an Open Hole	4-15
5-1	Principal Components of Hydraulic Test	
	Facility	5-4
6-1	Debris Test Results - Parallel Bar Grates	6-23
7-1	Maximum Efficiency Slopes - Reticuline	
	Grates	7-6
7-2	Debris Test Results - Reticuline Grates	7-22
8-1	Maximum Efficiency Slopes - 45° Tilt-	
	bar Grates	8-8
8-2	Debris Test Results - 45 - 2-1/4 - 4 Grates	8-33
8-3	Debris Test Results - 45 - 3-1/4 - 4 Grates	8-34
9-1	Maximum Efficiency Slopes - 30° Tilt-	
	bar Grates	9-7
9-2	Debris Test Results - 30° Tilt-bar Grates	9-18
10-1	Debris Test Results - Curved Vain Grates	10-17
11-1	Maximum Efficiency Slopes -	
	P - 1-7/8 - 4 Grates	11-10
11-2	Debris Test Results - P - 1-7/8 - 4 Grates	11-18
12-1	Maximum Efficiency Slopes - P - 1-1/8 Grates	12-16
12-2	Debris Test Results - P - 1-1/8 Grates	12-20
13-1	Minimum Longitudinal Slope Conditions for	
	Carryover Splash on at Least One Grate	
	Design	13-21

LIST OF TABLES - Continued

<u>Table</u>		<u>Page</u>
13-2	Comparison of Test Grates at 9 Percent Longitudinal Slope	13-23
13-3	Average Debris Handling Efficiencies for Test Grates	13-30
14-1	Grate Inlet Classification	14-4

SUMMARY

Eleven drain inlet grates were tested to evaluate their safety characteristics for bicycle as well as pedestrian traffic. Four of the grates that rated highest in the safety tests were selected for hydraulic testing. Three other grates with designs and bar spacings similar to grates proven safe were also selected for hydraulic testing. A parallel bar grate was included in the hydraulic test program as a standard with which to compare the performance of the other test grates. Hydraulic and debris tests were performed on full-size grates in sizes of 2 ft by 4 ft (0.61 m by 1.22 m) and 2 ft by 2 ft (0.61 m by 0.61 m). The grates were tested at cross slopes of 1:48, 1:24, 1:16 and longitudinal slopes of 0.5, 1, 2, 4, 6, 9, and 13 percent with gutter flows up to 5.6 ft³/s (0.158 m³/s). Debris tests were run using 150 pieces of 3 in (76 mm) by 4 in (102 mm) paper debris. Test results show that two of the grate designs (a cast and a steel fabricated grate) are nearly as hydraulically efficient as the parallel bar grate and considerably more efficient than the other grate designs tested. One other design (a steel fabricated grate) shows high hydraulic efficiencies at longitudinal slopes up to 6 percent. These three grate designs are recommended for additional testing. A grate's ability to handle debris without clogging was shown to be most dependent on the spacing of its longitudinal bars. Grates with the widest longitudinal bar spacing tested consistently outperformed grates with narrower longitudinal bar spacing.

ACKNOWLEDGMENTS

This study was conducted by the U.S. Bureau of Reclamation (USBR) at their Engineering and Research Center, Denver, Colorado, for the Federal Highway Administration under Purchase Order No. 5-3-0166. The Bureau of Reclamation's involvement in the study was a result of their interest in drop inlet designs.

The authors would like to acknowledge the following individuals for their contribution in selected areas of the study:

1. Model design - Charles Givens and Robert Sund
2. Structural analysis of grates - Michael Davister
3. Bicycle safety - Daniel Smith (DeLeuw, Cather and Company),
Larry Harrison and John Fegan (FHWA)
4. Hydraulic tests - James Francisco, Warren Frizell, Theresa
Satchell, Richard Straubinger, and William
Fiedler
5. Drafting - Joseph Santillana
6. Photography - W. M. Batts

The authors would also like to acknowledge Mr. Thomas Rhone, USBR Applied Hydraulics Section Head, for his advice, thorough manuscript review, and generous support throughout this study.

The contract was monitored by Dr. D. C. Woo, Contract Manager, Environmental Design and Control Division, Federal Highway Administration. The authors would like to acknowledge Dr. Woo for the overall direction of the study, his timely input during the test program, and his critical review and comments on research results.

NOTATION

A = cross sectional flow area

E = hydraulic efficiency

g = gravitational acceleration

L = length of grate

L_0 = length of grate needed to capture total roadway flow outside of gutter

n = Manning's coefficient of roughness

Q_c = carry over flow

Q_s = side flow into grate

Q_F = frontal flow into grate

Q_I = flow intercepted by grate

Q_T = gutter flow

R = hydraulic radius

S_0 = longitudinal slope

T = calculated width of spread

T' = measured width of spread

y = depth of flow at the curb

y' = depth of flow at the gutter line

V = gutter flow velocity

P = wetted perimeter

Z = reciprocal of the cross slope, T/y

CHAPTER 1

INTRODUCTION

In recent years Americans have shown increased interest in bicycling. The exposure of bicyclists to our nation's highways and streets has resulted in increased bicycle accidents with vehicular traffic as well as with various highway-related structures. Proper surface drainage of streets and highways is one of many requirements for the safe movement of traffic and is normally accomplished with curb inlets, grate inlets, or a combination of both.

Although curb inlets and combination inlets are used on flat street slopes, grate inlets are far more prevalent, particularly on steeper slopes. The purpose of this comprehensive investigation is to identify, develop, and analyze selected grate inlets which maximize hydraulic efficiency, bicycle safety, pedestrian safety, structural sufficiency, economy, and freedom from clogging.

It would seem that the safety and hydraulic efficiency characteristics of a grate inlet design are in conflict: that the safest grate inlet would be a solid plate covering the inlet and the most hydraulically efficient grate inlet would be an open hole. It is obvious that a compromise is needed which will optimize both the safety and hydraulic efficiency characteristics of the grate inlet.

There have been a number of experimental studies conducted to determine the hydraulic characteristics of various grate inlet designs, including those with transverse rods, diagonal bars, and curved or tilted transverse bar configurations. To accomplish the objectives of this investigation, 15 grate inlet designs were selected based on the major criteria of bicycle safety, hydraulic efficiency, and freedom from clogging. A steel fabricated parallel bar grate was selected as one of the test grates based on its proven performance as a hydraulically efficient grate inlet. Although its bicycle safety characteristics are very poor, it provides an excellent standard of hydraulic efficiency with which to compare other grate inlet designs. Three other grate configurations presently used as storm drain inlets were also selected for the test program. They included the parallel bar with transverse rods at the surface of the grate, the reticuline grate and a parallel bar grate with 3/4 in (19 mm) clear spacing between bars. Three cast grate inlet designs were also tested. They included a 45° tilt bar grate, a 30° tilt bar grate (30° from vertical), and a curved vane grate.

The selection of these grate inlets was based on previous investigations and engineering judgement using available knowledge and experience. All of the inlet grate designs have been previously studied

at various degrees of effort for hydraulic efficiency and/or bicycle safety:

1. Parallel Bar with transverse rods (1)*(2)
2. Reticuline (3)(1)
3. Parallel Bar with three-quarter-inch clear spacing between bars (1)(2)
4. 45° Tilted Bar (5)(1)
5. 30° Tilted Bar (4)
6. Curved Vane (5)(6)

A structural analysis of the new test grates not presently in use was also performed to determine proper sizes for the structural members of each grate. The designs of the test grates used for bicycle safety and hydraulic tests were based on this structural analysis.

A bicycle safety consultant was hired to help develop and conduct the bicycle safety tests. Meetings were held with manufacturers to determine the feasibility and economic factors to be considered in developing new grate inlet designs. Project personnel consulted with city and state highway officials to determine clogging tendencies of present grate designs and to establish debris test procedures for evaluating selected test grates.

The test program was carried out using two test facilities. Approximately 540 bicycle tests were conducted on eleven 2 ft by 4 ft (0.61 m by 1.22 m) grate inlets at an outdoor test site. The site consisted of a 22 ft (6.7 m) wide 500 ft (152 m) long abandoned roadway with a concrete vault in which to place various test grates. An 8 ft (2.44 m) wide 60 ft (18.3 m) long hydraulic roadway flume was constructed in the U.S. Bureau of Reclamation Hydraulic Research Laboratory and used as the test facility for the 1,680 hydraulic efficiency tests and 100 debris tests.

The grate inlet capacity curves developed for the 2 ft by 4 ft (0.61 m by 1.22 m) and 2 ft by 2 ft (0.61 m by 0.61 m) grates can be used to determine grate efficiency and intercepted flow capability for various combinations of gutter flow, longitudinal and cross slopes. The safety, structural integrity, and hydraulic efficiency characteristics of the tested grates are presented in individual chapters and summarized in the Discussion of Results chapter of the report.

* Numbers in parentheses refer to references at the end of the chapter.

REFERENCES

1. City of Los Angeles, "Hydraulic Model Study of Bicycle-Safe Catch Basin Grates", an interim report, Feb. 1975
2. Los Angeles County Flood Control District, "Evaluation of Three Types of Catch Basin Grates for Streets with Bicycle Traffic", Systems and Standards Group, Design Division
3. Ragan, R. M., Gingrich, T. E., and Jackson, T. J., "Hydraulic Characteristics of Reticular Inlet Grates, University of Maryland, Dept. of Civil Engineering, January 1976
4. Donahue, J. F., and Bahler, S., "Design and Evaluation of the D.C. Safety Grate for Drop Inlets", District of Columbia Department of Highways and Traffic, Experimental Project No. -03-11-74-001, June 1975
5. Woo, D. C., and Jones, J. S., "Hydraulic Characteristics of Two Bicycle-Safe Grate Inlet Designs", Federal Highway Administration, Report No. FHWA-RD-74-77, November 1974
6. Cassidy, J. J., Generalized Hydraulic Characteristics of Grate Inlets, Highway Drainage and Scour Studies, Highway Research Record, No. 123, pp 36-48, 1966

CHAPTER 2

ANALYSIS OF STRUCTURAL INTEGRITY

The structural analyses for the various inlet grate designs studied were based on the requirements stated in "Standard Specifications for Highway Bridges," American Association of State Highway and Transportation Officials - AASHTO (1)*. The grates were analyzed for a 8,000 lb (35.6 kN) tire load** with a 30 percent impact factor. The load was applied to the grate with a 9 in by 9 in (229 mm by 229 mm) contact area as recommended by Ballinger (2).

A U.S. Bureau of Reclamation general purpose computer program, STR5, was used to perform the structural analysis of the grates. In some cases it was determined by a preliminary STR5 analysis that the bearing bars of the grate acted independently as simply supported beams. In those cases a simple beam analysis was performed.

The STR5 program has the capability to analyze a wide variety of indeterminate structures from simple planar frames to complex three dimensional structures. A mathematical model of the structure is described using various structural elements positioned in any orientation in space. Points within a model may be restrained against rotation and/or displacement in any direction to reflect the behavior of the actual structure. In addition, the program contains graphical output for both the displaced and undisplaced shape to verify the correctness of the configuration, orientation, and displacement of the model.

Steel Grates

Three fabricated steel grates were structurally analyzed. These are shown in figure 2-1. A preliminary STR5 analysis of the grate shown in figure 2-1b indicated the transverse rods and the end bars do not aid in distributing the load from a loaded bar to an unloaded bar for the 2 ft by 2 ft (0.61 m by 0.61 m) grate size. Consequently, the 2 ft (0.61 m) grate performs structurally as the grate shown in figure 2-1a where each bar acts independently as a simply supported beam. However, the STR5 analysis of the 2 ft by 4 ft (0.61 m by 1.22 m) parallel bar with transverse rod grate indicated that there was transverse distribution of the load and; therefore, it was analyzed by the STR5 program. The spacers shown in figure 2-1c serve to provide lateral support to the loaded bars. An elastic stability

* Numbers in parentheses identify the references at the end of the chapter.

** HS-20-44 truckload (32,000-pound axle load with 8,000 pounds per wheel).

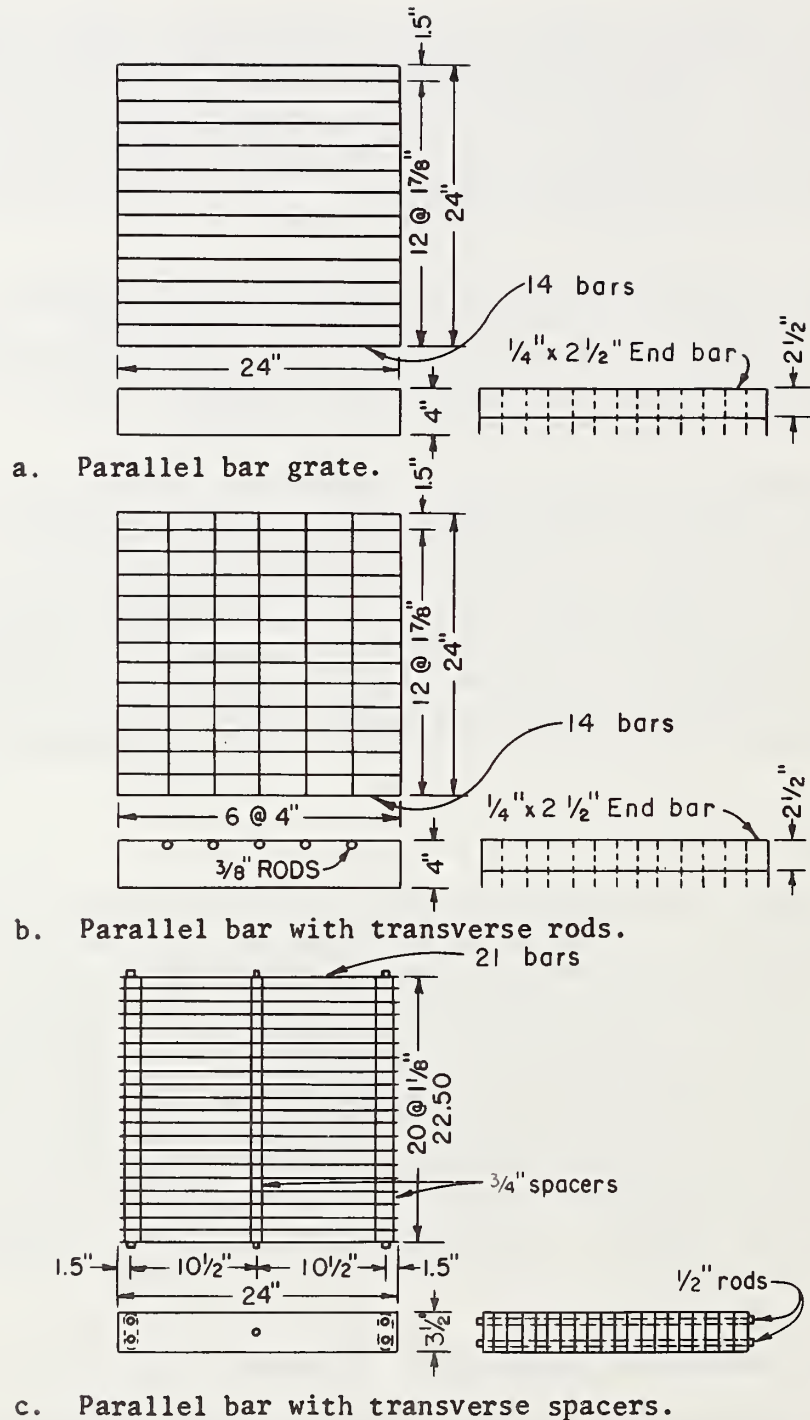


Figure 2-1. - Schematic drawings for three fabricated steel grate designs (Note: 1 in = 25.4 mm).

analysis indicated buckling is insignificant for typical steel grate sizes spanning 2 ft (0.61 m). However, lateral instability may exist for some bar sizes spanning 4 ft (1.22 m). Since lateral support is provided for the grate shown in figure 2-1c, a simple support beam analysis was used to design this grate for both the 2 ft (0.61 m) and 4 ft (1.22 m) span lengths.

AASHTO requirements specify the allowable bending stress as 20,000 lb/in² (138 MPa) for A36 steel. Also, Federal specifications (3) require that the grate show no permanent deformation when subjected to a 25,000 lb (111 kN) proof load on a 9 in by 9 in (229 mm by 229 mm) area. This proof load seems unduly conservative and was therefore not considered as part of the current design criteria.

The first analysis determined the bearing bar depth for a 2 ft by 2 ft (0.61 m by 0.61 m) parallel bar grate using bar thicknesses of 1/2 in (12.7 mm), 3/8 in (9.5 mm), and 1/4 in (6.4 mm) with the bearing bars spaced 1-7/8 in (48 mm) center to center (figure 2-1a). The STR5 analysis indicated that the end bars provide negligible rotational resistance to the longitudinal bars. Therefore, it was assumed that the longitudinal bars act as simply supported beams.

Using 1-7/8 in (47.6 mm) center-to-center bearing bar spacing and a 9 in (229 mm) wide load, the 8,000 lb (35.6 kN) tire load and impact load may be carried by as few as four bars. Therefore, the load per bar = $\frac{1.3(8,000)}{4} = 2,600$ lb/bar (111.6 kN/bar). Using simple support

beam equations the design moment, M, would be $M = R \left(a + \frac{R}{2w} \right)$, where:

R = beam reaction

w = uniformly distributed load per unit of length

a = measured distance along beam from end to start of uniform load (figure 2-2)

$$w = \frac{2,600 \text{ lb/bar}}{9 \text{ in}} = 289 \text{ lb/in (50.6 N/mm)}$$

$$R = \frac{(289)(9)}{2} = 1,300 \text{ lb (5.79 kN)}$$

or

$$M = (1,300) \left[7.5 + \frac{1,300}{(2)(289)} \right]$$

$$M = 12,674 \text{ lb-in (1432 N-m)}$$

Since the flexural stress at the extreme fiber is:

$$f_b = \frac{Mc}{I}$$

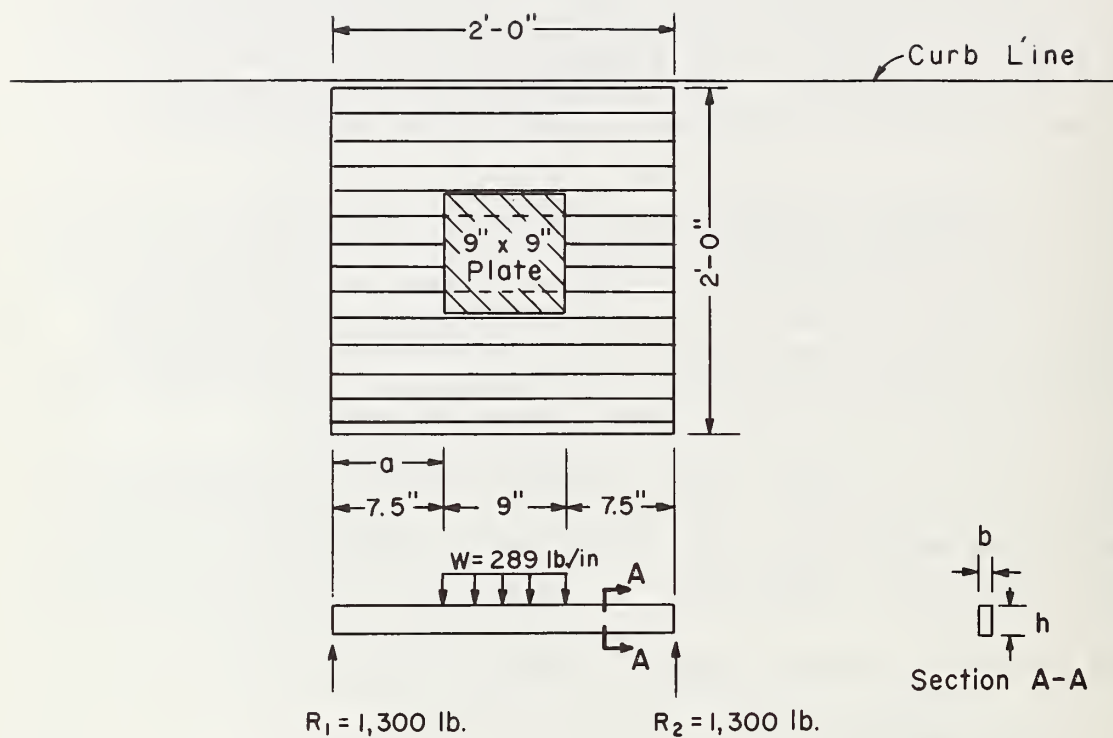


Figure 2-2. - Schematic load diagram
 (Note: 1 in = 25.4 mm, 1 lb = 4.45 N).

and

$$I = \frac{bh^3}{12}$$

$$C = h/2$$

$$f_b = \frac{6M}{bh^2}$$

or

$$H = \left(\frac{6M}{f_b b} \right)^{0.5}$$

A summary of these depths is given in table 2-1.

Fabricated grates commonly have the longitudinal bearing bars connected to a rectangular end member having the same dimensions as the bearing bars, resulting in a moment diagram approaching that of a simply supported beam (figure 2-3). A study was performed using tubular sections for the end members, giving more rotational stiffness to the ends of the bearing bars (figure 2-4). Consequently, the midspan moments would be reduced, resulting in smaller depths of the bearing bars, a reduction in grate weight, and possibly lower material costs. (This study is presented in the appendix of the chapter.)

Table 2-1

REQUIRED DEPTH OF BEARING BARS
PARALLEL BAR GRATES

(Note: 1 in = 25.4 mm, 1 kip/in² = 6.89 MPa)

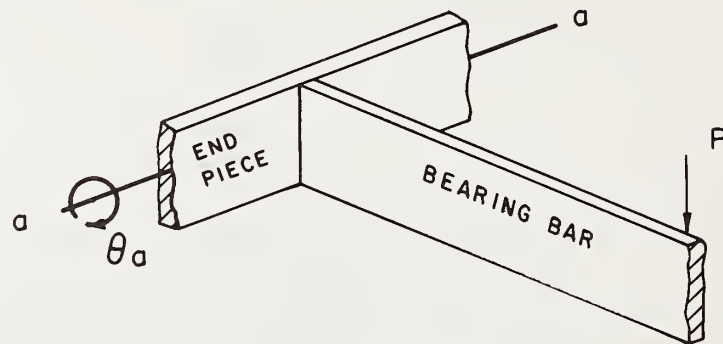
Bar thickness in (mm)	2 ft by 2 ft (0.61 m by 0.61 m) grate		2 ft by 4 ft (0.61 m by 1.22 m) grate*	
	in	(mm)	in	(mm)
1/2 (12.70)	2.76	(70.10)	4.12	(104.6)
3/8 (9.53)	3.18	(80.77)	4.76	(120.9)
1/4 (6.35)	3.90	(99.06)	5.82	(147.8)

* Assuming adequate lateral support.

Note: Bars spaced at 1-7/8 inches center to center - no transverse rods.

The second analysis determined bar depths for a parallel bar with transverse rod grates. The analysis was conducted for 1/4 in (6.4 mm), 3/8 in (9.5 mm) and 1/2 in (12.7 mm) bar thickness with center-to-center bar spacings of 1-7/8 in (48 mm) and 2-3/8 in

Statement: The connection shown below offers very little stiffness for rotation about the a-axis due to the small rotational stiffness of the rectangular end piece.



Consequently the moment diagram for the bearing bar will approach the moment diagram for a simply supported beam.

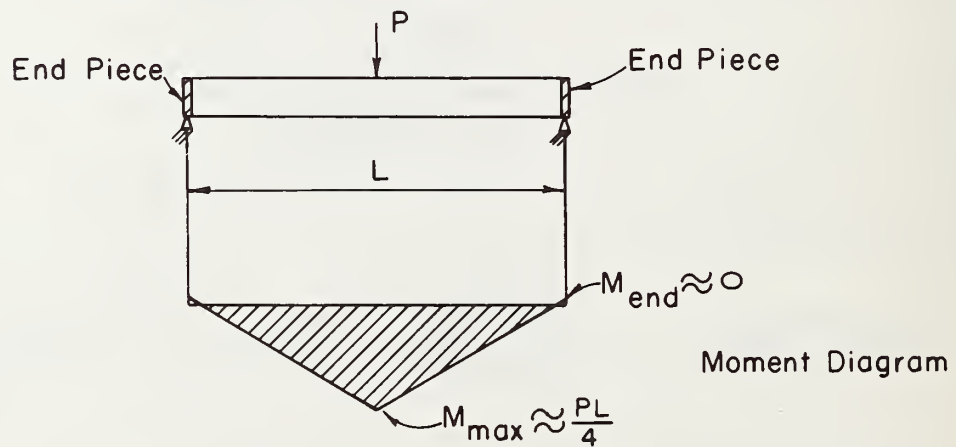
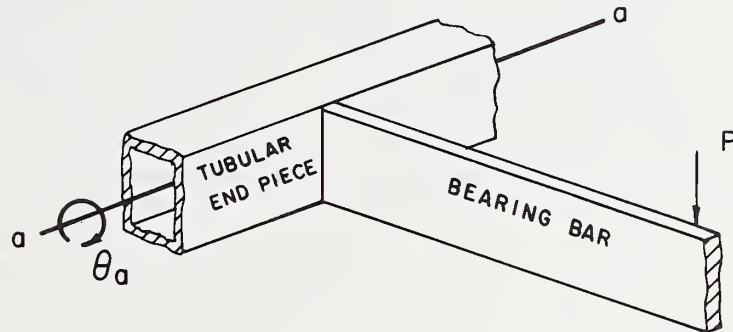
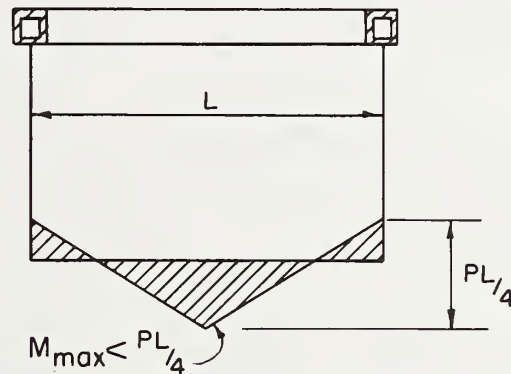


Figure 2-3. - Typical fabricated grate.

Statement: The connection shown below should offer more stiffness for rotation about the a-axis
(cont) more stiffness for rotation about the a-axis due to the increased rotational stiffness of the tubular end piece.



The moment diagram for this condition should produce end moments between 0 and $PL/8$.



Moment Diagram

Consequently, the depth of the bearing bar could be decreased because of the smaller mid-span moment.

Figure 2-4. - Tubular end piece design.

(60 mm). In addition, 3/8 in (9.5 mm) transverse rods were spaced at 4 in (102 mm) centers at the surface of the bearing bars (figure 2-1b).

With a 2 ft by 2 ft (0.61 m by 0.61 m) grate, the STR5 model analysis showed that the transverse rods do not aid in distributing the load to the adjacent unloaded bars. Again, the bars were designed assuming they act as simply supported beams. Although no transverse distribution of load occurred for a 2 ft by 2 ft (0.61 m by 0.61 m) grate, this was not the case when a larger grate was analyzed. An STR5 analysis indicated the maximum moment was approximately 90 percent of the simple span moment when a 40 in by 16-7/8 in (1.0 m by 0.43 m) manufacturer's grate was analyzed with the longitudinal bars spaced 1-7/8 in (48 mm) center to center and the transverse rods at 4 in (102 mm) centers. A summary of the analysis for a 2 ft by 2 ft (0.61 m by 0.61 m) and 2 ft by 4 ft (0.61 m by 1.22 m) grate are given in table 2-2.

Table 2-2

REQUIRED DEPTH OF BEARING BARS
PARALLEL BAR WITH TRANSVERSE ROD GRATES

(Note: 1 in = 25.4 mm, 1 kip/in² = 6.89 MPa)

Bar thickness in (mm)	2 ft by 2 ft (0.61 m by 0.61 m) grate		2 ft by 4 ft (0.61 m by 1.22 m) grate	
	in	(mm)	in	(mm)
Longitudinal bar spacing = 1-7/8 in (47.6 mm)				
1/2 (12.70)	2.76	(70.10)	3.60	(91.4)
3/8 (9.53)	3.18	(80.77)	4.45	(113.0)
1/4 (6.35)	3.90	(99.06)	5.67	(144.0)
Longitudinal bar spacing = 2-3/8 in (60.33 mm)				
1/2 (12.70)	3.18	(80.77)	4.35	(110.5)
3/8 (9.53)	3.68	(93.47)	5.25	(133.4)
1/4 (6.35)	4.50	(114.30)	6.66	(169.2)

Static plate load tests were conducted by the California Department of Transportation (4) using a 9 in by 9 in (229 mm by 229 mm) steel plate centered on a 40 in (1 m) long by 23-5/8 in (0.60 m) wide grate. The grate consisted of thirteen 3-1/2 in by 1/4 in (89 mm by 6.4 mm)

bearing bars on 1-7/8 in (48 mm) centers and 3/8 in (9.5 mm) transverse rods on 4 in (102 mm) centers. A proof load of 20,000 lb (89.0 kN) was applied to the five center bars of the grate resulting in a deflection of 0.123 in (3 mm). It was estimated that the yield load for this grate was approximately 20,000 lb (89.0 kN). Using the same test procedure on a 40 in (1 m) long by 16-7/8 in (0.43 m) wide grate, Ballinger (2) estimated that the grate yielded under a load of 18,000 lb (80 kN) when the 9 in by 9 in (229 mm by 229 mm) plate was located on the four center bearing bars. The grate had 3-1/2 in by 1/4 in (89 mm by 6.4 mm) bearing bars on 1-7/8 in (48 mm) centers and 3/8 in (9.5 mm) transverse rods on 4 in (102 mm) centers. These yield loads are less than the 25,000 lb (111 kN) proof load required by the Federal Specification RR-F-621b (3).

Tables 2-1 and 2-2 give greater bearing bar depths than recommended by the manufacturers for a 20-ton (178.0 kN) truck with a 32,000 lb (142 kN) single-axle load on a 2 ft (0.61 m) span. The 9 in by 9 in (229 mm by 229 mm) tire contact area used in this investigation is smaller than that used by the manufacturers. As a result, with 1-7/8 in (48 mm) center spacing of the bearing bars, it is possible that the load would be carried by as few as four bars if the area is based on the 9 in (229 mm) square. Five bars would carry the same load based on the tire contact area used by the manufacturers. The assumed lateral load distribution is another important factor. Our analysis indicates that the transverse rods do not aid in distributing the normal highway load to adjacent unloaded bars when the span is only 2 ft (0.61 m).

The third analysis determined bar depths for 2 ft by 2 ft (0.61 m by 0.61 m) and 2 ft by 4 ft (0.61 m by 1.22 m) sizes of a parallel bar grate with transverse spacers (figure 2-1c). Bar depths were determined for bar widths of 1/2 in (12.7 mm), 3/8 in (9.5 mm), and 1/4 in (6.4 mm) with clear spacing of 3/4 in (19.1 mm) between bearing bars. A summary of the results is shown in table 2-3.

The Reticuline grate was not structurally analyzed since it is commercially available and the manufacturer's publications provide vehicular load tables based on AASHTO specifications.

Cast Grates

The cast grates analyzed consisted of tilted and curved vane bars oriented perpendicular to the direction of flow and stiffened with 2 in deep by 1/2 in wide (51 mm by 13 mm) longitudinal bars. The cross sections of the bearing bars are shown in figure 2-5. The size of the longitudinal bars was suggested as the minimum recommended size by manufacturers of cast grates. Two different inclinations of 30° (from the vertical) and 45° were used for the tilted bars.

Table 2-3

REQUIRED DEPTH OF BEARING BARS
PARALLEL BAR WITH TRANSVERSE SPACER GRATES

(Note: 1 in = 25.4 mm, 1 kip/in² = 6.89 MPa)

Bar thickness		2 ft by 2 ft (0.61 m by 0.61 m) grate		2 ft by 4 ft (0.61 m by 1.22 m) grate	
in	(mm)	in	(mm)	in	(mm)
1/2	(12.70)	1.92	(48.77)	3.00	(76.20)
3/8	(9.53)	2.07	(52.58)	3.24	(82.30)
1/4	(6.35)	2.39	(60.71)	3.75	(95.25)

The structural analysis for the tilt bar grates was conducted to determine the depth of tilt bar required using three different tilt bar spacings and two different longitudinal bar spacings, giving a total of six grate designs for each of the two inclinations. The method used to determine the bar depths for the cast grates is listed below:

1. Assume a trial bar depth for the given bar thickness. (The bearing bar thickness of 3/4 in (19 mm) was recommended by manufacturers of cast grates.)
2. Perform an STR5 structural analysis using the assumed bar size.
3. Based on the STR5 analysis, compute the maximum biaxial bending stresses.
4. If the maximum stresses are significantly different from the allowable stresses, assume a new bar depth and proceed as in step 2.

An STR5 structural analysis was also performed on a curved vane bar to determine the maximum stresses for the shape shown in figure 2-5c.

Ductile cast iron with an allowable tensile stress of 16,000 lb/in² (110 MPa) and an allowable compressive stress of 22,000 lb/in² (152 MPa) in the extreme fibers was used in the design. Normal stresses were computed based on the biaxial bending moments obtained from a structural analysis using STR5 for each grate. A 2 ft by 2 ft (0.61 m by 0.61 m) grate was used in the structural analysis for the various spacings of the tilted bars and longitudinal bars.

Maximum stresses were determined for the curved vane bars based on moments obtained from models of a 2 ft by 2 ft (0.61 m by 0.61 m) grate and a 2 ft by 4 ft (0.61 m by 1.22 m) grate. In each case, the selected curved vane bar configuration was satisfactory. A summary of the required depths for the 12 tilt bar grates and the maximum stresses for the curved vane bar grates are given in tables 2-4, 2-5, and 2-6.

An analysis was performed using a 2 ft by 4 ft (0.61 m by 1.22 m) grate model with the largest bearing bar spacing of 6-1/4 in (159 mm) and the largest longitudinal bar spacing of 3-7/32 in (82 mm) for the 45° tilt bar grates. The results of this study indicated a 6.3 percent maximum stress reduction over the 2 ft by 2 ft (0.61 m by 0.61 m) grate. Based on this study, one could conservatively use the same tilt bar depths obtained from the 2 ft by 2 ft (0.61 m by 0.61 m) grate designs for the 2 ft by 4 ft (0.61 m by 1.22 m) grates.

Summary

Three fabricated steel bar grate configurations as shown in figure 2-1 were designed to meet AASHTO specifications. No lateral support is necessary for typical bar sizes spanning 2 ft (0.61 m). Lateral support should be provided when the span length is 4 ft (1.22 m).

Twelve cast grates were designed which used tilted transverse bearing bars for two different degrees of tilt and various bar spacings. The inherent size of the cast grate bar members result in a distribution of the load to unloaded bars making it necessary to perform an indeterminate structural analysis. One curved vane cast grate was analyzed and found to be structurally sound.

When structural tubing, rather than rectangular bars, is used for the end bars in the fabricated steel grates, some load is distributed to the unloaded bars resulting in decreased bar depths and an overall decrease in the grate weight. Study results for the tubular design are given in the appendix to this chapter.

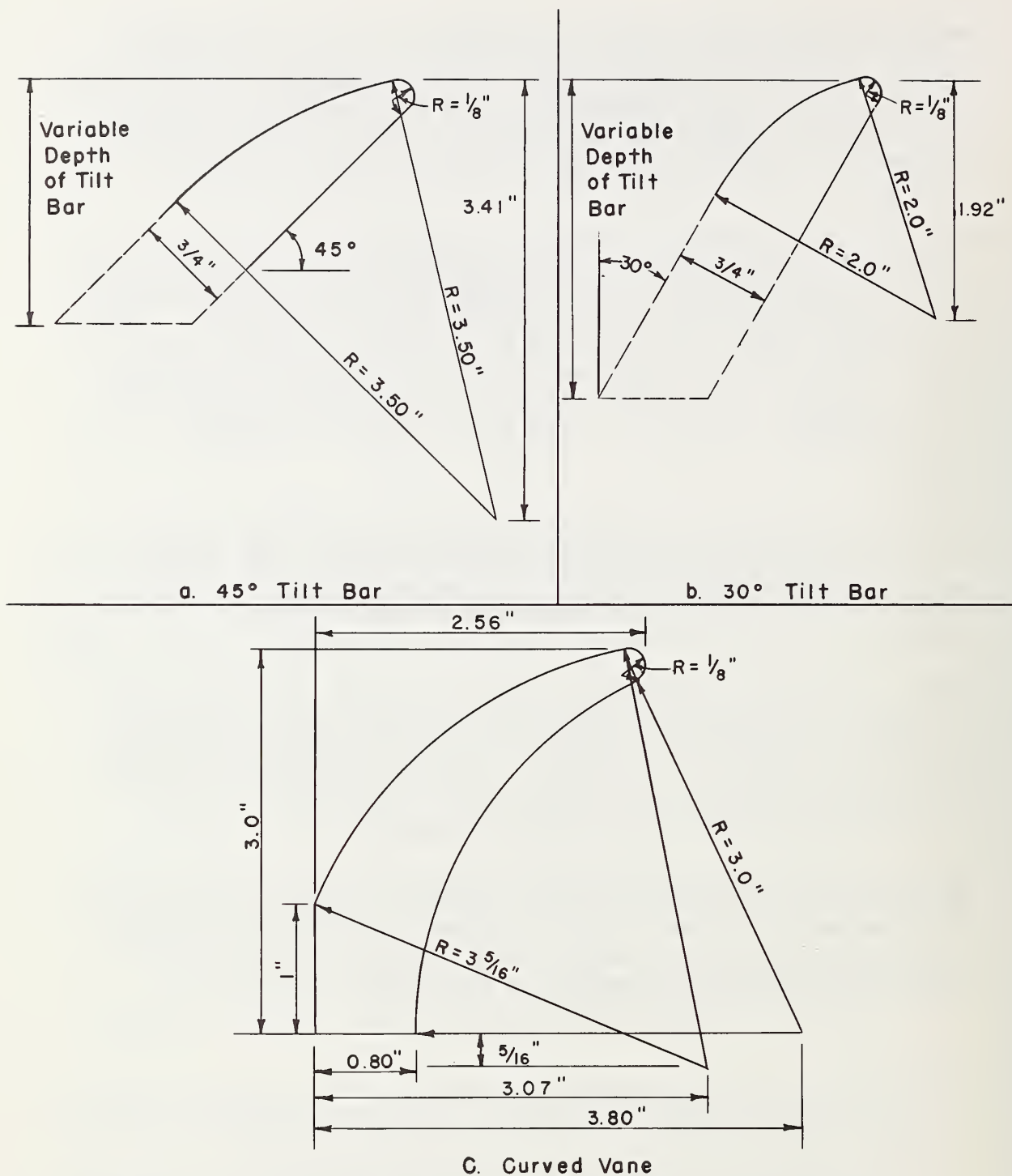

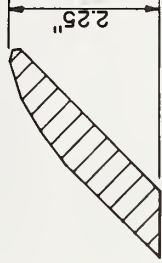
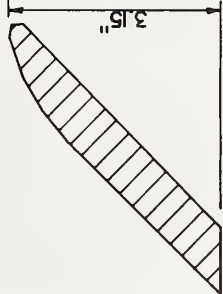

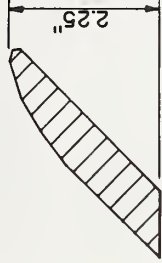
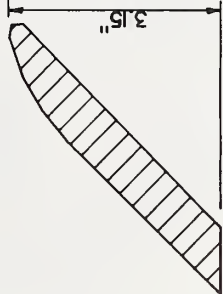
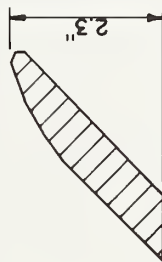
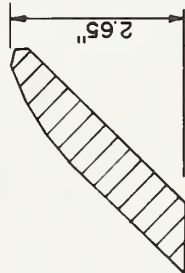
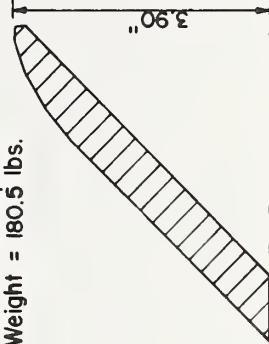


Figure 2-5. - Cross sections of bearing bars - cast grates
(Note: 1 in = 25.4 mm).

Table 2-4

REQUIRED DEPTH OF 45° TILT BEARING BARS

(Note: 1 in = 25.4 mm, 1b/in² = 6.89 kPa, 1 lb = 0.454 kg)

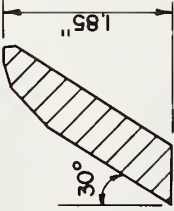
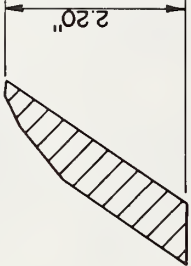
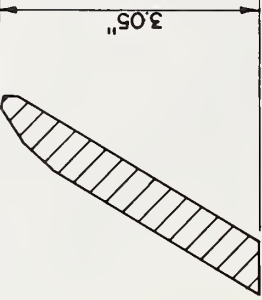
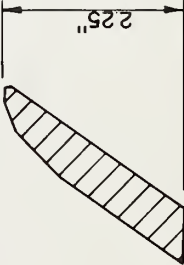
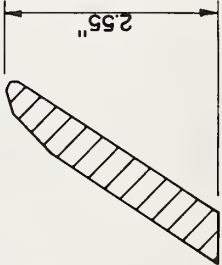
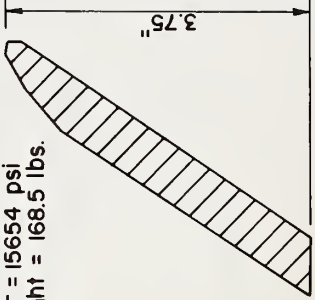
TILTED BAR SPACING LONG. BAR SPACING	3" (3 bar loading)	4" (2 bar loading)	6 1/4" (1 bar loading)
	 <p>$\sigma = 15978 \text{ psi}$ Weight = 213.6 lbs.</p>	 <p>$\sigma = 15773 \text{ psi}$ Weight = 195.6 lbs.</p>	 <p>$\sigma = 15882 \text{ psi}$ Weight = 186.5 lbs.</p>
2 1/4"	 <p>$\sigma = 15978 \text{ psi}$ Weight = 213.6 lbs.</p>	 <p>$\sigma = 15773 \text{ psi}$ Weight = 195.6 lbs.</p>	 <p>$\sigma = 15882 \text{ psi}$ Weight = 186.5 lbs.</p>
3 7/32"	 <p>$\sigma = 15858 \text{ psi}$ Weight = 209.6 lbs.</p>	 <p>$\sigma = 15984 \text{ psi}$ Weight = 191.6 lbs.</p>	 <p>$\sigma = 15624 \text{ psi}$ Weight = 180.5 lbs.</p>

All tilted bars are 3/4" thick, longitudinal bars are 2" x 1/2"

Table 2-5

REQUIRED DEPTH OF 30° TILT BEARING BARS

(Note: 1 in = 25.4 mm, 1b/in² = 6.89 kPa, 1 lb = 0.454 kg)

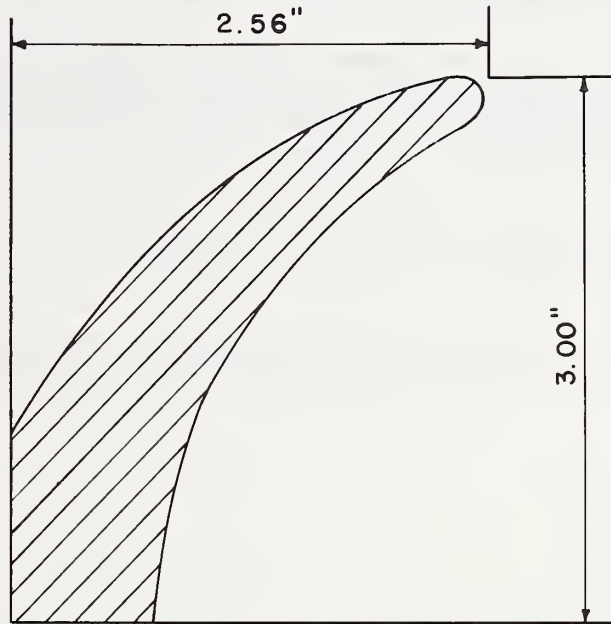
TILTED BAR LONG. BAR SPACING	3" (3 bar loading)	4" (2 bar loading)	6 1/4" (1 bar loading)
	2 1/4"	3 7/32"	
	 <p>$\sigma = 15795 \text{ psi}$ Weight = 193.6 lbs.</p>	 <p>$\sigma = 16240 \text{ psi}$ Weight = 187.6 lbs.</p>	 <p>$\sigma = 16156 \text{ psi}$ Weight = 172.5 lbs.</p>
	 <p>$\sigma = 15747 \text{ psi}$ Weight = 191.6 lbs.</p>	 <p>$\sigma = 16075 \text{ psi}$ Weight = 173.6 lbs.</p>	 <p>$\sigma = 15654 \text{ psi}$ Weight = 168.5 lbs.</p>

All tilted bars are 3/4" thick, longitudinal bars are 2"x 1/2"

Table 2-6

CURVED VANE BAR ANALYSIS

(Note: 1 in = 25.4 mm, 1 lb/in² = 6.89 kPa)



	Maximum Compressive stress* (psi)	Maximum Tensile stress* (psi)
2 ft. by 2 ft. (0.61 m by 0.61 m) Grate	-11,190	+14,646
2 ft. by 4 ft. (0.61 m by 1.22 m) Grate	-12,434	+15,669

Spacing of curved bars: $4\frac{1}{2}$ " for 2 ft. by 2 ft. (0.61 m by 0.61 m) grate

$4\frac{1}{4}$ " for 2 ft. by 4 ft. (0.61 m by 1.22 m) grate

Spacing of longitudinal bars: $3\frac{7}{32}$ "

* Allow. tensile stress = 16000 psi

* Allow. comp. stress = 22000 psi

REFERENCES

1. AASHTO, "Standard Specifications for Highway Bridges," American Association of State Highway and Transportation Officials, 11th Edition, 1973
2. Ballinger, C. A., and Gade, R. H., "Evaluation of the Structural Behavior of Typical Highway Inlet Grates, with Recommended Structural Design Criteria," Report No. FHWA-RD-73-90, December 1973
3. U.S. Government, "Federal Specification RR-F-621b - Frames, Covers, Gratings, Sump and Catch Basin, Manhole," September 1967
4. California Department of Transportation, "Highway Drainage Inlets," (A Value Engineering Study), April 29, 1971

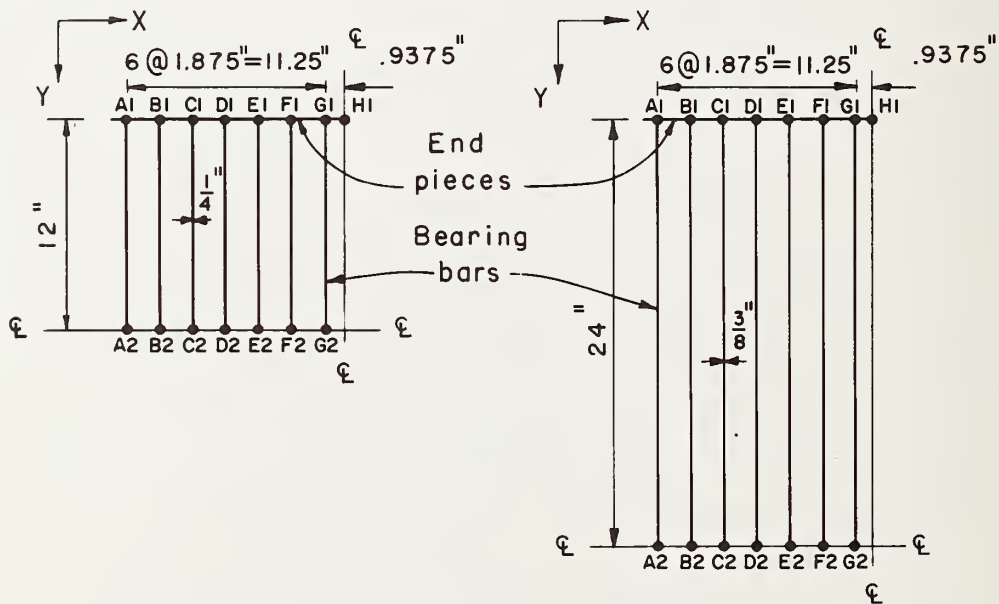
Appendix

A study was conducted using tubular sections for the end members of fabricated steel grates. The study included analysis of both the 2 ft by 2 ft (0.61 m by 0.61 m) and 2 ft by 4 ft (0.61 m by 1.22 m) grate models (figure 2-6).

Several different tubular sections were used in the analysis giving weight reductions as high as 14.2 percent for the larger grates. A tabulation of the results is given in tables 2-7 and 2-8 for the two grate sizes.

Problem : Calculate depths of grate bars using different size structural tubing for end pieces and compare weight of resulting grate with weight of grate using rectangular end pieces.

Solution: The analysis was made using two different grate sizes and modeled for STR5 analysis as shown below. The center 4.5" of members F1-F2 and G1-G2 were loaded with 289 lb./in which is equivalent to an H2O tire load with a 0.3 impact factor spread over a 9" x 9" area.



$\frac{1}{4}$ Model of 2ft. by 2ft. (0.61m by 0.61m) grate

$\frac{1}{4}$ Model of 2ft. by 4ft. (0.61m by 1.22m) grate

Figure 2-6. - STR5 tubular model
(Note: 1 in = 25.4 mm, 1 lb/in = 0.175 N/mm).

Table 2-7

RESULTS OF 2 FT BY 2 FT (0.61 M BY 0.61 M) TUBULAR GRATE ANALYSIS

(Note: 1 in = 25.4 mm, 1 lb = 0.454 kg)

END PIECE	SIZE BEARING BAR REQUIRED	WEIGHT OF GRATE	% REDUCTION
$\frac{1}{4}$ " x 3.90" Bar	$\frac{1}{4}$ " x 3.90"	106 #	—
2" x 2" x $\frac{3}{16}$ " Struct. Tube	$\frac{1}{4}$ " x 3.41"	98.5 #	7.3
2" x 2" x $\frac{1}{4}$ " Struct. Tube	$\frac{1}{4}$ " x 3.31"	100.4 #	5.4
3" x 2" x $\frac{3}{16}$ " Struct. Tube	$\frac{1}{4}$ " x 3.23"	99.3 #	6.5
3" x 2" x $\frac{1}{4}$ " Struct. Tube	$\frac{1}{4}$ " x 3.16"	103.7 #	2.4

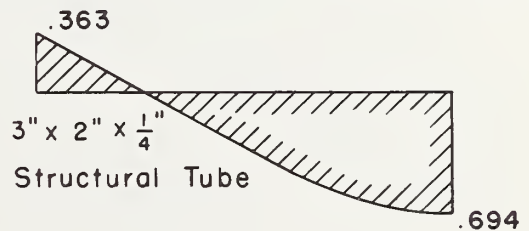
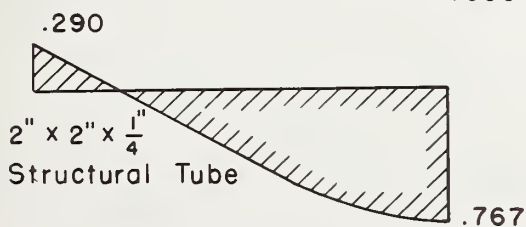
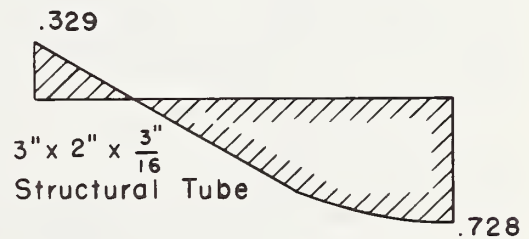
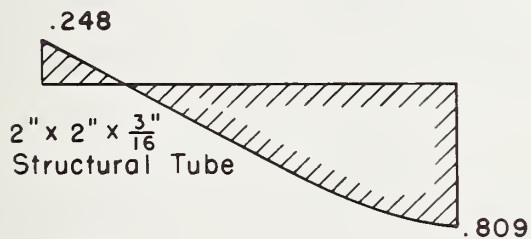
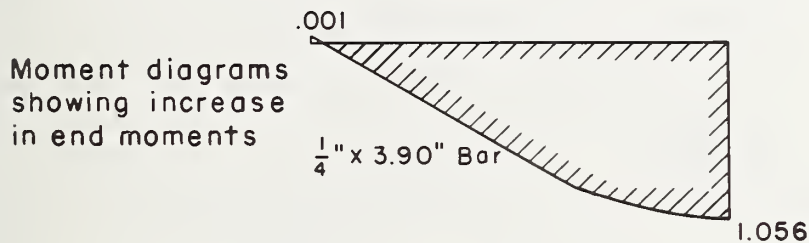


Table 2-8

RESULTS OF 2 FT BY 4 FT (0.61 M BY 1.22 M) TUBULAR GRATE ANALYSIS

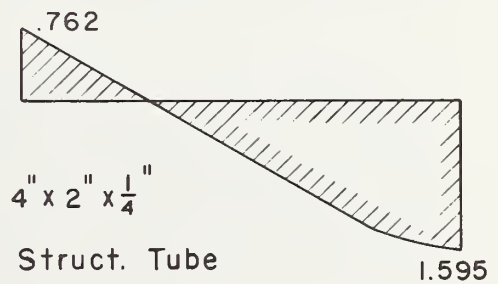
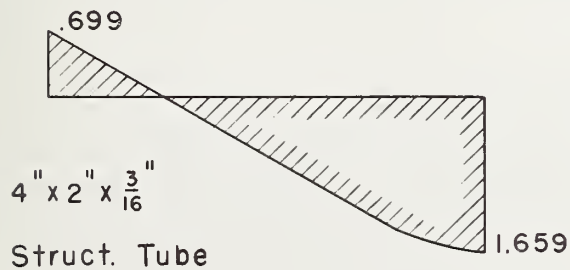
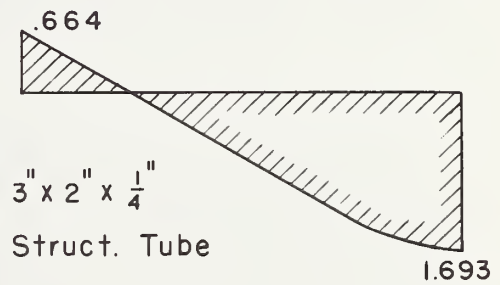
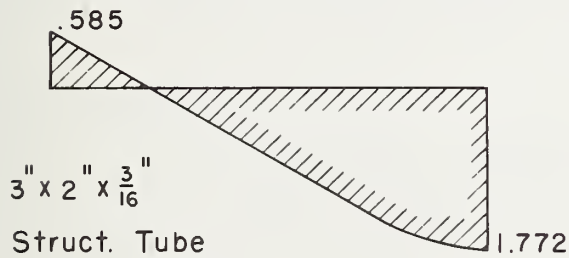
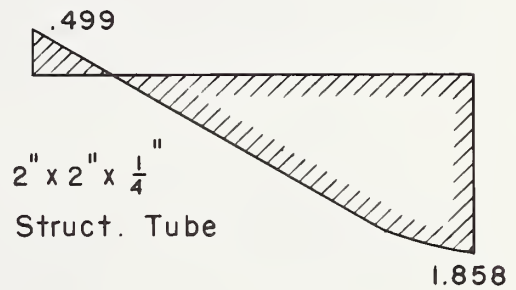
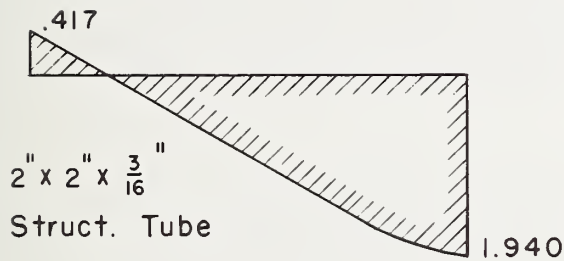
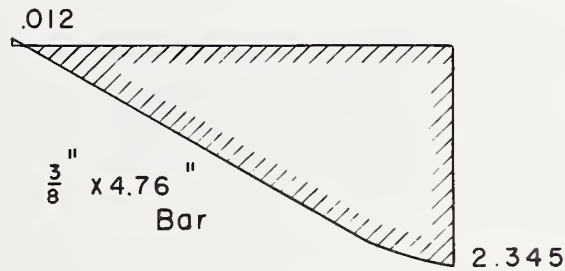
(Note: 1 in = 25.4 mm, 1 lb = 0.454 kg)

END PIECE	SIZE BEARING BAR REQUIRED	WEIGHT OF GRATE	% WEIGHT REDUCTION
$\frac{3}{8}$ " x 4.76" Bar	$\frac{3}{8}$ " x 4.76"	364.4 #	—
2" x 2" x $\frac{3}{16}$ " Struct. Tube	$\frac{3}{8}$ " x 4.31"	325.2 #	10.8
2" x 2" x $\frac{1}{4}$ " Struct. Tube	$\frac{3}{8}$ " x 4.22"	323.1 #	11.3
3" x 2" x $\frac{3}{16}$ " Struct. Tube	$\frac{3}{8}$ " x 4.12"	316.8 #	13.1
3" x 2" x $\frac{1}{4}$ " Struct. Tube	$\frac{3}{8}$ " x 4.03"	316.4 #	13.2
4" x 2" x $\frac{3}{16}$ " Struct. Tube	$\frac{3}{8}$ " x 3.99"	312.6 #	14.2
4" x 2" x $\frac{1}{4}$ " Struct. Tube	$\frac{3}{8}$ " x 3.91"	314.6 #	13.7

Table 2-8 (continued)

MOMENT DIAGRAMS

(Note: moments in kip-ft, 1 kip-ft = 1356 N/m)



CHAPTER 3

ANALYSIS OF BICYCLE AND PEDESTRIAN SAFETY

Introduction

This chapter summarizes findings from the grate safety tests conducted at the Denver Federal Center from September 29, 1975, through October 2, 1975. The purpose of the test program was to analyze grate performance in relation to bicyclist and pedestrian safety with the specific intent of input to the process of selecting grates for hydraulic testing. A grate size of 2 ft by 4 ft (0.61 m by 1.22 m) was selected for use in the bicycle safety tests. Table 3-1 presents principal features of grates evaluated in the test program. Four were fabricated steel parallel bar gates with transverse rods. Six were simulated cast grates with rectangularly spaced bars, the transverse bars being tilted at a 45° angle from vertical. The final grate was of reticuline or "honeycomb" design. The grates are shown in figure 3-1.

Test Site

Bicycle safety tests were conducted on a 22 ft (6.7 m) wide paved asphalt road with an average grade of 2 percent. The test grates were placed in a concrete vault which held the grates level (no longitudinal or cross slope) and even with the road surface. An 8 in (203 mm) high concrete curb was provided along the approach to the grate for the uphill and downhill straight runs. The curb was removed for turning tests. Figure 3-2 shows the test site set up for a straight downhill test.

Test Procedure

Male and female bicyclists, both adults and children, rode typical bicycles over a drop inlet for a total of 539 runs with 11 different test grates in place. A total of seven adults and four children served as subject riders. Table 3-2 presents physical data on test subjects. Each grate was tested on some 26 to 38 runs with cyclists traveling straight over the grate and some 12 to 27 runs with cyclists attempting to turn while on the grate. Grates were kept wet for all test runs to simulate the worst environmental conditions normally encountered by bicyclists.

Straight crossings of grates were made uphill in a speed range of 8 to 12 miles per hour (12.9 to 19.3 km/hr) and downhill in a speed range between 17 and 23 miles per hour (27.3 to 37.0 km/hr). Speed data were not recorded on the turning runs but turning approach speeds probably ranged from 5 to 12 miles per hour (8.0 to 19.3 km/hr) since bicyclists traveled uphill for these tests. A total of 174 uphill, 164 downhill, and 201 turning runs were made during the test program.

Table 3-1

PRINCIPAL GRATE DIMENSIONS

(Note: 1 in = 25.4 mm)

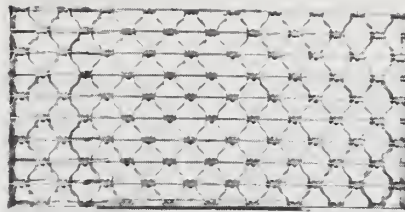
Type	Longitudinal spacing* (inches)	Longitudinal bar width (inches)	Transverse spacing** (inches)	Transverse bar width (inches)	Manufacturing process
Reticuline	2-5/8	1/4	***5	3/16	Fabricated steel
Parallel bar	1-7/8	1/4	4	3/8 rod	Fabricated steel
Parallel bar	1-7/8	1/4	6	3/8 rod	Fabricated steel
Parallel bar	1-7/8	1/4	8	3/8 rod	Fabricated steel
Parallel bar	2-3/8	1/4	4	3/8 rod	Fabricated steel
45° tilt-bar	2-1/4	1/2	3	3/4	Cast****
45° tilt-bar	2-1/4	1/2	4	3/4	Cast****
45° tilt-bar	2-1/4	1/2	6-1/4	3/4	Cast****
45° tilt-bar	3-1/4	1/2	3	3/4	Cast****
45° tilt-bar	3-1/4	1/2	4	3/4	Cast****
45° tilt-bar	3-1/4	1/2	6-1/4	3/4	Cast****

* Center to center spacing of bars parallel to direction of flow.

** Center to center spacing of bars transverse to direction of flow.

*** Center to center spacing of rivets - reticuline grate only.

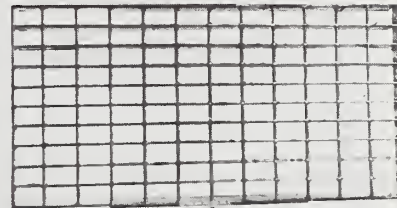
**** Grates used for the tests were made of white oak to simulate cast grates.



RETICULINE



$P=1\frac{1}{2}=4$



$P=2\frac{1}{2}=4$

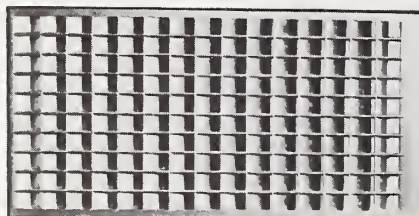


$P=1\frac{1}{2}=6$

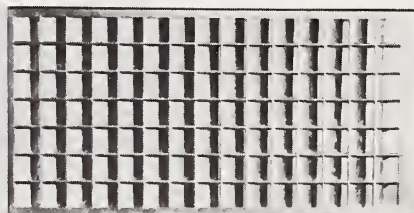


$P=1\frac{1}{2}=8$

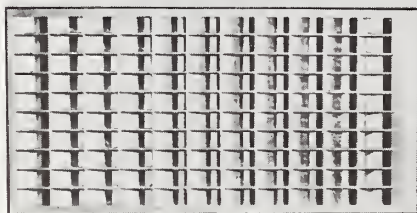
Figure 3-1. - 2 ft by 4 ft (0.61 m by 1.22 m) test grates.
Photo H-1765-345



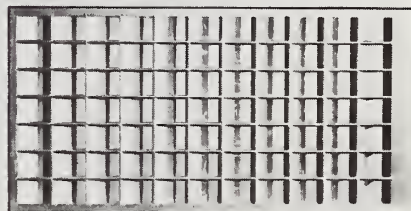
45-2 $\frac{1}{4}$ -3



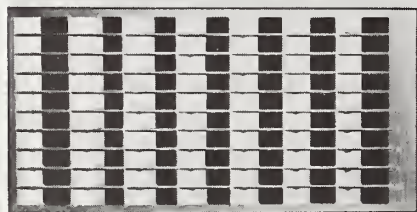
45-3 $\frac{1}{4}$ -3



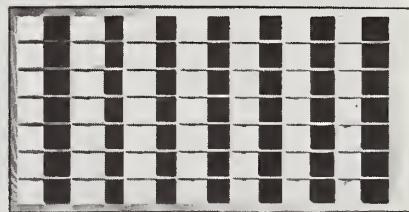
45-2 $\frac{1}{4}$ -4



45-3 $\frac{1}{4}$ -4



45-2 $\frac{1}{4}$ -6 $\frac{1}{4}$



45-3 $\frac{1}{4}$ -6 $\frac{1}{4}$

Figure 3-1. - (continued) Photo H-1765-363

BICYCLE SAFETY TEST SITE

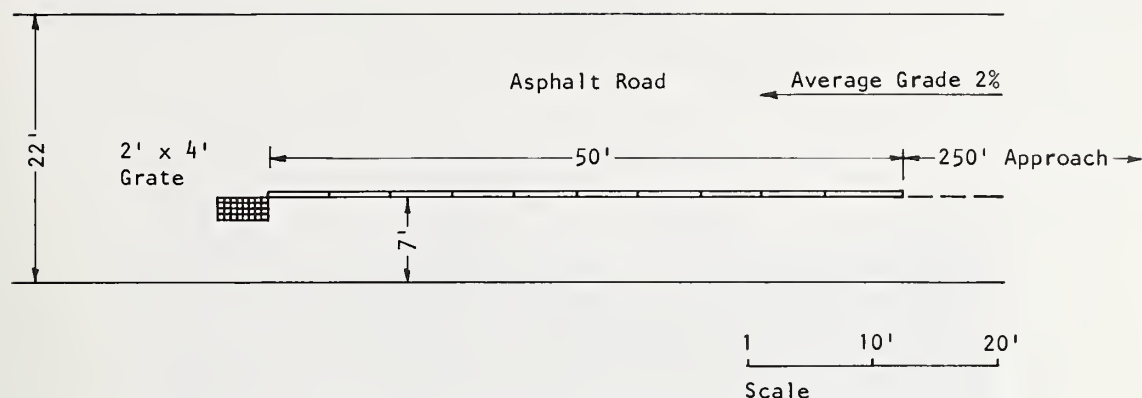


Figure 3-2. - Bicycle safety test site (Note: 1 ft = 0.305 m).

Table 3-2

TEST SUBJECTS - PHYSICAL DATA

Name	Sex	Height	Weight (lb)	Age
Dave	M	6'0"	168	33
Lynn	M	6'3"	240	35
Jane	F	5'3"	130	25
Bob	M	5'8"	175	35
Phil	M	6'0"	150	33
Pete	M	5'11"	140	22
Doug	M	6'3"	180	22
Ann	F	4'0"	50	7
Eric	M	4'6"	80	11
Doug	M	4'10"	75	9
Dave	M	5'2-1/2"	100	11

(NOTE: 1 in = 25.4 mm, 1 ft = 0.305 m, 1 lb = 0.454 Kg)

Three common types of bicycles were used in the tests, a 27 in (686 mm) 10-speed, a 26 in (660 mm) 3-speed, and a 20 in (508 mm) high-rise. Both "clincher" and "sew-up" tires were employed with the 10-speed and both "slick" and "knobby" balloon tires were employed with the high-rise. Tire widths for the various bicycles are shown in table 3-3.

Table 3-3

TIRE WIDTHS FOR TEST BICYCLES

Bicycle	Tire	Front tire width (inches)	Rear tire width (inches)
High-rise	"Knobby"	1-3/4	2-3/16
High-rise	"Slick"	1-3/4	2-3/16
3-speed		1-7/16	1-7/16
10-speed	"Clincher"	1-3/16	1-3/16
10-speed	"Sew-up"	7/8	7/8

(NOTE: 1 in = 25.4 mm)

Three types of data were collected. These included measurements by a team of observers, bicyclists' perceptions, and several types of video records. Observers attempted to note swerves to maintain control due to grate-induced disturbances, skidding on the straight runs, and skidding with and without braking on the turning runs. Observers were also prepared to note speed retardation which might result from wheels catching in the grate, but this phenomena did not occur at any time during the test program. Figure 3-3 shows the observation team during a typical downhill test.

After each straight pass over the grate, perceptions of the test riders were recorded in relation to the following characteristics:

- Comfort or bumpiness of the ride across the grate.
- Ability to recognize the grate as safe to ride across in advance of reaching it.
- Effect of the grate on steering control.
- Grate-induced skidding. Riders were never sure they had skidded and because of this uncertainty, only the skids recorded by the observers were used in the final analysis.
- Riders were questioned as to whether they felt that tire deformation when in contact with the transverse bars was so severe that the wheel rim had made contact with the grate. However, none of the riders ever had the impression of rim contact and this data item was discarded from the analysis.



Figure 3-3. - Test site and observation team. Photo H-1765-333

On the turning runs, rider perceptions were recorded on the following phenomena:

- Whether the grate affected the riders' turning control
- Whether the grate induced a skid
- Whether the rider had braked or not while executing the turn

Copies of the observers' log sheets and bicyclist perception forms are included in the Appendix to this chapter.

Video data included video tape of all runs, high-speed motion photography of selected runs, and still photography of selected runs.

Analysis of Data

Data were aggregated by grate type and test mode (straight or turning). Although straight runs were made at both high (typical downhill) and low (typical uphill) speed ranges, these were aggregated as a single test mode. This was done because the effects of high and low speeds are reflected in the other types of data recorded, particularly the control, comfort, skidding, and recognition categories. Evaluation criteria were developed on the basis of average performance for all grates in each category. In each data category, grates with above average performance received a rating of 1; grates below average received a zero. Grates exhibiting performance within ± 10 percent of the mean received a 0.5 rating. For instance, in the case of unbraked skids on turning runs, skids occurred on roughly 30 percent of that type runs on all grates taken together. Hence, if a grate experienced skids on more than 30 percent of the unbraked runs, it received a zero score for that category; if skids were experienced on less than 30 percent of the runs, it received a 1 score; and if skids comprised roughly 30 percent of the unbraked turning runs, a 0.5 score was given. Net scores were then accumulated for observer data and bicyclist data separately, and order rankings of grate performance were made on the basis of each type of data. Then a composite ranking was prepared on the basis of the separate observer and bicyclist based scores. A comprehensive listing of evaluation criteria is presented on table 3-4. Table 3-5 shows the ranking of 11 test grates on the basis of observer data. Table 3-6 shows rankings on the basis of rider perceptions. Table 3-7 presents a final ordering of the grates based upon the observer and rider scores. A summary of test data is appended.

Pedestrian Safety

Evaluation of grates in relation to pedestrian safety was based upon inspection of grates in relation to foot sizes and shoe types. Hence,

Table 3-4

EVALUATION CRITERIA

Characteristic	Criteria
<u>Observer Data</u>	
Swerve	Grate fails criteria if induced swerves exceed 2 percent of all rides.
Skid without brake:	
• Straight runs	Grate fails criteria if skids occur on more than 3 percent of all runs.
• Turning runs	Grate fails criteria if skids occur on more than 30 percent of all runs.
Skid with braking:	
• Turning runs	Grate fails criteria if skids occur on more than 46 percent of all runs.
<u>Bicyclist Perceptions</u>	
Steering control:	
• Straight runs	Grate fails criteria if moderate effect percentage exceeds 14 percent of all runs or significant incidence of strong effect perceived.
• Turning without braking	Grate fails criteria if control affected on more than 34 percent of all runs.
• Turning with braking	Grate fails criteria if control affected on 47 percent of all runs.
Comfort	Grate fails criteria if rated moderately rough or worse on more than 23 percent of all rides.
Grate recognition	Grate fails criteria if percent of times recognized too late to evade exceeds 8 percent or recognized in time to be evaded only by panic maneuver exceeds 21 percent.
Skid:	
• On turn with braking	Grate fails criteria if skids occur on more than 67 percent of all runs.
• On turn without braking	Grate fails if skids occur on more than 30 percent of all runs.

Table 3-5

OBSERVER EVALUATION

Grate type	Control (swerve)	Skids (straight runs)	Turning skids (unbraked)	Turning skids (braked)	Net score	Rank
45 - 2-1/4 - 4	1	1	1	1	4	1-2 tie
45 - 3-1/4 - 3	1	1	1	1	4	1-2 tie
45 - 3-1/4 - 4	0	1	1	1	3	3-5 tie
Reticuline	1	1	1	0	3	3-5 tie
P - 2-3/8 - 4	1	1	1	0	3	3-5 tie
P - 1-7/8 - 4	1	0	1	0.5	2.5	6
45 - 2-1/4 - 3	1	1	0	0	2	7
P - 1-7/8 - 6	0	1	0	0	1	8-10 tie
45 - 2-1/4 - 6-1/4	1	0	0	0	1	8-10 tie
45 - 3-1/4 - 6-1/4	1	0	0	0	1	8-10 tie
P - 1-7/8 - 8	0	0	0	0	0	11

A score of 0 indicates below average performance.

A score of 0.5 indicates average performance.

A score of 1 indicates above average performance.

Table 3-6

BICYCLIST EVALUATION

Grate type	Control (straight runs)	Com- fort	Recog- nition	Turning control (braked)	Turning control (unbraked)	Turning skids (braked)	Turning skids (unbraked)	Net score	Rank
P - 1-7/8 - 4	1	1	1	1	1	1	1	7	1
Reticuline	1	1	1	1	1	0.5	0.5	6	2-3 tie
45 - 3-1/4 - 3	1	1	0	1	1	1	1	6	2-3 tie
45 - 3-1/4 - 4	1	1	1	1	1	0	0.5	5.5	4
45 - 2-1/4 - 3	1	1	0	0.5	1	0.5	1	5	5
45 - 2-1/4 - 4	1	1	0.5	1	0	1	0	4.5	6-7 tie
P - 2-3/8 - 4	1	0.5	1	0	1	0	1	4.5	6-7 tie
P - 1-7/8 - 6	1	1	0.5	0	0	0	0	2.5	8
45 - 2-1/4 - 6-1/4	0	0	0	0.5	0.5	0.5	0.5	2	9
P - 1-7/8 - 8	0	0	0	0	0	0	0.5	0.5	10
45 - 3-1/4 - 6-1/4	0	0	0	0	0	0	0	0	11

A score of 0 indicates below average performance.

A score of 0.5 indicates average performance.

A score of 1 indicates above average performance.

Table 3-7

COMPOSITE EVALUATION

Grate type	Observer score	Bicyclist score	Final score	Final rank
45 - 3-1/4 - 3	4	6	10	1
P - 1-7/8 - 4	2.5	7	9.5	2
Reticuline	3	6	9	3
45 - 3-1/4 - 4	3	5.5	8.5	4-5 tie
45 - 2-1/4 - 4	4	4.5	8.5	4-5 tie
P - 2-3/8 - 4	3	4.5	7.5	6
45 - 2-1/4 - 3	2	5	7	7
P - 1-7/8 - 6	1	2.5	3.5	8
45 - 2-1/4 - 6-1/4	1	2	3	9
45 - 3-1/4 - 6-1/4	1	0	1	10
P - 1-7/8 - 8	0	0.5	0.5	11

it is judgmental in nature rather than based upon an ordered experimentation protocol as was the bicycle testing. With respect to pedestrian safety these observations can be made:

- The openings on the 45 - 3-1/4 - 6-1/4 and the 45 - 2-1/4 - 6-1/4 grates can easily admit a small child's foot, virtually any type of high-level heel, or the toe of a shoe and appear to be most hazardous among the 11 grates tested.
- Other grates with nearly square openings, the P - 2-3/8 - 4, the 45 - 3-1/4 - 3 and the 45 - 3-1/4 - 4 appear capable of admitting some of the thicker high-heeled shoes which would not be admitted through grates with closer parallel bar spacing and also appear more likely to induce ankle twisting than other types. In general, grates with long, narrow openings appear safer than ones with somewhat wider and shorter openings. This is irrespective of direction of pedestrian travel across the grate.
- The tilt-bar feature may be more likely to induce ankle twisting when high heels penetrate the openings than on grates without the tilt-bar feature.
- Virtually any grate will pose a hazard to persons wearing high-heeled shoes with narrow heel base.
- It must be reemphasized that these findings are judgmental in nature and not based on any analysis of accident records or rigorous test programs.

Summary of Results

Following are key findings of the safety tests and evaluation:

- All of the grates tested are markedly safer than many of the parallel bar grates in common use today. There were clear safety performance differences among the grates tested. But it must be emphasized that the ratings of safety contained herein are relative only to the grates tested and even those which are rated lowest in performance are judged to be significantly superior to many grates now in use on streets and highways.
- Of the 11 grates tested, 7 showed markedly superior performance over the remaining 4. Of the 7 in the high performance group, 4 were of the 45° tilt-bar type with transverse bar spacings at, or less than, 4 in (102 mm). Two were of the parallel bar with transverse rods type with transverse spacings of 4 in (102 mm). The reticuline grate type completed the high performance group.
- The lower performance group was comprised of four grates with transverse bar spacings at, or greater than, 6 in (152 mm). Two

were of the parallel bar with transverse rods type and two were of the 45° tilt-bar type.

- The inference of the immediately preceding two points is that transverse spacing is a critical factor in the bicycle safety performance of the grate - a more critical factor than whether the grate is of the reticuline, 45° tilt-bar, or parallel bar with transverse rods type. The analysis also suggests that deterioration in bicycle safety performance begins as transverse spacings are increased somewhat above 4 in (102 mm).
- A comparison of tables 3-1 and 3-3 shows that some of the tire widths are fairly close to the longitudinal bar spacings of several grates. However, no "pinching" of the bicycle tires was ever encountered. Bars spaced at or slightly less than the normal range of bicycle tire widths could possibly "pinch" a bicycle tire and pose a safety hazard. Bars spaced sufficiently close so as to be closer than the narrowest bicycle tire would be considered bicycle safe.
- No direct evidence of tire or rim damage attributable to a specific grate was evidenced. Although several flat tires were incurred during the test program, these were attributable to thistle punctures. Photographic evidence does show significant tire deformation (figure 3-4 illustrates a case of severe tire deformation) on grates with the larger transverse spacings.



Figure 3-4. - Severe tire deformation on a grate with 8 in (203 mm) transverse bar spacing. Photo H-1765-59

- Skidding was as prevalent a problem on the fabricated metal grates as on the wooden fabricated grates used to simulate cast metal gratings. This disproves the field supposition that the painted wooden grates were more slippery than the metal ones. If the wood grates were indeed more slippery than the metal grates, the high performance of the three 45° tilt-bar grates constructed of wood is all the more impressive.
- Significant skidding occurred on virtually all grates as a result of turning runs as illustrated on figure 3-5. The fact that the grates were kept wet during the tests increased the chances for skidding. The number of skids observed suggest that grates will remain a hazard to cyclists traversing them while turning a corner.



Figure 3-5. - Severe skidding in turn. Photo H-1765-255

- The fact that skidding while turning on the grates will remain a problem also emphasizes the importance of recognizability of

safe grates. The value of safe grates may be negated if bicyclists are injured in skidding falls due to bicyclists' panic maneuvers avoiding "safe" grates which did not appear safe on approach. Some form of distinctive marking to identify "safe" grates, if uniformly used by all jurisdictions, would help alleviate this problem. Use of paint treatments, signs, or other markings for this purpose should be studied.

- The grates which proved least satisfactory on bicycle safety testing were also those which appeared least satisfactory from a pedestrian standpoint. In addition, of the grates which performed well in the bicycle safety testing, those with the wider parallel bar spacings - those with more nearly square openings - appeared capable of catching some of the raised-heel shoe types. Also, the 45° tilt-bar feature appears to have some potential for inducing twisted ankles when heels do penetrate the openings.

In summary, clear performance differences in terms of bicycle safety are noted between grates having transverse bar spacings over 4 in (102 mm) (poor performance) and those having less spacing (better performance). Similar differences are presumed relative to pedestrian safety. In addition, grates having large, nearly square openings (i.e., 3-1/4 by 4) are also judged to pose some potential for pedestrian mishap.

Recommendations

Based upon these findings, the following recommendations were made for selection of grates for hydraulic testing:

- One parallel bar-transverse rod grate from the high-performance group (P - 1-7/8 - 4).
- Two 45° tilt-bar grates from the high-performance group (45 - 2-1/4 - 4 and 45 - 3-1/4 - 4).
- The reticuline grate.
- A grate selected from the low safety performance group. The grate from the low-performance group would be tested to obtain a measure of the increase in hydraulic efficiency which can be gained for some trade-off in safety.

APPENDIX

COMPOSITE DATA SUMMARY

Grate type	Number of tests		Observer data												Bicyclist perceptions																							
	Straight Turning		Swerve (S)						Skid (BT)						Control						Skid						Comfort (S)						Recognition (S)					
	N	Min	Maj	N	Min	Maj	(S)	N	Min	Maj	(BT)	N	Min	Maj	(UT)	Maj	N	Min	Maj	(S)	4	Y	N	Y	N	(UT)	Y	N	Y	N	(S)	1	2	3	4	1	2	3
Reticuline	32	12	32	0	0	32	0	0	2	3	0	6	1	0	0	0	1	31	2	3	2	5	3	2	2	5	0	1	13	18	25	5	2	0				
P - 1-7/8 - 4	28	12	28	0	0	27	1	0	4	1	1	4	2	0	0	0	2	26	2	5	1	4	3	4	1	4	0	2	13	13	22	5	1	0				
P - 1-7/8 - 6	35	12	34	1	0	35	0	0	2	3	0	4	3	0	0	0	3	32	3	-2	4	3	4	1	4	3	0	7	12	16	27	7	1	0				
P - 1-7/8 - 8	38	17	32	6	0	35	3	0	3	3	1	2	8	0	0	3	11	24	6	1	6	4	6	1	3	7	1	20	6	11	25	8	5	0				
P - 2-3/8 - 4	28	16	28	0	0	28	0	0	2	3	1	9	1	0	0	0	2	26	4	2	2	8	5	1	1	9	0	7	5	16	21	5	2	0				
45 - 2-1/4 - 3	28	24	28	0	0	28	0	0	6	2	3	10	3	0	0	0	0	28	5	6	1	12	7	4	2	11	0	5	12	11	20	7	1	0				
45 - 2-1/4 - 4	26	24	26	0	0	26	0	0	9	1	2	10	2	0	0	0	2	24	3	9	5	7	6	6	6	6	0	2	7	17	19	6	1	0				
45 - 2-1/4 - 6-1/4	31	15	31	0	0	27	4	0	4	5	0	2	4	0	0	2	8	21	4	5	2	4	6	3	2	4	1	8	15	7	17	11	3	0				
45 - 3-1/4 - 3	30	18	30	0	0	30	0	0	6	2	1	8	1	0	0	0	0	30	3	6	1	8	5	4	1	8	0	6	12	12	19	7	4	0				
45 - 3-1/4 - 4	28	24	27	1	0	28	0	0	8	1	1	12	2	0	0	0	2	26	3	7	3	11	8	2	4	10	0	5	12	11	22	4	2	0				
45 - 3-1/4 - 6-1/4	34	27	34	0	0	32	2	0	4	4	5	8	5	1	0	0	15	19	9	4	2	5	10	3	6	8	1	13	13	7	24	6	4	0				
Totals	338	201	330	8	0	328	10	0	50	28	15	75	32	1	0	5	46	287	44	50	36	71	63	31	32	75	3	76	120	139	241	71	26	0				

Legend:

(S) = Straight runs
 (BT) = Braked turning runs
 (UT) = Unbraked turning runs
 N = No incident observed
 Min = Minor incident observed
 Maj = Major incident observed
 Y = Adverse effect perceived
 Control 1 = Extreme effect
 2 = Strong effect
 3 = Moderate effect
 4 = No effect
 Comfort 1 = Very rough
 2 = Moderately rough
 3 = Somewhat rough
 4 = Smooth
 Recognition 1 = Comfortable distance
 2 = Panic maneuver range
 3 = After committed
 4 = Did not appear safe at all

[illegible]

Observer's Log

OBSERVER _____ DATE: _____

Test No.	Abort Fall	Swerve			Skid			Speed retarded		Damage (specify) or comment
		None	Minor	Major	None	Minor	Major	Yes	No	

Observer Instructions

For each run, note any significant effects of grate on rider performance:

- Abort - rider forced to stop to avoid spill or stopped or avoided grate because of panic.
- Fall - rider fell due to grate-induced loss of balance.
- Swerve - rider significantly deviated from course to maintain balance (note none, minor, major). On turning runs, note inability to complete turn.
- Skid - lateral slippage of tire on grate or pavement surface (note none, minor, major).
- Speed retardation - note any apparent speed retardation due to tire being "pinched" in grate.
- Damage - identify any equipment damage apparently resultant from traversing grates - tire deflation, broken spokes, rim damage, etc.
- Comment - note any significant features of ride which merit recording.

BICYCLIST OBSERVATION LOG
(straight runs)

Test No.	Control	Comfort	Recognition	Rim contact	Comment

Rider subjective evaluation information was filled out by each rider immediately after each pass over a grate. Following are response categories.

Control

- Did this grate seem to affect your control (ability to steer as desired and maintain balance and speed) of the bicycle?
 1. Extreme effect
 2. Strong effect
 3. Moderate effect
 4. No effect

In instructing the test subjects with regard to response to the above questions, they were told to interpret extreme effect as being an effect on the order of causing the rider to fall or to feel near to fall or causing them to travel off course in a radical maneuver to retain balance or causing them to feel unable to execute the test turn maneuver or to feel that their speed was sharply checked due to properties of the grate. A strong effect was interpreted as an incident in which significant corrective effort was required to maintain balance and directional control or speed was measurably retarded due to properties of the grate. This type of effect was distinguished from an extreme effect in that the bicyclist was not forced to come to a halt or to swerve out of what would be a normal 4 ft (1.22 m) wide bike lane. A moderate effect was interpreted as an incident in which minor corrective action was required to maintain course and balance or slight speed retardation was noticed. While these types of effects

Comfort

- ### Rim Contact

- ## Recognition

- 3-22

Comment

- Rider comment on any outstanding feature of the run

BICYCLIST OBSERVATION LOG
(turning runs)

Test No.	Turning control	Skidding	Brake applied?	Comment
----------	-----------------	----------	----------------	---------

Turning control: Did grate affect ability to turn? (yes, no).

Skidding: Did grate cause skid? (yes, no).

Brake applied?: Was brake applied in turn? (yes, no).

Comment: As before.

CHAPTER 4

HYDRAULIC CONSIDERATIONS

Figure 4-1a shows the full-scale laboratory gutter section used during the test program. The section width was selected based on the use of a 2 ft (0.61 m) wide gutter section and a 6 ft (1.83 m) wide traffic lane. Since the depth and/or width of the gutter flow are often limiting criteria in the hydraulic design for grate inlets, it is necessary to define the relationship between these variables and the gutter flow, Q_T . This relationship is commonly expressed in terms of the Manning equation,

$$Q_T = \frac{1.486}{n} A R^{2/3} S_0^{1/2}$$

where: Q_T = gutter flow

n = coefficient of roughness

A = cross sectional flow area

R = hydraulic radius

S_0 = slope of energy line

The Manning formula is the most widely used equation for uniform open channel flow. This formula, which deals with an average discharge and velocity, can be used incorrectly if not properly understood. The triangular gutter section is a case-in-point. The average velocity for the gutter section shown in figure 4-1b is:

$$V = \frac{1.486}{n} R^{2/3} S_0^{1/2}$$

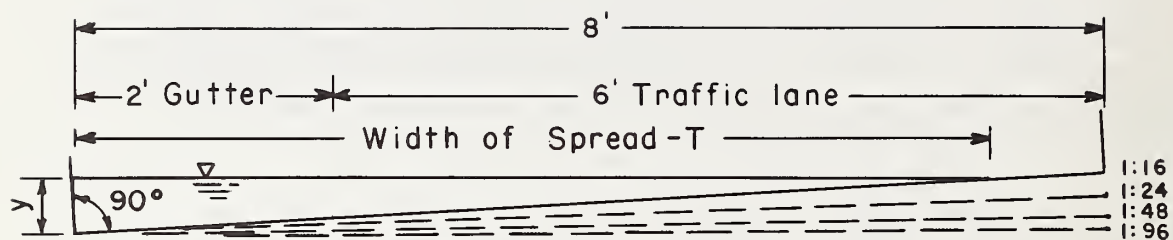
where: $R = A/P$

P = wetted perimeter

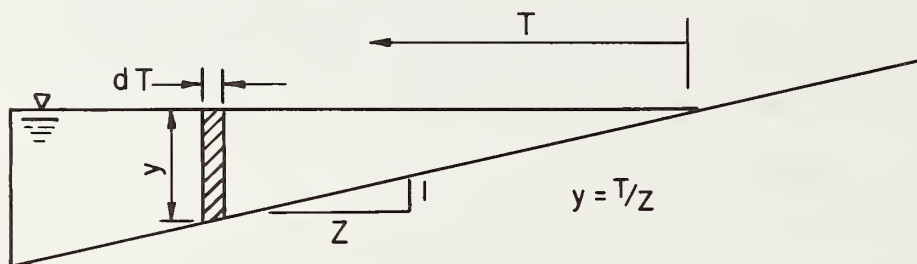
Neglecting the small triangular area near the curb,

$$A = y/2 (yz) = (y/2) T$$

$$P = y + yz \left(\frac{\sqrt{z^2 + 1}}{z} \right) = y (1 + \sqrt{z^2 + 1})$$



a. Laboratory gutter section.



b. Theoretical gutter section.

Figure 4-1. - Triangular gutter sections.

therefore,

$$V = \frac{1.486}{n} \left(\frac{(y/2)(yz)}{y(1+\sqrt{z^2+1})} \right)^{2/3} S_0^{1/2}$$

$$\text{or} \quad V = \frac{1.486}{n} \left(\frac{z}{1+\sqrt{z^2+1}} \right)^{2/3} (S_0)^{1/2} (y/2)^{2/3} \quad (4-1)$$

since $A = (y/2) T$

$$Q_T = \frac{1.486}{n} \left(\frac{z}{1+\sqrt{z^2+1}} \right)^{2/3} (S_0)^{1/2} (y/2)^{5/3} T \quad (4-2)$$

For a given longitudinal slope, S_0 , and cross slope, $1/Z$, the velocity and discharge are functions of $(y)^{2/3}$ and $(y)^{5/3}$, respectively. These functions are plotted in figure 4-2 for $n = 0.016$, $S_0 = 4$ percent, $Z = 16$, and $T = 5$ ft (1.52 m).

Therefore,

$$V = 17.82 (y/2)^{2/3} \quad (4-3)$$

$$Q = 89.08 (y/2)^{5/3} \quad (4-4)$$

Equations 4-3 and 4-4 give the average velocity and discharge for the gutter section based on the standard Manning equation.

The area in the rectangular block of figure 4-2 represents the average discharge based on the average depth, $y/2$ (equation 4-4). If instead of using the average depth, $y/2$, in equation 4-4, the depth, y , is summed using incremental widths of the section shown in figure 4-1, the crosshatched area in figure 4-2 will represent the actual discharge. The area under the $(y)^{5/3}$ curve which represents the actual discharge is 19 percent greater than the area enclosed in the rectangle representing the calculated discharge based on the average depth as calculated in equation 4-4.

Larson and Straub (1)* found that their laboratory results yielded gutter flow measurements up to 15 percent greater than the calculated values using the Manning equation. Izzard (2) in a discussion of his paper, "Hydraulics of Runoff from Developed Surfaces," notes a study conducted by the Bureau of Standards where an incremental width of a triangular section was integrated across the width of flow resulting in a flow discharge 19 percent greater than the discharge computed by

* Number in parenthesis indicates reference at the end of the chapter.

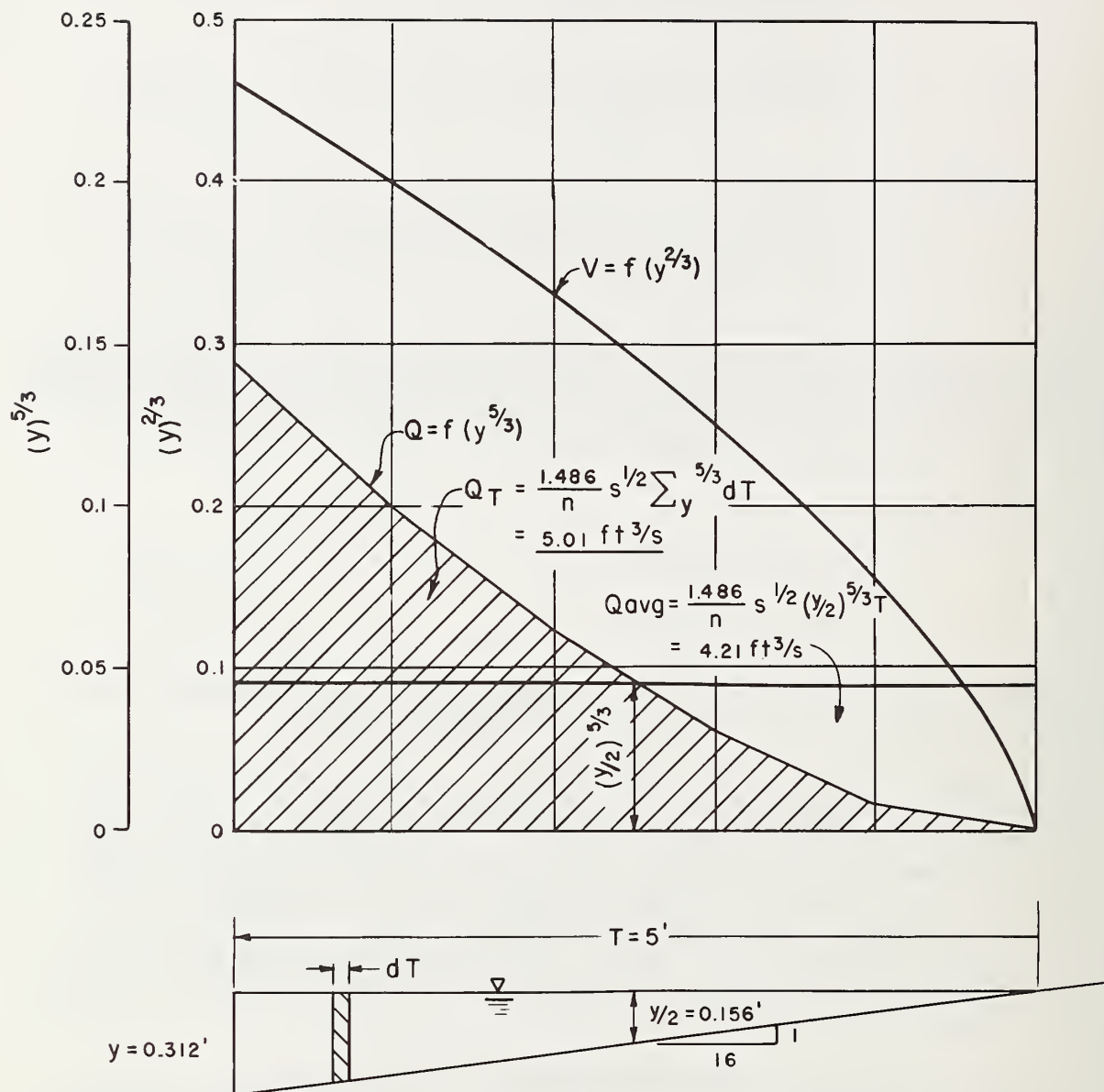


Figure 4-2. - Depth-discharge relationships for a gutter section, $T = 5 \text{ ft}$ (Note: $1 \text{ ft} = 0.305 \text{ m}$).

the Manning equation. The integration results in the following equation for a triangular section:

$$Q_T = \frac{0.557}{n} Z S_0^{1/2} y^{8/3} \quad (4-5)$$

adopted by the Federal Highway Administration.

For the same longitudinal slope, $S_0 = 4$ percent, and width of spread, $T = 5$ ft (1.52 m), the $(y)^{5/3}$ curve is plotted in figure 4-3 for cross slopes of $Z = 16, 24$, and 48 . For $Z = 16$, several curves of $(y)^{5/3}(S_0)^{1/2}$ for various longitudinal slopes, S_0 , are also plotted. Although the total gutter flow represented by the area under the curves changes with respect to S_0 and Z , the percent of gutter flow in the 2 ft (0.61 m) grate width, approximately 74 percent for $T = 5$ ft (1.52 m), does not vary with S_0 and Z for a constant width of spread, T . Therefore, the percent of gutter flow in the 2 ft (0.61 m) grate width is a function of the width of spread, T , and does not vary with longitudinal slope, S_0 or cross slope, $1/Z$.

The frontal flow, Q_F , (figure 4-4) can be approximated by calculating the roadway flow outside the gutter using the depth, y' , at the outer edge of the gutter and subtracting it from the total gutter flow, Q_T . For a gutter width of 2 ft (0.61 m),

$$Q_F = \frac{0.557}{n} Z S_0^{1/2} \left[y^{8/3} - y'^{8/3} \right] \quad (4-6)$$

$$\text{where, } y' = \left(y - \frac{2}{Z} \right)$$

$$\text{and } y = T/Z$$

The hydraulic efficiency can be calculated by dividing equation 4-6 by equation 4-5:

$$E = \frac{Q_F}{Q_T} = 1 - \left(1 - \frac{2}{T} \right)^{8/3} \quad (4-7)$$

If the intercepted gutter flow, Q_I , consisted only of frontal flow, Q_F , across the 2 ft (0.61 m) width of the grate, we could represent the hydraulic efficiency $E = Q_F/Q_T$ as a function of width of spread, T , with one curve as illustrated in figure 4-5. Using equations 4-5 and 4-6, the efficiency, E , would be the ratio of the quantity $(y)^{8/3}$ at the curb minus $(y')^{8/3}$ 2 ft (0.61 m) from the curb to the value of $(y)^{8/3}$ at the curb or $E = 1 - (1 - (2/T))^{8/3}$ for a 2 ft (0.61 m) gutter width. Since there will be flow entering along the length of the grate, it is obvious that this curve yields lower efficiencies than what can be expected with 2 ft (0.61 m) and 4 ft (1.22 m) grate lengths.

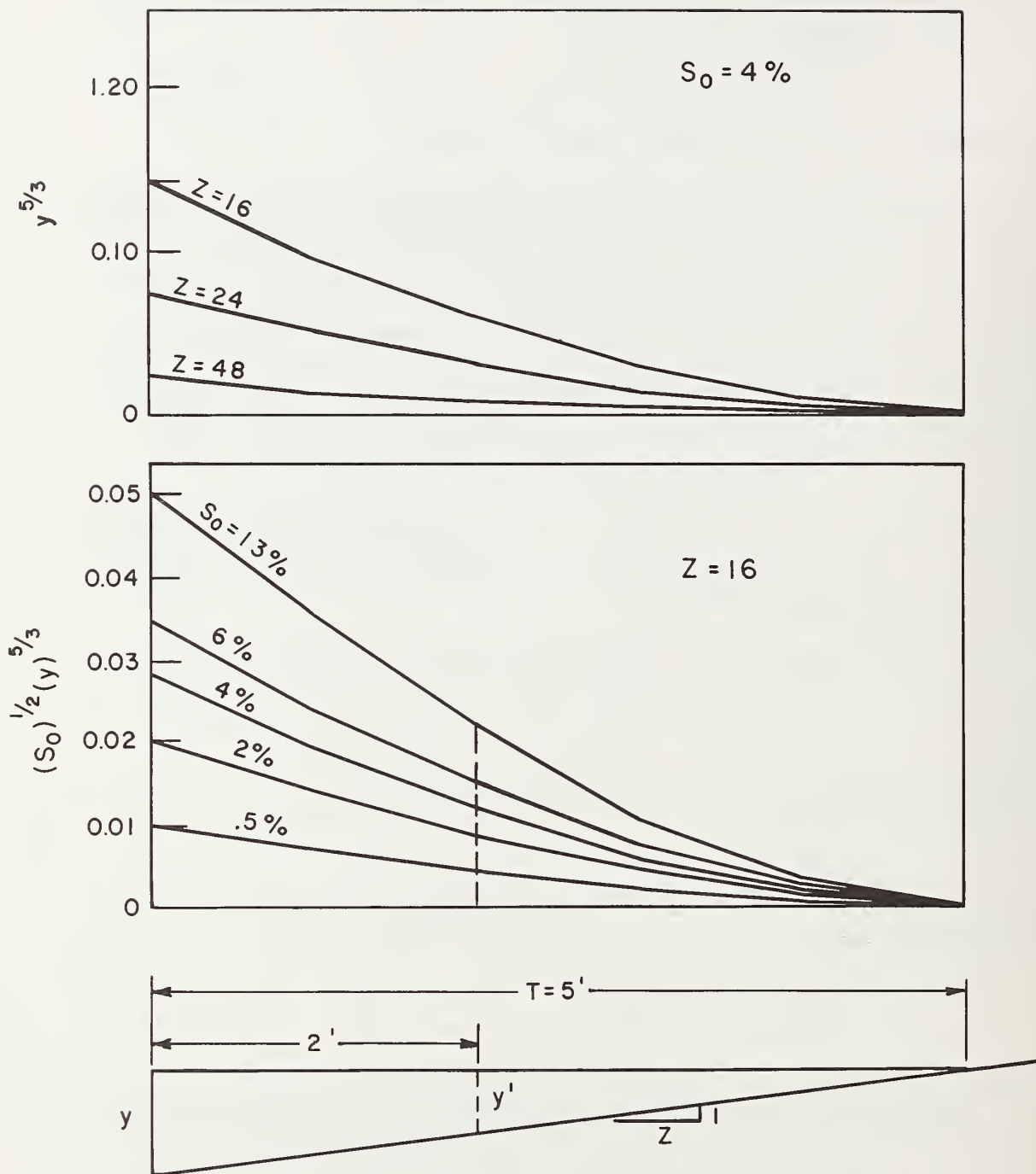


Figure 4-3. - Effect of longitudinal and cross slope on gutter flow with constant $T = 5$ ft (Note: 1 ft = 0.305 m).

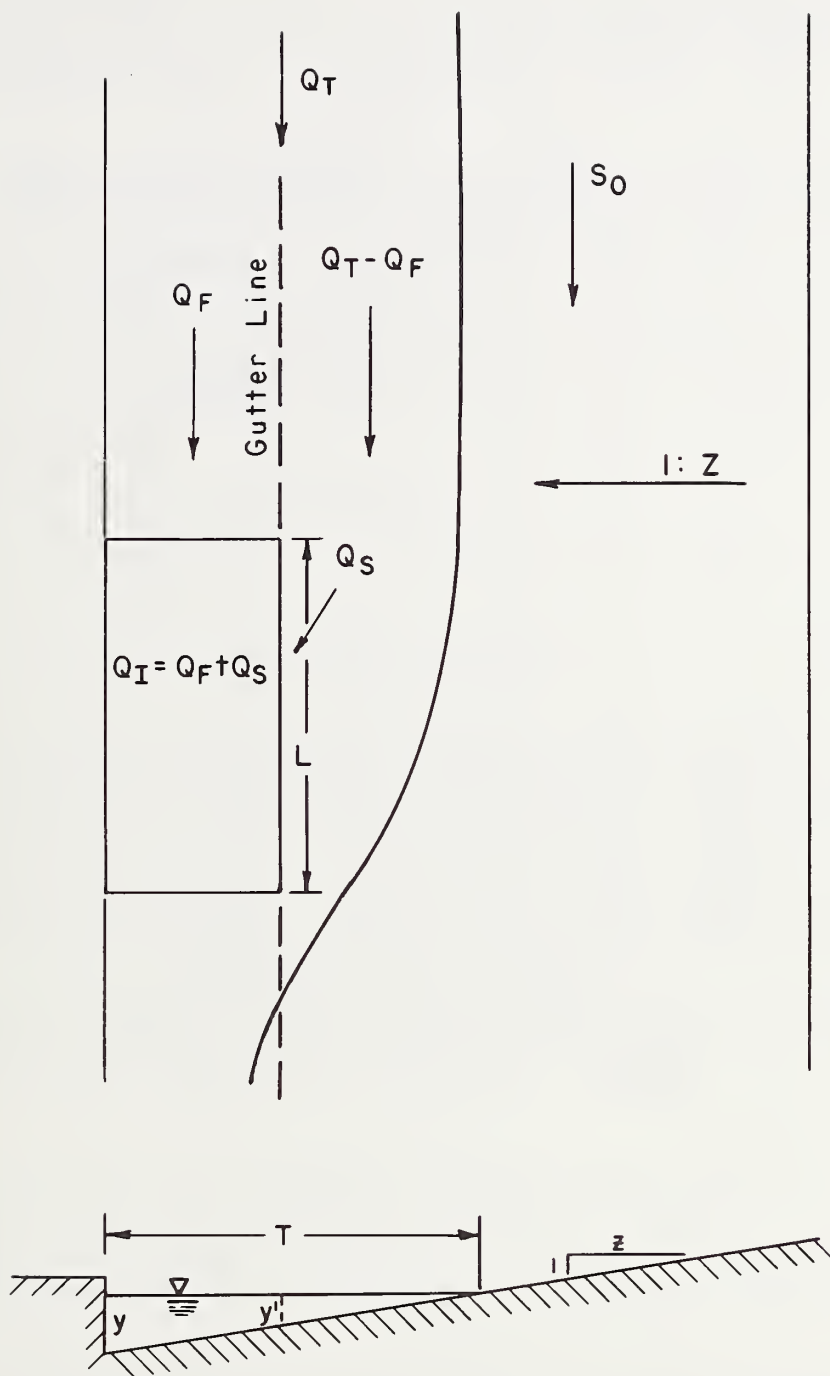


Figure 4-4. - Definition sketch of gutter flow near an open hole.

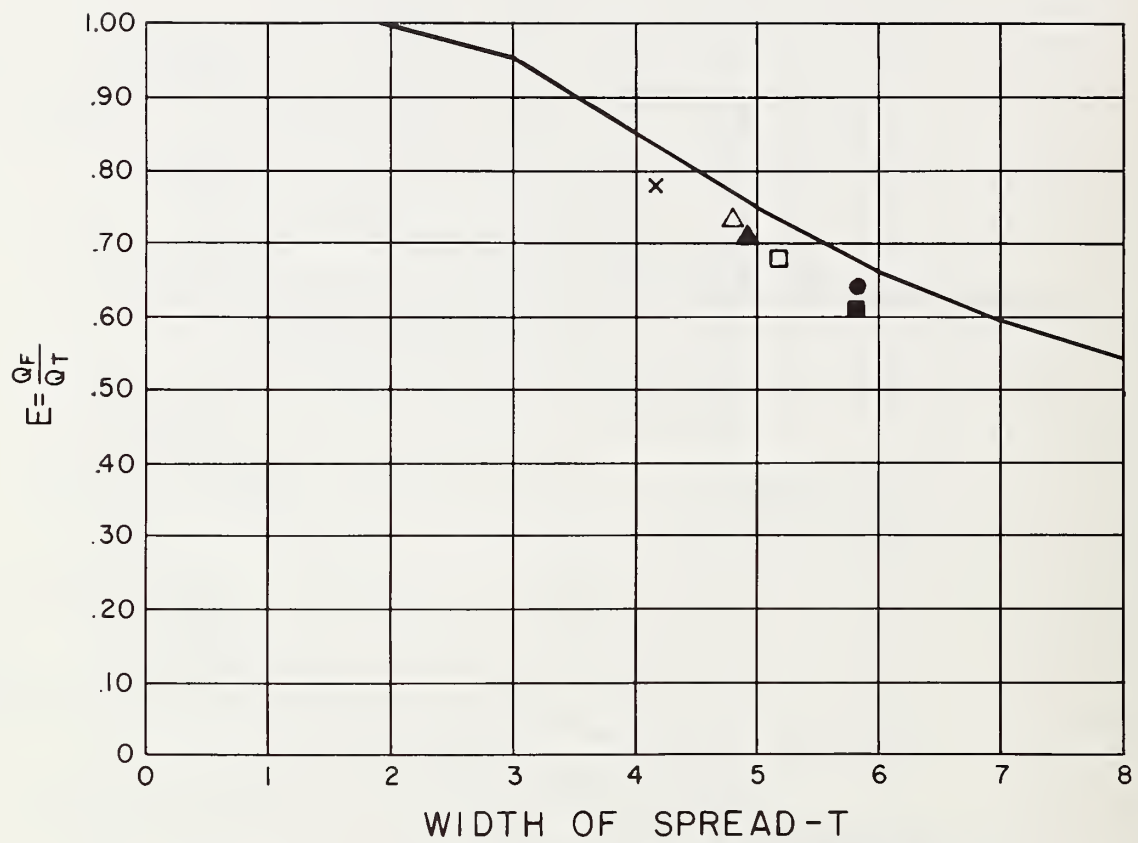


Figure 4-5. - Hydraulic efficiency of frontal flow vs. width of spread.

From figure 4-4, it is evident that the side flow, Q_S , can be analyzed assuming a curb inlet condition 2 ft (0.61 m) from the curb along the gutter line section. Li (3), at John Hopkins University, studied the curb inlet hydraulic capacity and developed the following equation for a curb inlet of length, L , less than the length, L_0 , needed to capture the total gutter flow, in this case, $Q_T - Q_F$:

$$\frac{Q_S}{Q_T - Q_F} = 2 \left(\frac{L}{L_0} \right)^2 - \left(\frac{L}{L_0} \right) \quad (4-8)$$

where: $L_0 = v_0 \sqrt{\frac{2(y')Z}{g}} \sqrt{1+Z^2}$

and $v_0 = \frac{1.486}{n} S_0^{1/2} (y')^{2/3}$

for $Z > 8$

$$L_0 = 23.15 S_0^{1/2} (y')^{7/6} Z$$

$$y' = \frac{T-2}{Z}$$

or $L_0 = 23.15 (T-2)^{7/6} S_0^{1/2} (1/Z)^{1/6} \quad (4-9)$

Therefore, for a constant width of spread, T , L_0 is directly proportional to $(S_0)^{1/2}$ and $(1/Z)^{1/6}$. This indicates that as the longitudinal slope, S_0 , or cross slope, $1/Z$, increases (becomes steeper), the optimum grate length L_0 , needed to capture all the gutter flow outside of the 2 ft (0.61 m) grate width Q_S also increases. Therefore the overall hydraulic efficiency, E , of the grate inlet will decrease with an increase in either longitudinal slope, S_0 , or cross slope, $1/Z$ until the line in figure 4-4 is reached indicating no side flow, Q_S . Actual grate inlet hydraulic efficiencies will remain above the curve in figure 4-5 until splash and spray caused by transverse bar members more than offset the side flow, Q_S , resulting in values below the curve represented in figure 4-5.

Hydraulic efficiencies of grate inlets can best be compared by plotting efficiency, E , as a function of total gutter flow, Q_T . Since $E = (Q_S + Q_F)/Q_T$, one can solve equations 4-5, 4-6, and 4-7 and plot the results as shown in figure 4-6 for a 2 ft (0.61 m) wide 4 ft (1.22 m) long open hole. Figure 4-6 represents the theoretical maximum efficiency for any 2 ft (0.61 m) by 4 ft (1.22 m) grate inlet.

Velocity profiles and flow measurements immediately upstream of the 2 ft by 4 ft (0.61 m by 1.22 m) opening were conducted to verify equations 4-5, 4-6, and 4-7. A 1/8 in (3 mm) pitot tube and differential pressure cell were used to measure velocities and develop the velocity profiles for $Z = 24$ presented in figure 4-7.

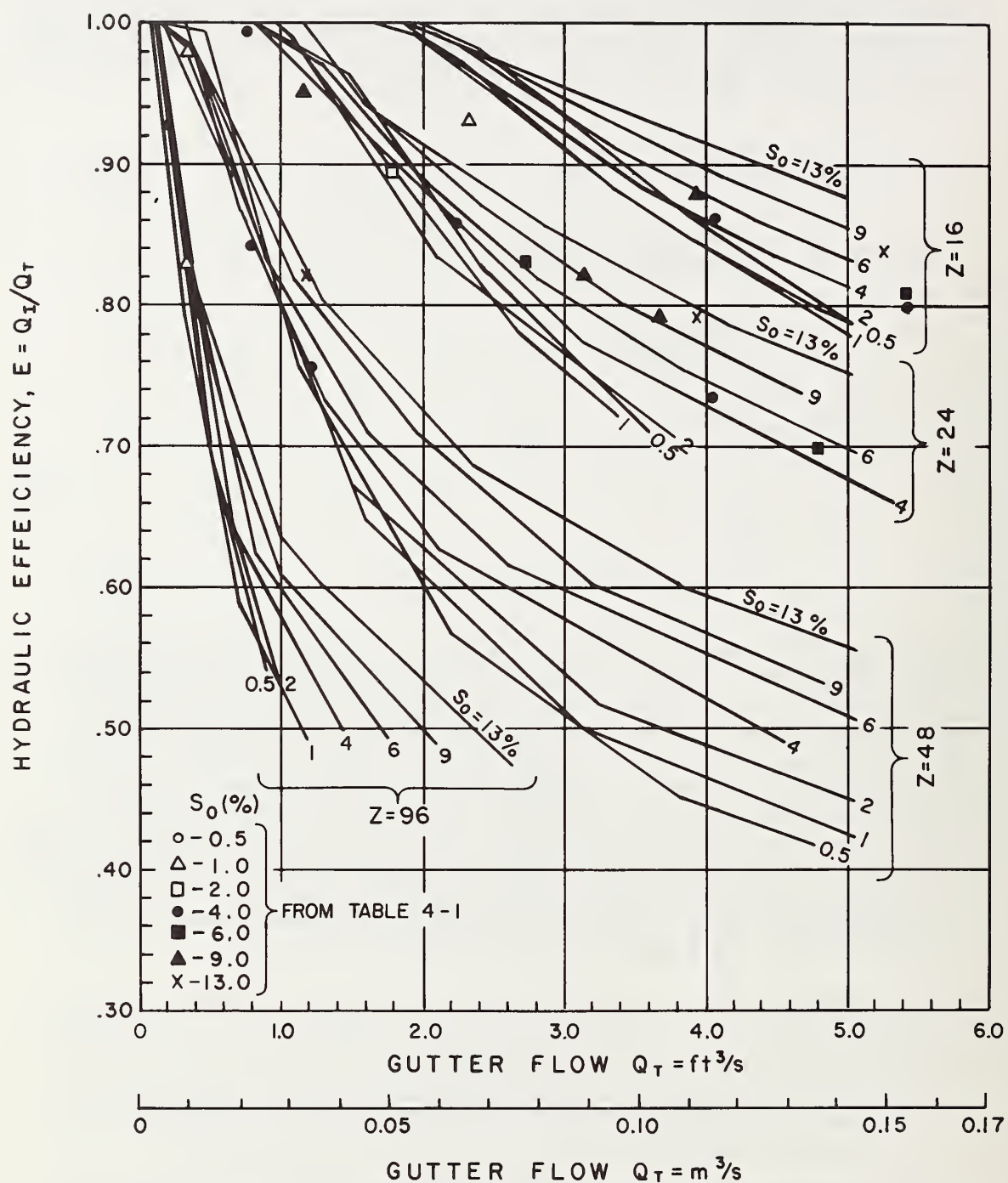
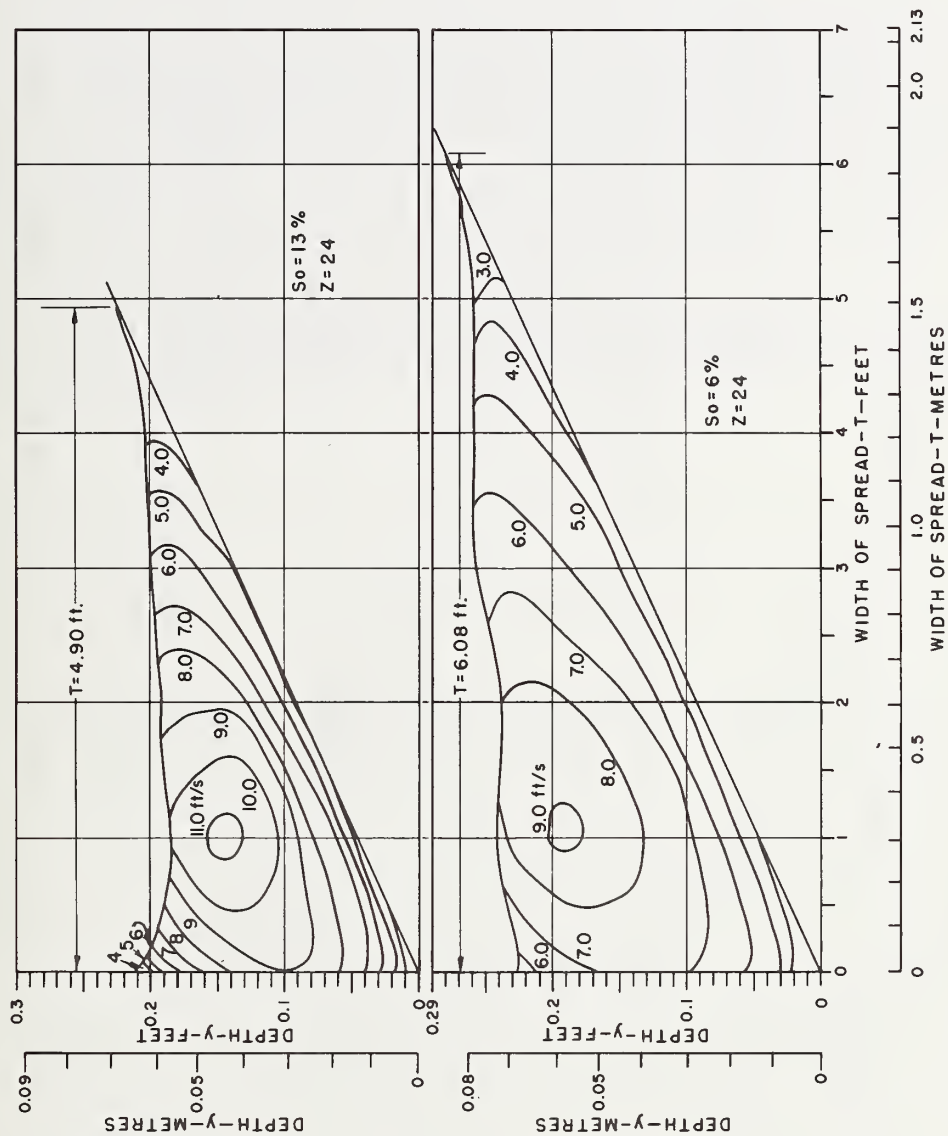


Figure 4-6. - Theoretical hydraulic efficiency vs. gutter flow, 2 ft by 4 ft (0.61 m by 1.22 m) open hole.



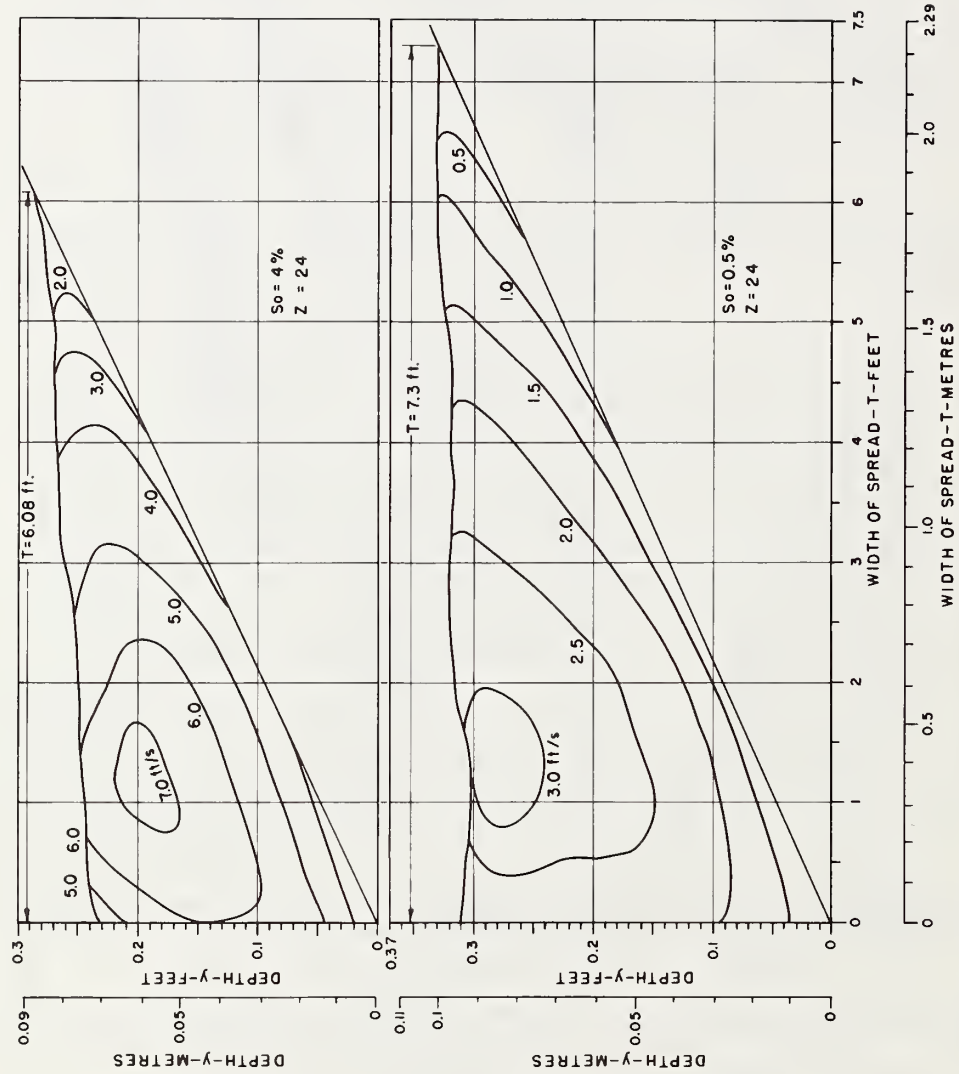
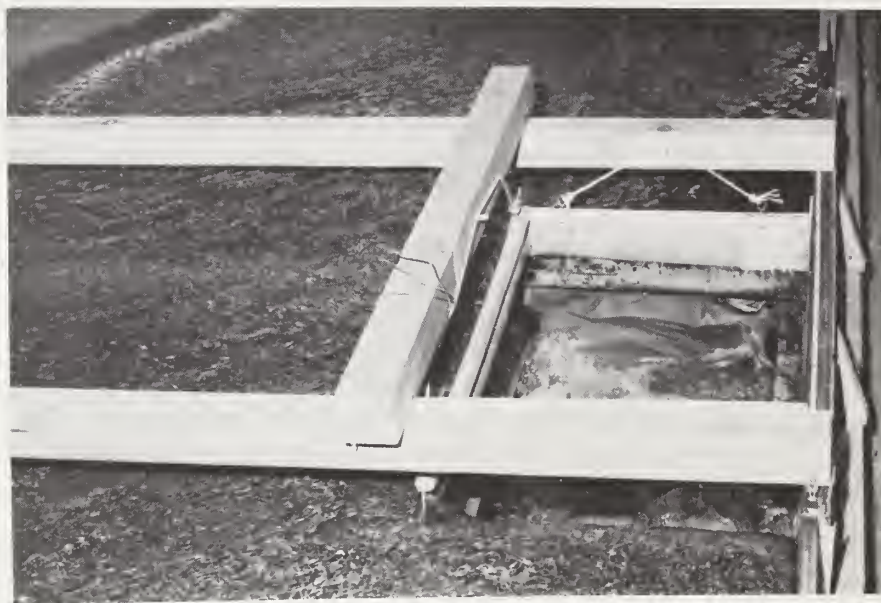


Figure 4-7b. - Typical velocity profiles, $S_o = 0.5\%$ and 4% , $Z = 24$ (Note: $1 \text{ ft/s} = 0.305 \text{ m/s}$).

The canvas device shown in figure 4-8 was used to measure intercepted frontal flow Q_F , in the 2 ft (0.61 m) wide gutter. The device was then dropped into the 2 ft by 4 ft (0.61 m by 1.22 m) open hole and the total intercepted flow, $Q_I = Q_F + Q_S$, was measured. These data as well as Q_T and Q_F measured by the velocity profiles in figure 4-7, are given in table 4-1. The calculated values are derived from equations 4-5, 4-6, and 4-8.

The Q_F/Q_T ratios from table 4-1 are plotted in figure 4-5 and are slightly less than the theoretical plot. This deviation is what would be expected since the theoretical curve does not take into consideration the decrease in velocity due to curb friction as shown in the velocity profiles of figure 4-7. Table 4-1 also gives comparisons between measured side flows, Q_S , and side flows calculated based on equation 4-8. The measured side flows, Q_S , are greater than the calculated values using equation 4-8.

The measured hydraulic efficiency, $E = (Q_S + Q_F)/Q_T$, values from table 4-1 are plotted in figure 4-6 and compare very well with the theoretical performance of a 2 ft by 4 ft (0.61 m by 1.22 m) open hole.



a. View looking downstream. Photo H-1765-382



b. Flow from left to right. Photo H-1765-384

Figure 4-8. - Device used to measure intercepted frontal flow, Q_F .

Table 4-1

INLET FLOW MEASUREMENT FOR AN OPEN HOLE

(Note: 1 ft = 0.305 m, 1 ft³/s = 0.028 m³/s)

S ₀ %	T ft	T' ft	Z	Q _T		Q _F		Q _F /Q _T		Q _S		E = $\frac{Q_F + Q_S}{Q_T}$	
				Meas. ft ³ /s	Cal.** ft ³ /s	Meas. ft ³ /s	Cal. ft ³ /s	Meas. %	Cal. %	Meas. ft ³ /s	Cal. ft ³ /s	Meas. %	Cal. %
0.5	4.78	5.0	24	0.80	0.80	0.615	0.611	76.9	76.4	0.180	0.189	99.4	100
1.0	4.88	5.0	16	2.35	2.35	1.73	1.775	73.6	75.5	0.455	0.500	93.0	96.8
1.0	4.85	5.0	24	1.18	1.18	0.85	0.894	72.0	75.8	0.274	0.267	95.3	98.4
1.0	4.75	5.0	48	0.35	0.35	0.249	0.270	71.1	77.0	0.094	0.080	98.0	100
2.0	4.99	5.0	24	1.79	1.79	1.33	1.328	74.3	74.2	0.268	0.255	89.3	88.4
4.0	5.17	5.40	16	5.47	5.47	3.72	3.99	68.0	72.9	0.61	0.355	79.2	79.4
4.0	4.62	5.00	16	4.08	4.08	3.06	3.182	75.0	78.0	0.44	0.321	85.8	85.9
4.0	5.95	6.08	24	4.06	4.06	2.54	2.69	62.6	66.3	0.43	0.23	73.2	71.9
4.0	4.78	5.0	24	2.27	2.27	1.690	1.735	74.4	76.4	0.240	0.190	85.0	84.8
4.0	5.85	5.85	48	1.22	1.22	0.78	0.82	63.9	67.2	0.140	0.088	75.4	74.4
4.0	5.04	5.0	48	0.81	0.81	0.59	0.60	72.8	74.1	0.090	0.077	84.0	83.6
6.0	4.75	5.1	16	5.41	5.41	3.80	4.16	70.2	76.9	0.56	0.277	80.6	82.0
6.0	4.75	5.0	24	2.74	2.74	2.00	2.090	73.0	76.3	0.280	0.160	83.2	82.1
6.0	5.88	6.0	24	4.82	4.82	2.92	3.21	60.6	66.6	0.43	0.19	69.5	70.5
9.0	3.94	4.2	16	3.99	3.99	3.20	3.37	80.2	84.5	0.30	0.195	87.7	89.3
9.0	4.66	4.83	24	3.17	3.17	2.38	2.46	75.1	77.6	0.22	0.132	82.0	81.8
9.0	4.92	5.00	24	3.69	3.69	2.61	2.772	70.7	75.1	0.30	0.138	78.9	78.8
13.0	4.10	4.3	16	5.29	5.29	4.11	4.401	77.7	83.2	0.30	0.174	83.4	86.5
13.0	4.39	4.9	24	3.27	3.27	2.15	2.621	65.7	80.2	0.26	0.107	73.7	83.4
13.0	4.73	5.0	24	3.95	3.95	2.83	3.029	71.6	76.7	0.28	0.113	78.7	79.5
13.0	4.61	5.0	48	1.18	1.18	0.84	0.929	71.2	78.7	0.127	0.043	81.9	82.4

* Measured values.

** Calculated values from equations.

*** Calculated values from measured velocities.

REFERENCES

1. Larson, Curtis L., Straub, Lorenz G., Grate Inlets for Surface Drainage of Streets and Highways, Bulletin No. 2, St. Anthony Falls Hydraulic Laboratory, June 1949.
2. Izzard, Carl F., Hydraulics of Runoff from Developed Surfaces, Highway Research Board, Vol. 26, pp. 129-150, 1946.
3. Li, Wen-Hsiung, The Design of Storm-Water Inlets, Department of Sanitary Engineering and Water Resources, John Hopkins University, June 1956.

CHAPTER 5

TEST FACILITY AND EXPERIMENTAL APPROACH

Experimental Equipment

To accurately investigate the hydraulic characteristics of grate inlets, the decision was made to use a full scale test facility. The width of roadbed selected for the test facility was 8 ft (2.44 m) including a 2 ft (0.61 m) gutter section and one half of a 12 ft (3.66 m) traffic lane - 6 ft (1.83 m), generally considered the allowable width of flow spread. The test roadbed was made 60 ft (18.3 m) long with the grate inlet test section located 40 ft (12.2 m) from the head box. The facility was designed and constructed to accommodate the following test conditions:

Longitudinal slopes	0.5 percent to 13 percent
Cross slopes	1:96 to 1:16
Maximum gutter flow	5.6 ft ³ /s (0.16 m ³ /s)
Manning roughness factor	0.016 to 0.017

To complete the 1,800 hydraulic tests in a reasonable amount of time, consideration was given to designing a hydraulic test facility which emphasized simplicity and ease of operation. Figures 5-1 and 5-2 are schematic drawings of the test facility. Principal components of the facility are identified in table 5-1 and are shown in figures 5-3 and 5-4. The roadbed was constructed of 3/4 in (19 mm), 4 ft (1.22 m) by 8 ft (2.44 m) sheets of Permaply supported every 2 ft (0.61 m) by transverse 3 in (76 mm) steel beams. The 3 in (76 mm) beams are fastened on one side to a 4 in (102 mm) steel angle and on the other to a 4 in (102 mm) steel beam running the 60 ft (18.3 m) length of the roadbed. The 4 in (102 mm) steel beam can be raised and lowered, thus rotating the roadbed on the 4 in (102 mm) angle. These 4 in (102 mm) members are in turn supported by two 60 ft (18.3 m) long, 16 in (406 mm) deep steel beams. The two large beams were welded together with 10 in (254 mm) beams to form a support structure 6 ft 9 in (2.06 m) wide. This support structure rests on an A-frame saddle support, 15 ft (4.6 m) from the downstream end of the facility and a lifting frame located 10 ft (3.0 m) from the upstream end of the facility. A 9 ft (2.74 m) wide, 4 ft (1.22 m) long, and 40 in (1 m) deep head box is attached to the upstream end of the roadbed by a flexible seal and supported by two 8 in (203 mm) beams welded to the 16 in (406 mm) beams. A 7 ft (2.13 m) sluice gate at the front of the head box is used to control the velocity of the flow onto the roadbed. The 8 in (203 mm) supply line, running from the pumps to the head box, is connected through a Dresser coupling to one of the 16 in (406 mm) beams at the A-frame support. This arrangement eliminates the need to change piping when the longitudinal slope is changed.

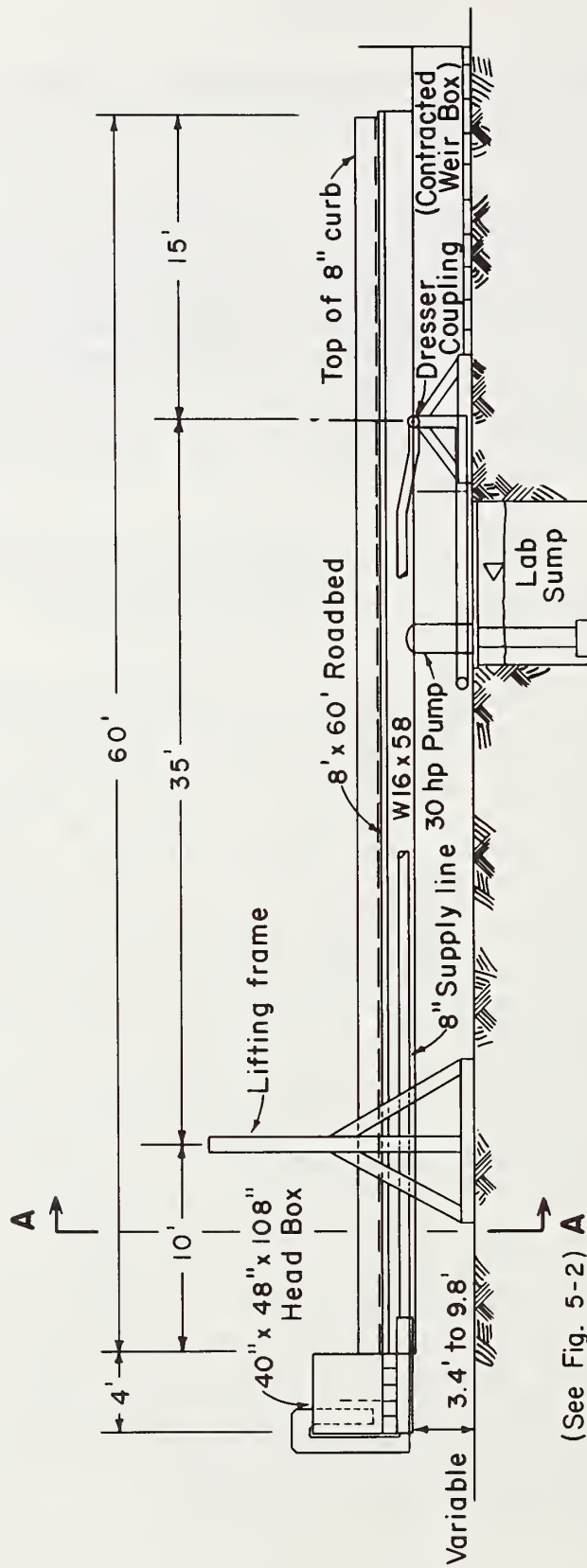


Figure 5-1. - Hydraulic test facility elevation view (schematic)
 (Note: 1 ft = 0.305 m, 1 in = 25.4 mm).

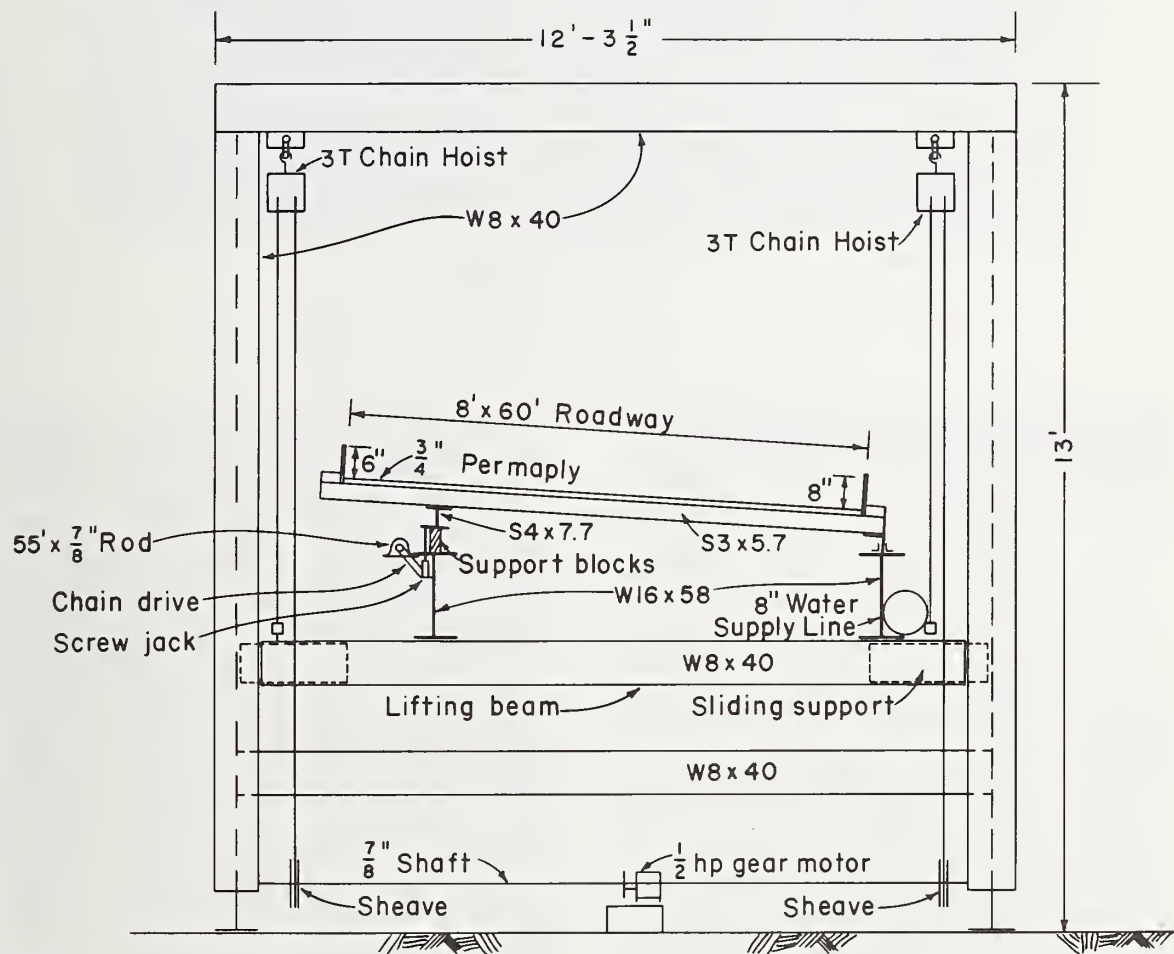


Figure 5-2. - Hydraulic test facility section A-A (schematic)
 (Note: 1 ft = 0.305 m, 1 in = 25.4 mm).

Table 5-1

PRINCIPAL COMPONENTS OF HYDRAULIC TEST FACILITY

No.	Feature	No.	Feature
1	Sand coated roadbed	17	Motor to drive chain hoists
2	Curb	18	Head box drain
3	Walkway	19	Vertical turbine pumps
4	Grate inlet	20	Control valve
5	Carriage	21	90° angle beam
6	Head box	22	Dresser coupling
7	Lifting frame	23	Diversion chute for intercepted flow
8	Chain hoist	24	Rectangular contracted weir
9	Orifice-Venturi meter	25	Slide gate
10	Water supply pipe	26	90° V-notch weir
11	Tail box	27	Motor and drive shaft to run screw jacks
12	W 16 x 58 beam	28	S 4 x 7.7 beam
13	W 10 x 49 beam	29	Support blocks
14	W 8 x 40 beam	30	Drive shaft
15	S 3 x 5.7 beam	31	Screw jack
16	Sliding support		

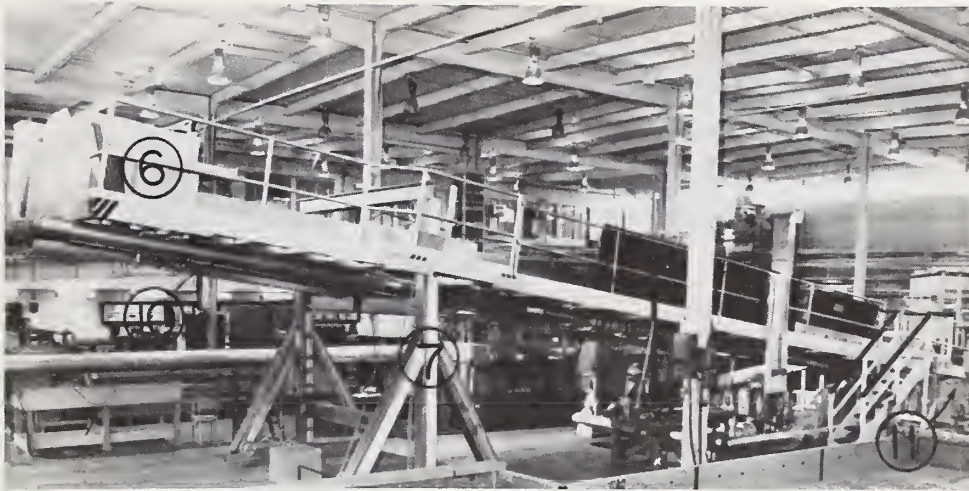


Photo H-1765-350.1

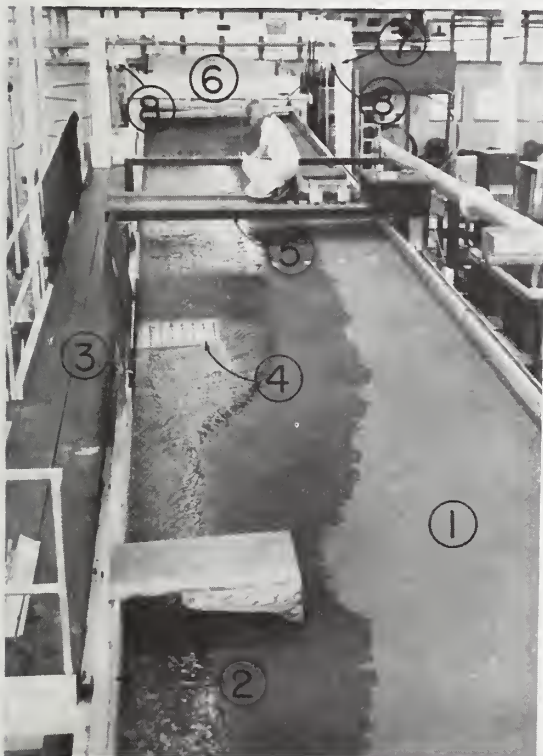


Photo H-1765-369.1

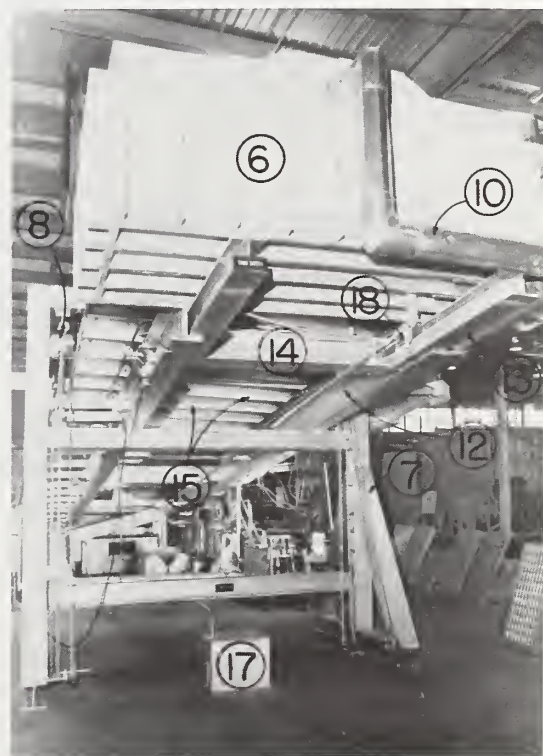


Photo H-1765-374.1

Figure 5-3. - Principal components of hydraulic test facility.

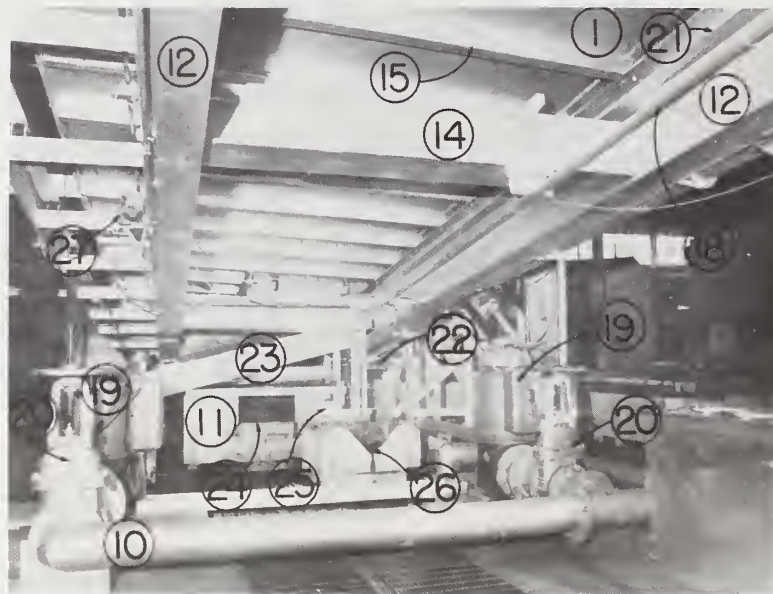


Photo H-1765-375.1

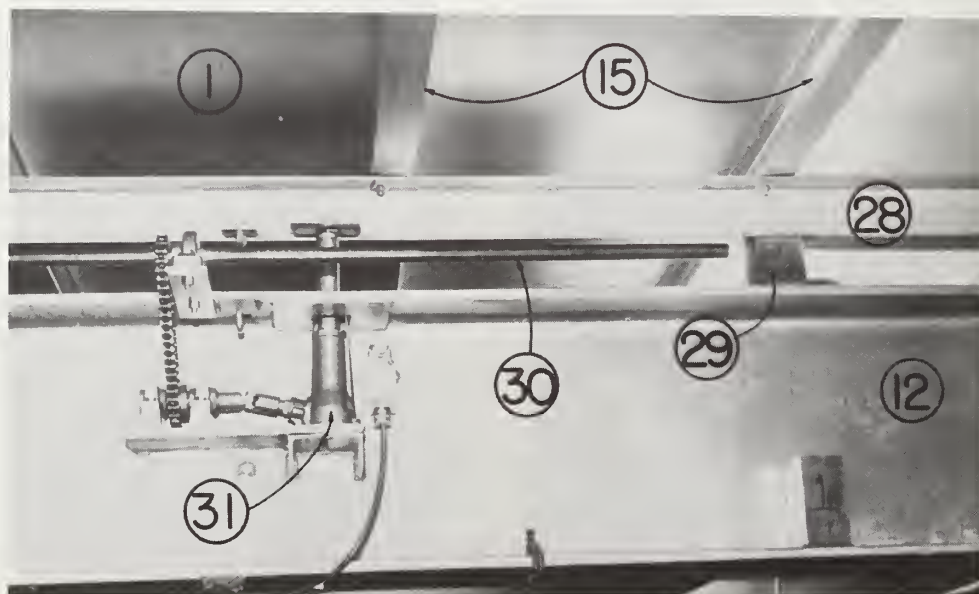


Photo H-1765-368.1

Figure 5-4. - Principal components of hydraulic test facility (continued).

The longitudinal slope is adjusted by a power system consisting of two 3 ton (2772 kg) chain hoists driven by a 1/2 hp (373 w) gear motor. The roadbed cross slope is adjusted by six automobile-type screw jacks positioned on 8 ft (2.44 m) centers along the 60 ft (18.3 m) length of the roadbed. The jacks are simultaneously driven by a 60 ft (18.3 m) long, 7/8 in (22 mm) diameter drive shaft connected to a 1/4 hp (187 w) gear motor.

The chain hoist and the cross slope jacks are used to adjust the roadbed conditions when the roadbed is dry. Flow instabilities which may result from a suspended roadbed, are eliminated by lowering the lifting beam onto supports in the lifting frame and supporting the cross slope with spacer blocks.

Water is supplied to the head box of the test facility from the laboratory sump through one or two 8 in (203 mm) vertical turbine pumps as needed. Since the total discharge can vary from 0.03 ft³/s to 5.60 ft³/s (0.0008 m³/s to 0.16 m³/s), a flow measuring device was needed which could accurately measure the discharge delivered to the head box, over the flow range. An 8 in (203 mm) combination orifice-Venturi meter was located on the 8 in (203 mm) pipeline between the pumps and the head box. The meter has a ring seal which automatically seals an orifice plate in place when the pump is operated. Five orifice plates ranging in size from 1-1/4 in to 5-1/2 in (32 mm to 140 mm) were used to accurately measure the discharge. To change orifice plates, it was necessary to shut off the pump, lift the orifice plate from the meter slot, replace it with one desired, and restart the pump. The meter was connected to a mercury differential manometer. The meter and various orifice plates had been calibrated previously in the hydraulic laboratory. The meter proved to be a simple and accurate measuring device for the study.

The roadbed flow which passed the grate inlet (referred to as carryover flow) was measured and subtracted from the total flow supplied to the roadbed to obtain the intercepted flow. This carryover flow was measured with one of three devices, depending on the quantity of flow past the grate. The flow left the downstream end of the roadbed and dropped into a large weir box which was constructed under the test facility (figure 5-4). This box, containing a 2 ft (0.61 m) wide contracted weir, extended under the downstream end of the test facility and was used to measure flows larger than 0.25 ft³/s (0.007 m³/s). Bypassed flows in the range from 0.25 ft³/s to 0.07 ft³/s (0.007 m³/s to 0.002 m³/s) were measured with a 90° V-notch weir connected to the large weir box by a 6 in (152 mm) pipeline and controlled by a slide gate. Both weirs were calibrated using the orifice-Venturi meter previously described. Bypassed flows below 0.07 ft³/s (0.002 m³/s) were diverted from the downstream end of the roadbed into a small volumetric tank for measurement.

A Manning roughness coefficient, "n" of 0.016 was specified for the road surface to be used in the study. Tests to determine the roughness coefficient of the road surface were done at several longitudinal slopes and at a horizontal cross slope. With a horizontal cross slope, the flow had a rectangular cross section and the normal Manning equation was used to calculate "n" based on the average of eight depth measurements across the road surface.

The Permaply surface was first sanded to remove the plastic coating, and then coated with epoxy paint. U.S. Standard Series No. 30 sand (0.59 mm to 1.9 mm diameter) was applied to the wet paint. Figure 5-5 shows this surface treatment in progress. Excess sand was washed from the surface when the paint had dried and tests indicated that $n = 0.014$. Since this value was too low, the existing surface was coated with marine varnish and U.S. Standard Series No. 8 sand (2.00 mm to 4.75 mm diameter) was applied to the wet surface. When the excess sand had been washed away, tests showed that $n = 0.022$. Since this roughness coefficient was also unacceptable, the surface was again coated with marine varnish and U.S. Standard Series No. 16 sand (1.0 mm to 2.44 mm diameter) was applied to the surface while it was wet. When the varnish dried, the excess sand was brushed off and the surface was sprayed with two coats of marine varnish to bind the sand particles together. Tests on this surface showed a Manning roughness coefficient of 0.016 to 0.017 which was acceptable for the purposes of the study. The surface proved to be durable and repeat tests at several intervals in the study showed the "n" value holding between 0.016 and 0.017.

Test Procedures

Hydraulic Tests. - The hydraulic test facility was designed to permit one man operation as far as hydraulic testing and changing longitudinal and transverse slopes are concerned. Changing from one longitudinal slope to the next took a maximum of 10 minutes. Cross slope changes took about 5 minutes. Because the facility was easily operated, each grate was tested over the complete range of longitudinal and cross slopes rather than setting one longitudinal and cross slope combination and then changing the grates.

For each longitudinal slope, cross slopes of $Z = 48$, 24, and 16 were tested. A $Z = 96$ cross slope was tested early in the program but was dropped because flowrates on this flat slope were too low to reveal differences in efficiency among the various grate designs.

For each cross slope, four or five different gutter flows were used. The maximum gutter flow Q_T used was governed by either the pump capacity of 5.3 ft³/s to 5.6 ft³/s (0.150 m³/s to 0.159 m³/s) or the width of the roadbed which limited the width of spread T' . Maximum flow spread widths, T' , tested were around 7 ft (2.13 m) to 7.5 ft (2.29 m). The minimum gutter flow used in each series of tests was that flow which was completely captured by the grate, or that flow



Figure 5-5. - Roadbed surface treatment. Photo H-1765-18

which provided a flow spread, T' , of 2 ft (0.61 m). The four or five data points obtained were sufficient to develop curves relating hydraulic efficiency, E , to gutter flow, Q_T , or width of spread, T' , for each combination of longitudinal and cross slopes.

Gutter flows were measured using a combination orifice-Venturi meter which is described in the experimental equipment section. Flow from the head box to the roadbed was controlled by a 7 ft (2.13 m) wide sluice gate. The gate could be moved up or down to adjust the vertical opening and the width of the opening could be controlled by blocking off sections with sheet metal plates. With the gate properly adjusted, the head that built up behind the sluice gate provided adequate gutter flow velocity at the beginning of the flume. Without the gate, the flow started out at near critical velocity and accelerated until it reached a flow velocity which was normal for the slope conditions being tested. This region where the flow accelerated had a steadily decreasing cross-sectional flow area and width of spread, T' , and was of course nonuniform flow. Use of the sluice gate resulted in a shorter reach of nonuniform flow at the beginning of the flume and therefore a longer reach of uniform flow upstream from the grate.

The sluice gate was rarely used for the $Z = 96$ and $Z = 48$ cross slopes because the normal flow velocities were attained within a few feet of the head box. The steep $Z = 16$ cross slope had the effect of concentrating the flow into a uniform width of spread without the use of the sluice gate even though the flow velocity was the highest of the cross slopes tested. The sluice gate was used most often at $Z = 24$. This cross slope was steep enough to result in fairly high flow velocities, but not steep enough to set up a uniform flow spread within a short distance from the head box. In general, the sluice gate was used for $Z = 24$ and $Z = 16$ in those instances when the longitudinal slope was steeper than the cross slope. The gate was most useful for the maximum gutter flow for each setup as this was the most difficult condition to stabilize. Lower flowrates tended to stabilize in a shorter distance.

The region of uniform flow spread upstream of the grate ranged from 35 ft (10.7 m) to as short as 5 ft (1.52 m) depending on the gutter flow, cross slope, and longitudinal slope.

The width of spread, T' , was measured using a point gage which could be moved along a graduated beam on the carriage. This measurement was taken at several locations upstream from the grate to be sure that the gutter flow was uniform when it reached the grate.

In measuring width of spread, the major problem was in deciding where the edge of the flow was. The edge was most irregular and difficult to identify at the flatter cross slopes, particularly $Z = 96$. The intersection of water surface and road surface is a

small angle at the flat cross slopes, and any small variation in the cross slope or irregularity in the road surface results in an uneven flow edge. Steeper cross slopes especially $Z = 16$, had a very even and well defined flow edge. Therefore, the flow spreads measured are less subject to error on the steep cross slopes and are questionable at $Z = 96$.

Flow which was not intercepted by the grate is referred to as carry-over flow, Q_c and was measured by either the 2 ft (0.61 m) wide contracted weir, the 90° V-notch weir or the volumetric tank depending on the flowrate.

The time required to complete a test was governed by the time needed to reach a uniform flow condition in the weir box. Once the water level became stable, the head on the weir was read using a hook gage that was mounted in a stilling well connected to the weir box. The water level in the V-notch weir box was particularly slow to stabilize. The V-notch crest was lower than the crest of the contracted weir and when the slide gate connecting the two boxes was opened (figure 5-4) the stored water in the contracted weir box drained over the V-notch weir. Therefore, it was necessary to wait for this stored water to drain out before the true carryover flowrate became established.

The procedure for making a typical test began with selecting the proper size orifice plate, based on the gutter flow to be used, and inserting it into the flow meter. The pump(s) would then be started, the orifice-Venturi meter and manometer bled to remove any air, and the required discharge set by adjusting the control valve. The sluice gate was then adjusted (if necessary) to produce a uniform flow spread for the maximum possible distance upstream of the grate. With a uniform flow spread set up, the carriage and point gage were used to measure the width of spread, T' , at several locations upstream of the grate. The grate area was then photographed. Finally, the hook gage was read (if the weirs were being used) and reread several minutes later to be sure that the water surface in the weir box had stabilized. With the hook gage reading known, the head on the weir could be calculated, and the carryover flowrate, Q_c , determined from the weir capacity curves.

Debris Tests. - To determine debris problems encountered at grate inlets, several engineers and maintenance personnel from the City and County of Denver, State of Colorado, and State of Wyoming were asked for their observations and suggested test procedures. The debris and test procedure used in the study evolved from these meetings and from contacts with FHWA engineers.

Debris tests were run on both the 2 ft by 4 ft (0.61 m by 1.22 m) and 2 ft by 2 ft (0.61 m by 0.61 m) grates. The debris testing was done at a cross slope of $Z = 24$ since it was a good average between

$Z = 16$ and $Z = 48$. Tests were run on slopes of 0.5 percent and 4 percent to evaluate the effect of longitudinal slope on debris-handling efficiency.

Debris tests were conducted using 150 pieces of 3 in (76 mm) by 4 in (102 mm) brown craft paper to represent leaves. The "leaves" were first saturated and placed on the wet road surface in an area 3 ft (0.91 m) wide by 25 ft (7.6 m) long starting immediately upstream from the grate. Gutter flow was begun slowly until advancing water reached the first "leaves." At this point stop watches were started to time the test. The gutter flow was slowly increased to reach $0.5 \text{ ft}^3/\text{s}$ ($0.014 \text{ m}^3/\text{s}$) in 2 minutes. Debris which failed to move naturally was loosened from the road surface and allowed to move downstream. Any debris which passed by the grate was retrieved and placed in the gutter area upstream from the grate. This was done to insure that all 150 "leaves" made contact with the grate for each test. At 5 minutes, the debris which had passed through the grate was recovered and counted. At 7 minutes, the gutter discharge, Q_T , was increased according to the hydrograph in figure 5-6. The maximum gutter flow of $2.67 \text{ ft}^3/\text{s}$ ($0.076 \text{ m}^3/\text{s}$) was reached in 10 minutes. At 15 minutes the debris that passed through the grate, debris caught on the grate, and debris which washed off the grate was counted. Photos were taken during the tests at 5 minutes, 10 minutes, and 15 minutes, and the debris remaining on the grate was photographed at the end of the test. Each test was repeated three times to average the somewhat variable results. The paper "leaves" were used for 2 tests before being replaced. After 2 tests, the paper became soggy and very flexible. If the "leaves" were not replaced, the results of the third test did not agree with the results of the first two tests.

The debris handling efficiency was calculated as the ratio of debris that passed through the grate plus the debris that washed off the grate to the total debris. Debris handling efficiencies were calculated at 5 minutes and at the end of 15 minutes.

Development and Use of Figures

Chapters 6 through 12 deal with one particular grate design. In each chapter there are three types of graphs:

- E vs. Q_T curves
- E vs. T' curves
- Inlet capacity curves

The hydraulic efficiency vs. gutter flow (E vs. Q_T) curves are based on actual data from the test facility and these data points are shown. For each cross slope, there is one curve for each of the seven longitudinal slopes.

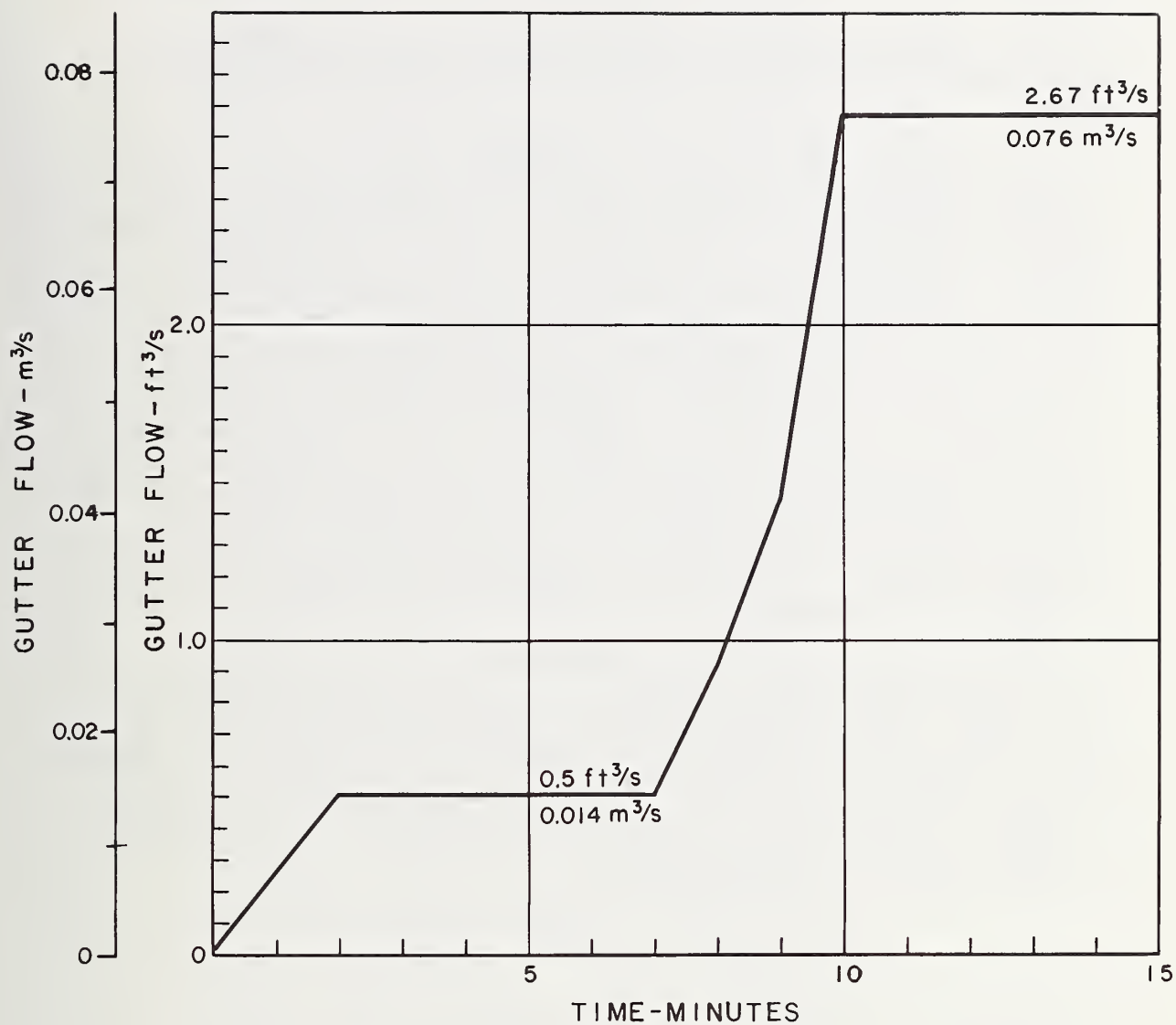


Figure 5-6. - Hydrograph for debris tests
(Note: 1 ft³/s = 0.028 m³/s).

The hydraulic efficiency vs. width of spread (E vs. T') curves are also based on actual data and the data points are shown. Again for each cross slope, there are curves for each of the seven longitudinal slopes tested.

The inlet capacity curves are developed from the E vs. Q_T curves. Since the curves are not based directly on the data, no points are shown.

The inlet capacity curves relate longitudinal slope, S_0 , cross slope, $1/Z$, gutter flow, Q_T , intercepted flow, Q_I , width of spread, T , and hydraulic efficiency, E . Figure 5-7 shows an inlet capacity curve complete with data points. In plotting the curves, points for each hydraulic efficiency line were obtained from the E vs. Q_T curves and points for the intercepted flow lines were obtained from Q_I vs. Q_T graphs which have not been presented in the report. The efficiency and intercepted flow lines were interpolated between the data points and the points from the graphs. Since these lines are interpolated between points, they are not as accurate as the E vs. Q_T curves which are straight line fits of actual data points. The width of spread, T , curves are theoretical and have been calculated using Izzard's modified Manning equation (equation 4-5) for triangular sections. For this reason, the widths of spread, T , in the inlet capacity curves do not necessarily agree with the actual measured widths of spread as shown on the E vs. T' graphs.

Each inlet capacity curve is plotted for one particular grate and cross slope, $1/Z$. With a known cross slope, $1/Z$, and grate size, the proper curve can be selected. A point can then be plotted using the design gutter flow and longitudinal slope as coordinates. It is likely that this point will not fall exactly on any of the lines so interpolation will be necessary. By interpolating between the various lines, the intercepted flow, Q_I , the width of flow spread, T , and the hydraulic efficiency, E , can be determined.

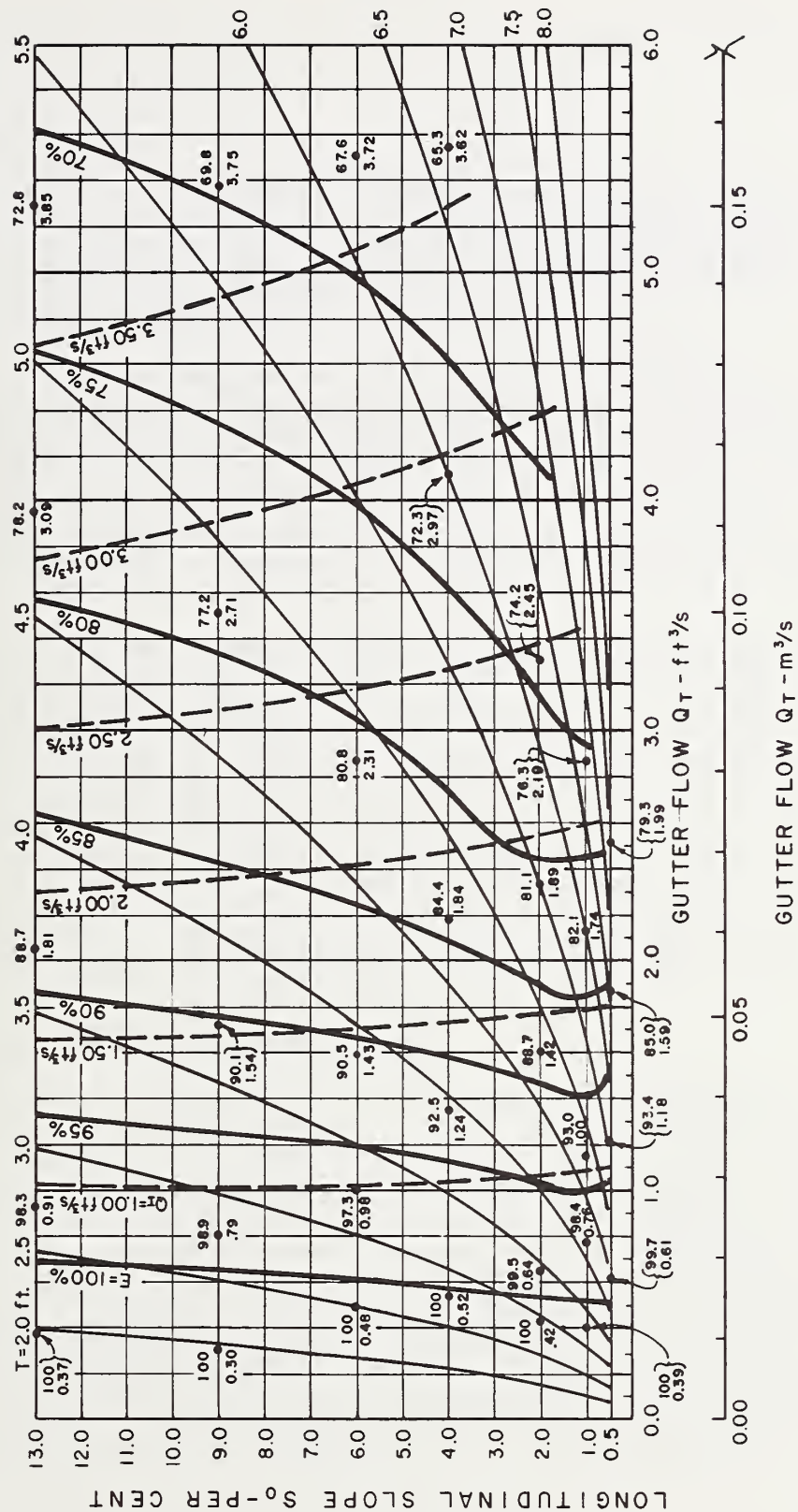


Figure 5-7. - Sample inlet capacity curve
(Note: $1 \text{ ft}^3/\text{s} = 0.028 \text{ m}^3/\text{s}$, $1 \text{ ft} = 0.305 \text{ m}$).

CHAPTER 6

HYDRAULIC EFFICIENCY AND DEBRIS TESTS - PARALLEL BAR GRATES

Introduction

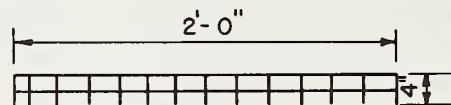
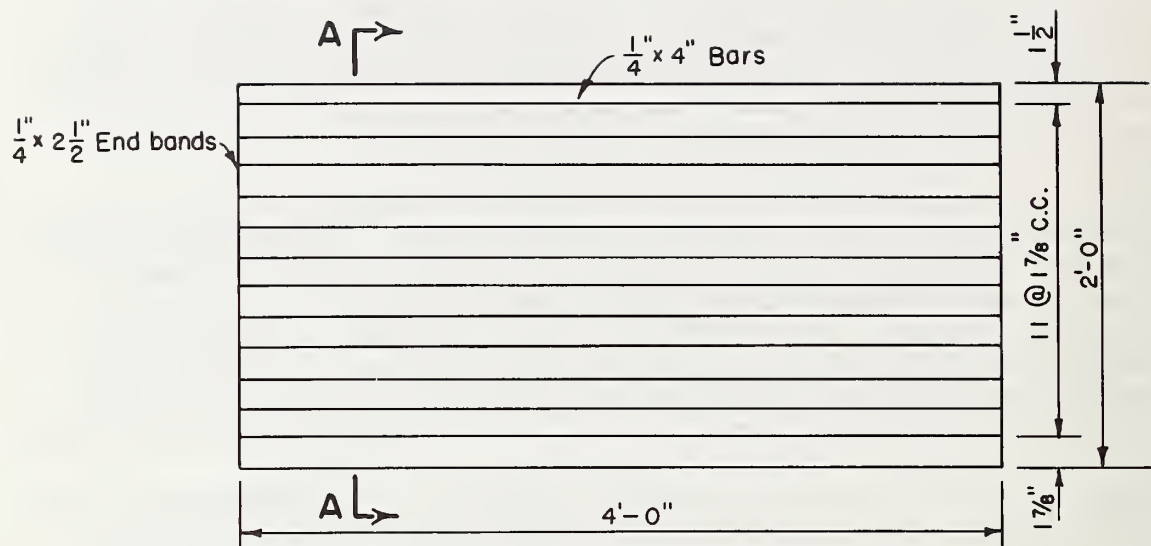
This is the first in a series of chapters describing hydraulic test results of grate inlet designs. As stated previously in this report, the major objective of the investigation was to identify grate inlets which are bicycle and pedestrian safe, hydraulically efficient, and demonstrate good debris-handling characteristics.

For some time, the parallel bar grate has been recognized as a very efficient grate inlet. However, in recent years, it has become evident that the standard parallel bar grate with 1 in to 2 in (25.4 mm to 51 mm) clear openings between bars is not safe for bicycle traffic. Since a comparison of the relative safety, hydraulic efficiency, and debris-handling capability of several grate inlets is desired, the parallel bar grate is included as the standard with which to compare hydraulic efficiencies of the various grate designs used in this study.

Figure 6-1 illustrates the physical dimensions of the fabricated steel grate tested, which represents the commonly used average dimensions for a 2 ft by 4 ft (0.61 m by 1.22 m) grate inlet. This particular grate has clear space openings of 1-5/8 in (41.3 mm) between 1/4 in (6.4 mm) wide and 4 in (102 mm) deep parallel bars based on the results of the structural analysis for a 2 ft by 2 ft (0.61 m by 0.61 m) parallel bar grate in Chapter 2 (Table 2-1). The same size parallel bar (1/4 in by 4 in (6.4 mm by 102 mm)) was used for the 2 ft by 4 ft (0.61 m by 1.22 m) test grate assuming the prototype grate would have a midspan support beam under the grate and midspan lateral support would be provided. The parallel bar grate was not tested for bicycle safety characteristics since it is obviously unsafe for bicycle traffic.

Experimental Results and Observations

Hydraulics. - Figures 6-2 and 6-3 present the experimental results for the 2 ft by 4 ft (0.61 m by 1.22 m) and 2 ft by 2 ft (0.61 m by 0.61 m) parallel bar grates. The smaller grate is less efficient than the larger grate since it is shorter and, therefore, less flow is captured along its outside edge. Since the steeper cross slopes confine the gutter flow near the curb a larger percentage of the flow passes over the grate and is intercepted by the inlet resulting in higher hydraulic efficiencies for the steeper cross slopes. Following the same rationale, a larger percentage of the flow will pass over the grate inlet as the longitudinal slope, S_0 , is increased for a given cross slope, $1/Z$, and gutter flow, Q_T . This will result in improved hydraulic efficiency as the longitudinal slope, S_0 , is



SECTION A-A

Figure 6-1. - 2 ft by 4 ft (0.61 m by 1.22 m) fabricated steel parallel bar grate.

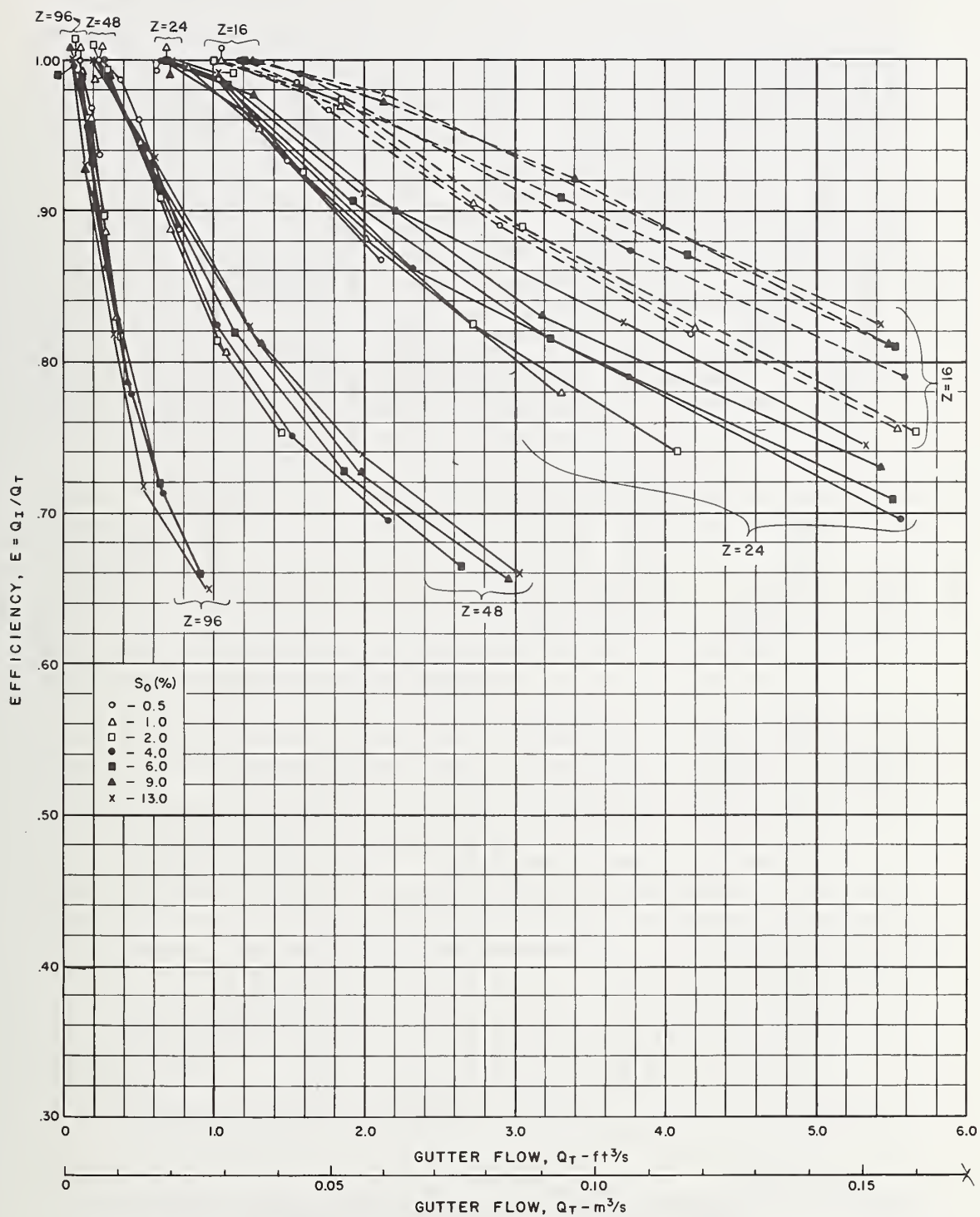


Figure 6-2. - Hydraulic efficiency vs. gutter flow, 2 ft by 4 ft (0.61 m by 1.22 m) parallel bar grate.

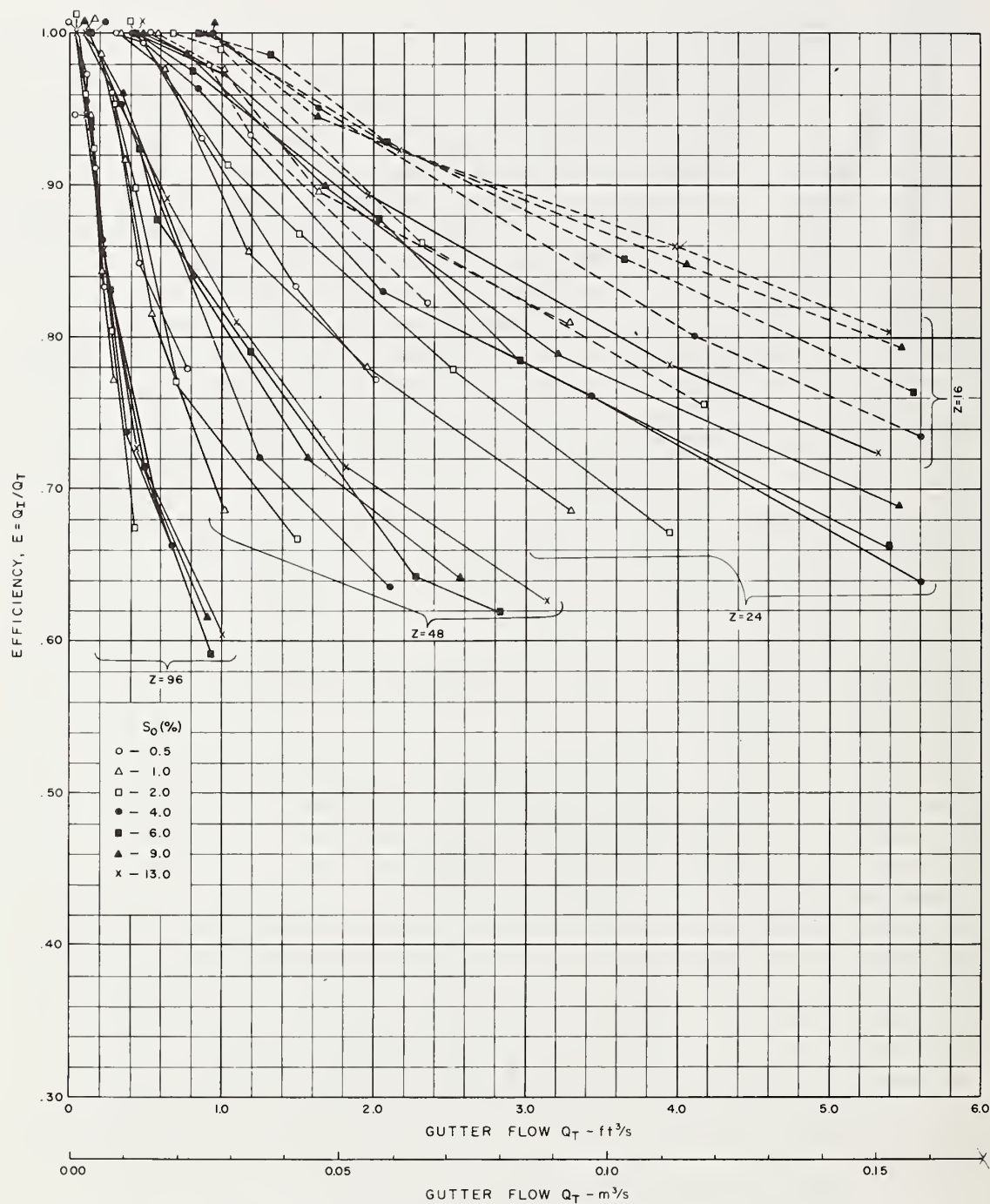


Figure 6-3. - Hydraulic efficiency vs. gutter flow, 2 ft by 2 ft (0.61 m by 0.61 m) parallel bar grate.

increased as evidenced in figures 6-2 and 6-3. However, the resulting consequences of confining the gutter flow, Q_T , near the curb and thus passing a greater percentage over the 2 ft (0.61 m) wide grate are higher velocities and larger flow depths at the grate inlet. This high energy flow produces increased splashing when the inlet grates have transverse members. Figure 6-4 shows the performance of the two sizes of parallel bar grates on a 13 percent longitudinal slope.

For 100 percent hydraulic efficiency, the 2 ft by 4 ft (0.61 m by 1.22 m) parallel bar grate with $Z = 16$ will capture a gutter flow, Q_T , equal to approximately 1.1 ft³/s (0.031 m³/s). This gutter flow is equal to approximately 0.69 ft³/s (0.02 m³/s) for $Z = 24$, 0.25 ft³/s (0.007 m³/s) for $Z = 48$, and 0.10 ft³/s (0.003 m³/s) for $Z = 96$. These values for the 2 ft by 2 ft (0.61 m by 0.61 m) parallel bar grate at 100 percent hydraulic efficiency reduce to $Q_T = 0.70, 0.41, 0.12$, and 0.05 ft³/s (0.020, 0.012, 0.003, and 0.001 m³/s) for values of $Z = 16, 24, 48$, and 96 .

Figure 6-5 shows the flow capture for the 2 ft by 2 ft (0.61 m by 0.61 m) parallel bar grate on longitudinal slopes of 6 percent and 13 percent and a gutter discharge near 5.3 ft³/s (0.15 m³/s).

Figure 6-6 illustrates measured width of spread, T' , near the parallel bar grate inlet for two cross slopes, $Z = 24$ and 96 and longitudinal slopes, $S_0 = 13, 9, 6, 4, 2, 1$, and 0.5 percent with efficiency, E , equal to 100 percent.

Figures 6-7 through 6-10 illustrate the hydraulic efficiencies, E , for the two parallel bar grates as a function of measured width of spread, T' . The flatter longitudinal slopes are more efficient for the same width of spread, T' . The gutter flow velocities on the roadbed outside the 2 ft (0.61 m) gutter line are slower at the flatter longitudinal slopes. As the grate captures the flow in the 2 ft (0.61 m) gutter, the water on the roadbed will flow toward the grate and some of the flow will be captured along the length of the grate. The amount of side capture is a function of the depth of flow 2 ft (0.61 m) from the curb, Y' . Figure 6-6 illustrates a 100 percent flow capture with a 2 ft by 4 ft (0.61 m by 1.22 m) grate and a width of spread, $T' = 4.5$ ft (1.37 m) at 0.5 percent longitudinal slope and $Z = 24$. Figure 6-7 shows an 87 percent efficiency for the same grate, width of spread, and cross slope at 13 percent longitudinal slope. The higher velocity of gutter flow on the roadbed resulting from the steeper slope allows more flow to pass outside the 2 ft (0.61 m) grate width than what the grate can capture as side flow along its length. Although the grate efficiencies are higher at the flatter longitudinal slopes, the total gutter flow is considerably less.

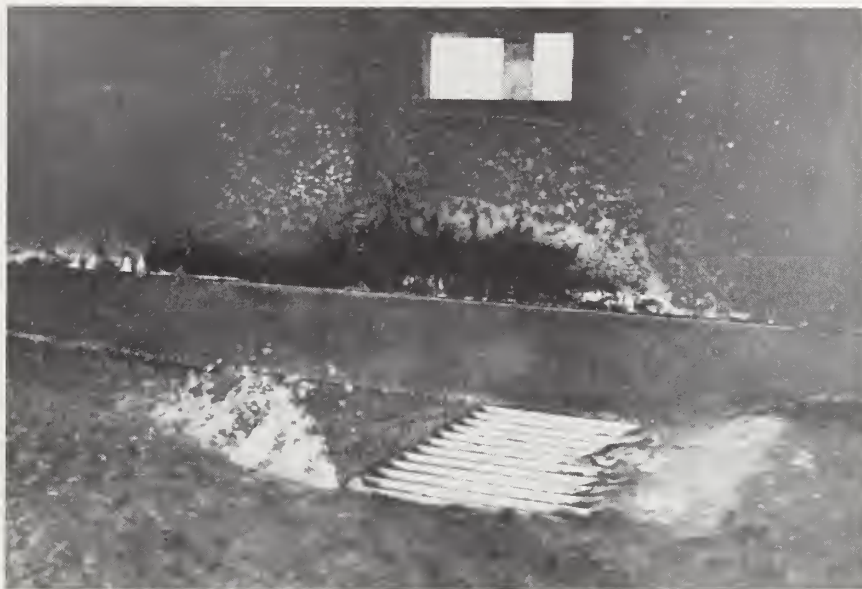


- a. 2 ft by 2 ft (0.61 m by 0.61 m) grate $T' = 5.9 \text{ ft (1.80 m)}$
 $Q_T = 5.3 \text{ ft}^3/\text{s (0.15 m}^3/\text{s)}$ $E = 72\%$
 Photo 9-9A

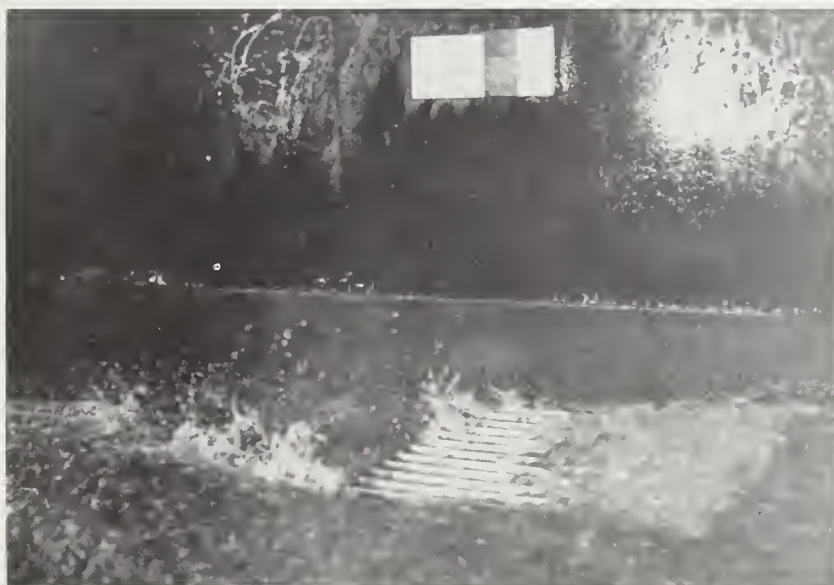


- b. 2 ft by 4 ft (0.61 m by 1.22 m) grate $T' = 5.8 \text{ ft (1.77 m)}$
 $Q_T = 5.3 \text{ ft}^3/\text{s (0.15 m}^3/\text{s)}$ $E = 75\%$
 Photo 9-14A

Figure 6-4. - Parallel bar grates, $S_0 = 13\%$, $Z = 24$.



- a. $S_0 = 6\%$ $T' = 6.4 \text{ ft (1.95 m)}$
 $Q_T = 5.4 \text{ ft}^3/\text{s (0.15 m}^3/\text{s)}$ $E = 66\%$
 Photo 6-5



- b. $S_0 = 13\%$ $T' = 5.9 \text{ ft (1.80 m)}$
 $Q_T = 5.3 \text{ ft}^3/\text{s (0.15 m}^3/\text{s)}$ $E = 72\%$
 Photo 4-13A

Figure 6-5. - View of 2 ft by 2 ft (0.61 m by 0.61 m) parallel bar grate, $Z = 24$.

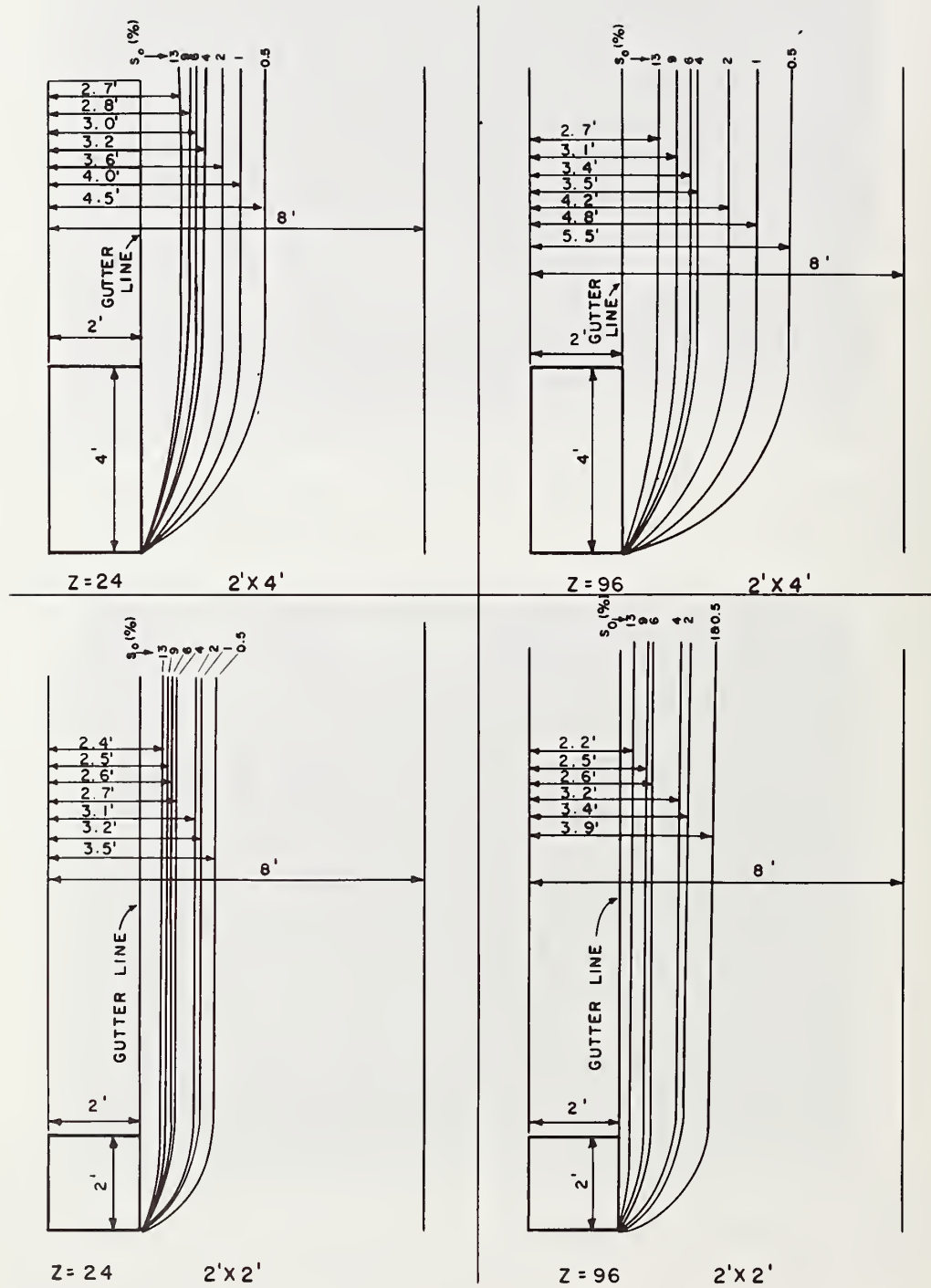


Figure 6-6. - Gutter flow patterns, parallel bar grate, E = 100%
(Note: 1 ft = 0.305 m).

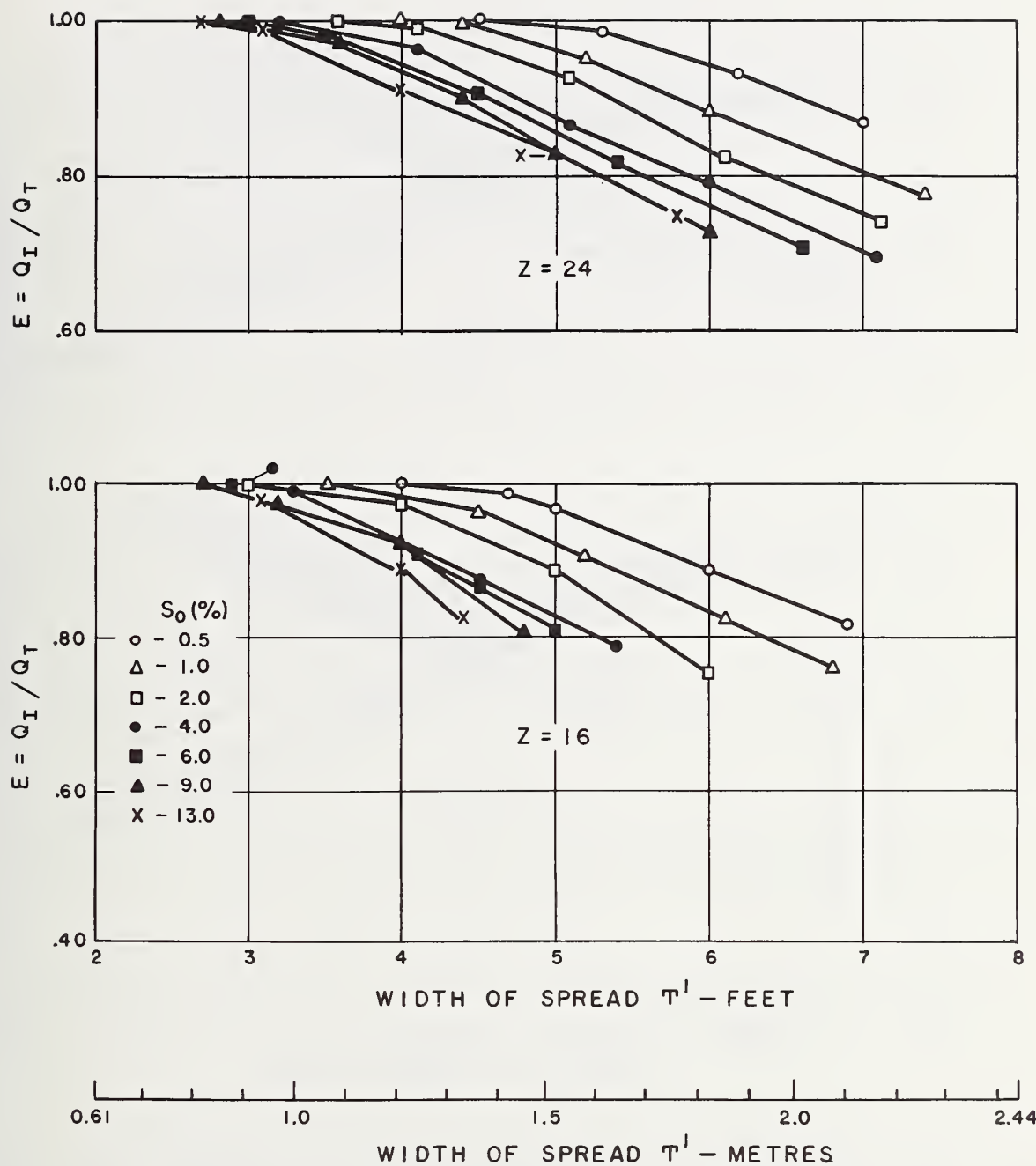


Figure 6-7. - Hydraulic efficiency vs. width of spread, 2 ft by 4 ft (0.61 m by 1.22 m) parallel bar grate, Z = 24, 16.

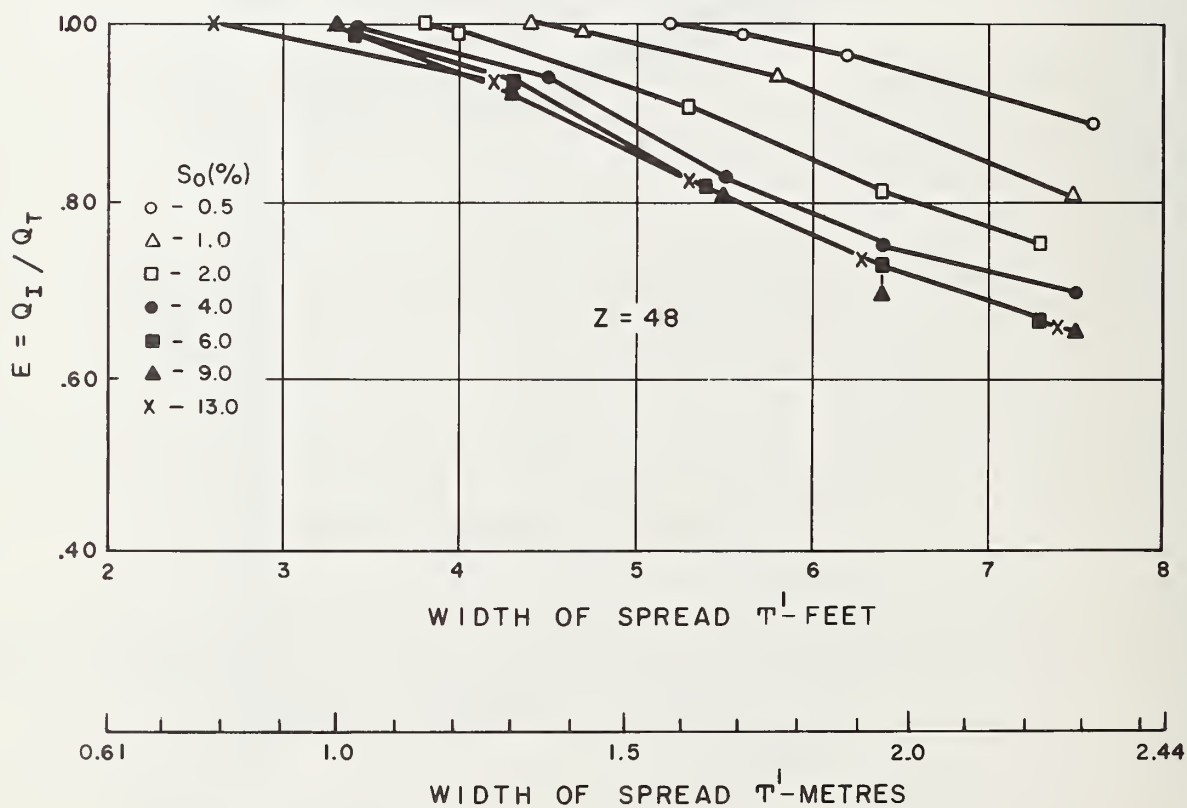
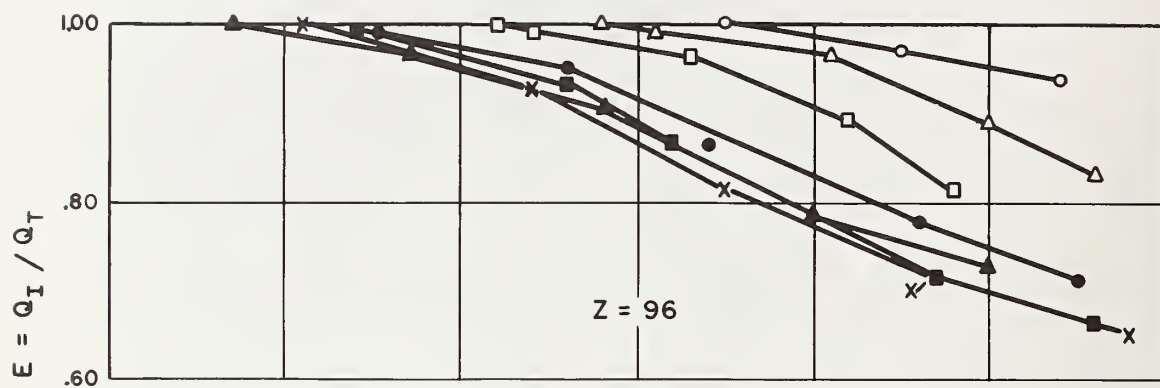


Figure 6-8. - Hydraulic efficiency vs. width of spread, 2 ft by 4 ft (0.61 m by 1.22 m) parallel bar grate, $Z = 96, 48$.

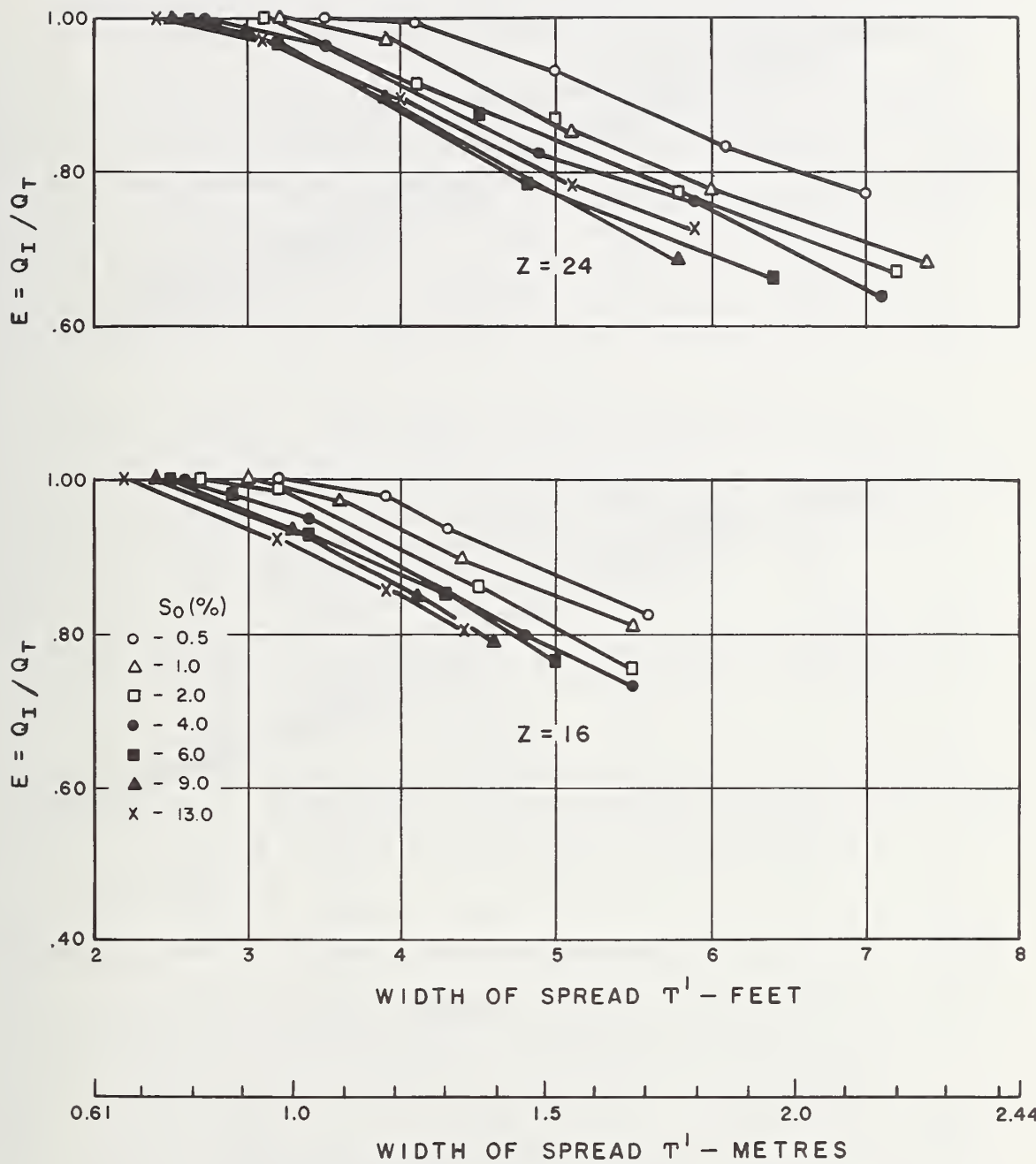


Figure 6-9. - Hydraulic efficiency vs. width of spread, 2 ft by 2 ft (0.61 m by 0.61 m) parallel bar grate, $Z = 24, 16$.

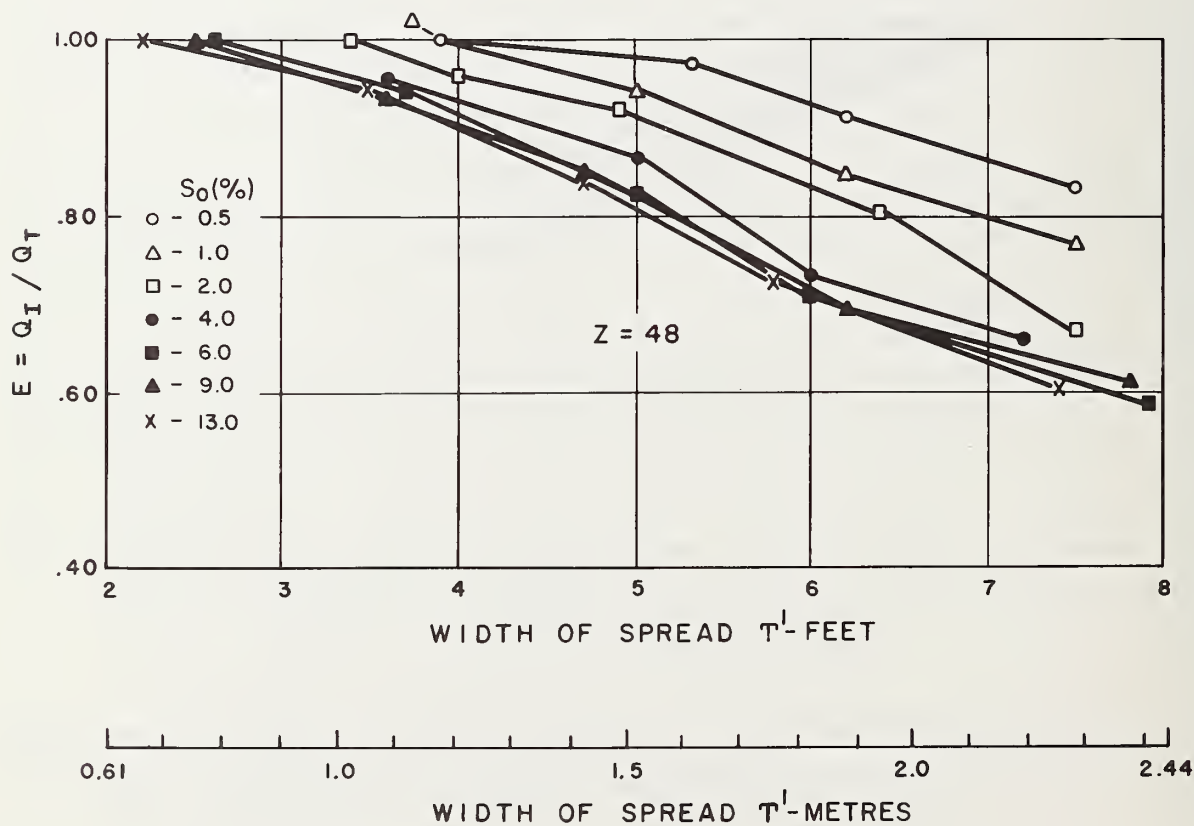
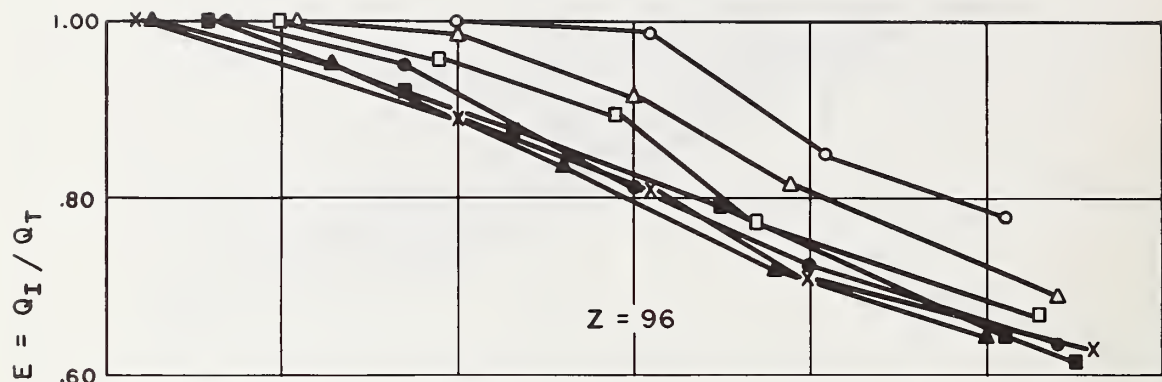


Figure 6-10. - Hydraulic efficiency vs. width of spread, 2 ft by 2 ft (0.61 m by 0.61 m) parallel bar grate, $Z = 96, 48$.

The grate inlet capacity curves shown in figures 6-11 through 6-18 relate gutter flow, Q_T , and longitudinal slope, S_0 , to hydraulic efficiency, E , intercepted flow, Q_I , and calculated width of spread, T . There is one figure for each cross slope, $1/Z$ and grate size. In general, for the parallel bar grate, an increase in the longitudinal slope, S_0 , will increase the grate inlet efficiency for the same gutter flow, Q_T .

Debris Test. - Debris tests were conducted to compare the debris-clogging potential of the parallel bar grate with other grates to be tested and determine its self-cleaning characteristics. Although the types and amount of debris one can expect in a gutter upstream from a particular grate inlet vary widely with time and location, floating debris consisting of leaves, twigs, and paper are quite common in most locations. A standard debris test procedure was developed and used for all the grates tested. The debris used and the test procedure are outlined in Chapter 5 dealing with test procedures.

Each debris test was conducted three times to average the somewhat variable results. One hundred and fifty pieces of 3 in by 4 in (76 mm by 102 mm) paper "leaves" were placed in the gutter upstream from the grate inlet. Each test was conducted in such a manner to insure that all 150 "leaves" arrived at the grate. Tests were conducted at 0.5 percent and 4 percent longitudinal slopes with $Z = 24$. The same test procedure was used for all tests.

Figure 6-19a illustrates the 2 ft by 4 ft (0.61 m by 1.22 m) parallel bar grate during the debris test at a gutter discharge of 2.7 ft³/s (0.076 m³/s). Figure 6-19b shows the distribution of debris on the grate after the test.

The results of these tests for the two grate sizes are presented in table 6-1. Although the debris test results are essentially the same for the two grate sizes at $S_0 = 0.5$ percent, for $S_0 = 4$ percent, the 2 ft by 2 ft (0.61 m by 0.61 m) grate is more efficient at passing debris.

Summary

The parallel bar grate has excellent hydraulic characteristics. Observations during the testing program indicated that the 2 ft by 2 ft (0.61 m by 0.61 m) and 2 ft by 4 ft (0.61 m by 1.22 m) parallel bar grates appear to be as efficient as the same size open holes.

For a given gutter discharge, Q_T , both parallel bar grates were more efficient at steeper longitudinal and cross slopes (figures 6-2 and 6-3). For a given width of spread, T' , both parallel bar grates were more efficient at flatter longitudinal and cross slopes (figures 6-7 through 6-10).

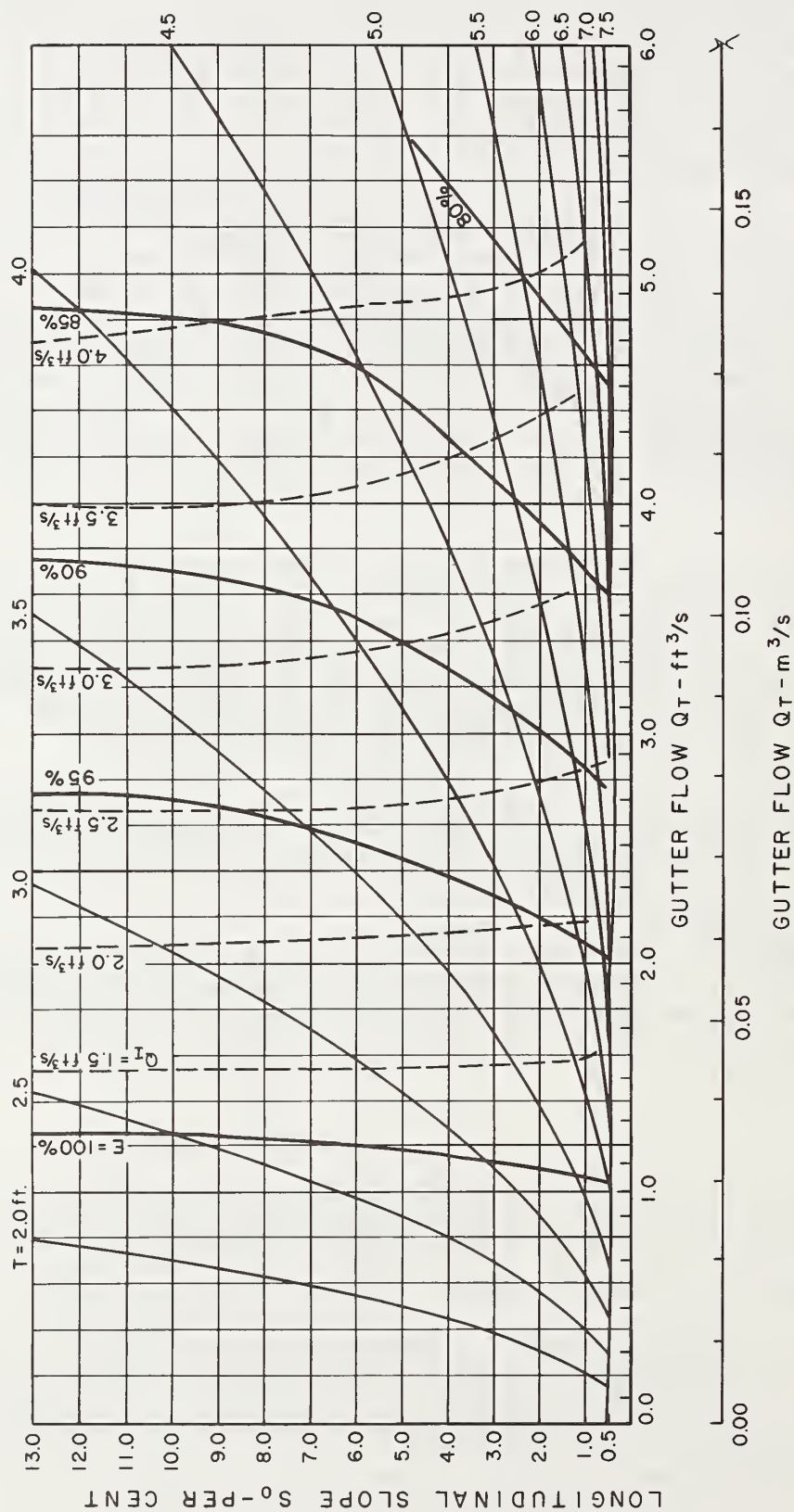


Figure 6-11. - Grate inlet capacity curves, 2 ft by 4 ft (0.61 m by 1.22 m) parallel bar grate, $Z = 16$ (Note: $1 \text{ ft}^3/\text{s} = 0.028 \text{ m}^3/\text{s}$, $1 \text{ ft} = 0.305 \text{ m}$).

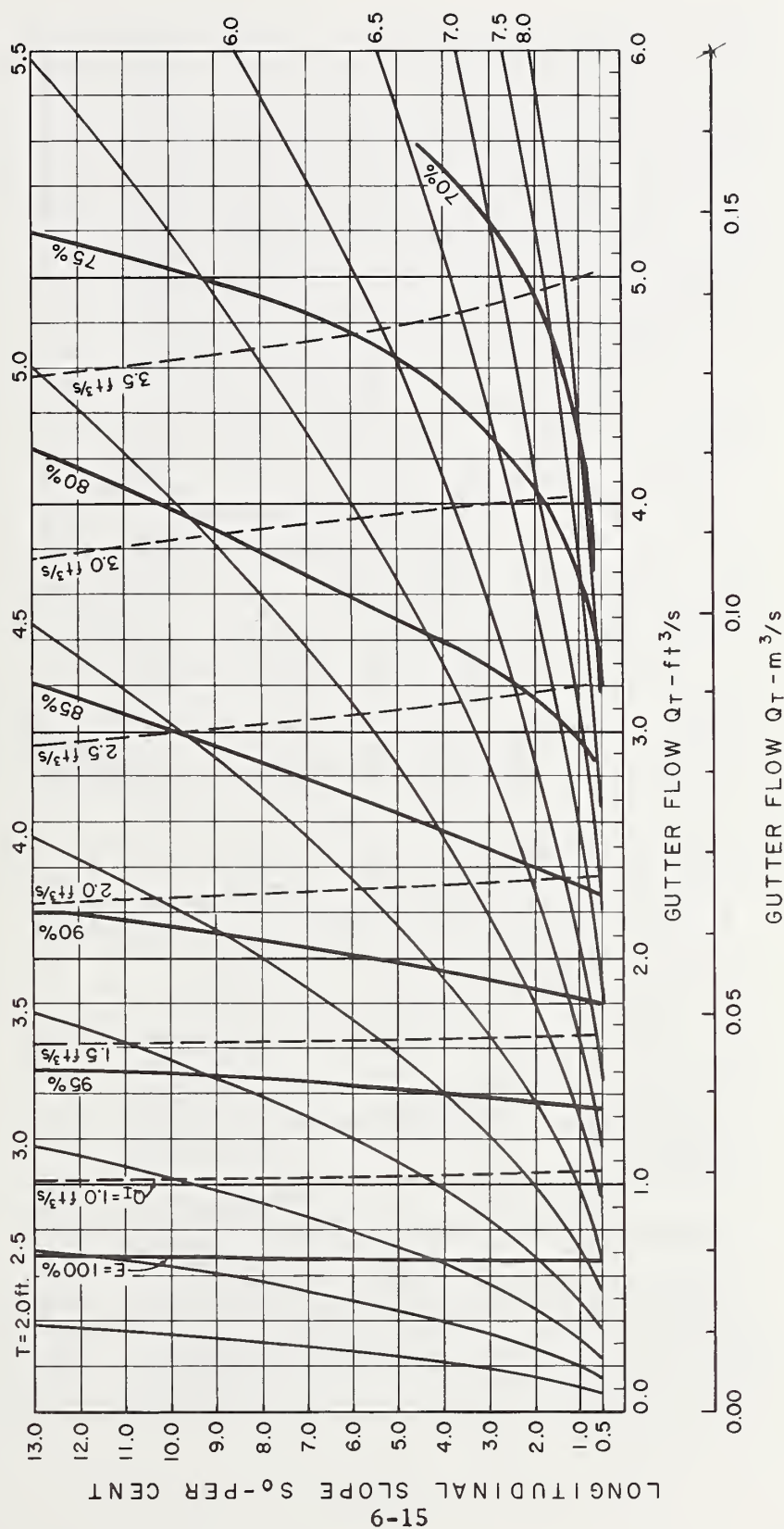


Figure 6-12. - Grate inlet capacity curves, 2 ft by 4 ft (0.61 m by 1.22 m) parallel bar grate, $Z = 24$ (Note: $1 \text{ ft}^3/\text{s} = 0.028 \text{ m}^3/\text{s}$, $1 \text{ ft} = 0.305 \text{ m}$).

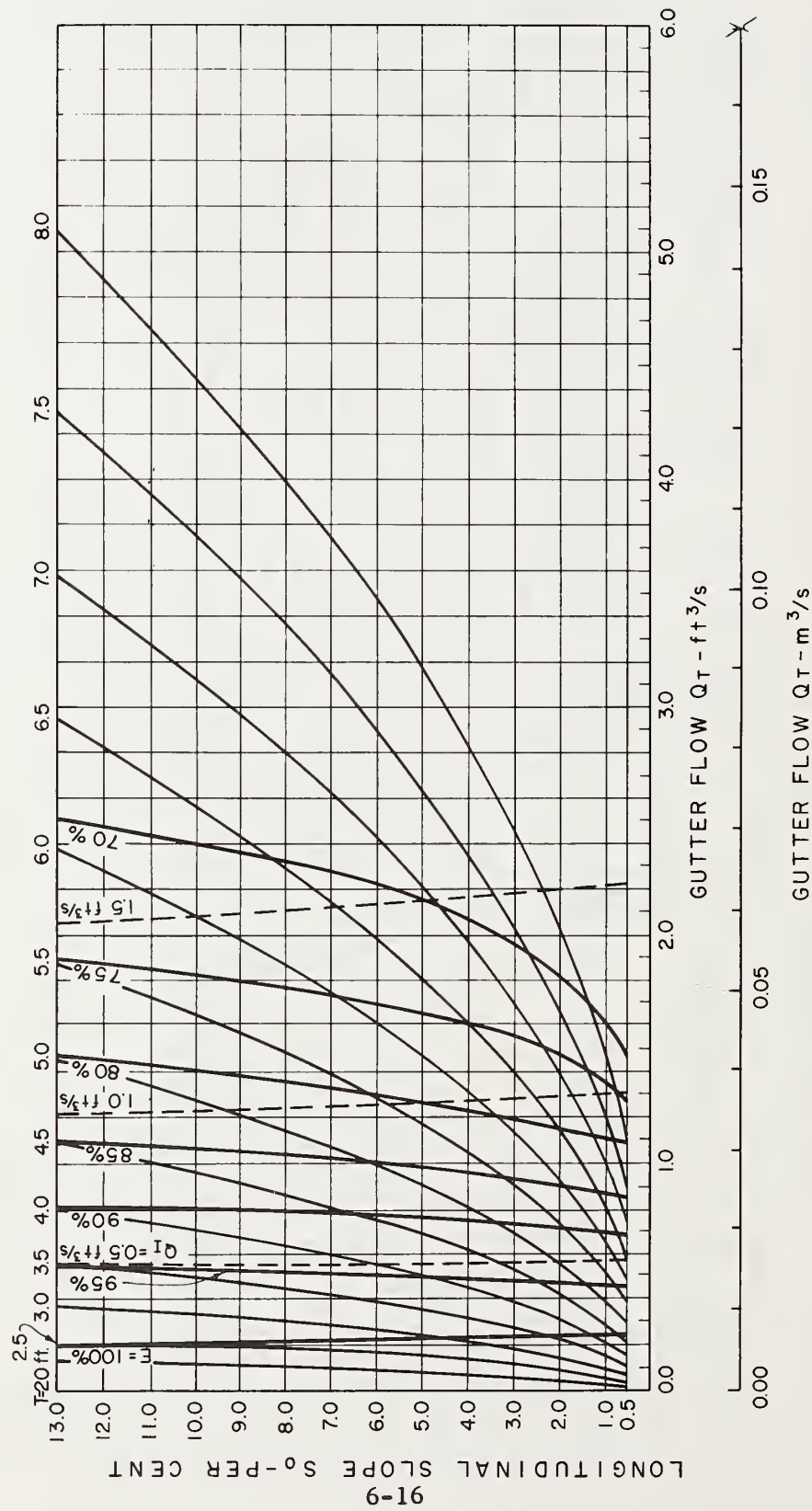


Figure 6-13. - Grate inlet capacity curves, 2 ft by 4 ft (0.61 m by 1.22 m) parallel bar grate, $Z = 48$ (Note: $1 \text{ ft}^3/\text{s} = 0.028 \text{ m}^3/\text{s}$, $1 \text{ ft} = 0.305 \text{ m}$).

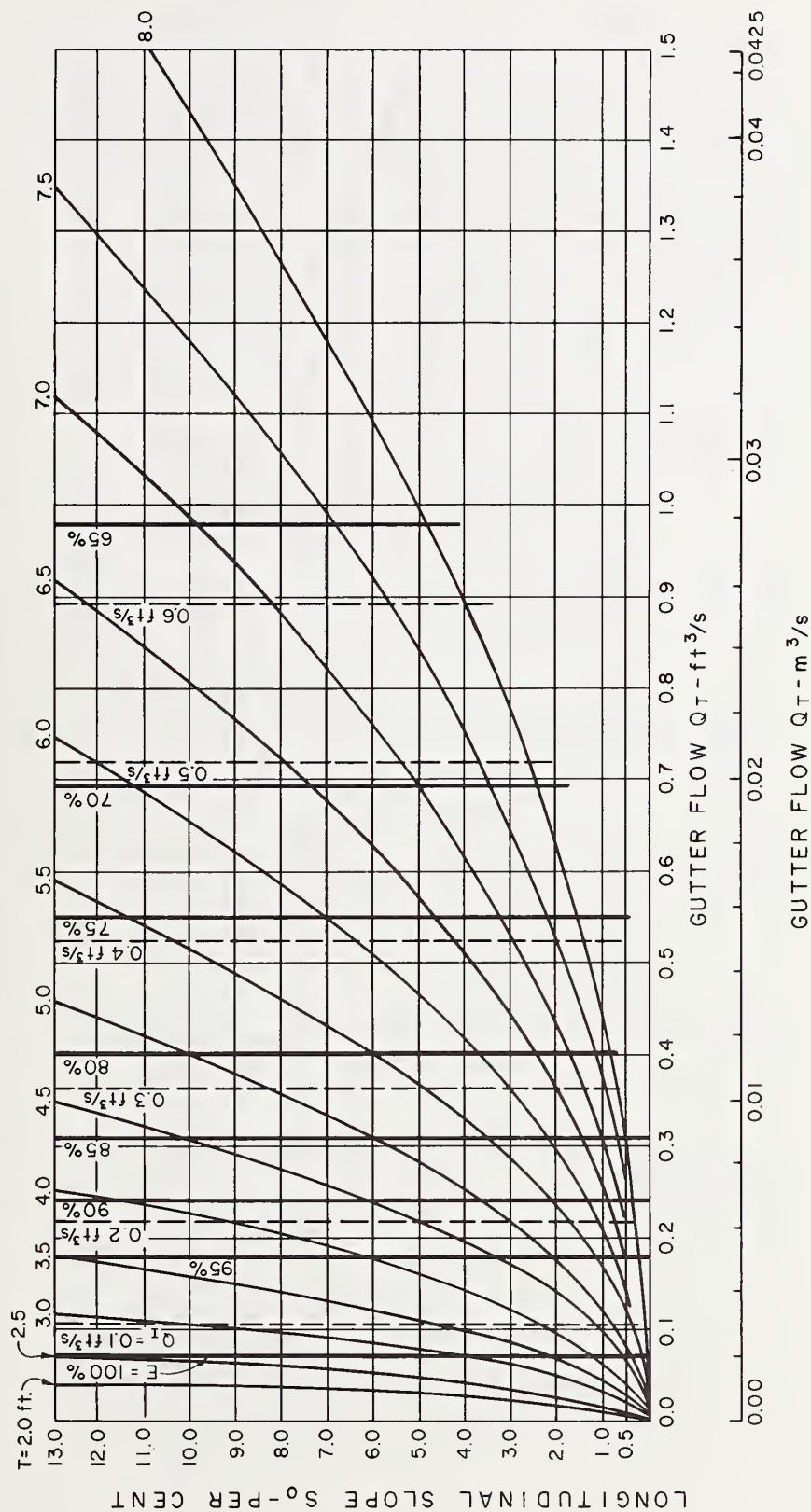


Figure 6-14. - Grate inlet capacity curves, 2 ft by 4 ft (0.61 m by 1.22 m) parallel bar grate, $Z = 96$ (Note: $1 \text{ ft}^3/\text{s} = 0.028 \text{ m}^3/\text{s}$, $1 \text{ ft} = 0.305 \text{ m}$).

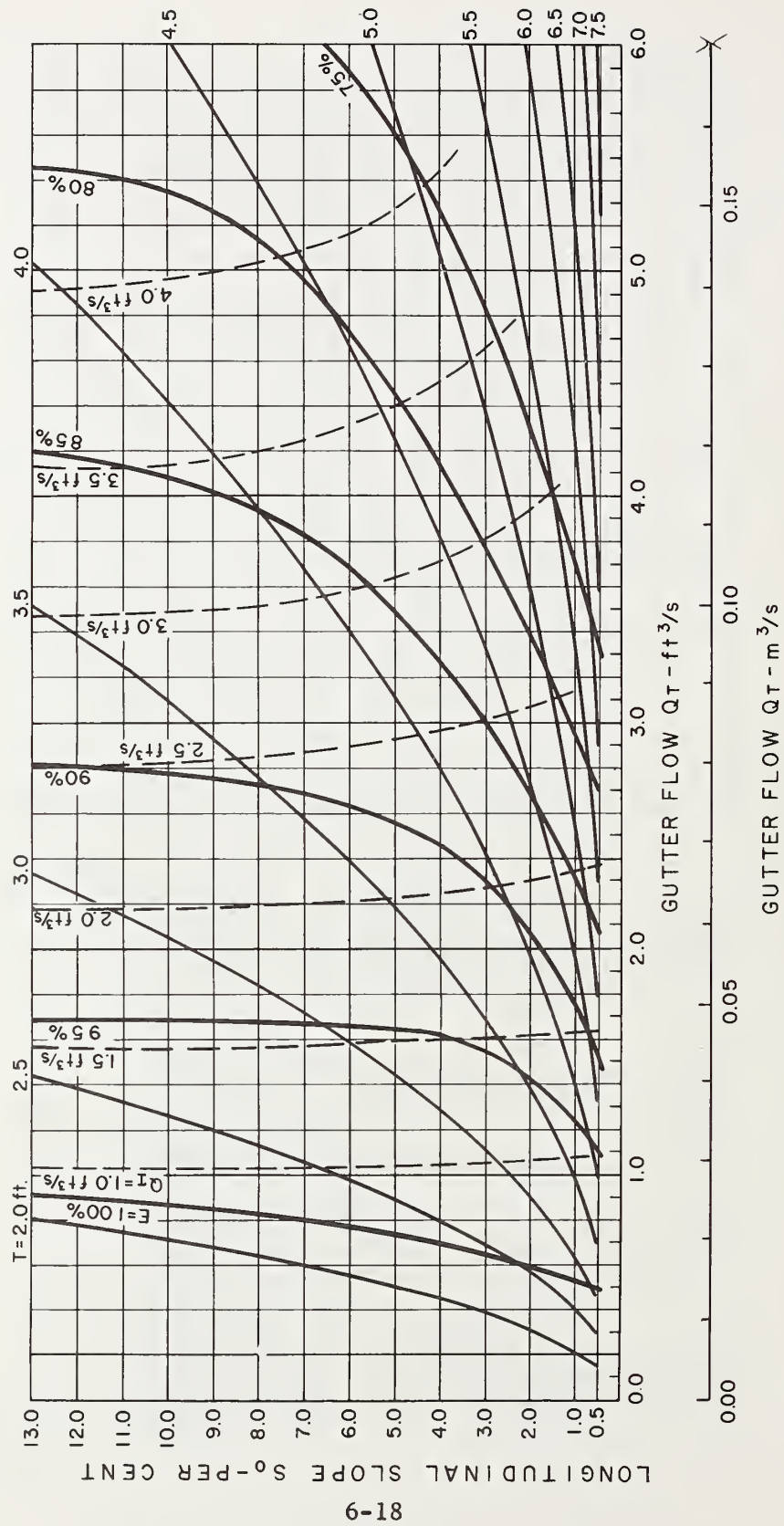


Figure 6-15. - Grate inlet capacity curves, 2 ft by 2 ft (0.61 m by 0.61 m) parallel bar grate, $Z = 16$ (Note: $1 \text{ ft}^3/\text{s} = 0.028 \text{ m}^3/\text{s}$, $1 \text{ ft} = 0.305 \text{ m}$).

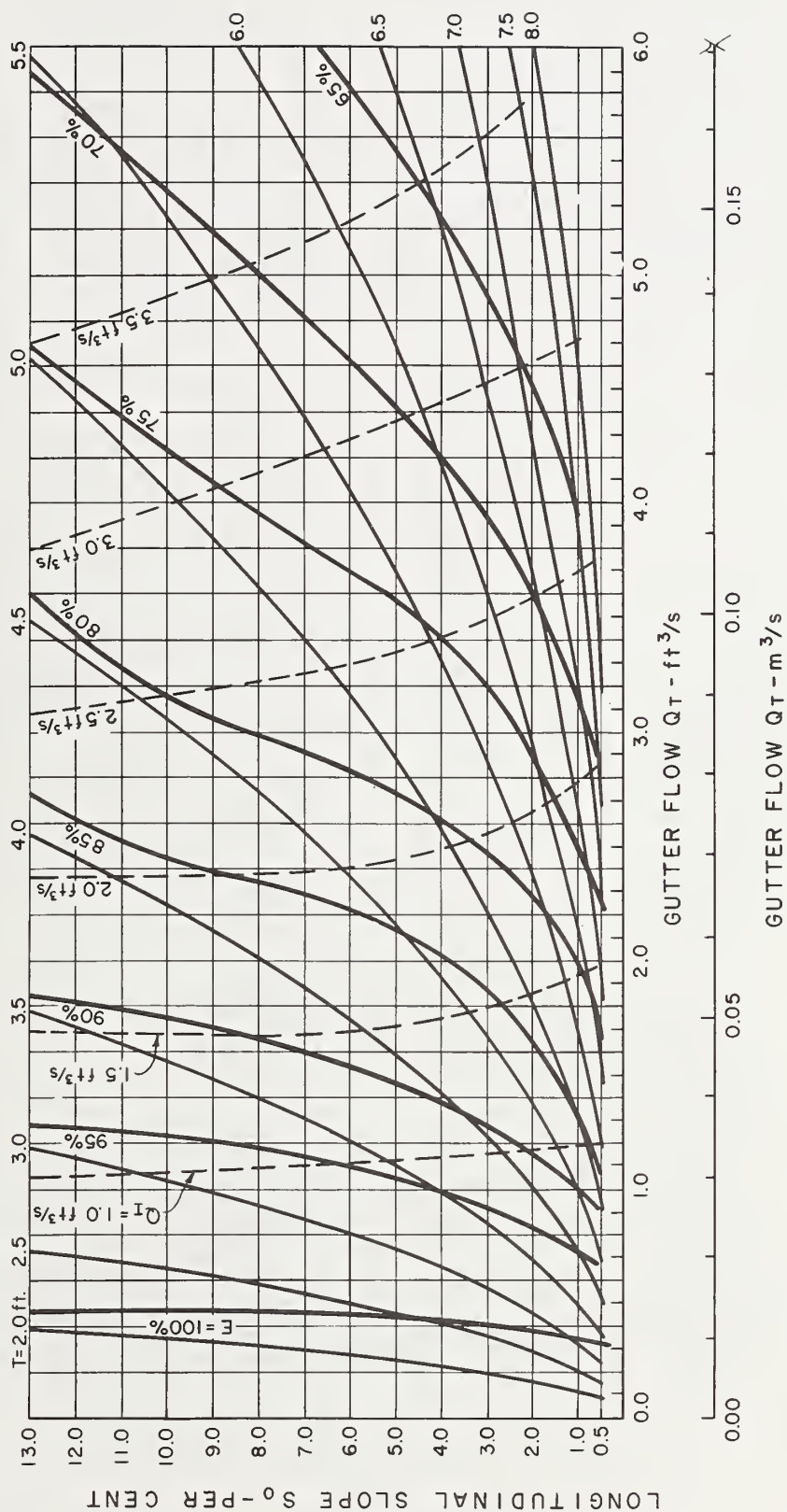


Figure 6-16. - Grate inlet capacity curves, 2 ft by 2 ft (0.61 m by 0.61 m) parallel bar grate,
 $Z = 24$ (Note: $1 \text{ ft}^3/\text{s} = 0.028 \text{ m}^3/\text{s}$, $1 \text{ ft} = 0.305 \text{ m}$).

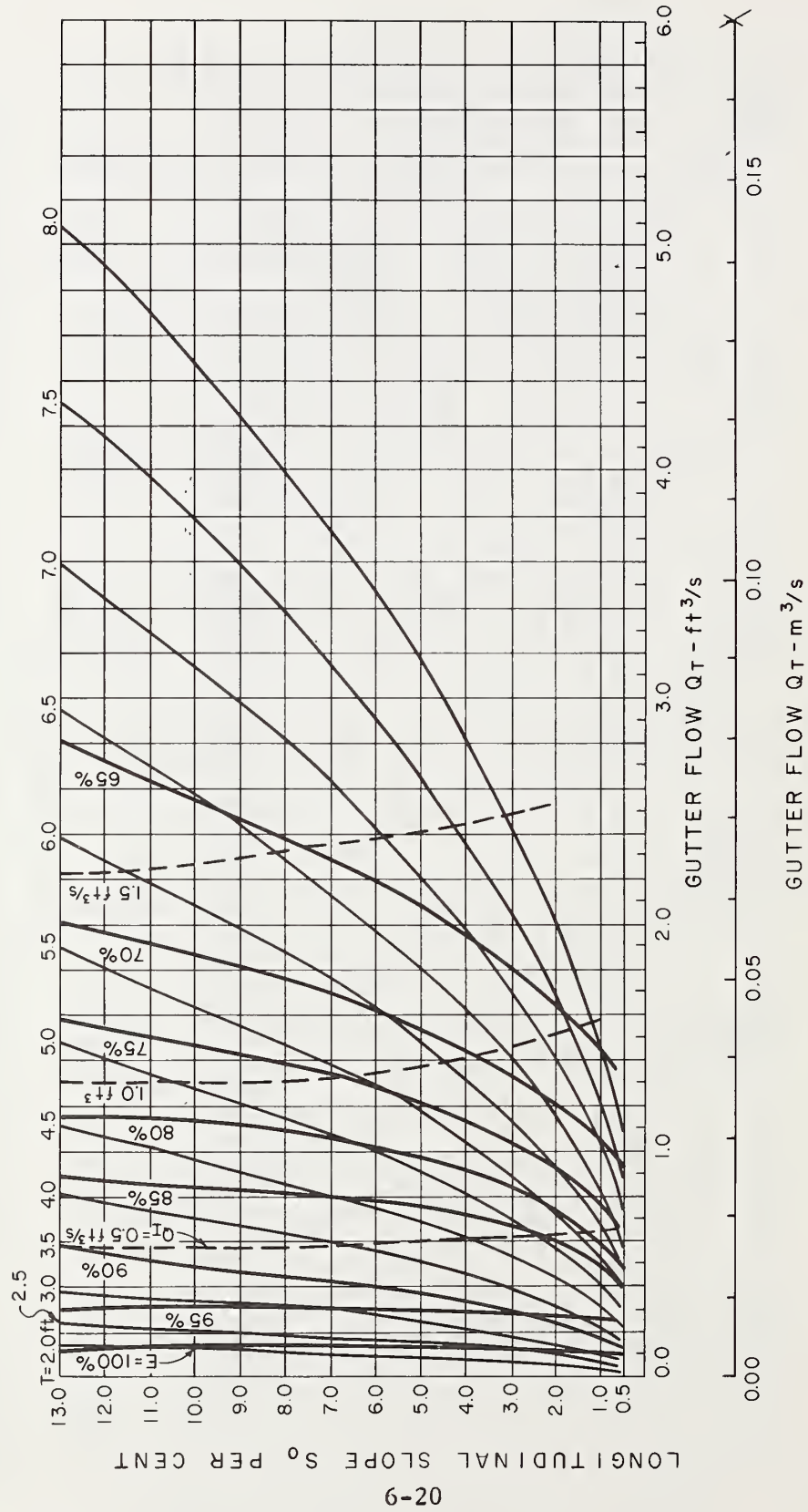


Figure 6-17. - Grate inlet capacity curves, 2 ft by 2 ft (0.61 m by 0.61 m) parallel bar grate,
 $Z = 48$ (Note: $1 \text{ ft}^3/\text{s} = 0.028 \text{ m}^3/\text{s}$, $1 \text{ ft} = 0.305 \text{ m}$).

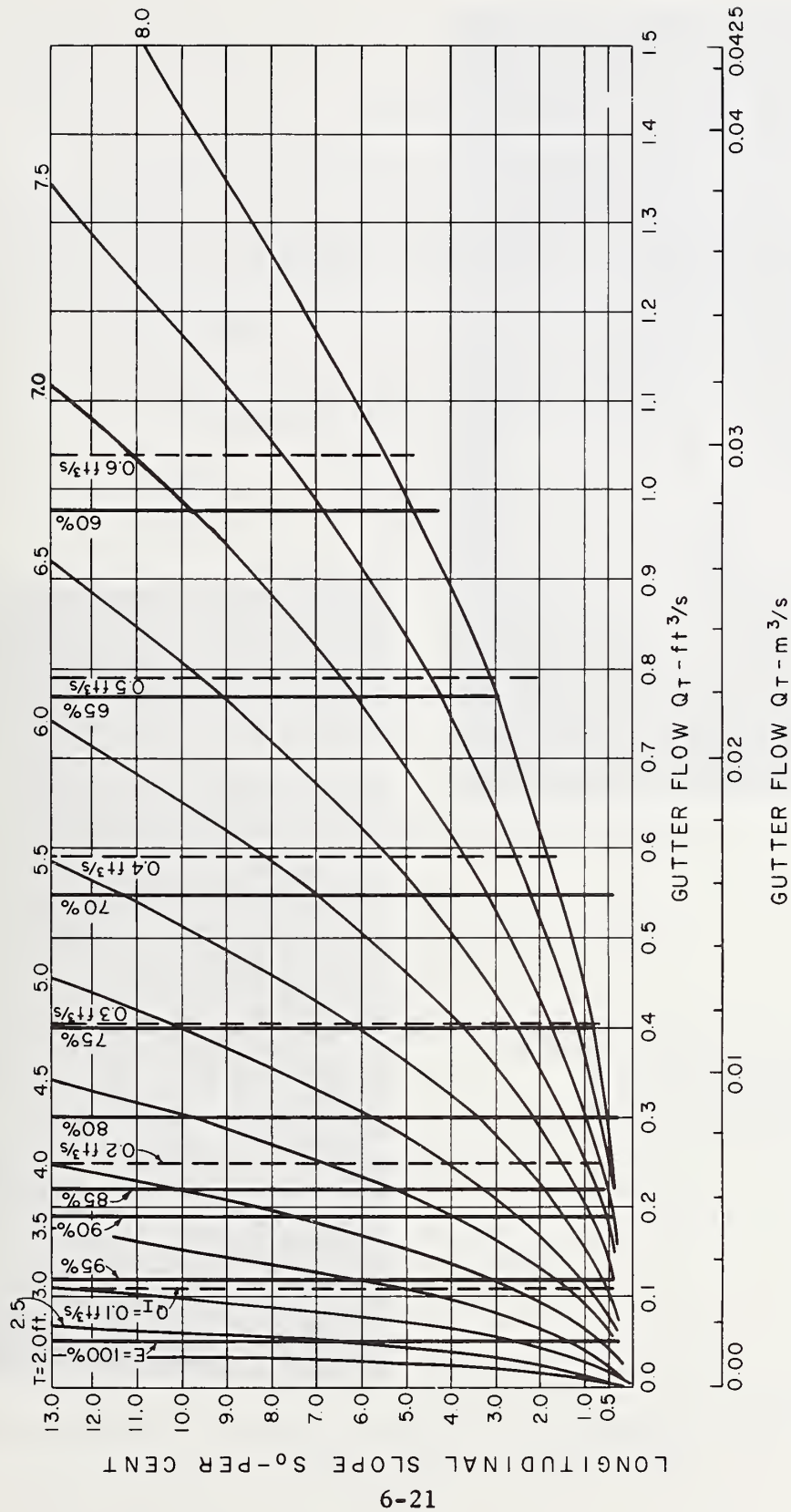


Figure 6-18. - Grate inlet capacity curves, 2 ft by 2 ft (0.61 m by 0.61 m) parallel bar grate,
 $Z = 96$ (Note: 1 $\text{ft}^3/\text{s} = 0.028 \text{ m}^3/\text{s}$, 1 ft = 0.305 m).



a. $Q_T = 2.7 \text{ ft}^3/\text{s} \text{ (} 0.076 \text{ m}^3/\text{s)}$

$T' = 5.4 \text{ ft (} 1.65 \text{ m)}$

Photo 63-5

- b. View looking downstream at
106 pieces of debris
caught on the grate.
Photo 63-6



Figure 6-19. - Debris test, 2 ft by 4 ft (0.61 m by 1.22 m) parallel bar grate, $S_0 = 4\%$, $Z = 24$.

Table 6-1

DEBRIS TEST RESULTS - PARALLEL BAR GRATES

Test No.	Number of "leaves" lodged on grate*			
	$S_0 = 0.5\%$		$S_0 = 4.0\%$	
	5 minutes	15 minutes	5 minutes	15 minutes
<u>2 ft by 2 ft (0.61 m by 0.61 m) grate</u>				
1	116	101		
2	106	99		
3	119	108		
4			120	94
5			106	94
6			110	101
Debris handling efficiency* (%)	24	32	25	36
<u>2 ft by 4 ft (0.61 m by 1.22 m) grate</u>				
1			-	-
2			130	110
3			126	106
4	107	91		
5	129	113		
6	117	99		
Debris handling efficiency* (%)	22	33	15	28

* Based on 150 "leaves" arriving at the grate.

Since the hydraulic efficiency, E , is a ratio of the intercepted flow, Q_I , to the total gutter flow, Q_T , it is apparent that a rather high efficiency, E , could yield a low intercepted flow, Q_I , if the gutter flow, Q_T , is low. Figures 6-2 and 6-3 illustrate the much higher capacity for gutter flow, Q_T , and therefore intercepted flow, Q_I , with $Z = 16$ and 24 as compared to $Z = 48$ and 96 .

The debris tests showed that a considerable number of the "leaves" straddled the parallel bars of the grate. Approximately 33 percent of the "leaves" passed through the grate for 15 minutes of gutter flow, but only 22 percent during the first 5 minutes of gutter flow.

CHAPTER 7

HYDRAULIC EFFICIENCY AND DEBRIS TESTS - RETICULINE GRATES

Introduction

This chapter describes the results of hydraulic tests conducted on the reticuline or "honeycomb" grate. The reticuline or honeycomb pattern has been recommended in several publications as a bicycle-safe alternative to the parallel bar grate. This design has proven to be bicycle-safe, but little data have been available on its hydraulic efficiency or debris handling characteristics.

The tested grate sizes were modifications of a standard 24 in by 40 in (0.61 m by 1.02 m) manufactured grate. The grate is constructed of 1/4 in (6.4 mm) wide by 4 in (102 mm) deep bearing bars to which 3/16 in (4.8 mm) wide by 2 in (51 mm) deep reticuline bars are riveted on 5 in (127 mm) centers. Figure 7-1 shows the actual dimensions of the 2 ft by 4 ft (0.61 m by 1.22 m) grate tested. In the report, the grates are identified by their nominal sizes of 2 ft by 2 ft (0.61 m by 0.61m) and 2 ft by 4 ft (0.61 m by 1.22 m).

Experimental Results and Observations

Hydraulics. - Hydraulic test results for the reticuline grates are shown in figures 7-2 and 7-3. Hydraulic efficiencies, E , for the 2 ft (0.61m) long grate were always lower than those for the 4 ft (1.22 m) long grate.

At mild longitudinal slopes, the 4 ft (1.22 m) grate is more efficient because it captures more flow along its side. At steep longitudinal slopes, the 4 ft (1.22 m) grate captures more of the flow passing over it because of its greater area.

Major differences in efficiency for similar flow and cross slope conditions on different longitudinal slopes, are caused by flow splashing completely across the grate.

Flowrates for $Z = 96$ were not great enough to cause any splash which would reduce the efficiency of the grates as the longitudinal slope was increased. Even at a 13 percent street grade, all splash was recaptured within the first 2 ft (0.61 m) of the grate. At $Z = 48$, some of the flow splashed over the 2 ft (0.61 m) long grate but not the 4 ft (1.22 m) long grate. The sequence of photographs in figure 7-4 shows the development of splash on the 2 ft by 2 ft (0.61 m by 0.61 m) grate at $Z = 48$ as the longitudinal slope is increased from 4 to 13 percent. At cross slopes of $Z = 24$ and $Z = 16$, the actual height of the splash above the grate decreased as the longitudinal slope was increased. Though the splash was much less

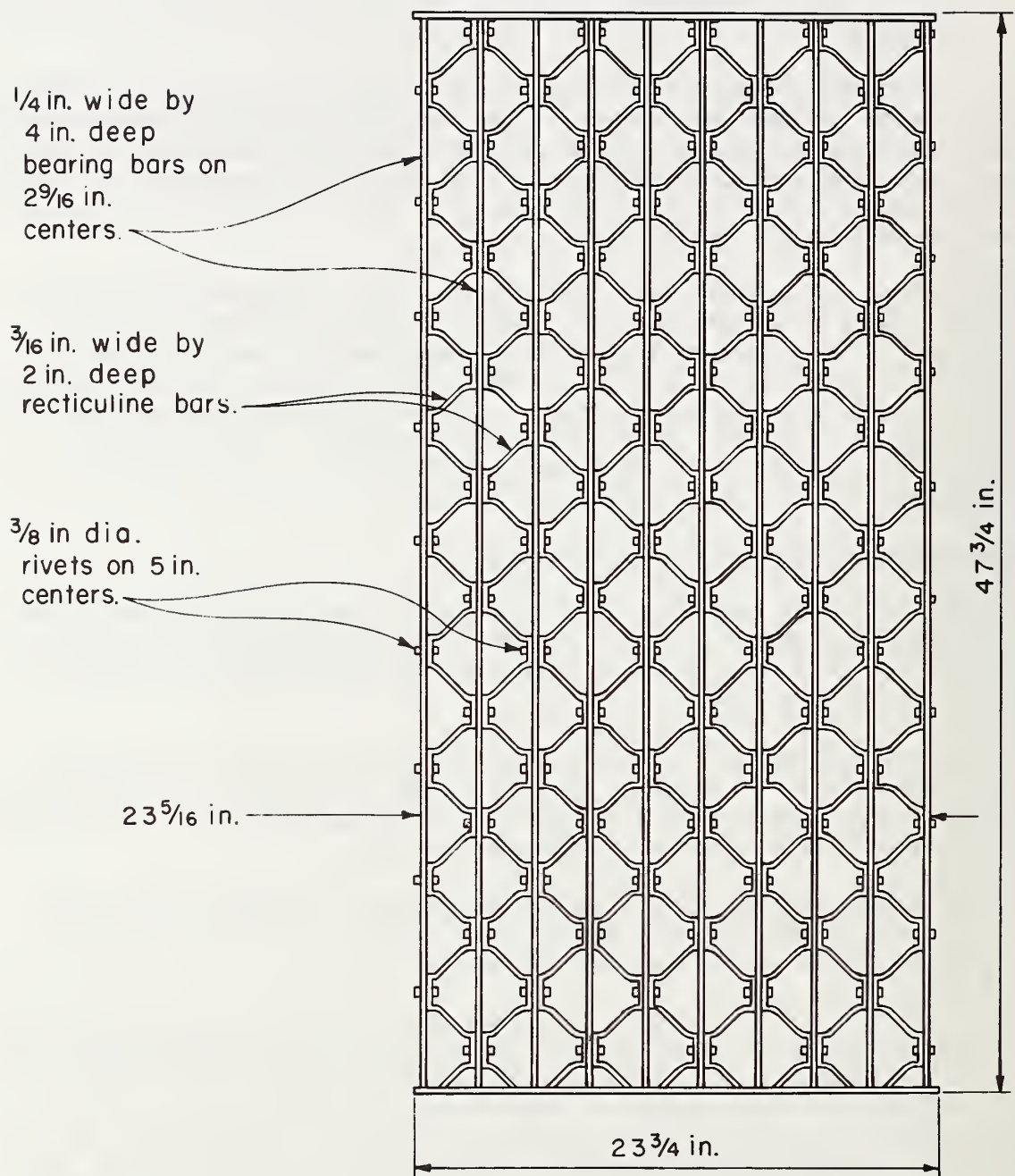


Figure 7-1. - 2 ft by 4 ft (0.61 m by 1.22 m) steel fabricated reticuline grate (Note: 1 in = 25.4 mm).

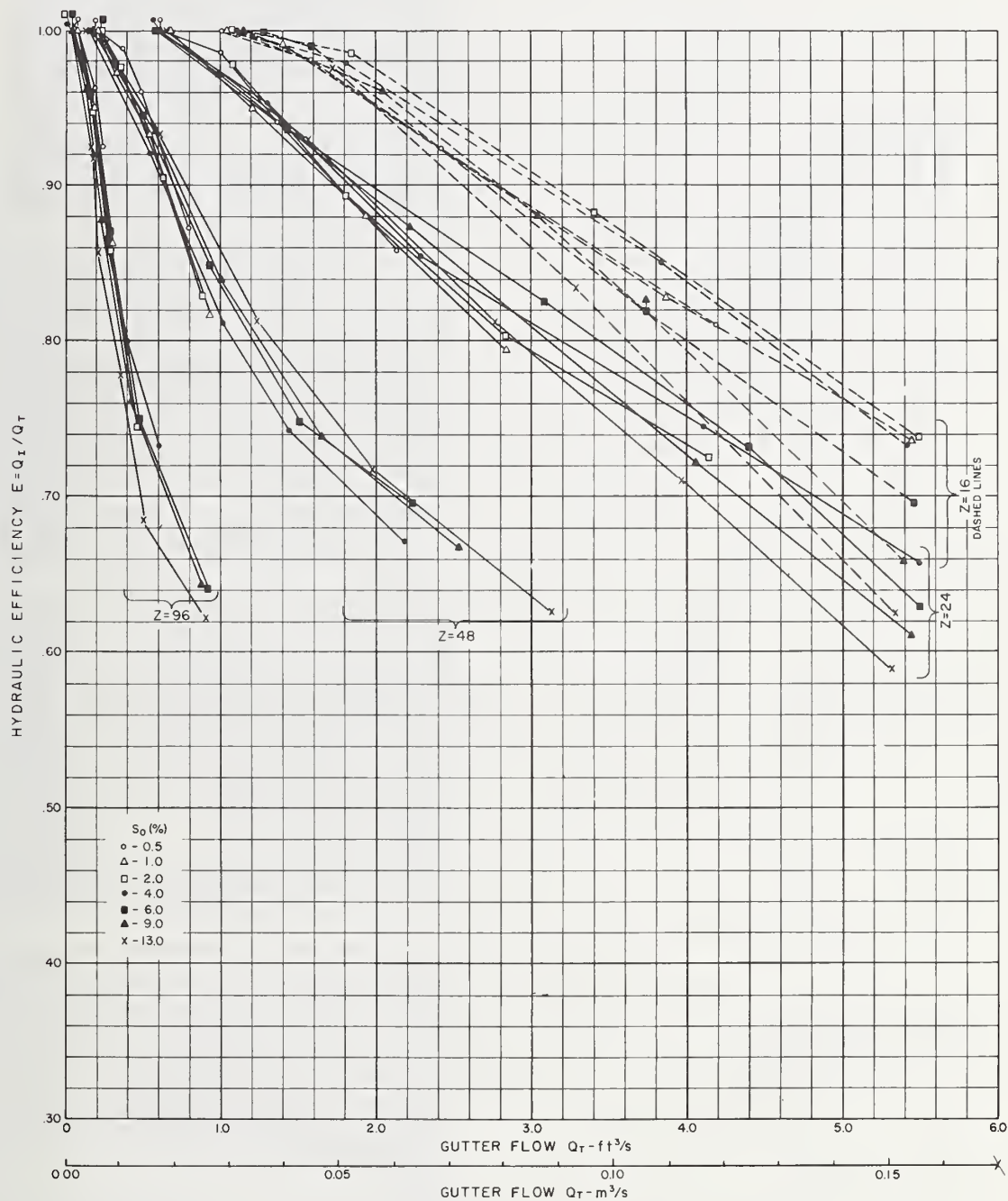


Figure 7-2. - Hydraulic efficiency vs. gutter flow, 2 ft by 4 ft (0.61 m by 1.22 m) reticulate grate.

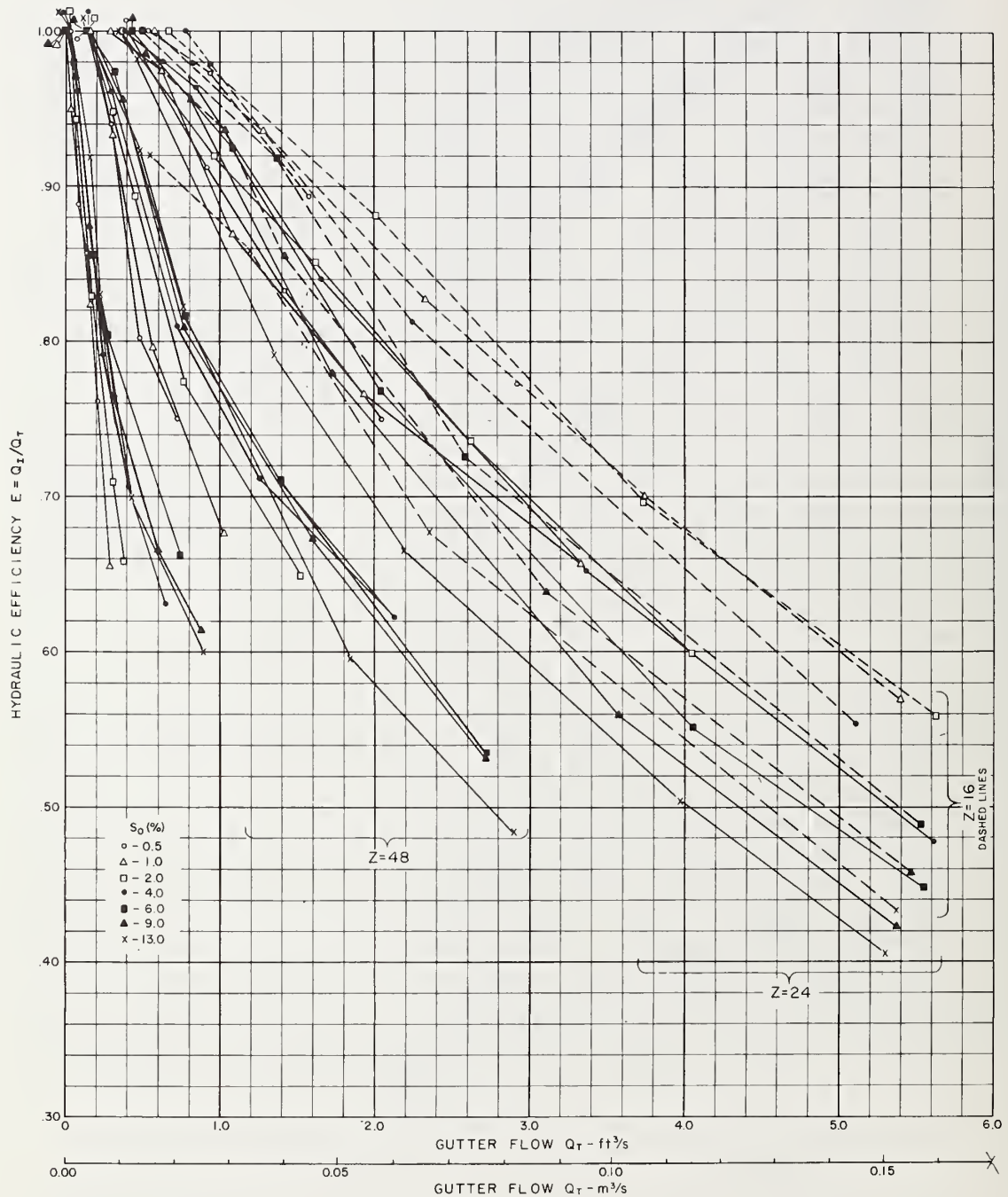
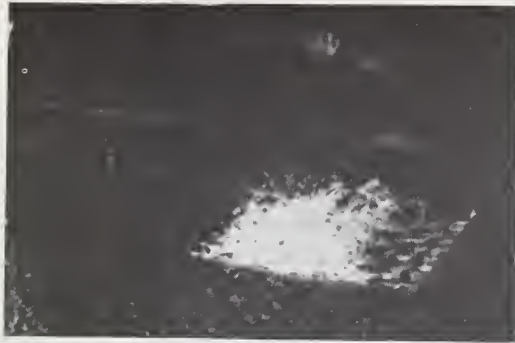
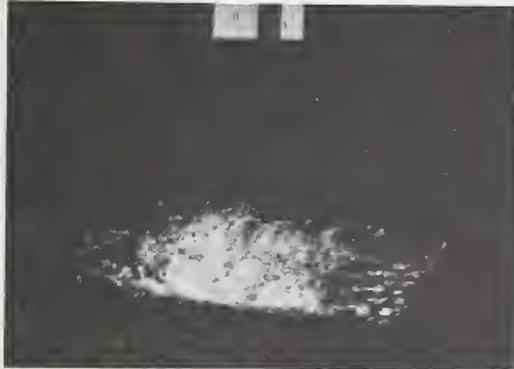


Figure 7-3. - Hydraulic efficiency vs. gutter flow, 2 ft by 2 ft (0.61 m by 0.61 m) reticulate grate.



- a. $S_0 = 4\%$
 $Q_T = 2.12 \text{ ft}^3/\text{s} \text{ (} 0.06 \text{ m}^3/\text{s)}$
 $T' = 7.3 \text{ ft (} 2.22 \text{ m)}$
 $E = 62\%$



- b. $S_0 = 6\%$
 $Q_T = 2.69 \text{ ft}^3/\text{s} \text{ (} 0.075 \text{ m}^3/\text{s)}$
 $T' = 7.0 \text{ ft (} 2.13 \text{ m)}$
 $E = 54\%$



- c. $S_0 = 9\%$
 $Q_T = 2.71 \text{ ft}^3/\text{s} \text{ (} 0.077 \text{ m}^3/\text{s)}$
 $T' = 7.3 \text{ ft (} 2.22 \text{ m)}$
 $E = 53\%$



- d. $S_0 = 13\%$
 $Q_T = 2.89 \text{ ft}^3/\text{s} \text{ (} 0.082 \text{ m}^3/\text{s)}$
 $T' = 7.2 \text{ ft (} 2.19 \text{ m)}$
 $E = 48\%$

Figure 7-4. - Development of splash on 2 ft by 2 ft (0.61 m by 0.61 m) reticuline grate, $Z = 48$. Photo H-1765-359

noticeable at the steeper longitudinal slopes, the hydraulic efficiency was still lower. Much of the flow actually skipped across the reticuline bars without splashing or passing through the grate. Figure 7-5 shows this phenomenon occurring on the 4 ft (1.22 m) long reticuline grate for $Z = 24$ at slopes of 6 and 13 percent. Figures 7-2 and 7-3 show the effects of longitudinal and cross slope on the amount of splash. For any gutter flow, Q_T , the S_0 lines for $Z = 96$ are very close together since no splash carries across the grates. At the other extreme, the lines for different longitudinal slopes, S_0 , on $Z = 16$ are spread apart as much as 13 percent because of the loss of efficiency due to splash at the steep longitudinal slopes.

Figures 7-6 and 7-7 show the relationship between the measured width of spread, T' , and the hydraulic efficiency, E , for the two grates. For the same width of spread, hydraulic efficiencies increase as the street grade and cross slope are decreased.

The grate inlet capacity curves in figures 7-8 through 7-15 relate gutter flow Q_T , and longitudinal slope, S_0 , to hydraulic efficiency, E , intercepted flow, Q_I , and width of spread, T . In these figures, width of spread, T , has been calculated using Izzard's equation. For a given gutter flow, the hydraulic efficiencies of the reticuline grates increase with increasing longitudinal slope until they reach some maximum value. The longitudinal slope where this maximum efficiency is reached depends on the grate's length, the cross slope, and the gutter flow. The maximum efficiency slopes for the reticuline grates are shown in table 7-1. The slopes are obtained from the inlet capacity curves by following a line of constant gutter flow and noting where the efficiency is maximum. Since the maximum efficiency slope is dependent on the gutter flow, the table shows a range of longitudinal slopes where each grate is most efficient.

Table 7-1

MAXIMUM EFFICIENCY SLOPES - RETICULINE GRATES

Grate Size	$Z = 96$	$Z = 48$	$Z = 24$	$Z = 16$
2 ft by 2 ft (0.61 m by 0.61 m)	8% to 13%	5% to 6%	2% to 3%	.5% to 2%
2 ft by 4 ft (0.61 m by 1.22 m)	4% to 7%	13%	4% to 6%	2% to 3%



a. $S_0 = 6\%$ $T' = 5.8 \text{ ft (1.77 m)}$
 $Q_T = 4.20 \text{ ft}^3/\text{s (0.119 m}^3/\text{s)}$ $E = 75\%$
 Photo 24.1-9



b. $S_0 = 13\%$ $T' = 5.8 \text{ ft (1.77 m)}$
 $Q_T = 5.31 \text{ ft}^3/\text{s (0.150 m}^3/\text{s)}$ $E = 59\%$
 Photo 23-3

Figure 7-5. - Variation in splash height with changing longitudinal slope for 2 ft by 4 ft (0.61 m by 1.22 m) reticuline grate, $Z = 24$.

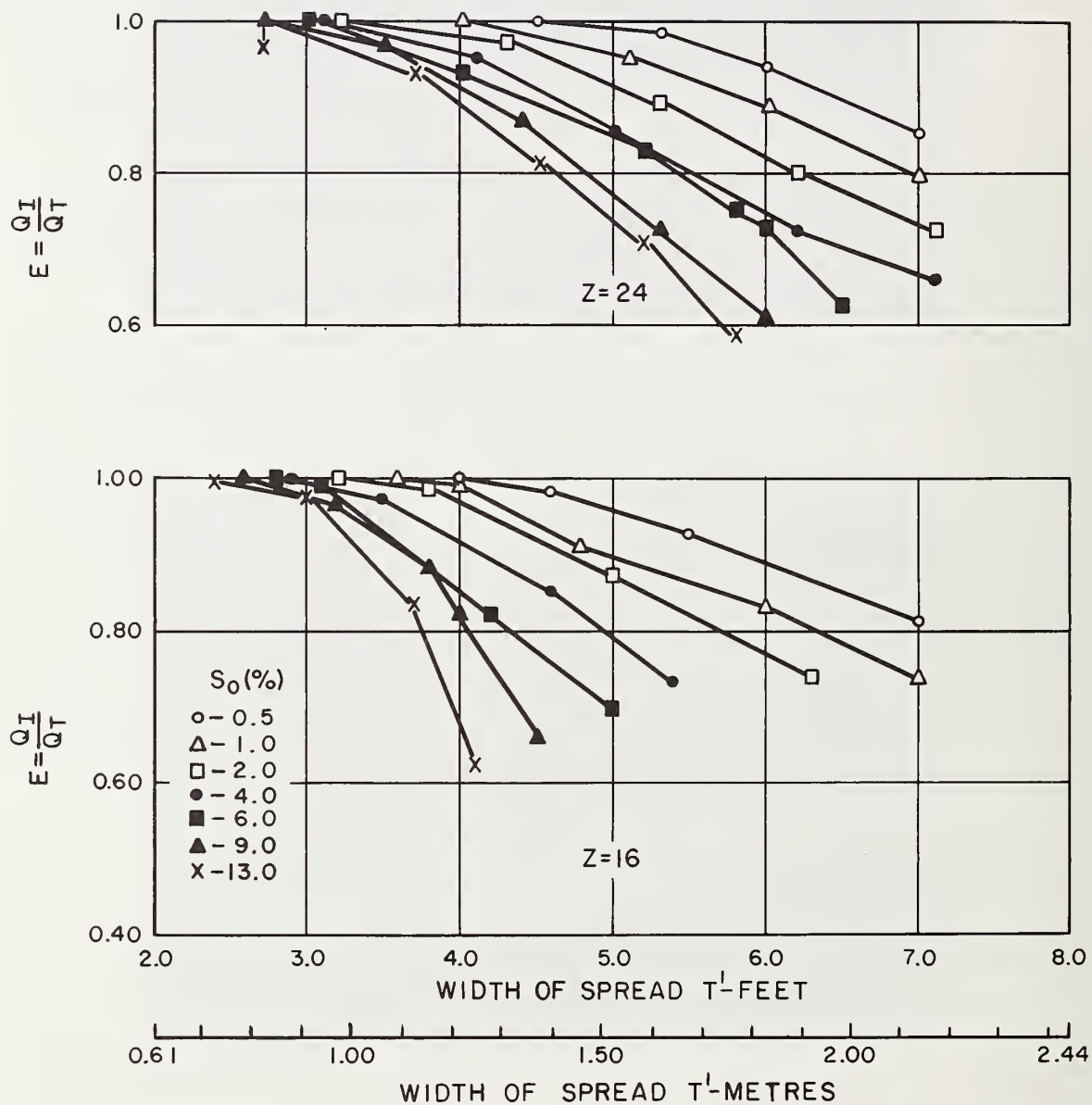


Figure 7-6. - Hydraulic efficiency vs. width of spread, 2 ft by 4 ft (0.61 m by 1.22 m) reticuline grate, $Z = 24$ and 16.

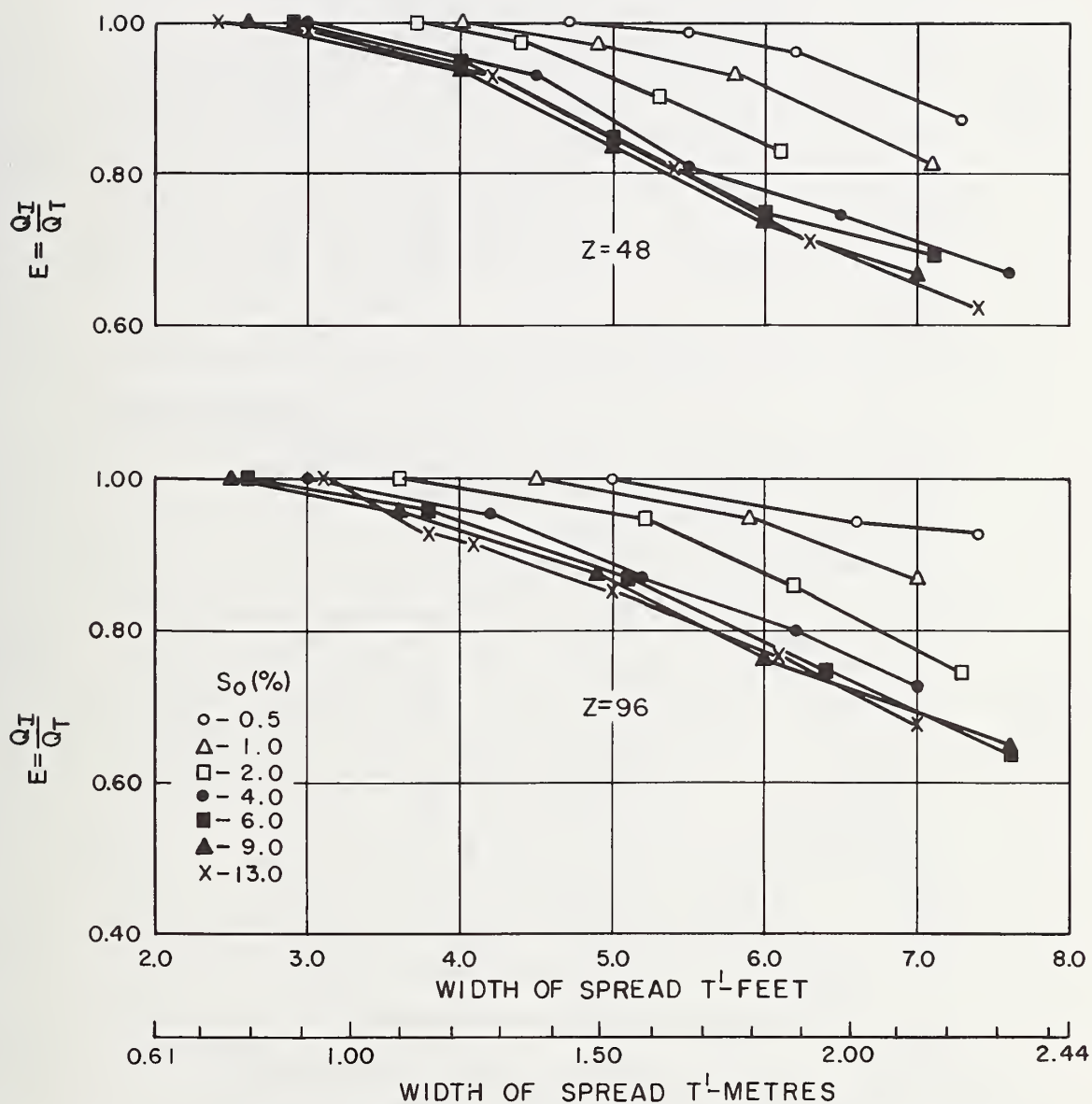


Figure 7-6. - (continued) Hydraulic efficiency vs. width of spread, 2 ft by 4 ft (0.61 m by 1.22 m) reticuline grate, $Z = 48$ and 96.

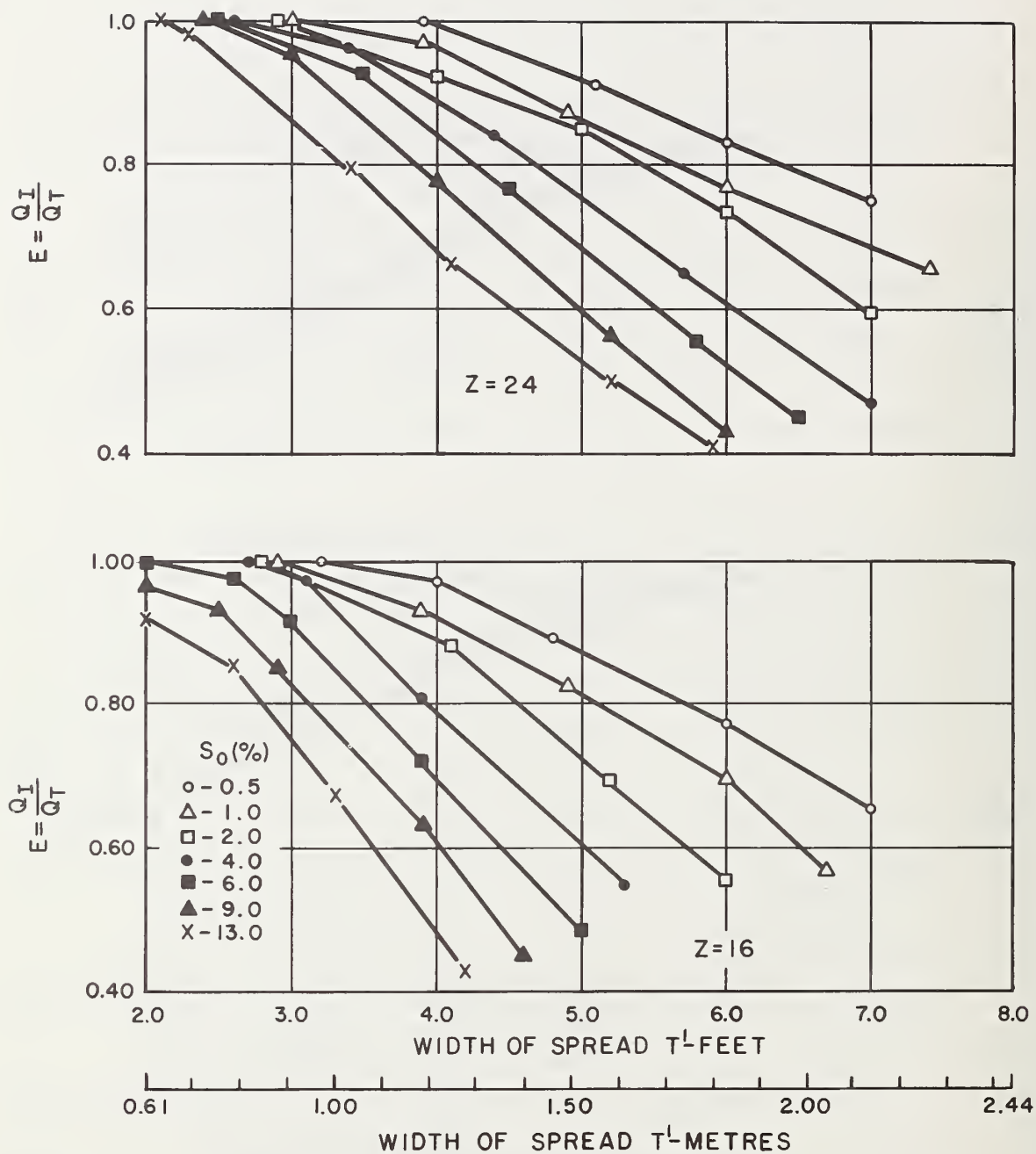


Figure 7-7. - Hydraulic efficiency vs. width of spread, 2 ft by 2 ft (0.61 m by 0.61 m) reticuline grate, Z = 24 and 16.

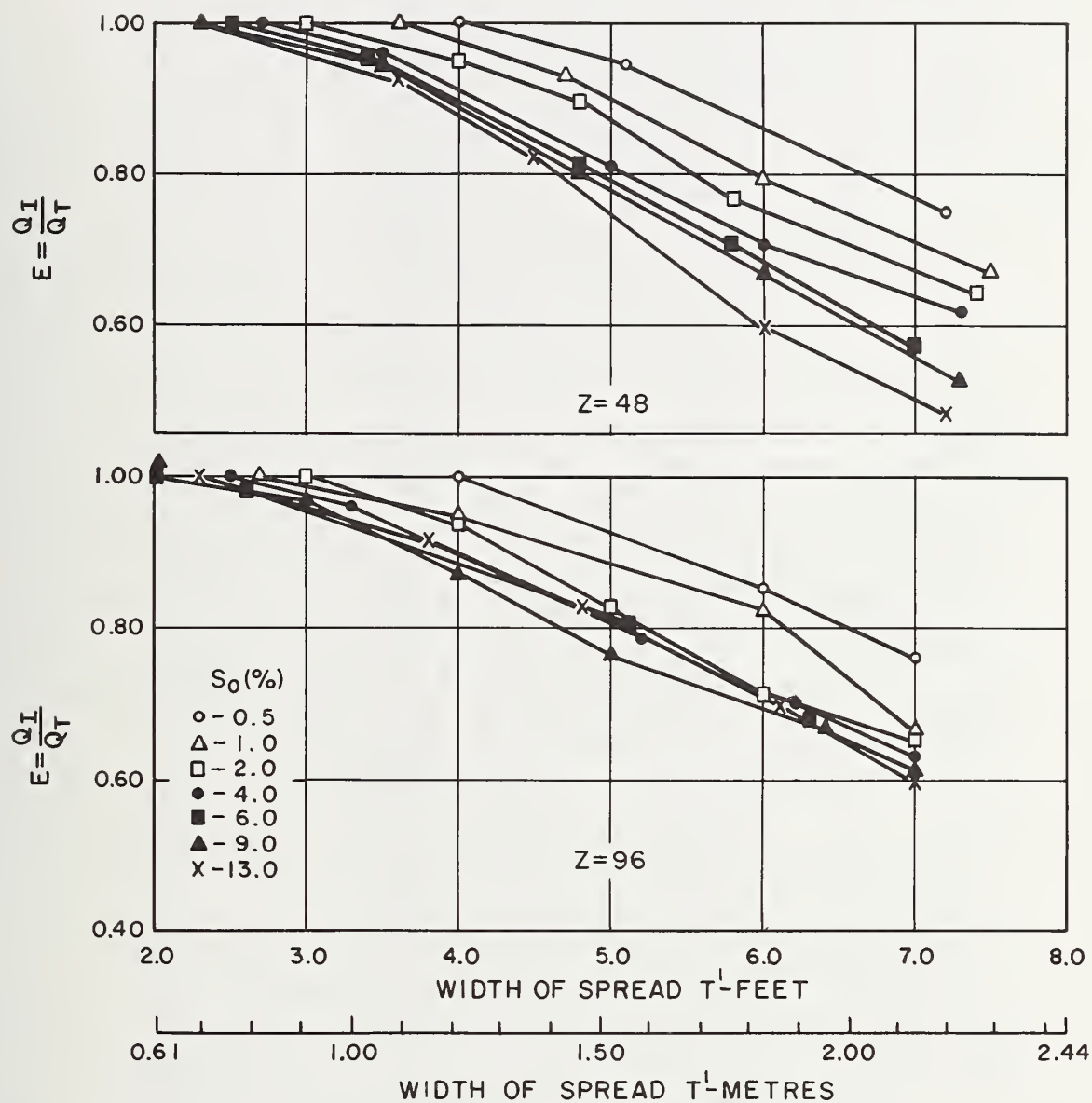


Figure 7-7. - (continued) Hydraulic efficiency vs. width of spread, 2 ft by 2 ft (0.61 m by 0.61 m) reticuline grate, $Z = 48$ and 96.

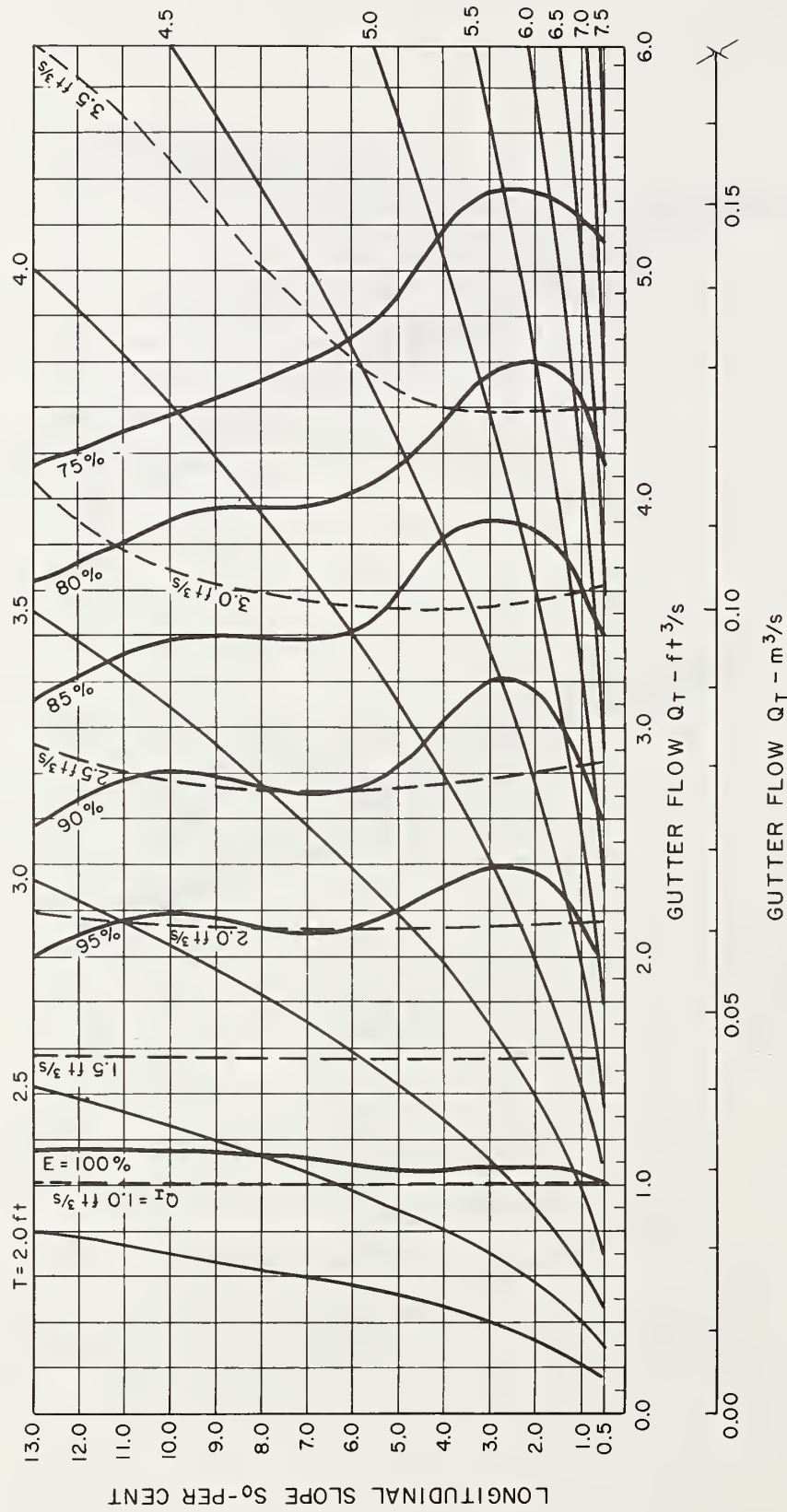


Figure 7-8. - Grate inlet capacity curves, 2 ft by 4 ft (0.61 m by 1.22 m) reticulate grate, $Z = 16$
(Note: 1 ft = 0.305 m, 1 ft^3/s = 0.028 m^3/s).

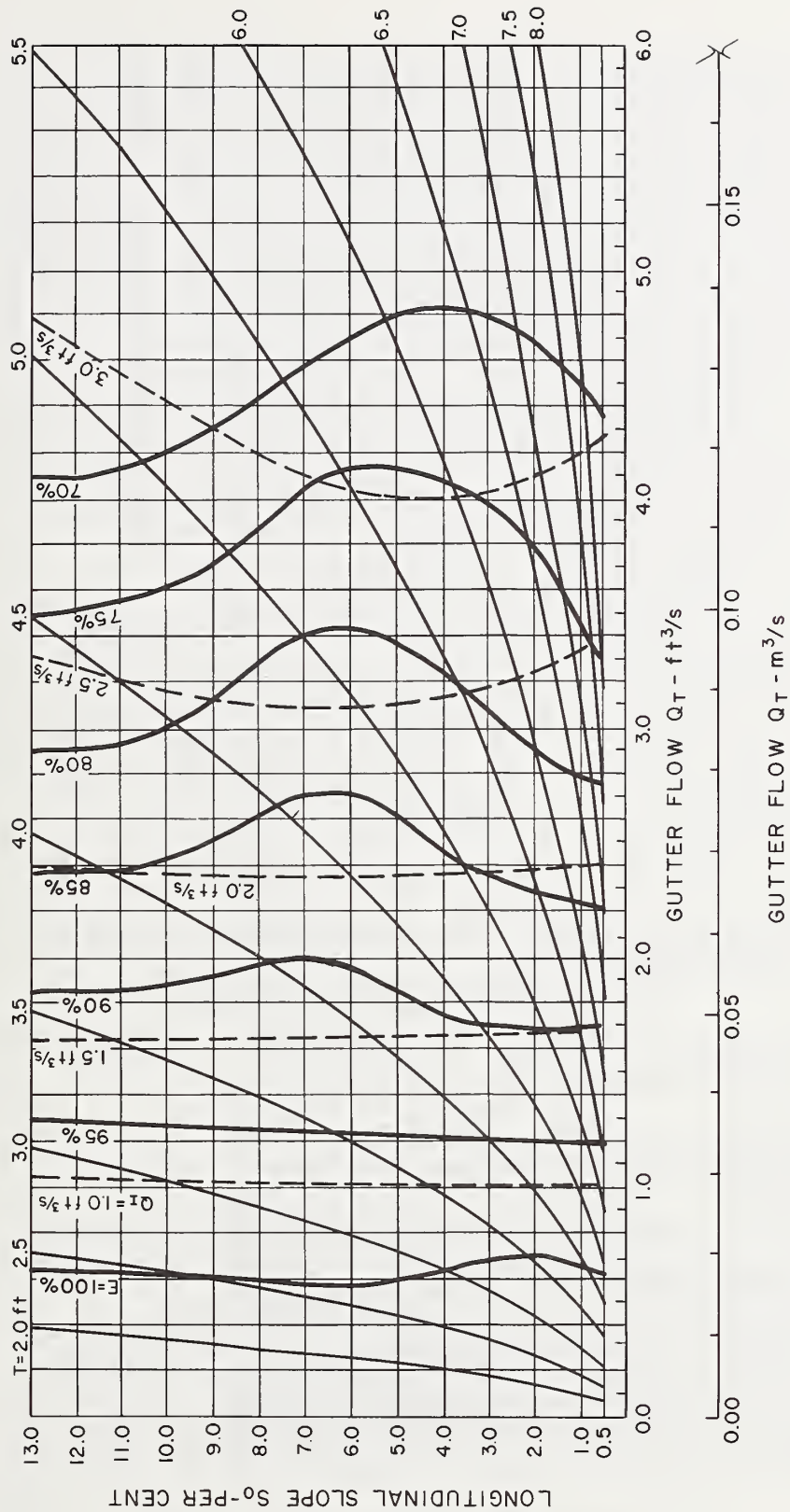


Figure 7-9. - Grate inlet capacity curves, 2 ft by 4 ft (0.61 m by 1.22 m) reticulate grate, $Z = 24$
 (Note: $1 \text{ ft} = 0.305 \text{ m}$, $1 \text{ ft}^3/\text{s} = 0.028 \text{ m}^3/\text{s}$).

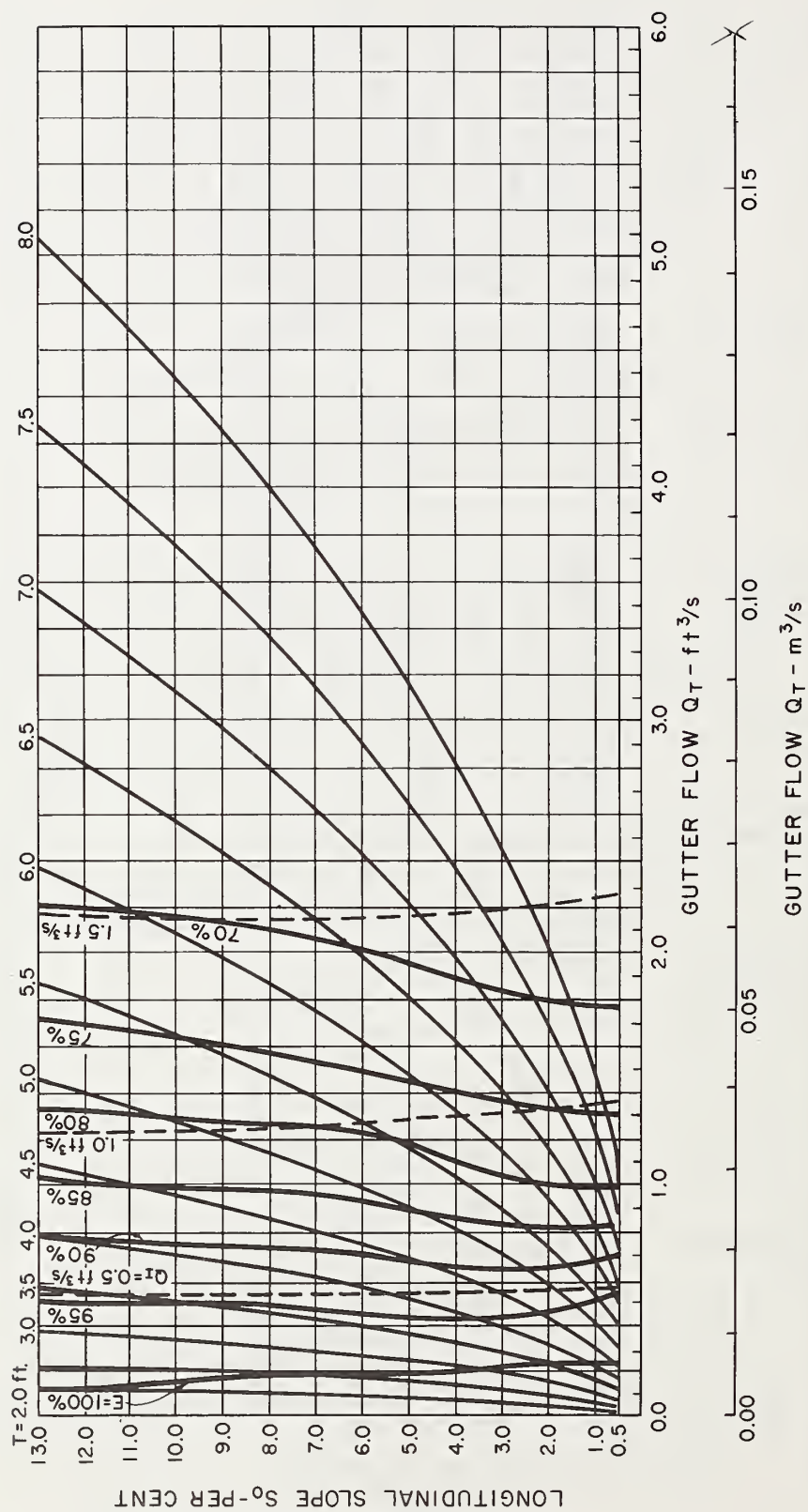


Figure 7-10. - Grate inlet capacity curves, 2 ft by 4 ft (0.61 m by 1.22 m) reticulate grate, $Z = 48$
 (Note: 1 ft = 0.305 m, 1 $\text{ft}^3/\text{s} = 0.028 \text{ m}^3/\text{s}$).

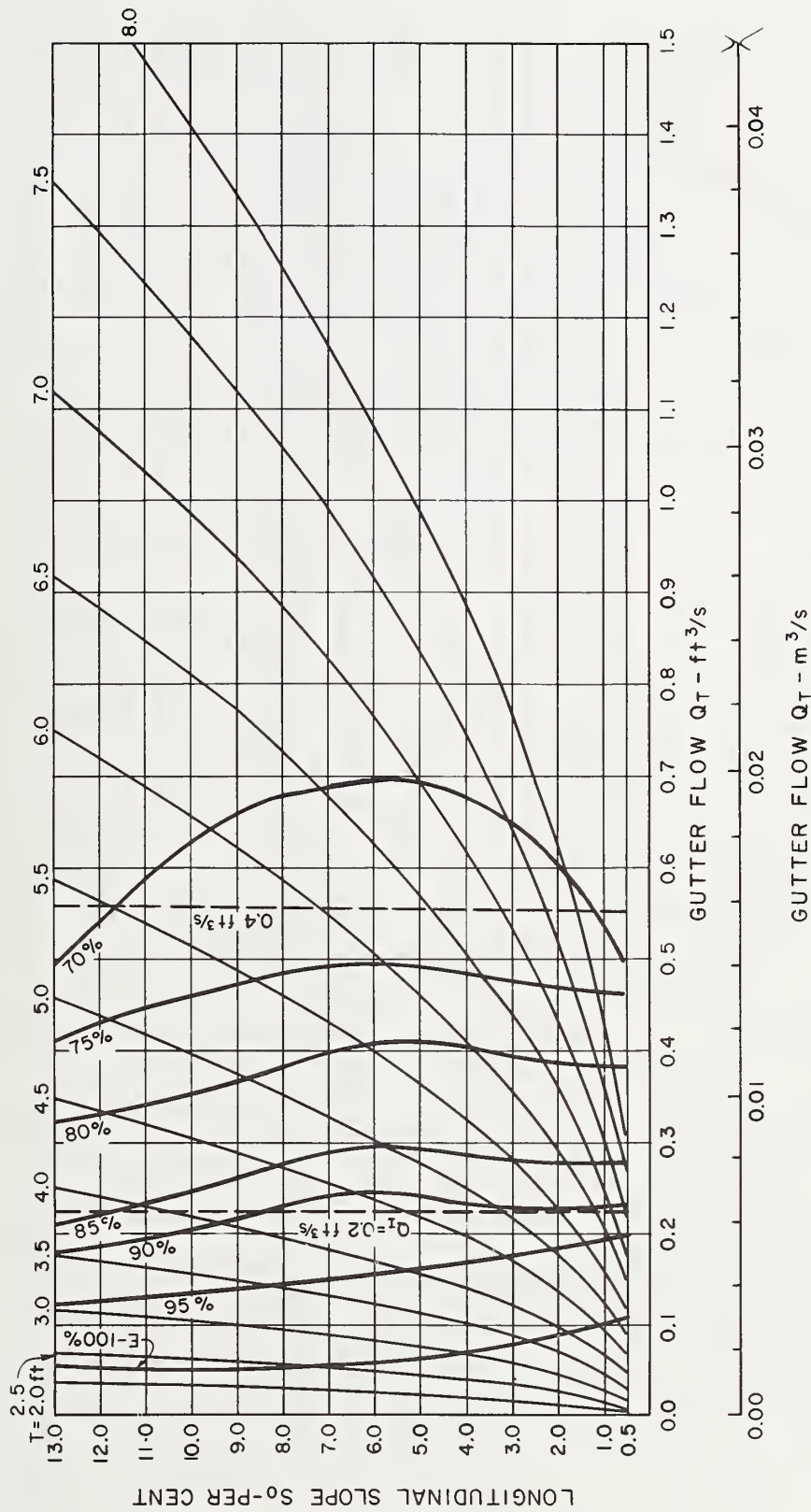


Figure 7-11. - Grate inlet capacity curves, 2 ft by 4 ft (0.61 m by 1.22 m) reticulate grate, $Z = 96$
 (Note: 1 ft = 0.305 m, 1 $\text{ft}^3/\text{s} = 0.028 \text{ m}^3/\text{s}$).

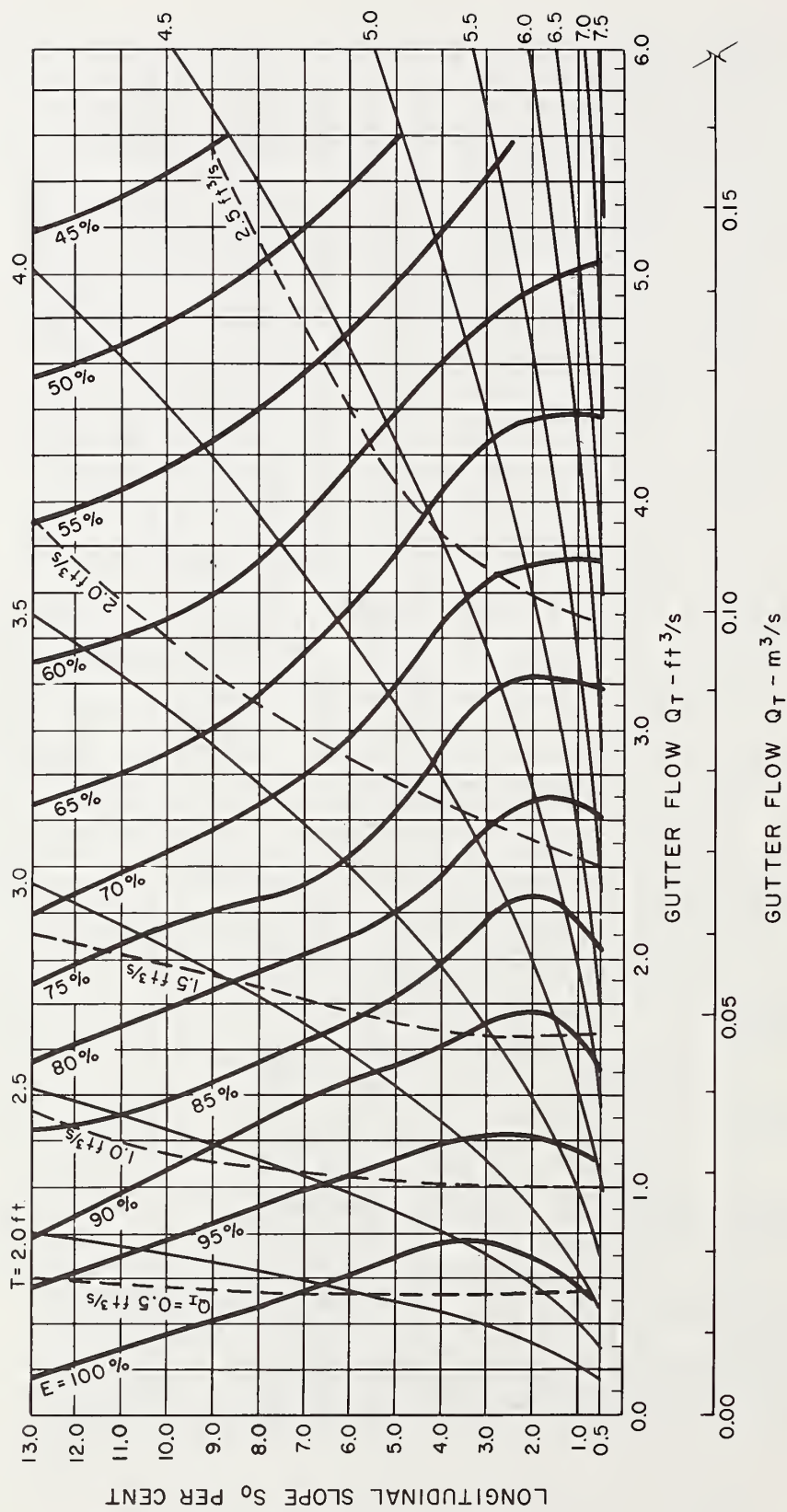


Figure 7-12. - Grate inlet capacity curves, 2 ft by 2 ft (0.61 m by 0.61 m) reticulate grate, $Z = 16$
 (Note: 1 ft = 0.305 m, 1 $\text{ft}^3/\text{s} = 0.028 \text{ m}^3/\text{s}$).

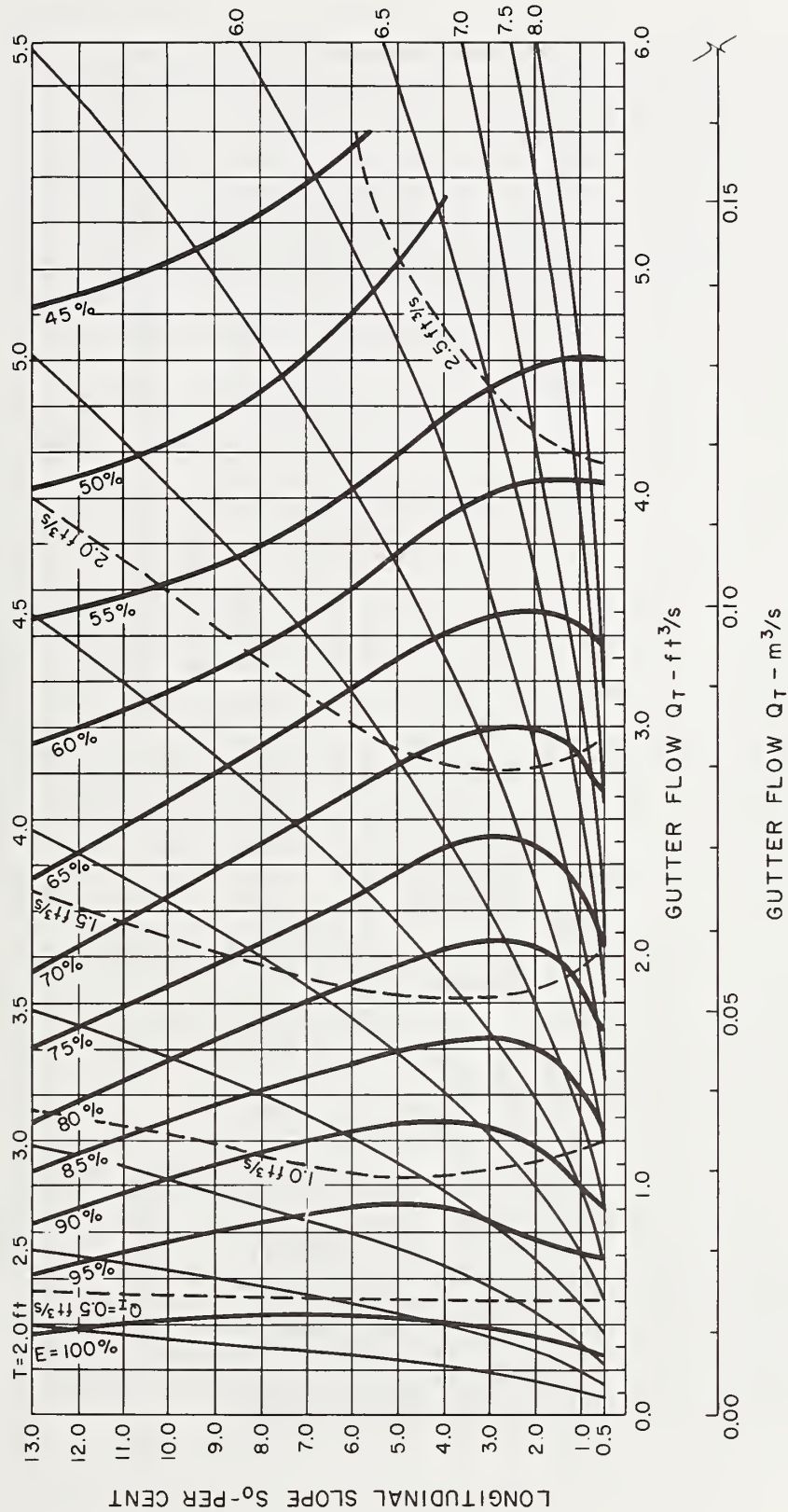


Figure 7-13. - Grate inlet capacity curves, 2 ft by 2 ft (0.61 m by 0.61 m) reticulate grate, $Z = 24$
 (Note: 1 ft = 0.305 m, 1 $\text{ft}^3/\text{s} = 0.028 \text{ m}^3/\text{s}$).

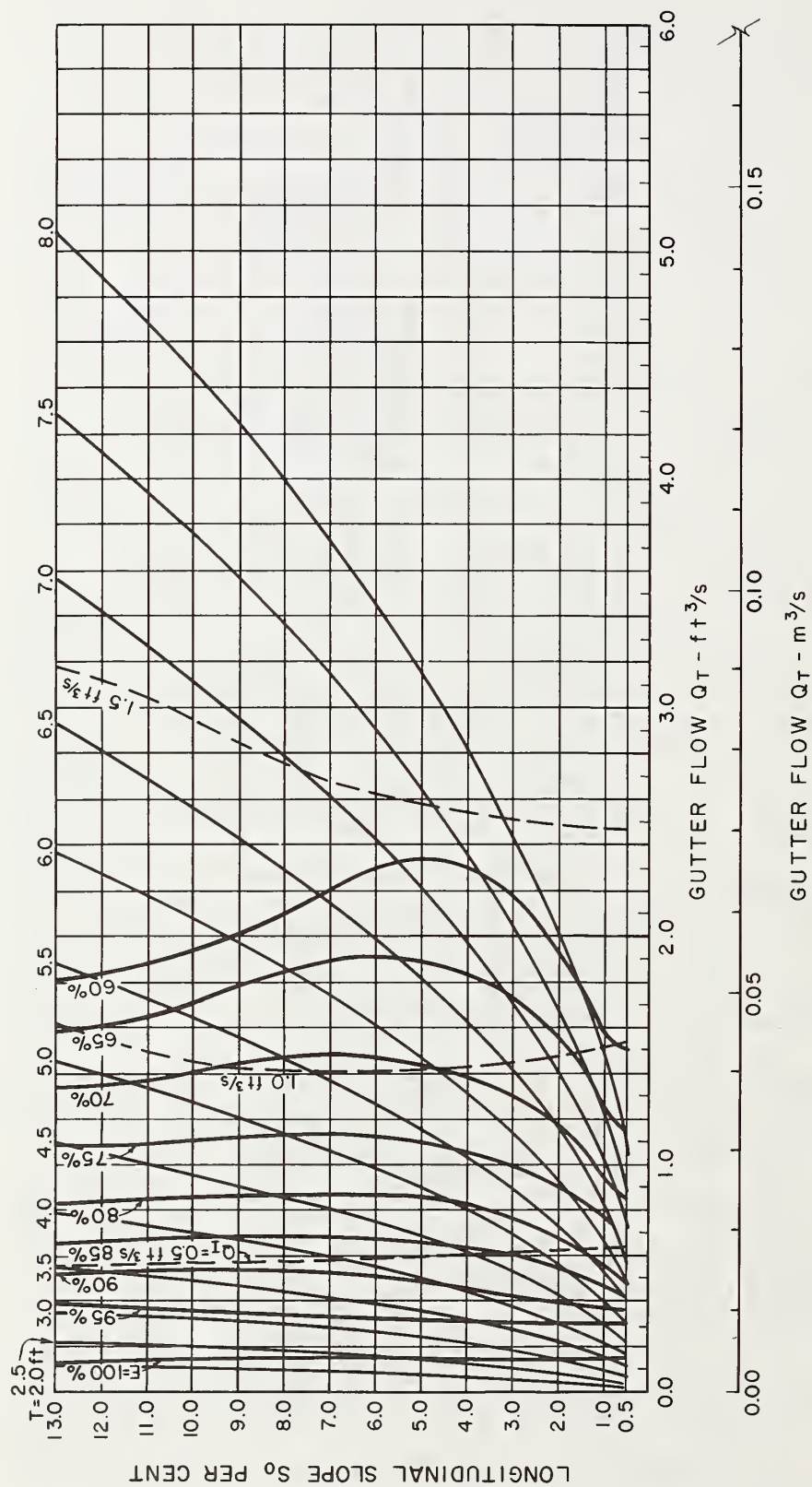


Figure 7-14. - Grate inlet capacity curves, 2 ft by 2 ft (0.61 m by 0.61 m) reticuline grate, $Z = 48$
 (Note: 1 ft = 0.305 m, 1 $\text{ft}^3/\text{s} = 0.028 \text{ m}^3/\text{s}$).

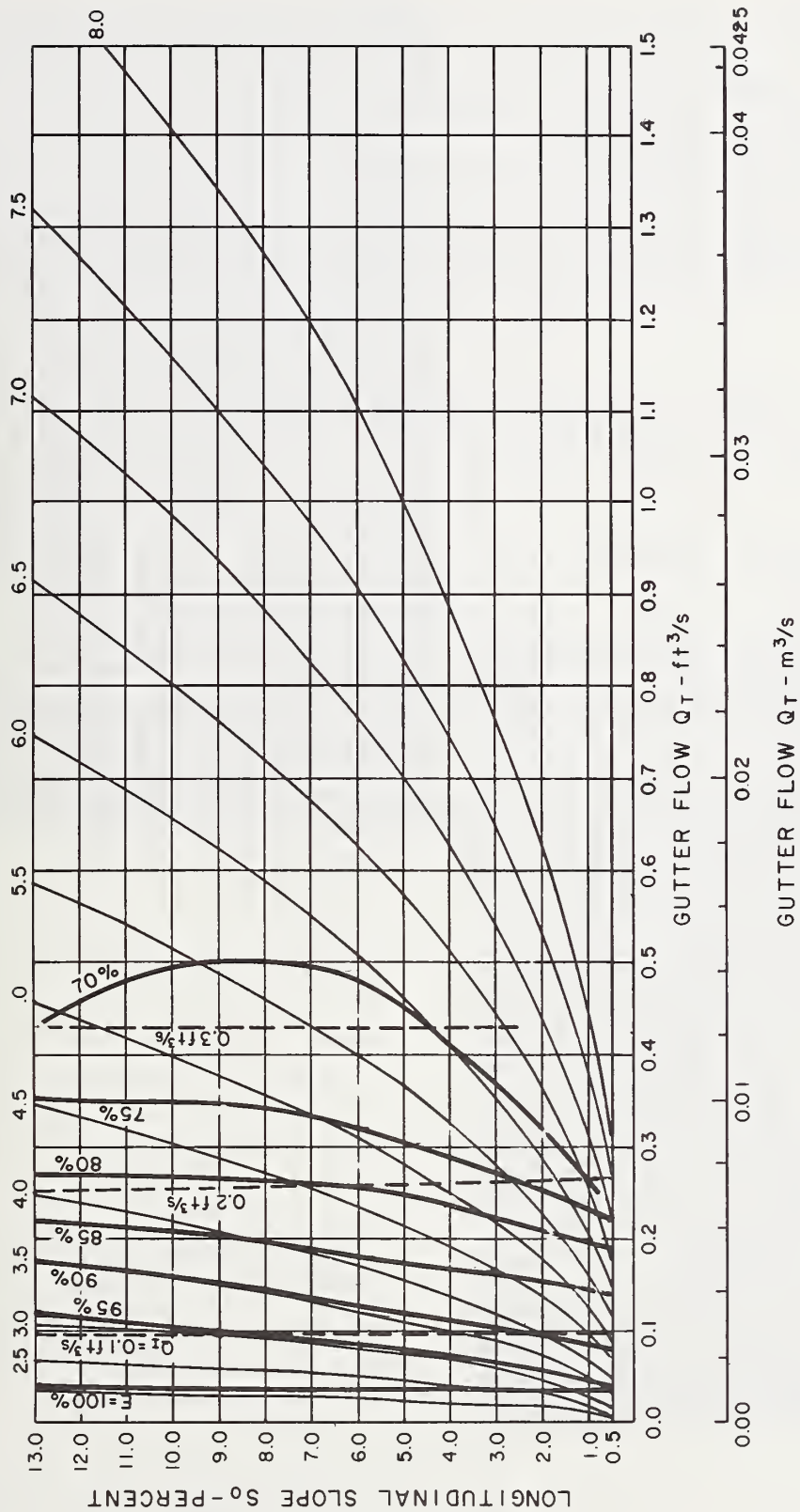


Figure 7-15. - Grate inlet capacity curves, 2 ft by 2 ft (0.61 m by 0.61 m) reticulate grate, $Z = 96$
 (Note: $1 \text{ ft} = 0.305 \text{ m}$, $1 \text{ ft}^3/\text{s} = 0.028 \text{ m}^3/\text{s}$).

Debris Tests. - Debris tests were conducted on the reticuline grates according to the test procedure described in Chapter 5. Figure 7-16a shows the 2 ft by 4 ft (0.61 m by 1.22 m) reticuline grate during a debris test with a gutter discharge of $0.5 \text{ ft}^3/\text{s}$ ($0.014 \text{ m}^3/\text{s}$). Figure 7-16b shows the final distribution of debris after the test. The results of the debris tests are shown in table 7-2.

The test results are very close for the two grate sizes at the 4 percent grade. At the 0.5 percent grade, however, the 2 ft by 2 ft (0.61 m by 0.61 m) grate is more efficient at handling debris.

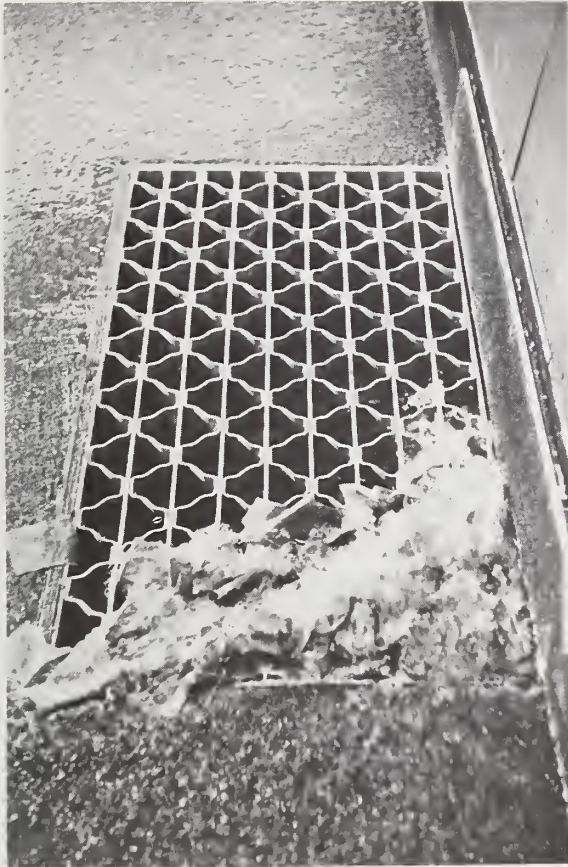
Summary

The reticuline grate has adequate hydraulic characteristics at mild longitudinal slopes. The grate's efficiency deteriorates rapidly as slopes and flow velocities increase.

For a given gutter flow, Q_T , both reticuline grates show an improvement in hydraulic efficiency as the longitudinal slope is increased. There is, however, a limiting slope above which the hydraulic efficiencies steadily decrease. This maximum efficiency slope depends on both the grate length and the cross slope (table 7-1).

At any given flow spread, the reticuline grates are more efficient at the flatter street slopes and cross slopes (figures 7-6 and 7-7).

The tests showed that the reticuline grates are not very efficient in passing debris. On the average, they passed 7 percent of the "leaves" in the first 5 minutes and 14 percent at the end of 15 minutes (table 7-2).



a. $Q_T = 0.5 \text{ ft}^3/\text{s}$ ($0.014 \text{ m}^3/\text{s}$)

$T' = 3.4 \text{ ft}$ (1.04 m)

Photo 62 11A-12

b. View looking downstream at
126 pieces of debris caught
on the grate.

Photo 62 14A-15

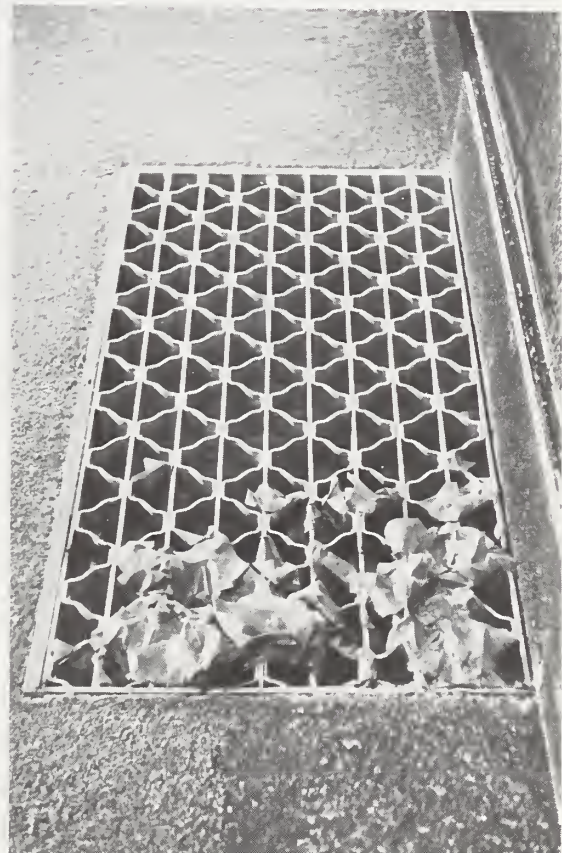


Figure 7-16. - Debris test, 2 ft by 4 ft (0.61 m by 1.22 m) reticuline
grate, $Z = 24$, $S_0 = 4\%$.

Table 7-2

DEBRIS TEST RESULTS - RETICULINE GRATES

Test No.	Number of "leaves" lodged on grate*			
	$S_0 = 0.5\%$		$S_0 = 4.0\%$	
	5 minutes	15 minutes	5 minutes	15 minutes
<u>2 ft by 2 ft (0.61 m by 0.61 m) grate</u>				
1			138	128
2			141	128
3			139	123
4	131	122		
5	141	131		
6	134	126		
Debris handling efficiency* (%)	10	16	7	16
<u>2 ft by 4 ft (0.61 m by 1.22 m) grate</u>				
1	148	144		
2	144	139		
3	140	132		
4			136	126
5			138	122
6			-	-
Debris handling efficiency* (%)	4	8	9	17

* Based on 150 "leaves" arriving at the gate.

CHAPTER 8

HYDRAULIC EFFICIENCY AND DEBRIS TESTS - 45° TILT-BAR GRATES

Introduction

This chapter describes the results of hydraulic tests conducted on two 45° tilt-bar gates. Tilt-bar gates that are now in use are typically cast gates. The two tilt-bar designs tested were reviewed by several foundry and grate manufacturing representatives to assure that the design was compatible with the casting process. The gates used in the study were constructed of white oak and are illustrated in figure 8-1.

The spacing of the longitudinal and transverse bars was based on the recommendations of the bicycle safety tests described in Chapter 3.

Both gates have transverse tilted bars spaced on 4 in (102 mm) centers. These tilted bars are 3/4 in (19 mm) thick, 3 in (76 mm) deep and are inclined 45° from horizontal. Several foundries suggested a minimum thickness of 3/4 in (19 mm) for the tilted bars. Based on this minimum thickness, the structural analysis in Chapter 2 recommended vertical depths of 2.25 in (57 mm) and 2.65 in (67 mm) for the tilted bars for longitudinal bar spacings of 2-1/4 in (57 mm) and 3-7/32 in (82 mm), respectively.

The tilted bars for all the test gates were made 3 in (76 mm) deep. The 1/2 in (13 mm) thick longitudinal bars were 2 in (50 mm) deep. Two different longitudinal bar spacings were tested. Actual dimensions are shown in figure 8-1, but the nominal center-to-center bar spacings of 2-1/4 in (57 mm) and 3-1/4 in (82 mm) will be referred to throughout the report. The gates have been code-named the 45 - 2-1/4 - 4 and the 45 - 3-1/4 - 4. The first symbol indicates the grate style, in this case a 45° tilt-bar grate. The second number is the nominal center-to-center longitudinal bar spacing in inches. The last number is the nominal center-to-center transverse bar spacing, also in inches. In an effort to streamline the flow surfaces, the tops of the longitudinal bars and the upstream edges of the transverse bars were rounded, as shown in the figure. Each of the gates was tested in a 2 ft by 2 ft (0.61 m by 0.61 m) and a 2 ft by 4 ft (0.61 m by 1.22 m) size.

Experimental Results and Observations

Hydraulics. - Results of hydraulic tests on the 45 - 2-1/4 - 4 gates are shown in figures 8-2 and 8-3. Results for the 45 - 3-1/4 - 4 gates are shown in figures 8-4 and 8-5.

For the same test conditions, hydraulic efficiencies E , for the 4 ft (1.22 m) long gates are always greater than those for the

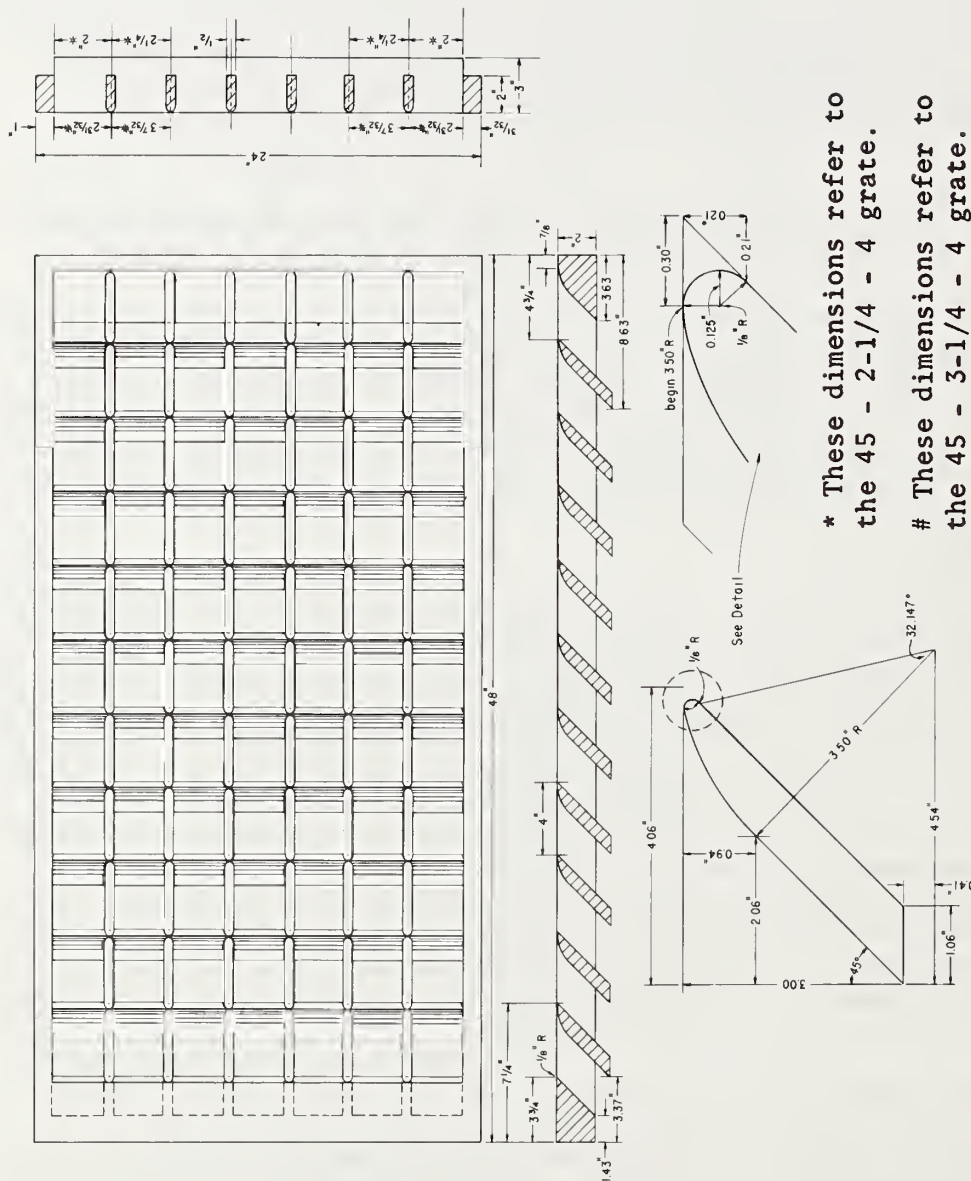


Figure 8-1. - 2 ft by 4 ft (0.61 m by 1.22 m) cast 45° tilt-bar grates
(Note: 1 ft = 0.305 m, 1 in = 25.4 mm).

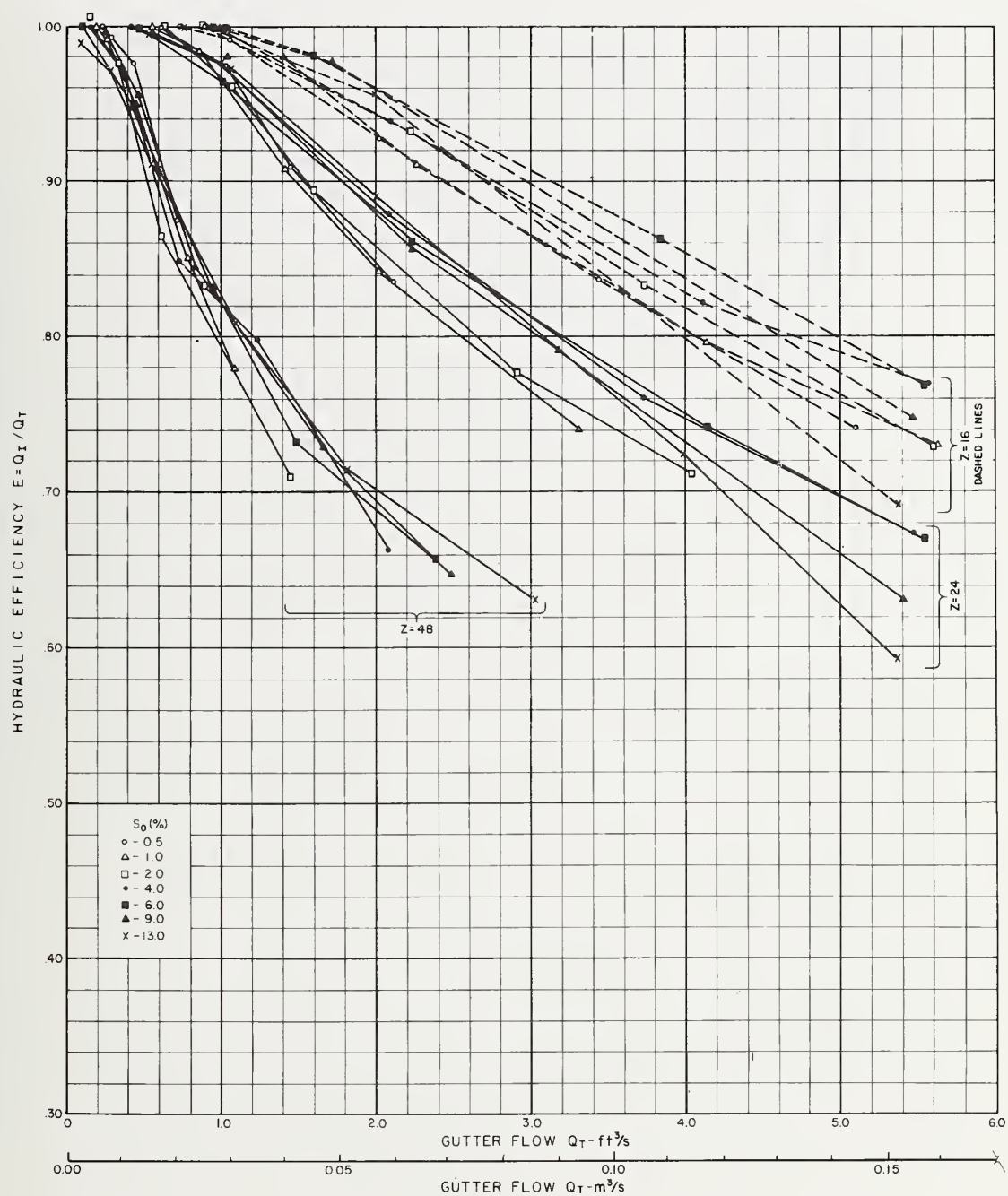


Figure 8-2. - Hydraulic efficiency vs. gutter flow, 2 ft by 4 ft (0.61 m by 1.22 m) 45 - 2-1/4 - 4 grate.

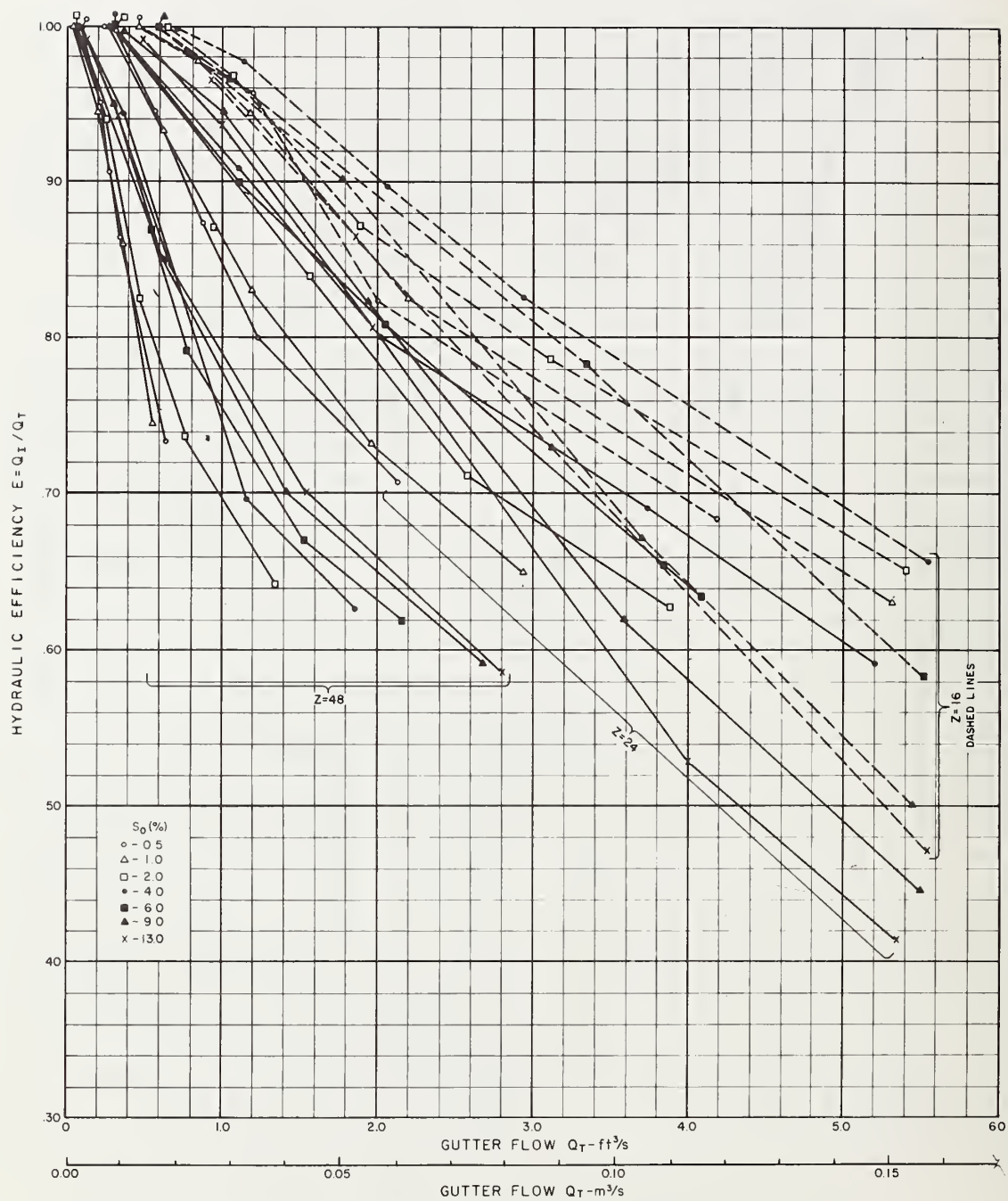


Figure 8-3. - Hydraulic efficiency vs. gutter flow, 2 ft by 2 ft (0.61 m by 0.61 m) 45 - 2-1/4 - 4 grate.

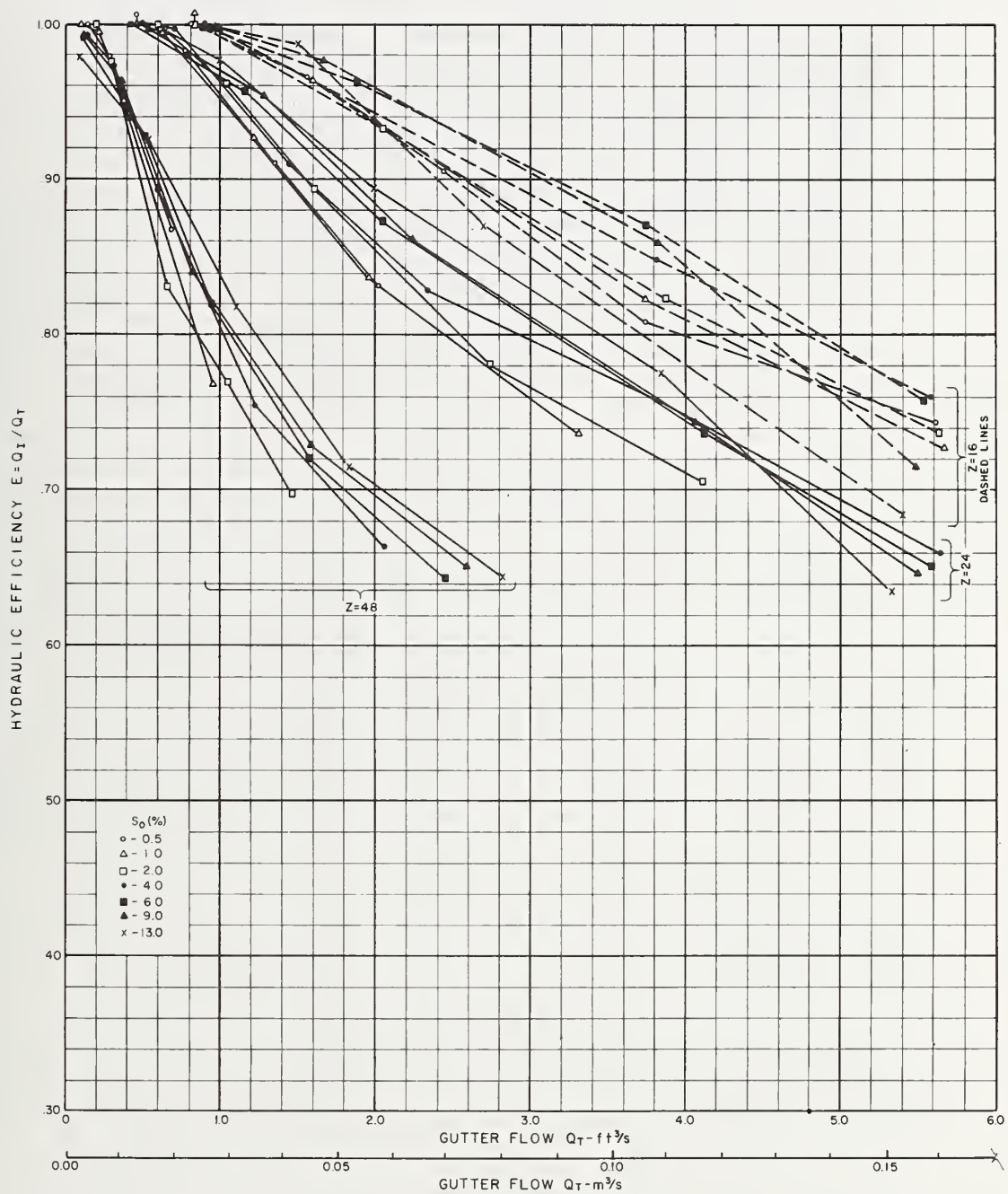


Figure 8-4. - Hydraulic efficiency vs. gutter flow, 2 ft by 4 ft (0.61 m by 1.22 m) 45 - 3-1/4 - 4 grate.

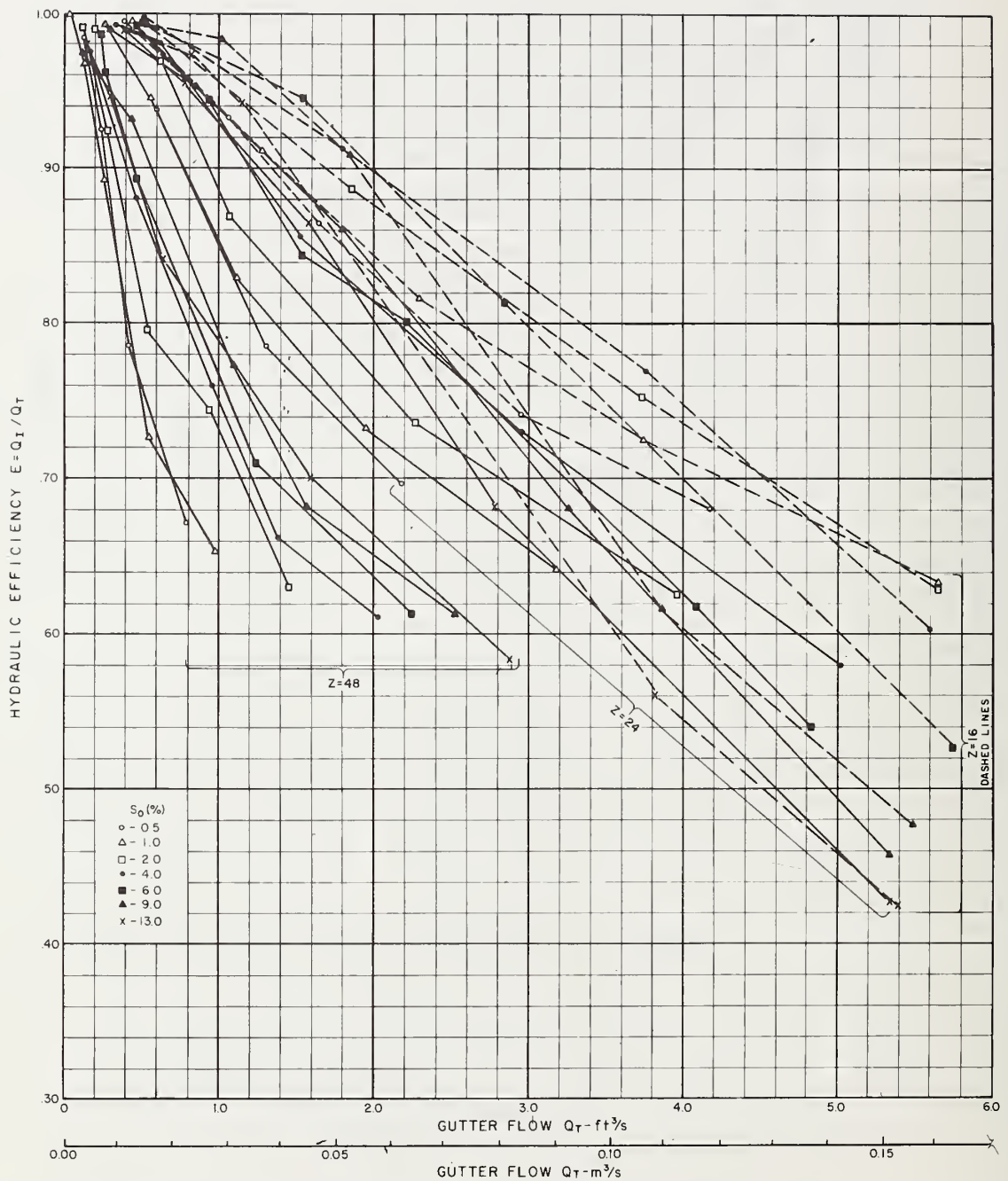


Figure 8-5. - Hydraulic efficiency vs. gutter flow, 2 ft by 2 ft (0.61 m by 0.61 m) 45 - 3-1/4 - 4 grate.

2 ft (0.61 m) long grates. At the flatter longitudinal slopes, S_0 , the shorter grates have lower hydraulic efficiencies because their sides are 2 ft (0.61 m) shorter. At the lowest longitudinal slopes, the 45° tilt-bar grates intercept all flow in their 2 ft (0.61 m) widths well within the length of the grate. Therefore, the extra length of the 4 ft (1.22 m) long grate brings an increase in hydraulic efficiency only because it captures more of the flow along the side. Most of the grate area is not being utilized. At steeper longitudinal slopes, flow velocities increase enough for flow to carry completely across the 2 ft (0.61 m) long grate. In this case, the longer grate is more efficient because of its greater area.

To save time, the 4 ft (1.22 m) long grates were tested first. These grates were then cut in half and modified into 2 ft (0.61 m) long grates. A problem developed with the 45 - 3-1/4 - 4 grates as testing progressed. The first tilted bar swelled and warped and eventually rose up above the grate surface nearly 0.25 in (6 mm). This offset set up an unusual splash pattern at the front of the grate. Figure 8-6 illustrates the splash phenomenon which was most evident visually at 13 percent slope for $Z = 48$. At steeper cross slopes and greater flow rates, the splash was not noticeable, but the offset is suspected of causing a loss in hydraulic efficiency. Comparisons of figures 8-2 and 8-4 and figures 8-3 and 8-5 show that the efficiencies for the 45 - 3-1/4 - 4 grates are generally slightly less than those for the 45 - 2-1/4 - 4 grates. The 45 - 3-1/4 - 4 has a greater open area and would be expected to provide higher hydraulic efficiencies than the 45 - 2-1/4 - 4 with actual cast grates which would not warp or change dimensions.

Figures 8-7 and 8-8 show the relationship between the measured width of spread, T' , and hydraulic efficiency E , for both sizes of the 45 - 2-1/4 - 4 grate. Figures 8-9 and 8-10 show the same relationships for the two 45 - 3-1/4 - 4 grates. In general, for the same width of spread, hydraulic efficiencies are higher at the lower longitudinal and cross slopes.

For the same gutter flow, hydraulic efficiencies are lower at the steeper longitudinal slopes. Flow that splashes completely across the grate is the biggest cause of this decrease in efficiency. Both the 45 - 2-1/4 - 4 grates and the 45 - 3-1/4 - 4 grates are efficient enough to recapture all of the splash for $Z = 48$. For $Z = 24$ and 16, however, flow splashes completely across the grate at the steeper longitudinal slopes. Figures 8-11 and 8-12 show the performance of the 2 ft by 4 ft (0.61 m by 1.22 m) 45 - 2-1/4 - 4 and 45 - 3-1/4 - 4 grates at slopes of 6 percent and 13 percent for $Z = 24$.

The grate inlet capacity curves in figures 8-13 through 8-24 relate gutter flow, Q_T , and longitudinal slope, S_0 , to hydraulic efficiency, E , intercepted flow, Q_I , and width of spread, T . Figures 8-13 through 8-18 are for the 45 - 2-1/4 - 4 grates, and figures 8-19

through 8-24 are for the 45 - 3-1/4 - 4 grates. There is one graph for each grate size and cross slope.

The development of the inlet capacity curves and directions for their use are presented in Chapter 5.

For a constant gutter flow, hydraulic efficiencies of the 45° tilt-bar grates increase with increasing longitudinal slope until some maximum efficiency is reached. The slope where efficiency is maximum depends on the grate length, grate style, cross slope, and gutter flow. Since the maximum efficiency slope depends on gutter flow, the table shows a range of slopes where the grates are most efficient for the gutter flows tested.

Table 8-1 shows the maximum efficiency slopes for both sizes of the 45 - 2-1/4 - 4 and 45 - 3-1/4 - 4 grates.

Table 8-1

MAXIMUM EFFICIENCY SLOPES - 45° TILT-BAR GRATES

Grate		Maximum efficiency slope		
		Z = 48	Z = 24	Z = 16
2 ft by 2 ft (0.61 m by 0.61 m)	45 - 2-1/4 - 4	>13%	4% to 8%	4%
2 ft by 4 ft (0.61 m by 1.22 m)	45 - 2-1/4 - 4	>13%	5% to 13%	6% to 7%
2 ft by 2 ft (0.61 m by 0.61 m)	45 - 3-1/4 - 4	>13%	4% to 7%	1% to 6%
2 ft by 4 ft (0.61 m by 1.22 m)	45 - 3-1/4 - 4	>13%	5% to 13%	5% to 7%

Figures 8-25 and 8-26 show the performance of the 2 ft by 2 ft (0.61 m by 0.61 m) 45 - 2-1/4 - 4 and 45 - 3-1/4 - 4 grates as longitudinal slopes are increased from 4 percent to 13 percent. It is apparent that both grates begin to exhibit splash problems at slopes above 4 percent.

Debris Tests. - The 45° tilt-bar grates were debris tested according to the procedure described in Chapter 5. Figures 8-27 and 8-28 show debris tests of the 4 ft (1.22 m) long 45 - 2-1/4 - 4 and



a. Normal 45 - 2-1/4 - 4 grate

$$Q_T = 2.80 \text{ ft}^3/\text{s} \text{ (} 0.079 \text{ m}^3/\text{s)}$$

Photo 43 5A-6

$$T' = 7.1 \text{ ft (} 2.16 \text{ m)}$$

$$E = 59\%$$



b. Warped 45 - 3-1/4 - 4 grate

$$Q_T = 2.88 \text{ ft}^3/\text{s} \text{ (} 0.081 \text{ m}^3/\text{s)}$$

Photo 44-4

$$T' = 7.1 \text{ ft (} 2.16 \text{ m)}$$

$$E = 58\%$$

Figure 8-6. - Splash patterns at 13 percent slope, $Z = 48$, 2 ft by 2 ft (0.61 m by 0.61 m) 45° tilt-bar grates.

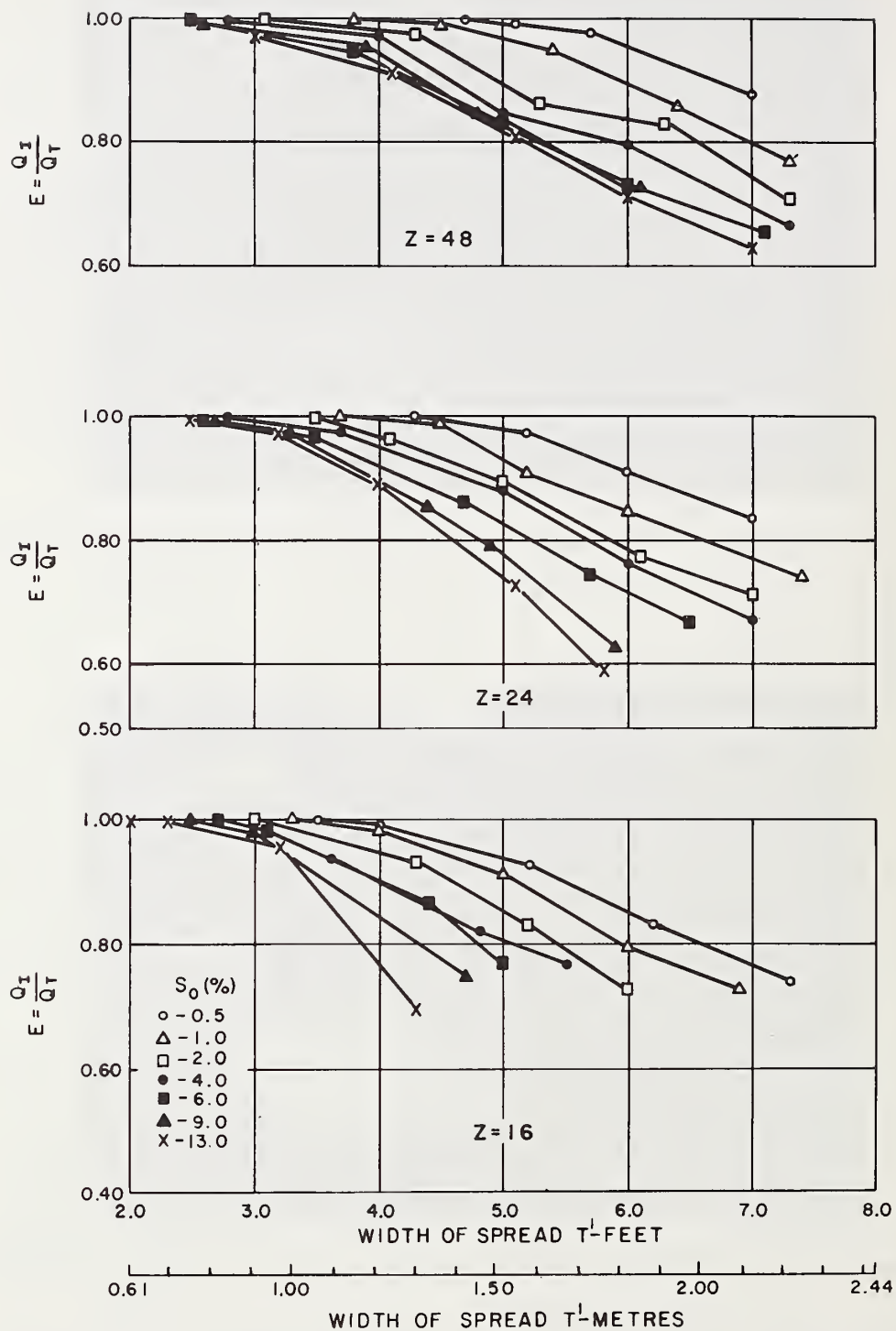


Figure 8-7. - Hydraulic efficiency vs. width of spread, 2 ft by 4 ft (0.61 m by 1.22 m) 45 - 2-1/4 - 4 grate.

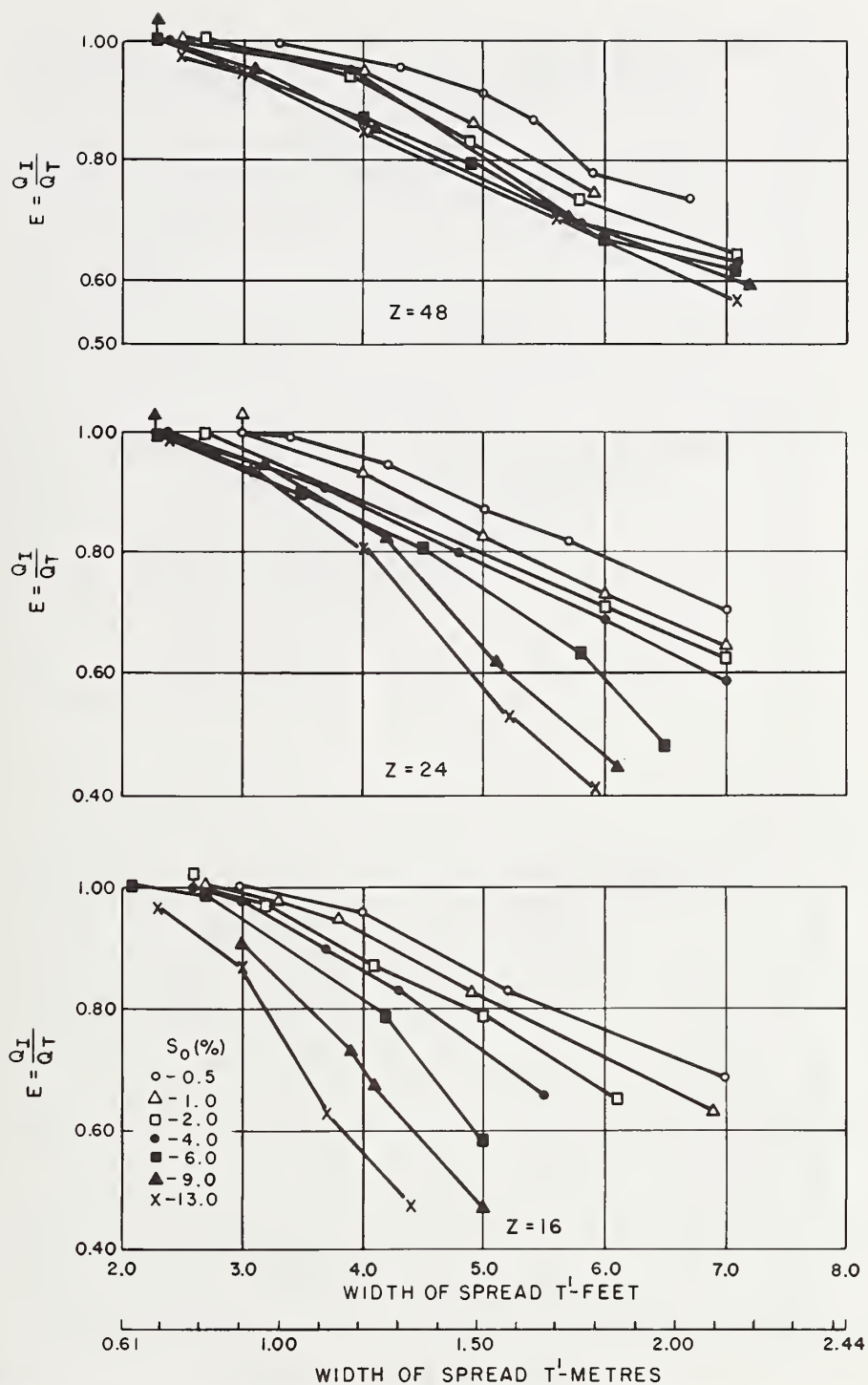


Figure 8-8. - Hydraulic efficiency vs. width of spread, 2 ft by 2 ft (0.61 m by 0.61 m) 45 - 2-1/4 - 4 grate.

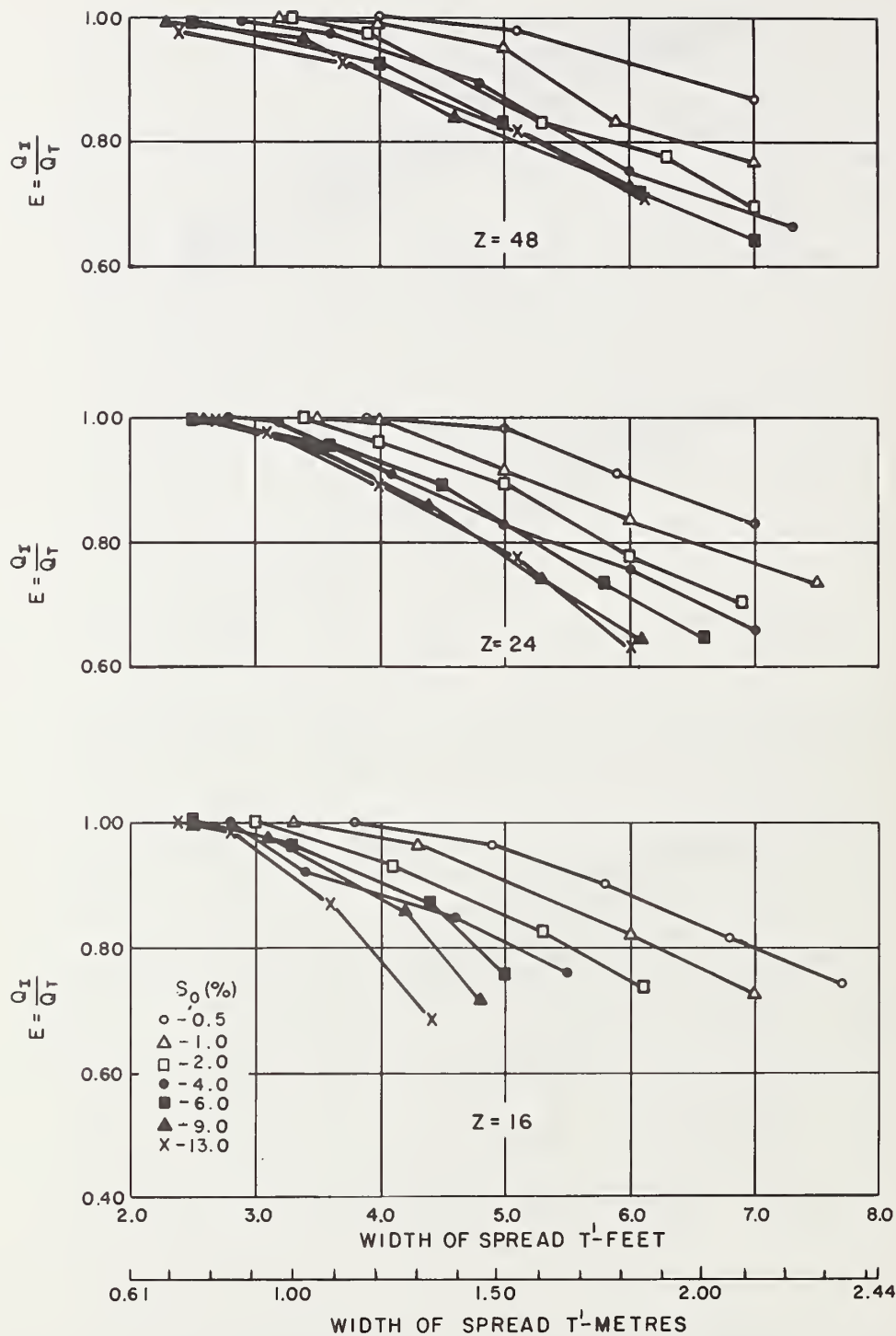


Figure 8-9. - Hydraulic efficiency vs. width of spread, 2 ft by 4 ft (0.61 m by 1.22 m) 45 - 3-1/4 - 4 grate.

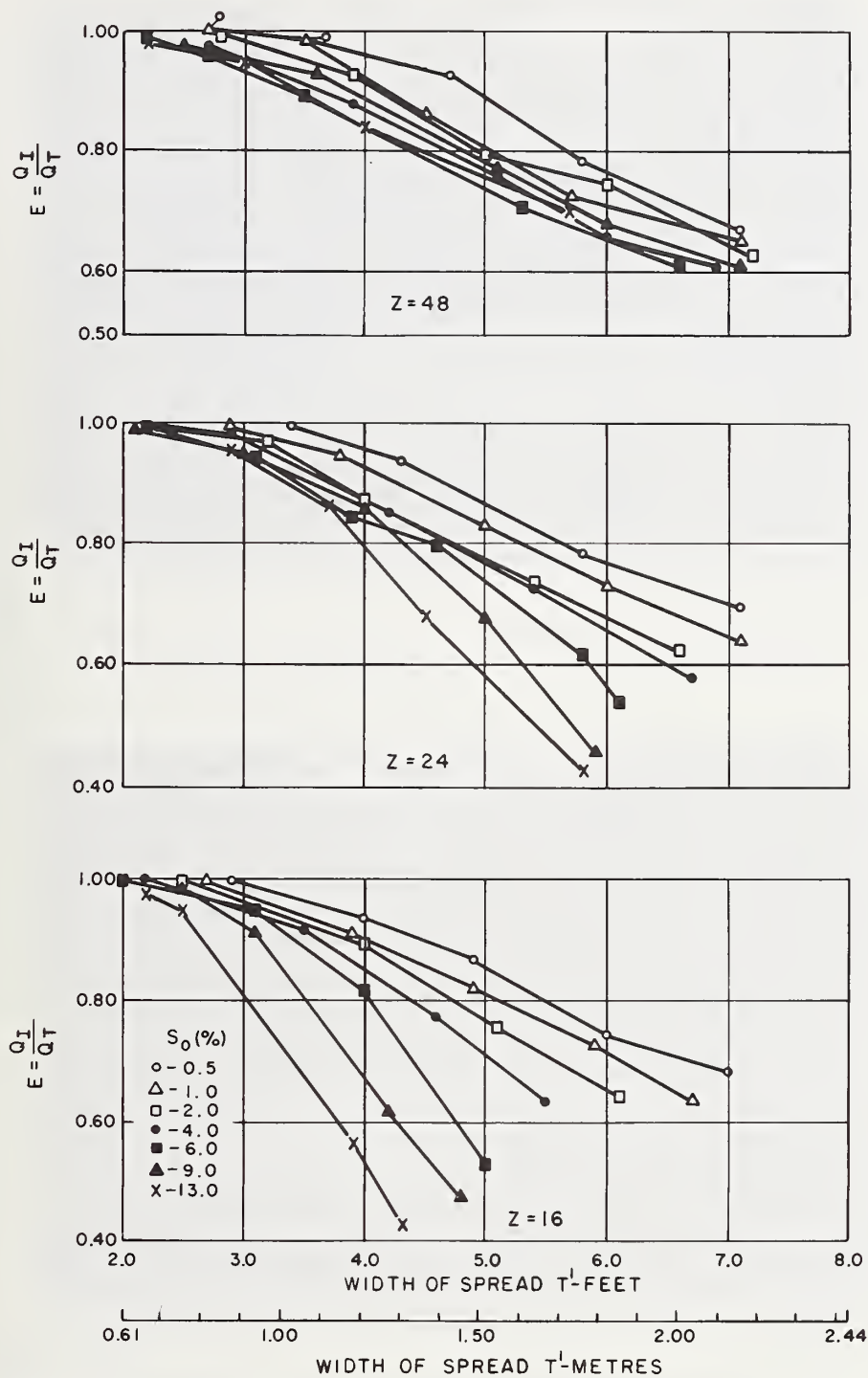


Figure 8-10. - Hydraulic efficiency vs. width of spread, 2 ft by 2 ft (0.61 m by 0.61 m) 45 - 3-1/4 - 4 grate.



a. $S_0 = 6\%$
 $Q_T = 5.54 \text{ ft}^3/\text{s} \text{ (} 0.157 \text{ m}^3/\text{s)}$
 Photo 31-15

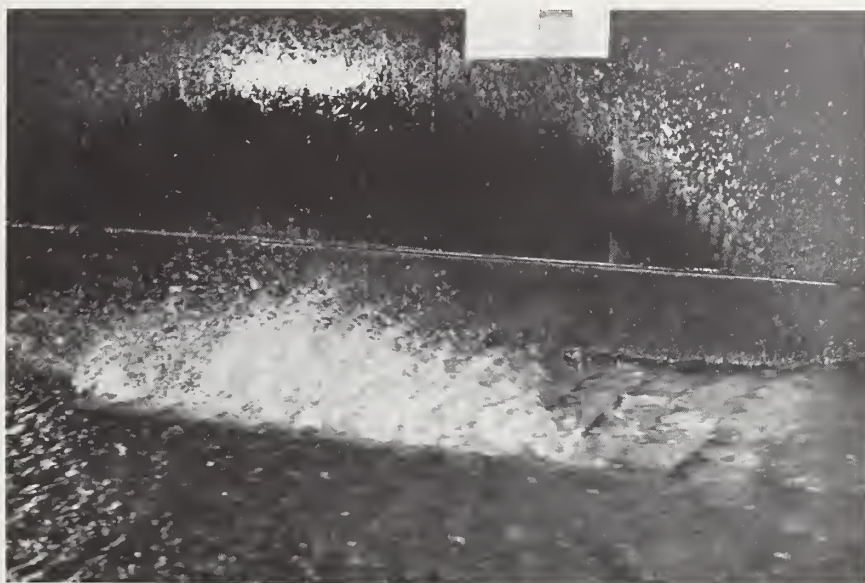
$T' = 6.5 \text{ ft (} 1.98 \text{ m)}$
 $E = 67\%$



b. $S_0 = 13\%$
 $Q_T = 5.36 \text{ ft}^3/\text{s} \text{ (} 0.152 \text{ m}^3/\text{s)}$
 Photo 34-15A

$T' = 5.8 \text{ ft (} 1.77 \text{ m)}$
 $E = 59\%$

Figure 8-11. - Flow carrying completely across the 2 ft by 4 ft
 (0.61 m by 1.22 m) 45 - 2-1/4 - 4 grate, $Z = 24$.



a. $S_0 = 6\%$

$T' = 6.6 \text{ ft (2.01 m)}$

$Q_T = 5.57 \text{ ft}^3/\text{s (0.158 m}^3/\text{s)}$

$E = 65\%$

Photo 36-3



b. $S_0 = 13\%$

$T' = 6.0 \text{ ft (1.83 m)}$

$Q_T = 5.31 \text{ ft}^3/\text{s (0.150 m}^3/\text{s)}$

$E = 64\%$

Photo 35-3

Figure 8-12. - Flow carrying completely across the 2 ft by 4 ft
(0.61 m by 1.22 m) 45 - 3-1/4 - 4 grate, $Z = 24$.

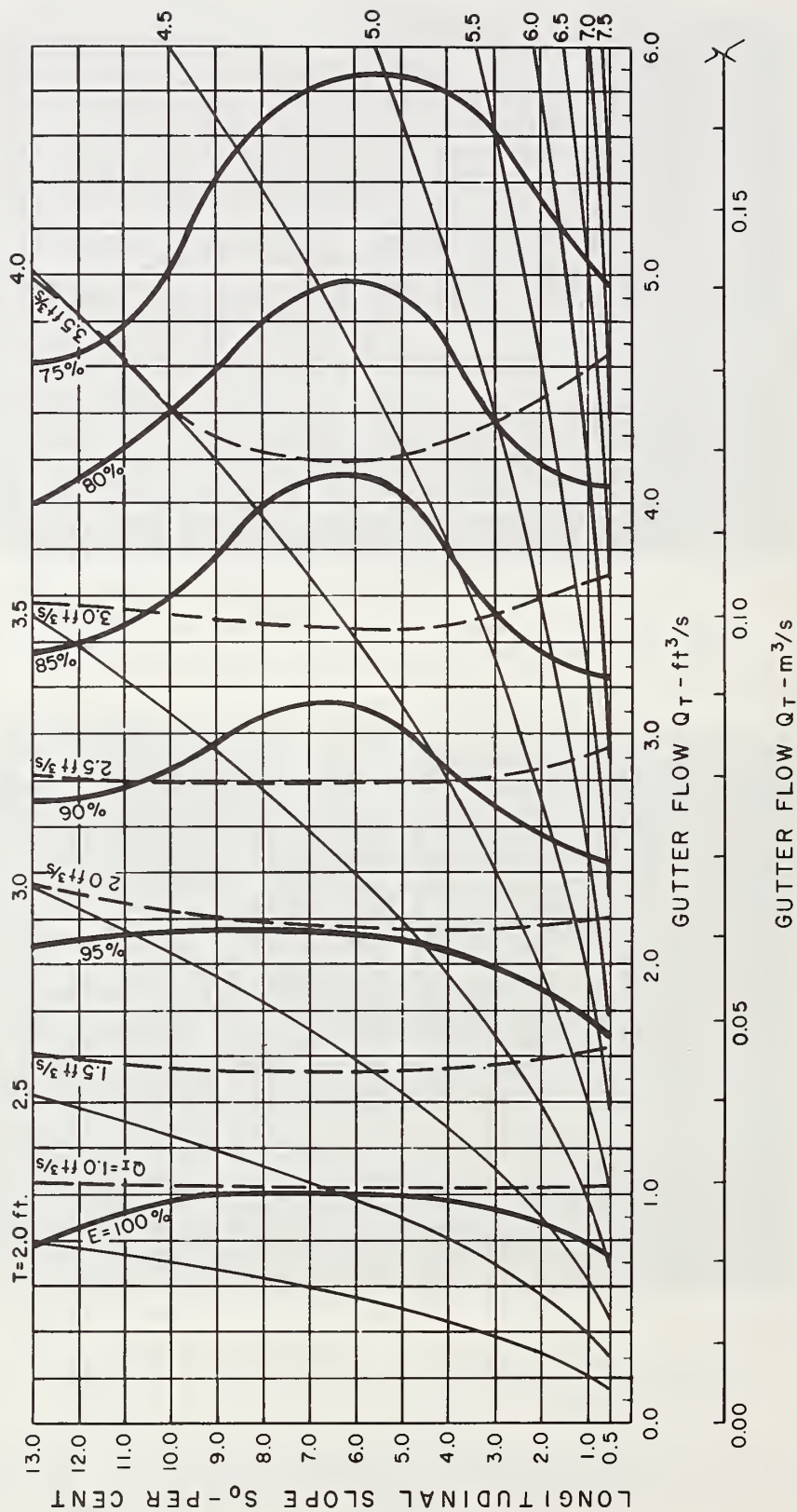


Figure 8-13. - Grate inlet capacity curves, 2 ft by 4 ft (0.61 m by 1.22 m) 45 - 2-1/4 - 4 grate, $Z = 16$ (Note: $1 \text{ ft}^3/\text{s} = 0.028 \text{ m}^3/\text{s}$, $1 \text{ ft} = 0.305 \text{ m}$).

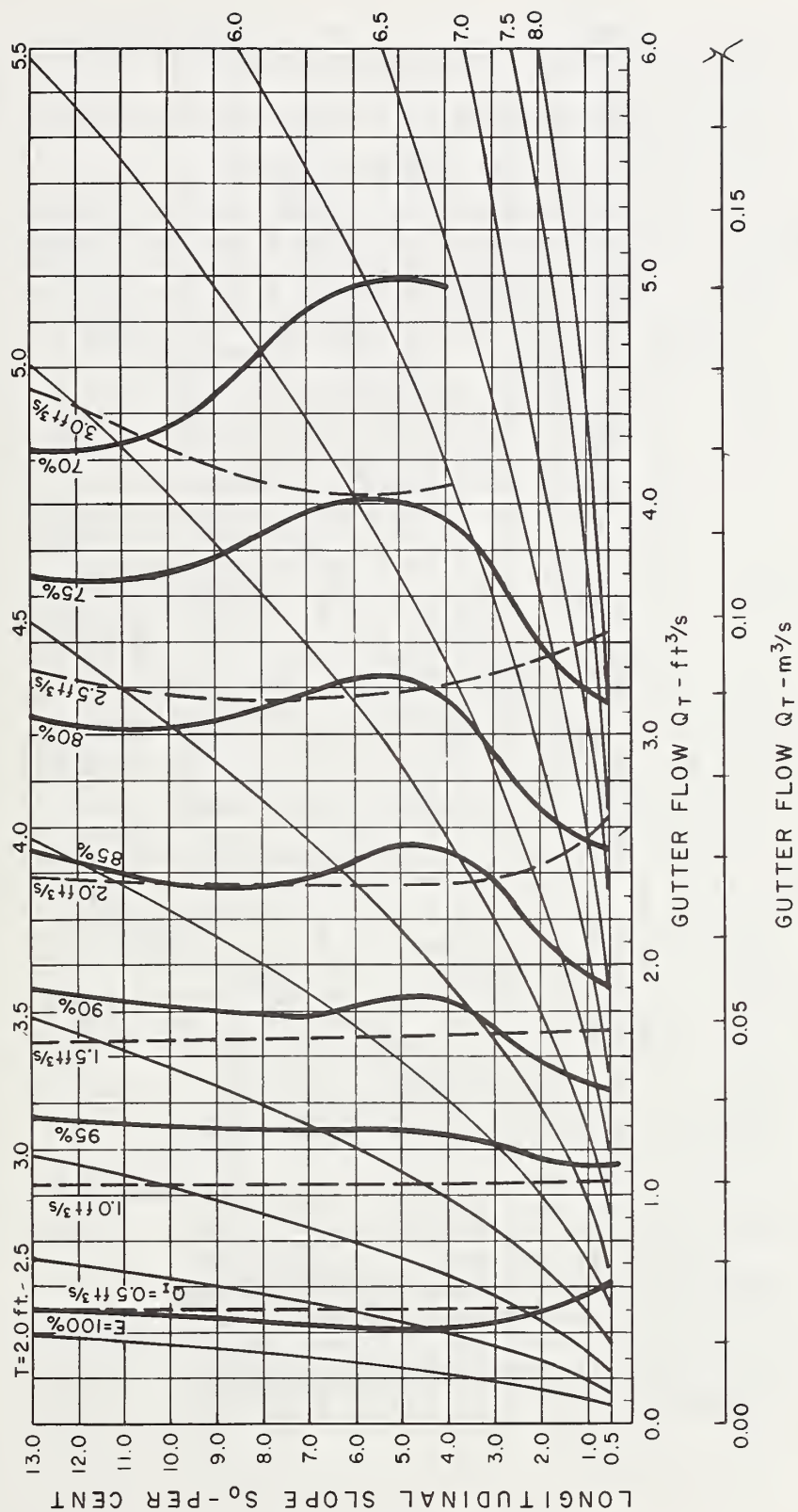


Figure 8-14. - Grate inlet capacity curves, 2 ft by 4 ft (0.61 m by 1.22 m) 45 - 2-1/4 - 4 grate, $Z = 24$ (Note: $1 \text{ ft}^3/\text{s} = 0.028 \text{ m}^3/\text{s}$, $1 \text{ ft} = 0.305 \text{ m}$).

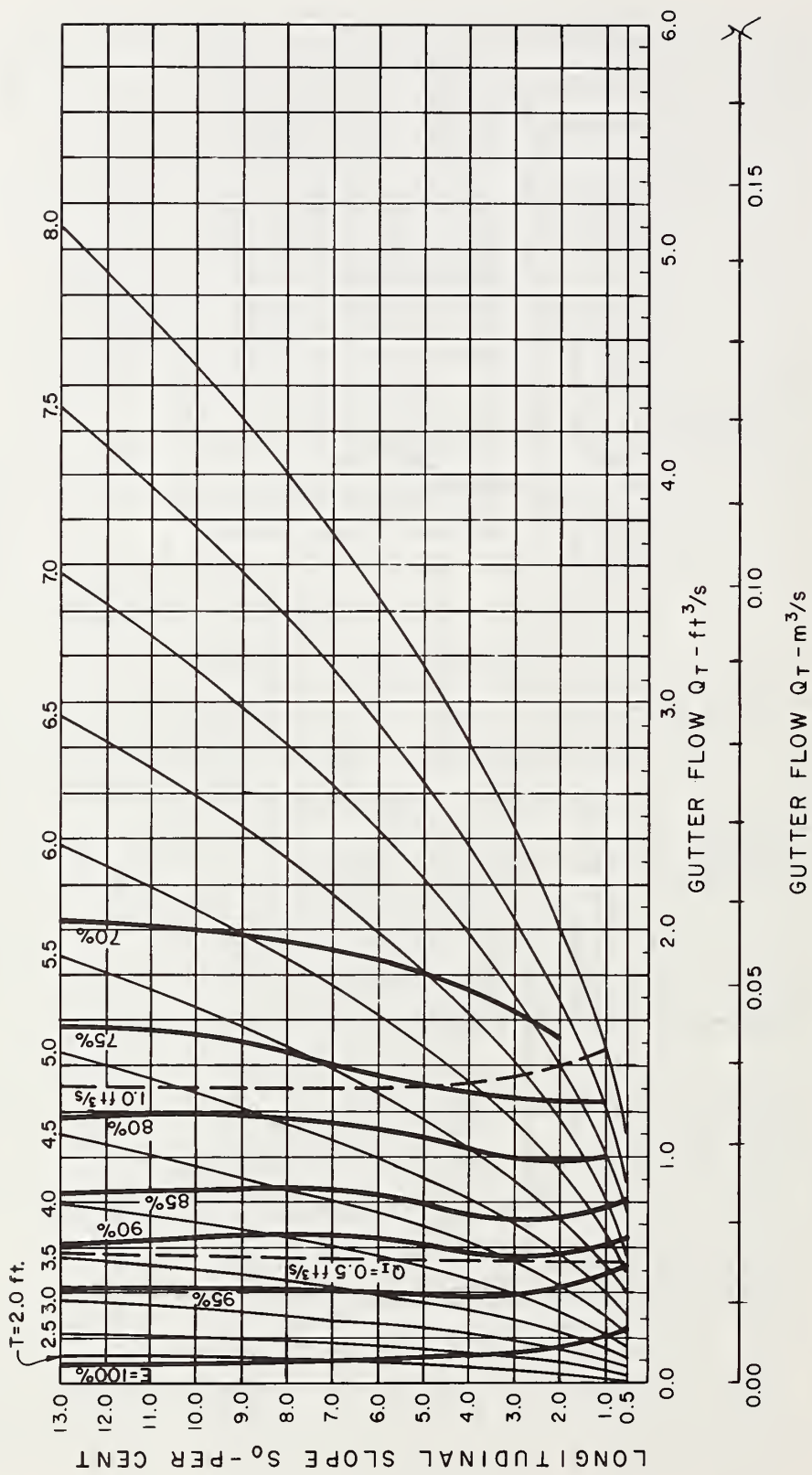


Figure 8-15. - Grate inlet capacity curves, 2 ft by 4 ft (0.61 m by 1.22 m) 45 - 2-1/4 - 4 grate, $Z = 48$ (Note: $1 \text{ ft}^3/\text{s} = 0.028 \text{ m}^3/\text{s}$, $1 \text{ ft} = 0.305 \text{ m}$).

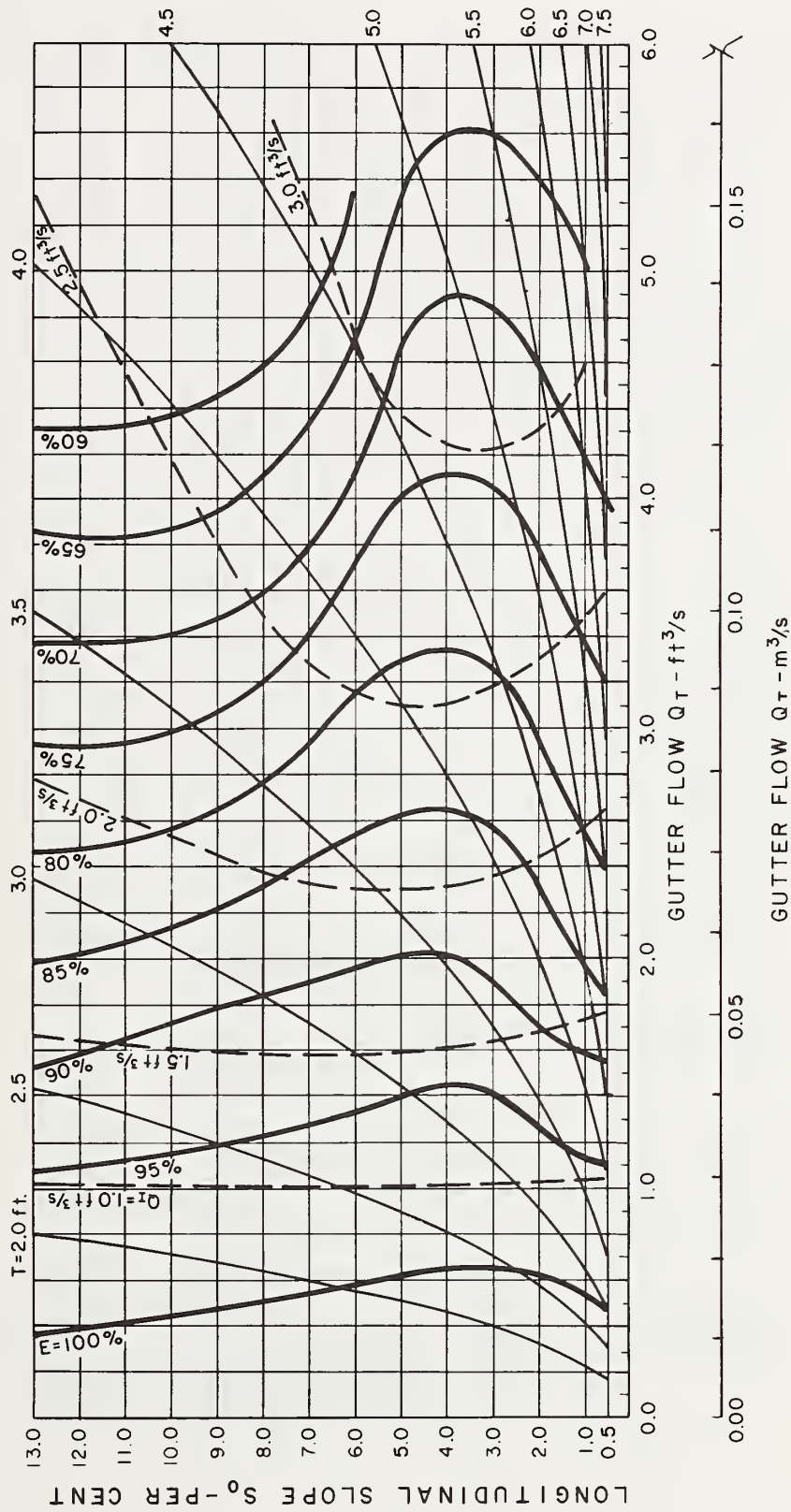


Figure 8-16. - Grate inlet capacity curves, 2 ft by 2 ft (0.61 m by 0.61 m) 45 - 2-1/4 - 4 grate, Z = 16 (Note: 1 ft³/s = 0.028 m³/s, 1 ft = 0.305 m).

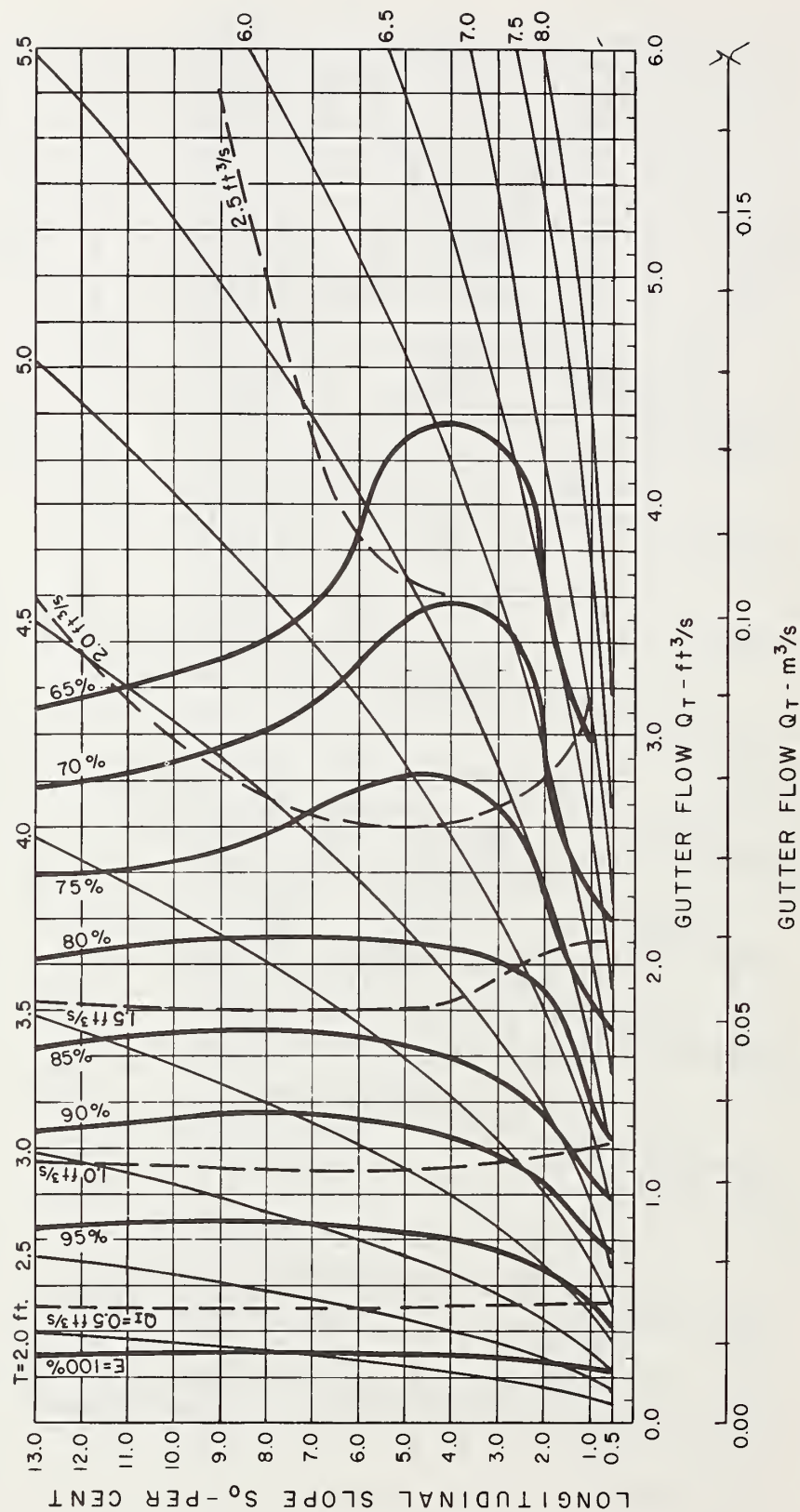


Figure 8-17. - Grate inlet capacity curves, 2 ft by 2 ft (0.61 m by 0.61 m) 45 - 2-1/4 - 4 grate, $Z = 24$ (Note: 1 $\text{ft}^3/\text{s} = 0.028 \text{ m}^3/\text{s}$, 1 ft - 0.305 m).

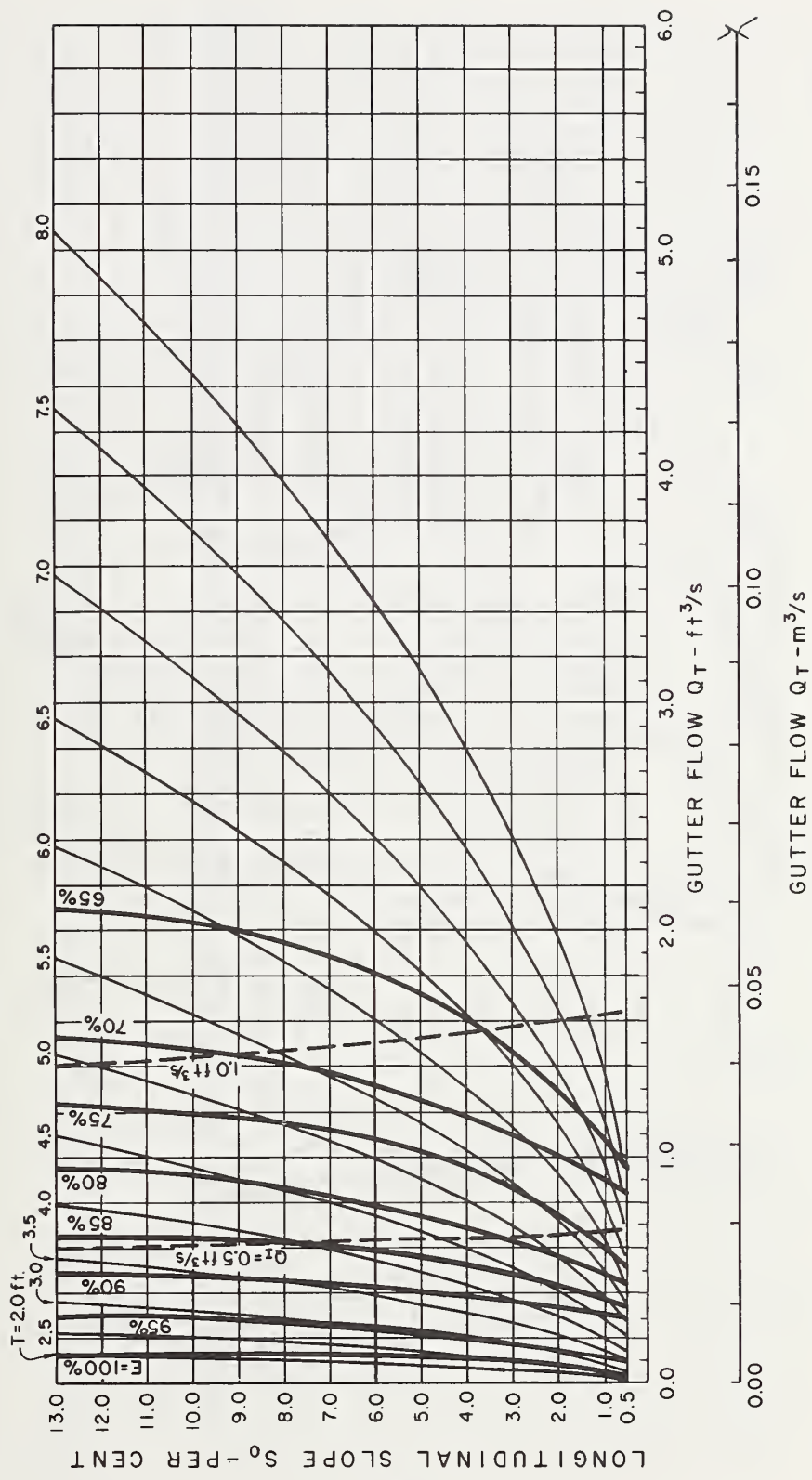


Figure 8-18. - Grate inlet capacity curves, 2 ft by 2 ft (0.61 m by 0.61 m) 45 - 2-1/4 - 4 grate, $Z = 48$ (Note: 1 $\text{ft}^3/\text{s} = 0.028 \text{ m}^3/\text{s}$, 1 ft = 0.305 m).

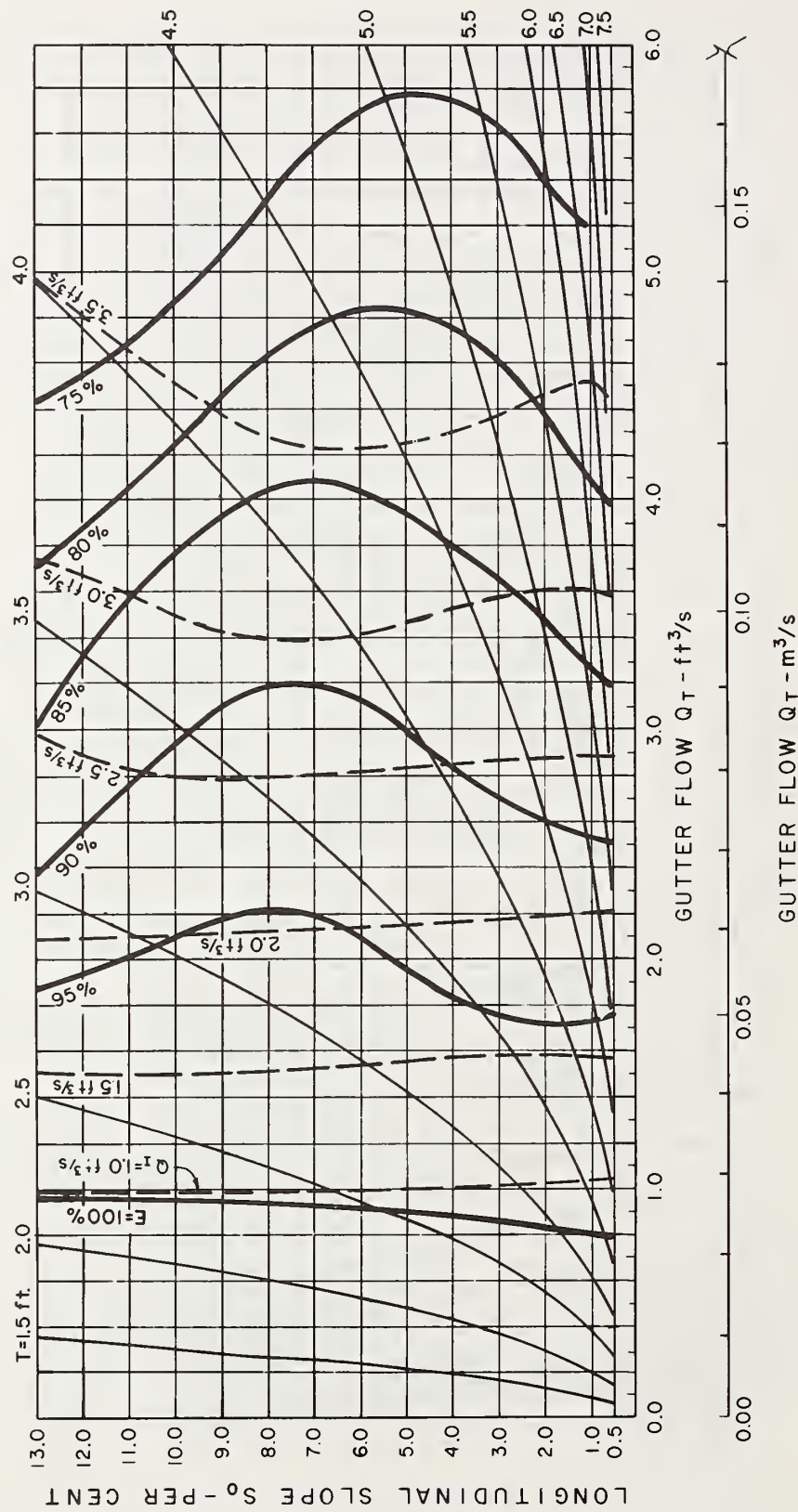


Figure 8-19. - Grate inlet capacity curves, 2 ft by 4 ft (0.61 m by 1.22 m) 45 - 3-1/4 - 4 grate, $Z = 16$ (Note: $1 \text{ ft}^3/\text{s} = 0.028 \text{ m}^3/\text{s}$, $1 \text{ ft} = 0.305 \text{ m}$).

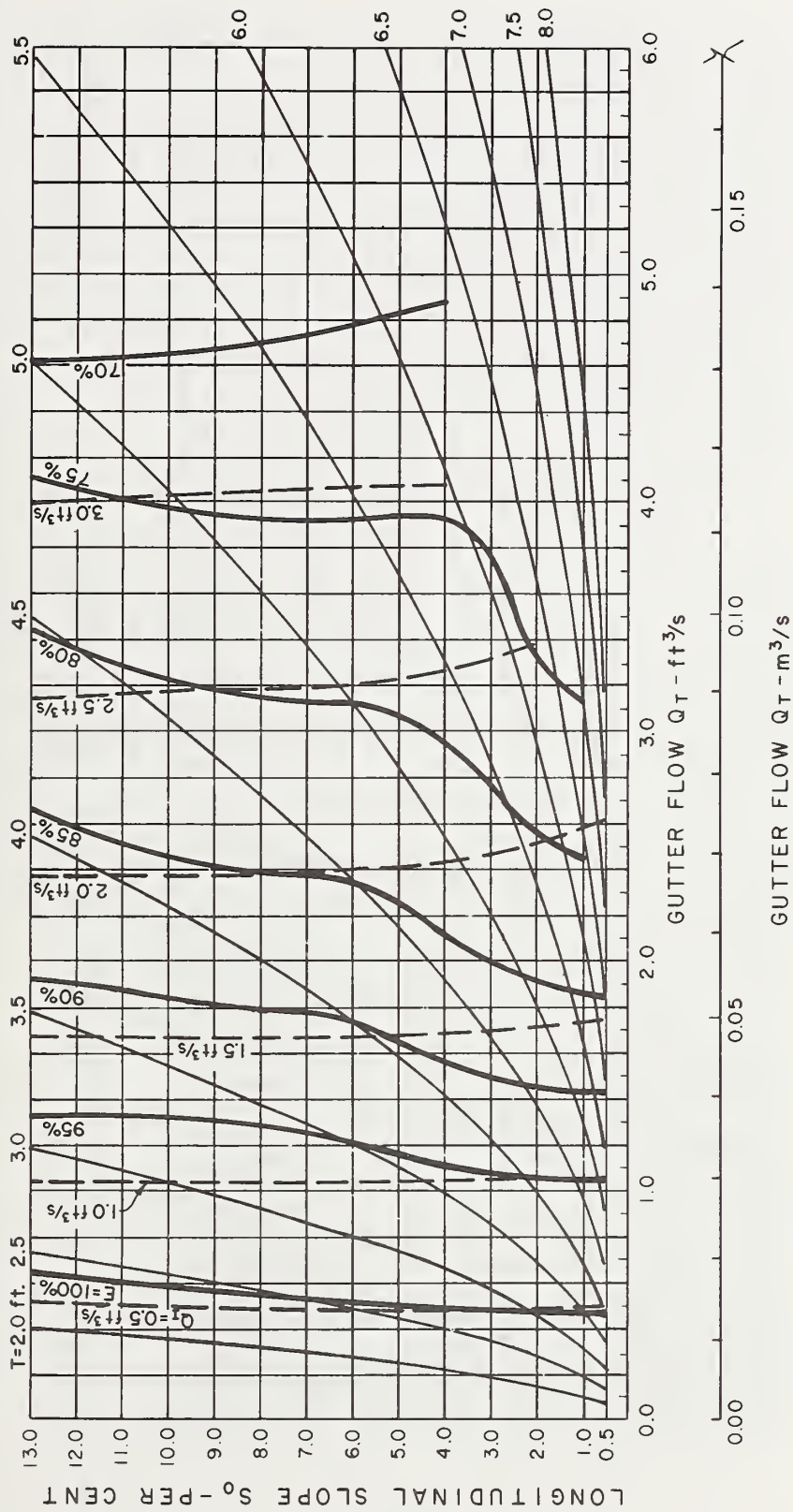


Figure 8-20. - Grate inlet capacity curves, 2 ft by 4 ft (0.61 m by 1.22 m) 45 - 3-1/4 - 4 grate, $Z = 24$ (Note: 1 $\text{ft}^3/\text{s} = 0.028 \text{ m}^3/\text{s}$, 1 ft = 0.305 m).

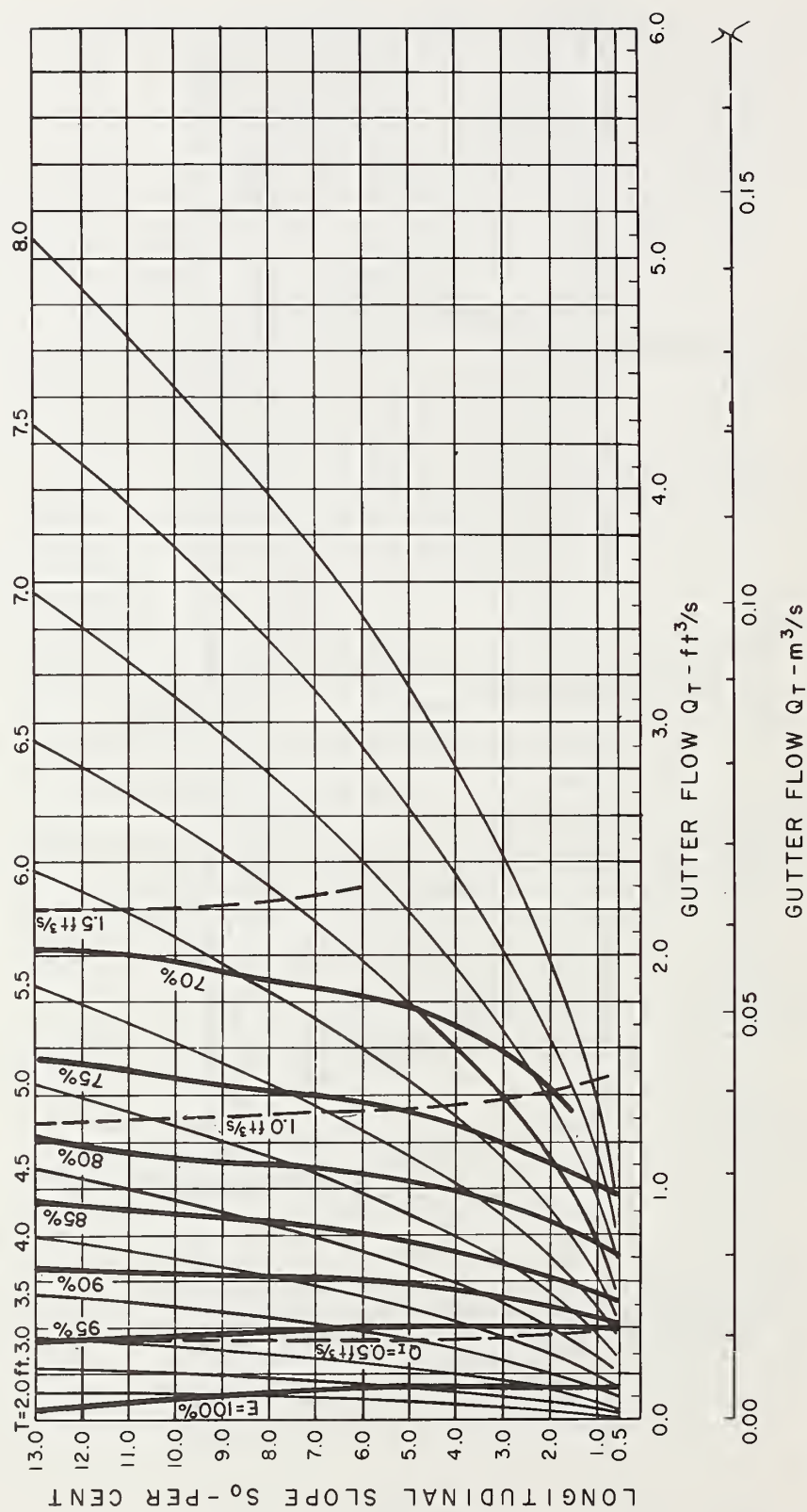


Figure 8-21. - Grate inlet capacity curves, 2 ft by 4 ft (0.61 m by 1.22 m) 45 - 3-1/4 - 4 grate, $Z = 48$ (Note: 1 $\text{ft}^3/\text{s} = 0.028 \text{ m}^3/\text{s}$, 1 ft = 0.305 m).

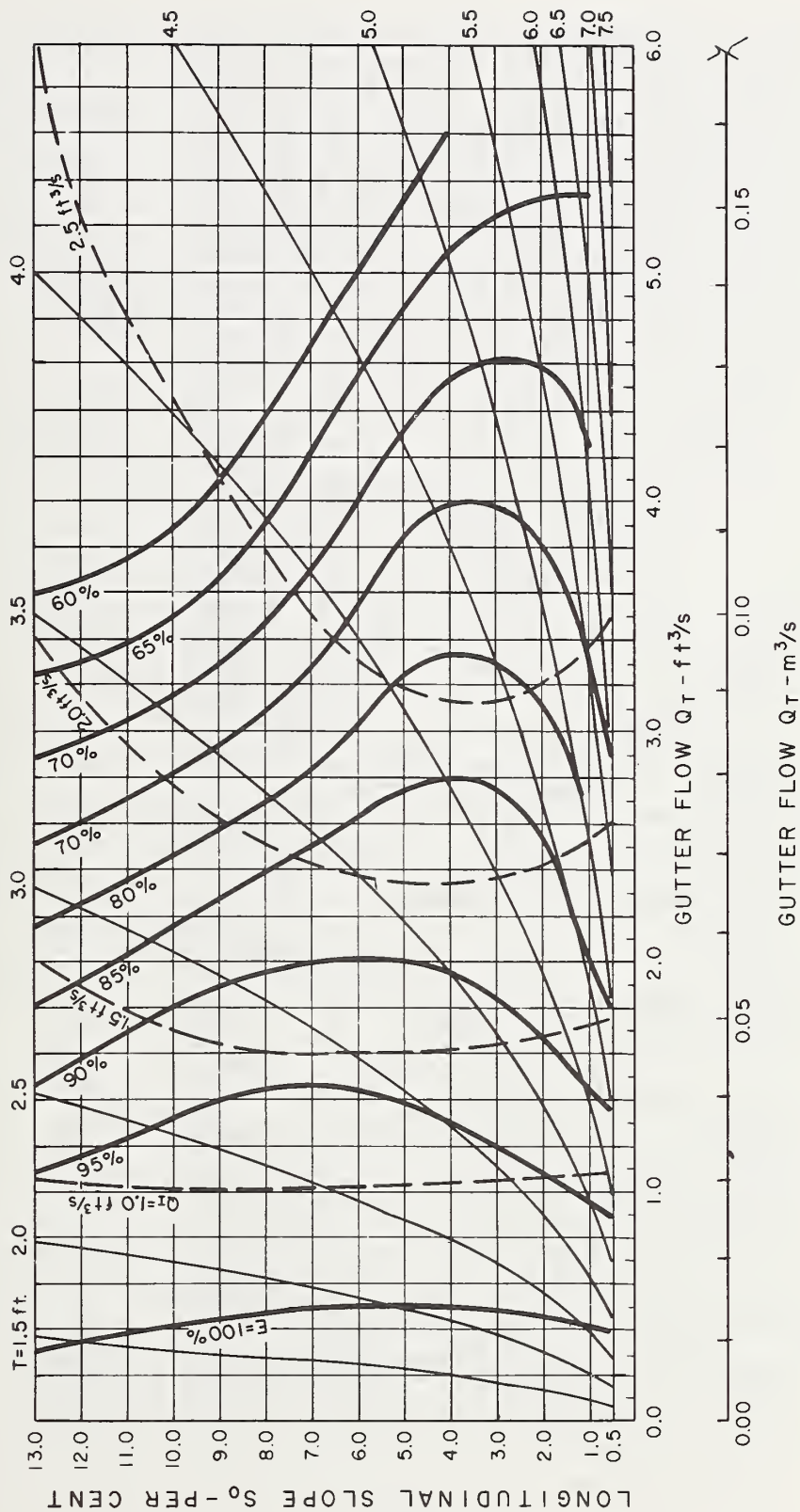


Figure 8-22. - Grate inlet capacity curves, 2 ft by 2 ft (0.61 m by 0.61 m) 45 - 3-1/4 - 4 grate, $Z = 16$ (Note: $1 \text{ ft}^3/\text{s} = 0.028 \text{ m}^3/\text{s}$, $1 \text{ ft} = 0.305 \text{ m}$).

Figure 8-23. - Grate inlet capacity curves, 2 ft by 2 ft (0.61 m by 0.61 m) 45 - 3-1/4 - 4 grate, Z = 24 (Note: 1 ft³/s = 0.028 m³/s, 1 ft = 0.305 m).

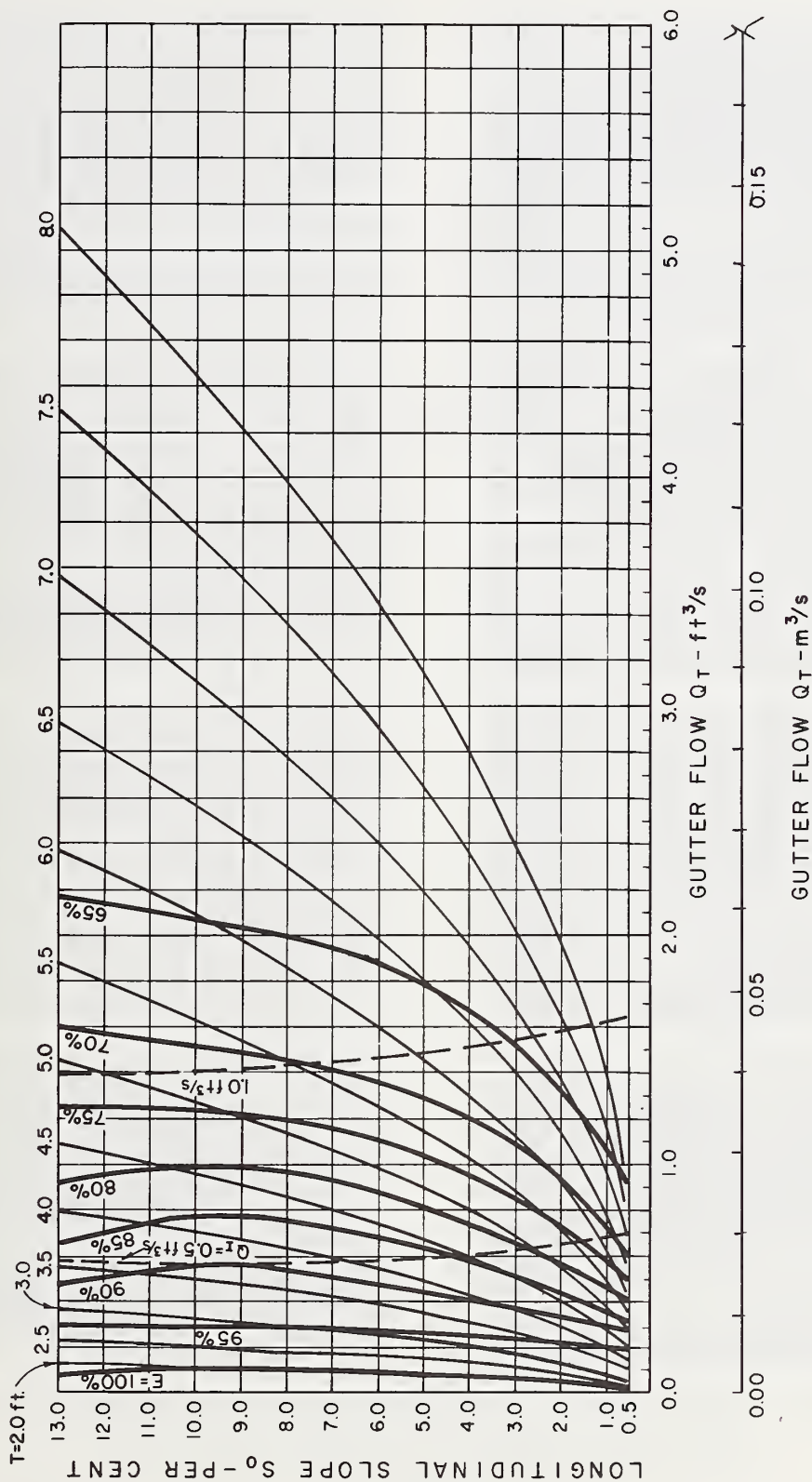
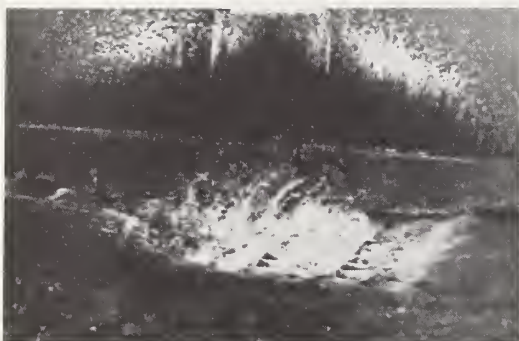


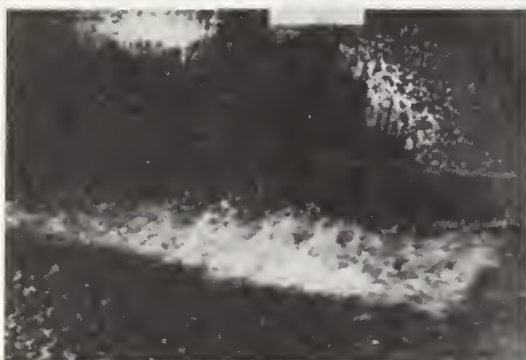
Figure 8-24. - Grate inlet capacity curves, 2 ft by 2 ft (0.61 m by 0.61 m) 45 - 3-1/4 - 4 grate, $Z = 48$ (Note: $1 \text{ ft}^3/\text{s} = 0.028 \text{ m}^3/\text{s}$, $1 \text{ ft} = 0.305 \text{ m}$).



- a. $S_0 = 4\%$
 $Q_T = 5.20 \text{ ft}^3/\text{s} \text{ (} 0.147 \text{ m}^3/\text{s)}$
 $T' = 7.0 \text{ ft (} 2.13 \text{ m)}$
 $E = 59\%$



- b. $S_0 = 6\%$
 $Q_T = 5.49 \text{ ft}^3/\text{s} \text{ (} 0.155 \text{ m}^3/\text{s)}$
 $T' = 6.5 \text{ ft (} 1.98 \text{ m)}$
 $E = 48\%$

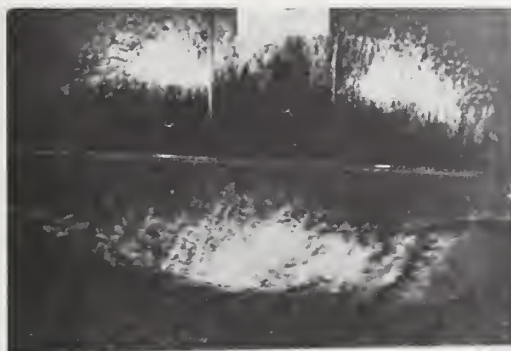


- c. $S_0 = 9\%$
 $Q_T = 5.49 \text{ ft}^3/\text{s} \text{ (} 0.155 \text{ m}^3/\text{s)}$
 $T' = 6.1 \text{ ft (} 1.86 \text{ m)}$
 $E = 45\%$

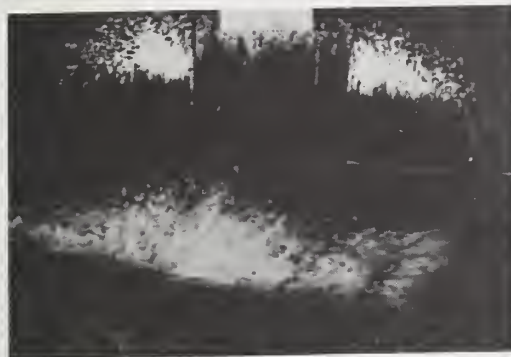


- d. $S_0 = 13\%$
 $Q_T = 5.34 \text{ ft}^3/\text{s} \text{ (} 0.151 \text{ m}^3/\text{s)}$
 $T' = 5.8 \text{ ft (} 1.77 \text{ m)}$
 $E = 41\%$

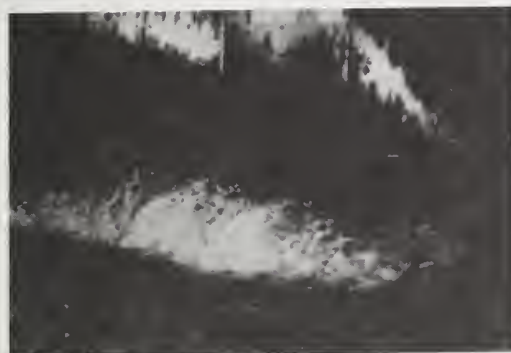
Figure 8-25. - Development of splash on 2 ft by 2 ft (0.61 m by 0.61 m)
 45 - 2-1/4 - 4 grate, $Z = 24$.
 Photo H-1765-379



- a. $S_0 = 4\%$
 $Q_T = 5.02 \text{ ft}^3/\text{s} \text{ (} 0.142 \text{ m}^3/\text{s)}$
 $T' = 6.7 \text{ ft} \text{ (} 2.04 \text{ m)}$
 $E = 58\%$



- b. $S_0 = 6\%$
 $Q_T = 4.83 \text{ ft}^3/\text{s} \text{ (} 0.137 \text{ m}^3/\text{s)}$
 $T' = 6.1 \text{ ft} \text{ (} 1.86 \text{ m)}$
 $E = 54\%$



- c. $S_0 = 9\%$
 $Q_T = 5.34 \text{ ft}^3/\text{s} \text{ (} 0.151 \text{ m}^3/\text{s)}$
 $T' = 5.9 \text{ ft} \text{ (} 1.80 \text{ m)}$
 $E = 46\%$



- d. $S_0 = 13\%$
 $Q_T = 5.34 \text{ ft}^3/\text{s} \text{ (} 0.151 \text{ m}^3/\text{s)}$
 $T' = 5.8 \text{ ft} \text{ (} 1.77 \text{ m)}$
 $E = 43\%$

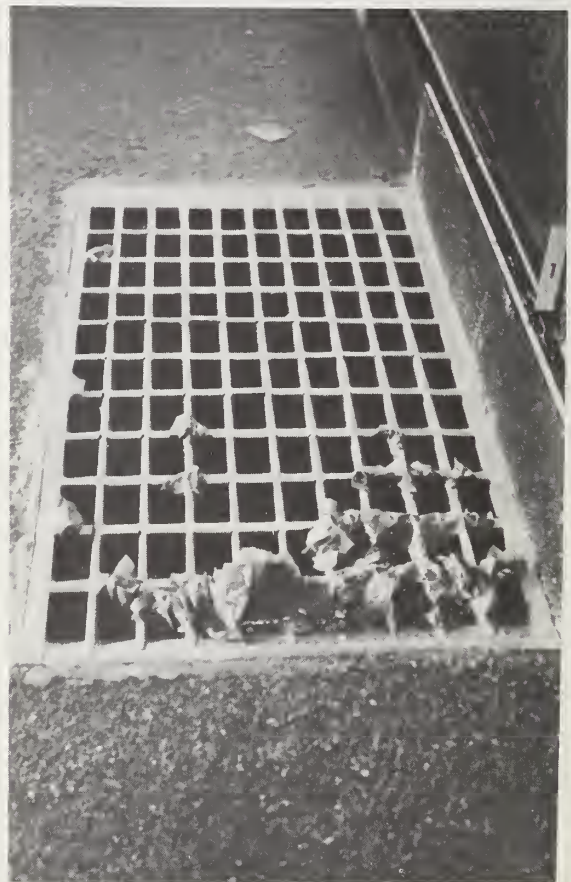
Figure 8-26. - Development of splash on 2 ft by 2 ft (0.61 m by 0.61 m)
 45 - 3-1/4 - 4 grate, $Z = 24$.
 Photo H-1765-380



a. $Q_T = 2.67 \text{ ft}^3/\text{s}$ ($0.076 \text{ m}^3/\text{s}$)

$T' = 5.0 \text{ ft}$ (1.52 m)

Photo 78 1A



b. View looking downstream
at 115 pieces of debris
caught on the grate.

Photo 78-3A

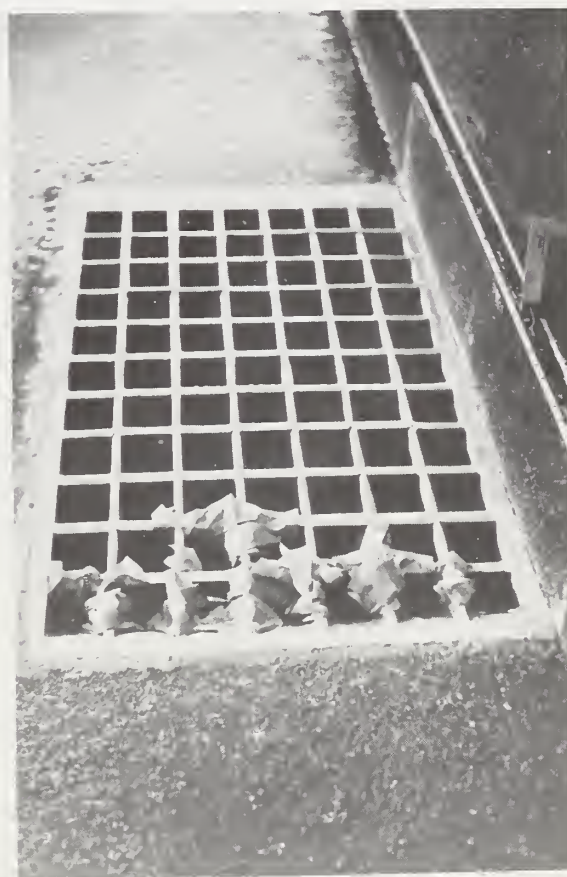
Figure 8-27. - Debris test, 2 ft by 4 ft (0.61 m by 1.22 m)
45 - 2-1/4 - 4 grate, $S_0 = 4\%$, $Z = 24$.



a. $Q_T = 0.5 \text{ ft}^3/\text{s}$ ($0.014 \text{ m}^3/\text{s}$)

$T' = 3.0 \text{ ft}$ (0.91 m)

Photo 83 17-17A



b. View looking downstream
at 72 pieces of debris
caught on the grate.
Photo 83 20-20A

Figure 8-28. - Debris test, 2 ft by 4 ft (0.61 m by 1.22 m)
45 - 3-1/4 - 4 grate, $S_0 = 4\%$, $Z = 24$.

45 - 3-1/4 - 4 grates, respectively. Results of the debris tests for both sizes of these grates are shown in tables 8-2 and 8-3.

The 45 - 2-1/4 - 4 and 45 - 3-1/4 - 4 grates are both more efficient at passing debris in the 4 ft (1.22 m) length than in the 2 ft (0.61 m) length. All of the grates are better at passing debris at a 4 percent slope than at 0.5 percent. The effect of the 1 in (25.4 mm) wider longitudinal bar spacing on the 45 - 3-1/4 - 4 grates is evident as these grates passed about twice as much debris as the 45 - 2-1/4 - 4 grates.

Summary

The 45° tilt-bar grates have good hydraulic characteristics at slopes of 4 percent to 7 percent. Steeper longitudinal slopes, particularly in combination with steeper cross slopes, cause decreasing hydraulic efficiencies.

For a given gutter flow, the 45° tilt-bar grates show an improvement in hydraulic efficiency with increasing longitudinal slope until some maximum efficiency is reached (figures 8-13 through 8-24). Above this slope, efficiencies are lower. Maximum efficiency slope depends on cross slope, gutter flow, and grate length (table 8-1).

The 45 - 2-1/4 - 4 and 45 - 3-1/4 - 4 grates are hydraulically identical for all practical purposes. The problem of the warped bar on the 45 - 3-1/4 - 4 grates is enough to account for the small efficiency differences between the 45 - 2-1/4 - 4 and 45 - 3-1/4 - 4 grates.

For any given width of flow spread, the 45° tilt-bar grates are more efficient at the flatter longitudinal and cross slopes than at the steeper longitudinal and cross slopes (figures 8-7 through 8-10).

The 45 - 2-1/4 - 4 grates are not particularly efficient at passing debris. On the average, they passed 13 percent of the "leaves" in the first 5 minutes and 20 percent at the end of 15 minutes. The 45 - 3-1/4 - 4 grates are much more efficient, passing 36 percent in the first 5 minutes and 46 percent at the end of 15 minutes (tables 8-2 and 8-3).

Table 8-2

DEBRIS TEST RESULTS - 45 - 2-1/4 - 4 GRATES

Test No.	Number of "leaves" lodged on grate*			
	$S_0 = 0.5\%$		$S_0 = 4.0\%$	
	5 minutes	15 minutes	5 minutes	15 minutes
<u>2 ft by 2 ft (0.61 m by 0.61 m) grate</u>				
1	143	129		
2	138	135		
3	135	124		
4			125	113
5			131	120
6			121	113
Debris handling efficiency* (%)	8	14	16	23
<u>2 ft by 4 ft (0.61 m by 1.22 m) grate</u>				
1			122	115
2			122	116
3			129	112
4	137	122		
5	125	115		
6	136	128		
Debris handling efficiency* (%)	12	19	17	24

* Based on 150 "leaves" arriving at the grate.

Table 8-3

DEBRIS TEST RESULTS - 45 - 3-1/4 - 4 GRATES

Test No.	Number of "leaves" lodged on grate*			
	$S_0 = 0.5\%$		$S_0 = 4.0\%$	
	5 minutes	15 minutes	5 minutes	15 minutes
<u>2 ft by 2 ft (0.61 m by 0.61 m) grate</u>				
1			97	85
2			90	80
3			94	87
4	102	81		
5	105	92		
6	88	73		
Debris handling efficiency* (%)	34	45	38	44
<u>2 ft by 4 ft (0.61 m by 1.22 m) grate</u>				
1			85	72
2			87	67
3			98	76
4	109	90		
5	109	96		
6	86	73		
Debris handling efficiency* (%)	32	42	40	52

* Based on 150 "leaves" arriving at the grate.

CHAPTER 9

HYDRAULIC EFFICIENCY AND DEBRIS TESTS - 30° TILT-BAR GRATES

Introduction

The spacings and sizes of the transverse and longitudinal bars for the 30° tilt-bar grate was based on the bicycle safety tests of the 45° tilt-bar grates (Chapter 3) and a structural analyses for the 30° tilt-bar grate (Chapter 2). The 30° tilt-bar grate is shown in figure 9-1. The center-to-center spacing of the longitudinal and transverse members are 3-7/32 in (81.8 mm) and 4 in (102 mm), respectively. Based on a bearing bar thickness of 3/4 in (19 mm), the structural analysis (Chapter 2) determined the required vertical depth to be 2.55 in (65 mm). Although the prototype ductile cast grate would require a 2.55 in (65 mm) depth, the wood test grates were made 2.5 in (64 mm) deep. In this report, we will refer to the grates by their nominal sizes of 2 ft by 4 ft (0.61 m by 1.22 m) and 2 ft by 2 ft (0.61 m by 0.61 m).

Experimental Results and Observations

Hydraulics. - Figures 9-2 and 9-3 present the experimental results for the 2 ft by 4 ft (0.61 m by 1.22 m) and 2 ft by 2 ft (0.61 m by 0.61 m) 30° tilt-bar grates. The figures evidence a loss in hydraulic efficiency for the 30° grate as the flow energy increases for a given gutter flow. The combination of flow velocity and depth is low enough for the $Z = 48$ cross slope that hydraulic efficiency improves for both grate sizes as longitudinal slope, S_0 , increases for the same gutter flow, Q_T (figures 9-2 and 9-3). For the steeper cross slopes, $1/Z$, which produce deeper flow depths, the hydraulic efficiency curves drop off at the higher longitudinal slopes, S_0 .

Figures 9-4a and 9-4b illustrate flow conditions similar to those shown in figure 7-5 (Chapter 7) for the reticuline grate. Instead of the low profile, "flow layer," produced by the reticuline grate, the 30° tilt-bar grate produces an arching spray pattern as the high velocity flow impacts on the first transverse bar.

The sequence of photographs in figure 9-5 shows the development of the spray pattern on the 2 ft by 2 ft (0.61 m by 0.61 m) grate at $Z = 48$ as the longitudinal slope is increased from 4 percent to 13 percent. This sequence can be compared to figure 7-4 of the reticuline grate report (Chapter 7). Although the spray pattern develops on the 30° tilt-bar grate for the $1/48$ cross slope, the hydraulic efficiency increases for steeper longitudinal slopes, S_0 , at a given gutter flow, Q_T , (figures 9-2 and 9-3), since the flow deflected over the grate is offset by the larger portion of flow

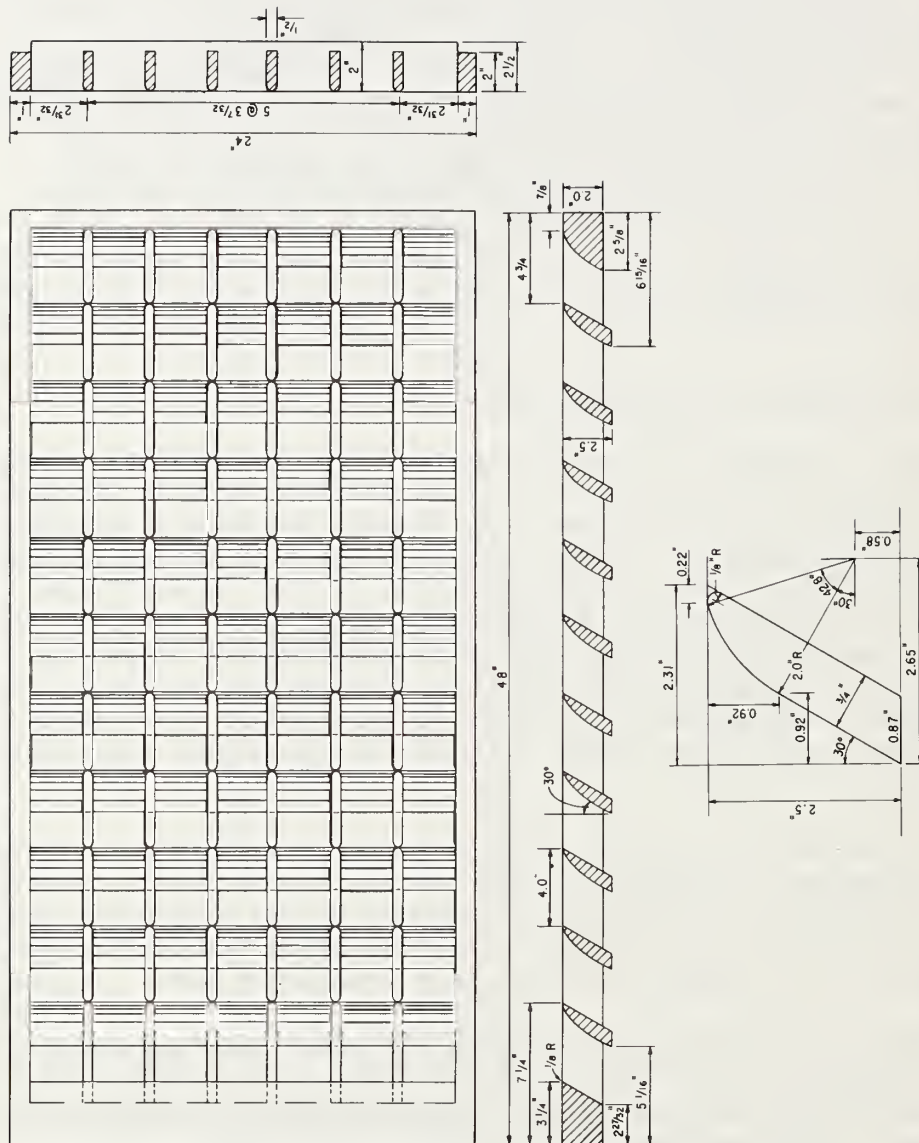


Figure 9-1. - 2 ft by 4 ft (0.61 m by 1.22 m) cast 30° tilt-bar grate (Note: 1 in = 25.4 mm).

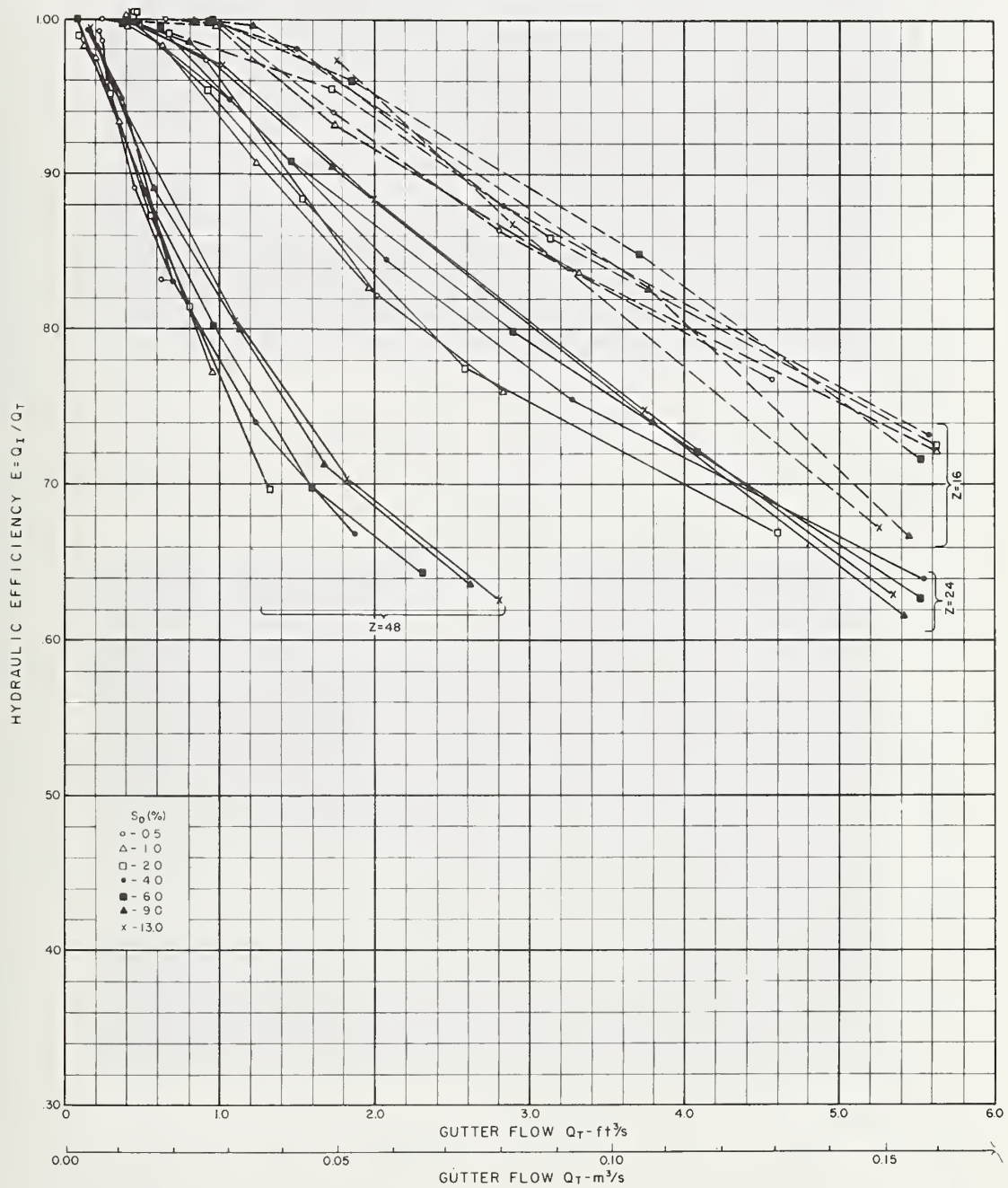


Figure 9-2. - Hydraulic efficiency vs. gutter flow, 2 ft by 4 ft (0.61 m by 1.22 m) 30° tilt-bar grate.

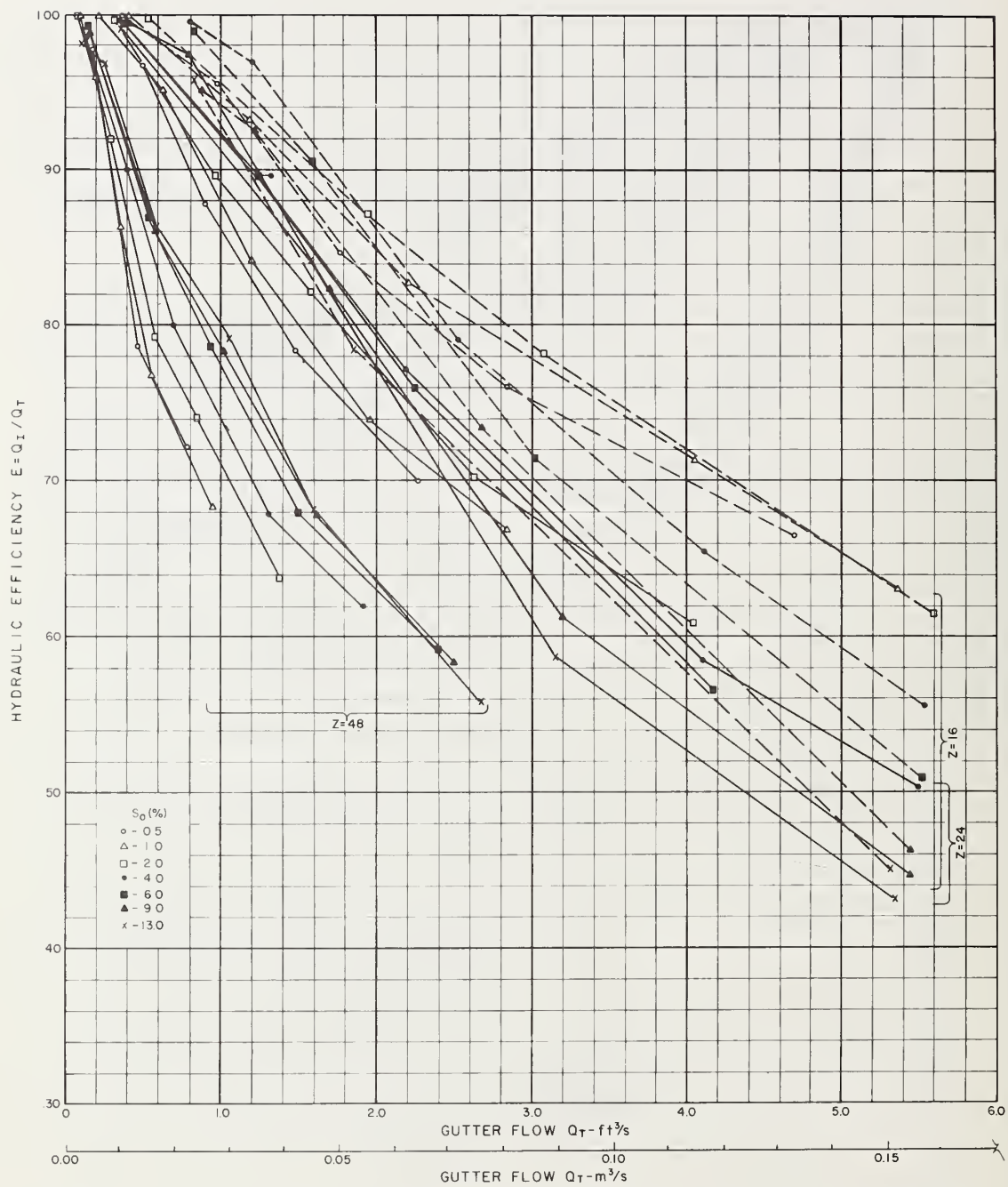
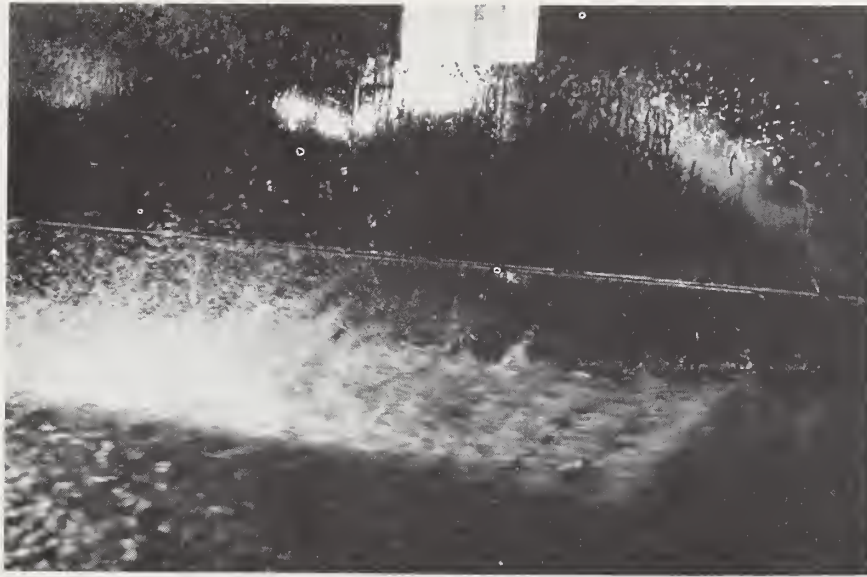


Figure 9-3. - Hydraulic efficiency vs. gutter flow, 2 ft by 2 ft (0.61 m by 0.61 m) 30° tilt-bar grate.



a. $S_0 = 6\%$
 $Q_T = 5.52 \text{ ft}^3/\text{s} \text{ (} 0.156 \text{ m}^3/\text{s)}$
 Photo 90-12

$T' = 6.4 \text{ ft (} 1.95 \text{ m)}$
 $E = 62.7$



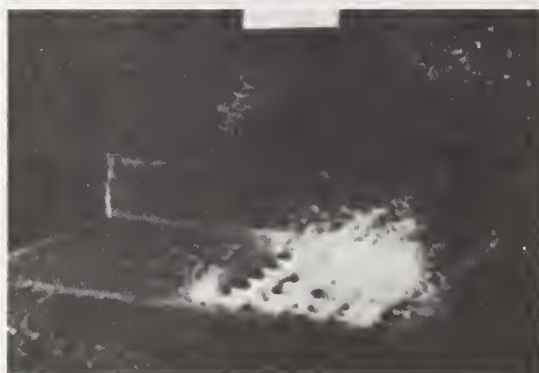
b. $S_0 = 13\%$
 $Q_T = 5.23 \text{ ft}^3/\text{s} \text{ (} 0.148 \text{ m}^3/\text{s)}$
 Photo 95-3

$T' = 5.7 \text{ ft (} 1.74 \text{ m)}$
 $E = 61.8$

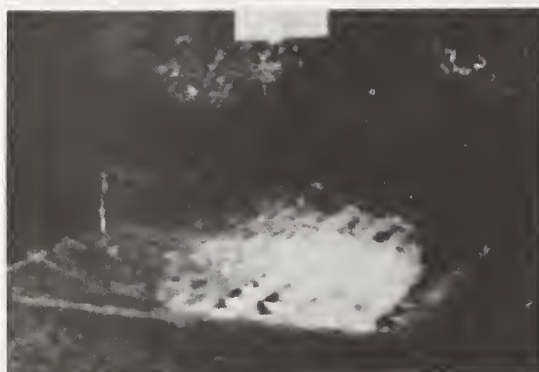
Figure 9-4. - Spray pattern on 2 ft by 4 ft (0.61 m by 1.22 m)
 30° tilt-bar grate, $Z = 24$.



- a. $S_O = 4\%$
 $Q_T = 1.92 \text{ ft}^3/\text{s} \text{ (} 0.054 \text{ m}^3/\text{s)}$
 $T' = 7.0 \text{ ft (} 2.13 \text{ m)}$
 $E = 62\%$



- b. $S_O = 6\%$
 $Q_T = 2.40 \text{ ft}^3/\text{s} \text{ (} 0.068 \text{ m}^3/\text{s)}$
 $T' = 7.0 \text{ ft (} 2.13 \text{ m)}$
 $E = 59.2\%$



- c. $S_O = 9\%$
 $Q_T = 2.50 \text{ ft}^3/\text{s} \text{ (} 0.071 \text{ m}^3/\text{s)}$
 $T' = 7.0 \text{ ft (} 2.13 \text{ m)}$
 $E = 58.4\%$



- d. $S_O = 13\%$
 $Q_T = 2.67 \text{ ft}^3/\text{s} \text{ (} 0.076 \text{ m}^3/\text{s)}$
 $T' = 7.0 \text{ ft (} 2.13 \text{ m)}$
 $E = 55.8\%$

Figure 9-5. - Development of spray pattern on 2 ft by 2 ft (0.61 m by 0.61 m) 30° tilt-bar grate, $Z = 48$. Photo H-1765-376

closer to the curb at steeper longitudinal slopes, S_0 , resulting in a net higher efficiency, E .

Figures 9-6 and 9-7 illustrate the hydraulic efficiency, E , for the two 30° tilt-bar grate sizes as a function of measured width of spread, T' .

The grate inlet capacity curves in figures 9-8 through 9-13 relate gutter flow, Q_T , and longitudinal slope, S_0 , to hydraulic efficiency, E , intercepted flow, Q_I , and calculated width of spread, T . There is one figure for each grate size and cross slope, $1/Z$. Figures 9-10 and 9-13 for a 1/48 cross slope illustrate the fact that as the longitudinal slope, S_0 , increases, there is no decrease in efficiency with respect to gutter flow, Q_T . For the 1/16 and 1/24 cross slopes (figures 9-8, 9-9, 9-11, and 9-12), there is a maximum efficiency slope, S_0 , above which the hydraulic efficiency of the grate begins to decrease with increase in slope, S_0 . The range of maximum efficiency slopes is given in table 9-1.

Table 9-1

MAXIMUM EFFICIENCY SLOPES - 30° TILT-BAR GRATES

Grate size	Z = 48	Z = 24	Z = 16
2 ft by 2 ft (0.61 m by 0.61 m)	>13%	2% to 7%	1% to 4%
2 ft by 4 ft (0.61 m by 1.22 m)	>13%	9%	3% to 6%

It is evident from the inlet capacity curves that the hydraulic efficiency, E , reaches a maximum at lower longitudinal slopes, S_0 , as the gutter flow, Q_T increases. For example, when $Z = 16$, for $Q_T = 3.00 \text{ ft}^3/\text{s}$ ($0.085 \text{ m}^3/\text{s}$) the large grate reaches its maximum hydraulic efficiency, $E = 88$ percent at $S_0 = 6$ percent. For $Q_T = 5.00 \text{ ft}^3/\text{s}$ ($0.142 \text{ m}^3/\text{s}$) the large grate reaches its maximum hydraulic efficiency, $E = 74$ percent at $S_0 = 3$ percent. For steeper longitudinal slopes, S_0 , when $Q_T = 5.00 \text{ ft}^3/\text{s}$ ($0.142 \text{ m}^3/\text{s}$) the efficiency reduces to $E = 69$ percent at $S_0 = 13$ percent. Therefore, the maximum efficiency slope is also a function of the gutter flow, Q_T .

Debris Tests. - Debris tests were conducted on the 30° tilt-bar grates according to the test procedure described in Chapter 5. Figure 9-14a shows the 2 ft by 4 ft (0.61 m by 1.22 m), 30° tilt-bar grate during a debris test at $S_0 = 4$ percent. Figure 9-14b shows

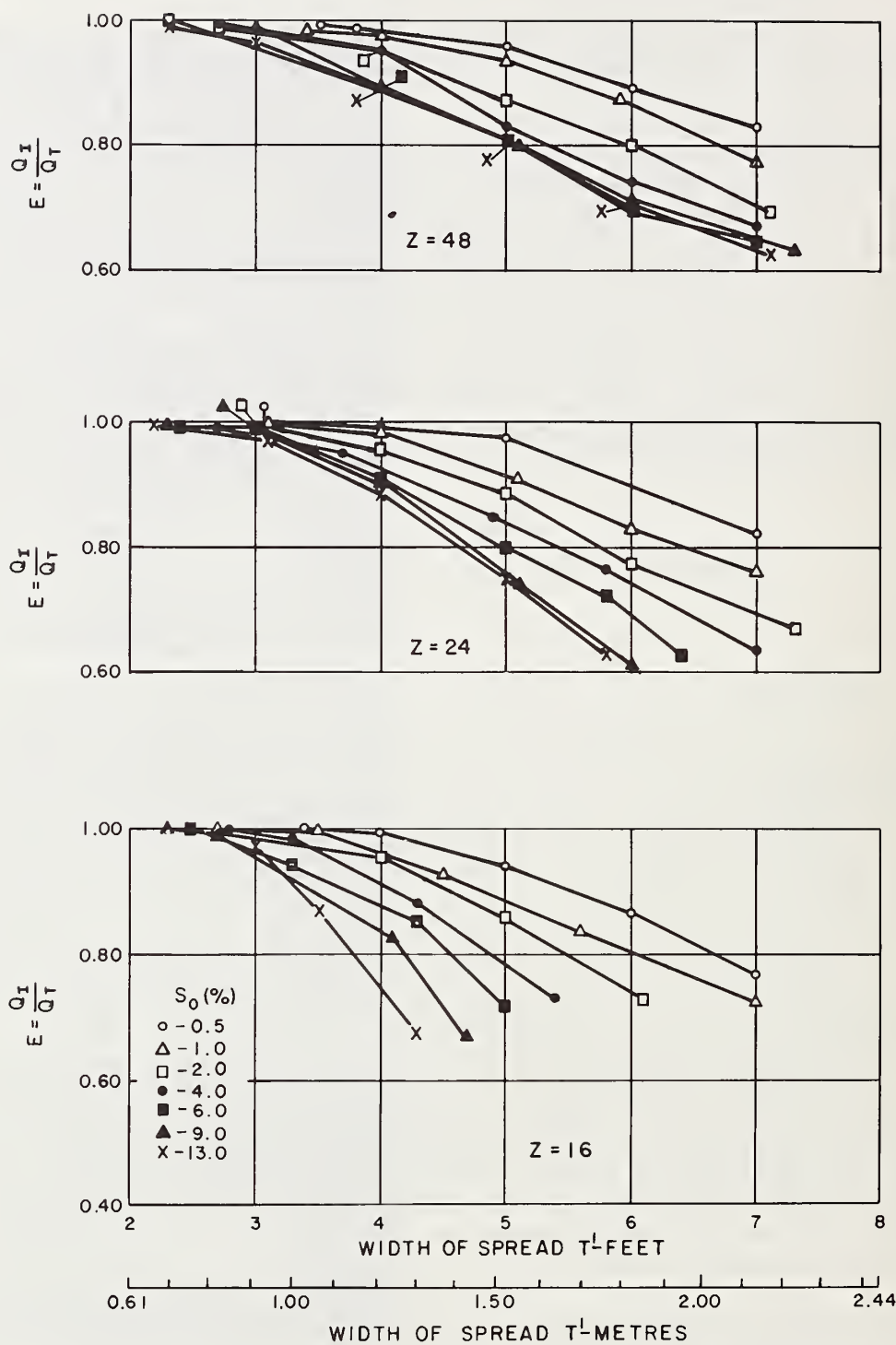


Figure 9-6. - Hydraulic efficiency vs. width of spread, 2 ft by 4 ft (0.61 m by 1.22 m) 30° tilt-bar grate.

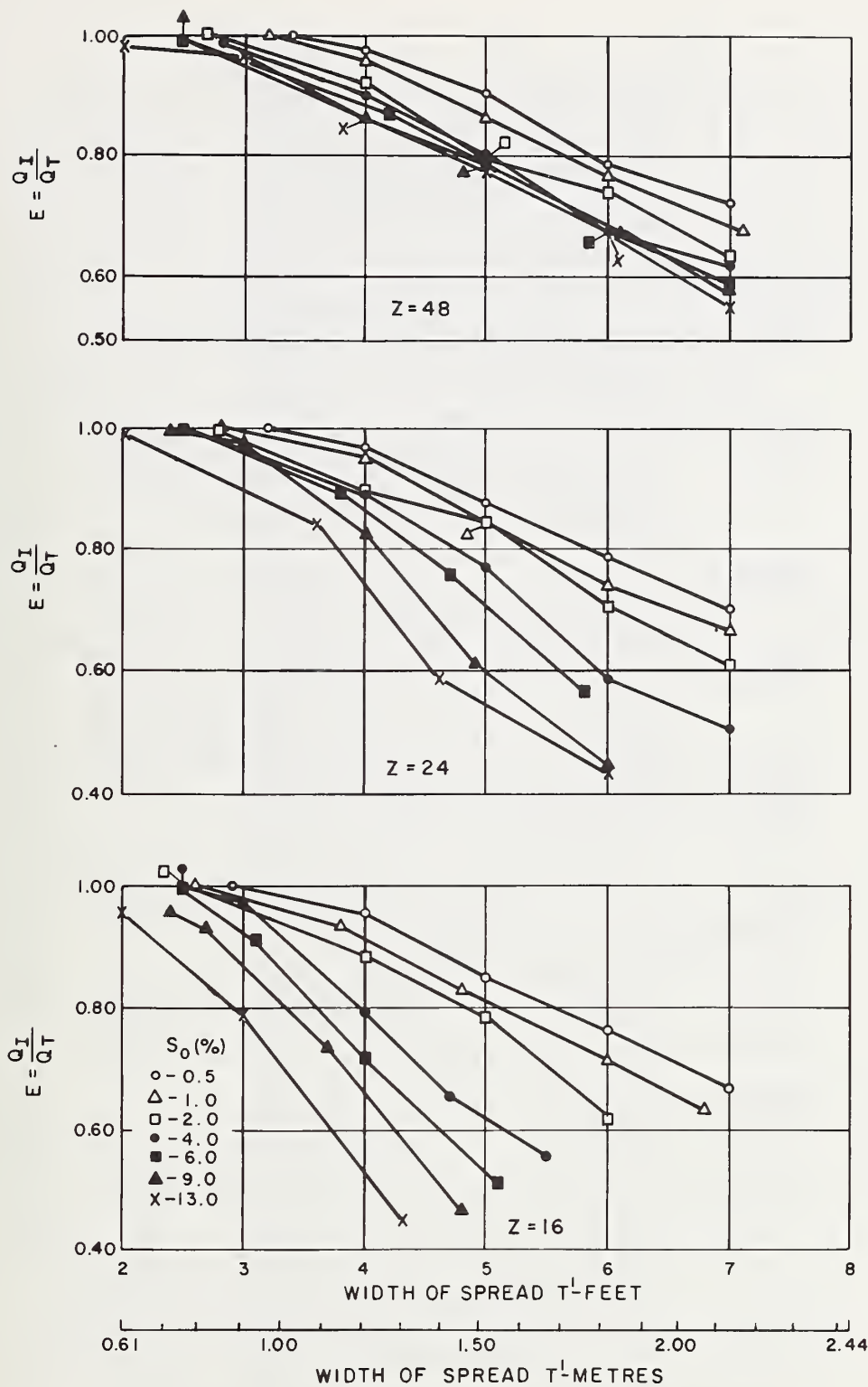


Figure 9-7. - Hydraulic efficiency vs. width of spread, 2 ft by 2 ft (0.61 m by 0.61 m) 30° tilt-bar grate.

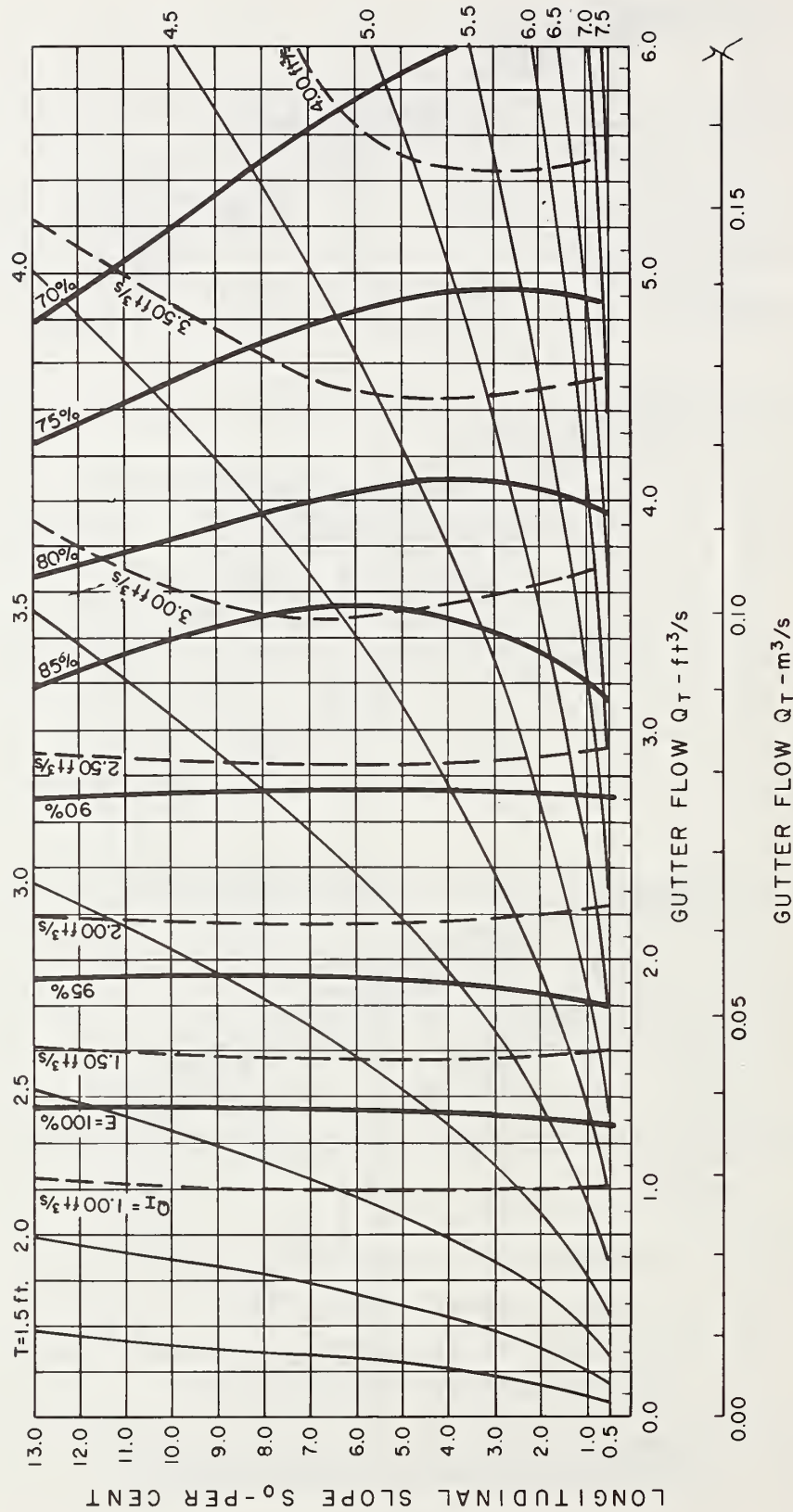


Figure 9-8. - Grate inlet capacity curves, 2 ft by 4 ft (0.61 m by 1.22 m) 30° tilt-bar grate, $Z = 16$ (Note: $1 \text{ ft}^3/\text{s} = 0.028 \text{ m}^3/\text{s}$, $1 \text{ ft} = 0.305 \text{ m}$).

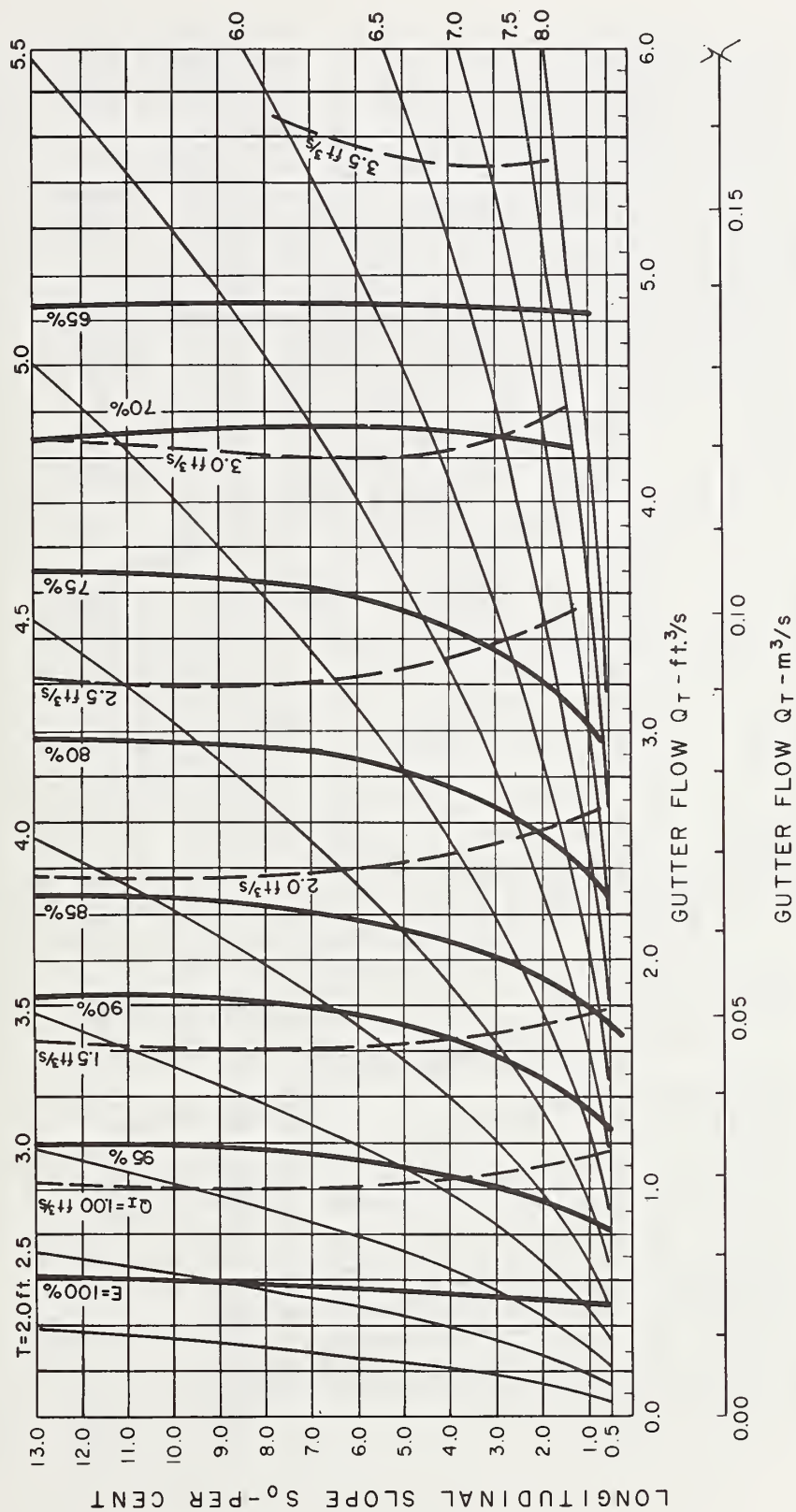


Figure 9-9. - Grate inlet capacity curves, 2 ft by 4 ft (0.61 m by 1.22 m) 30° tilt-bar grate, $Z = 24$ (Note: $1 \text{ ft}^3/\text{s} = 0.028 \text{ m}^3/\text{s}$, $1 \text{ ft} = 0.305 \text{ m}$).

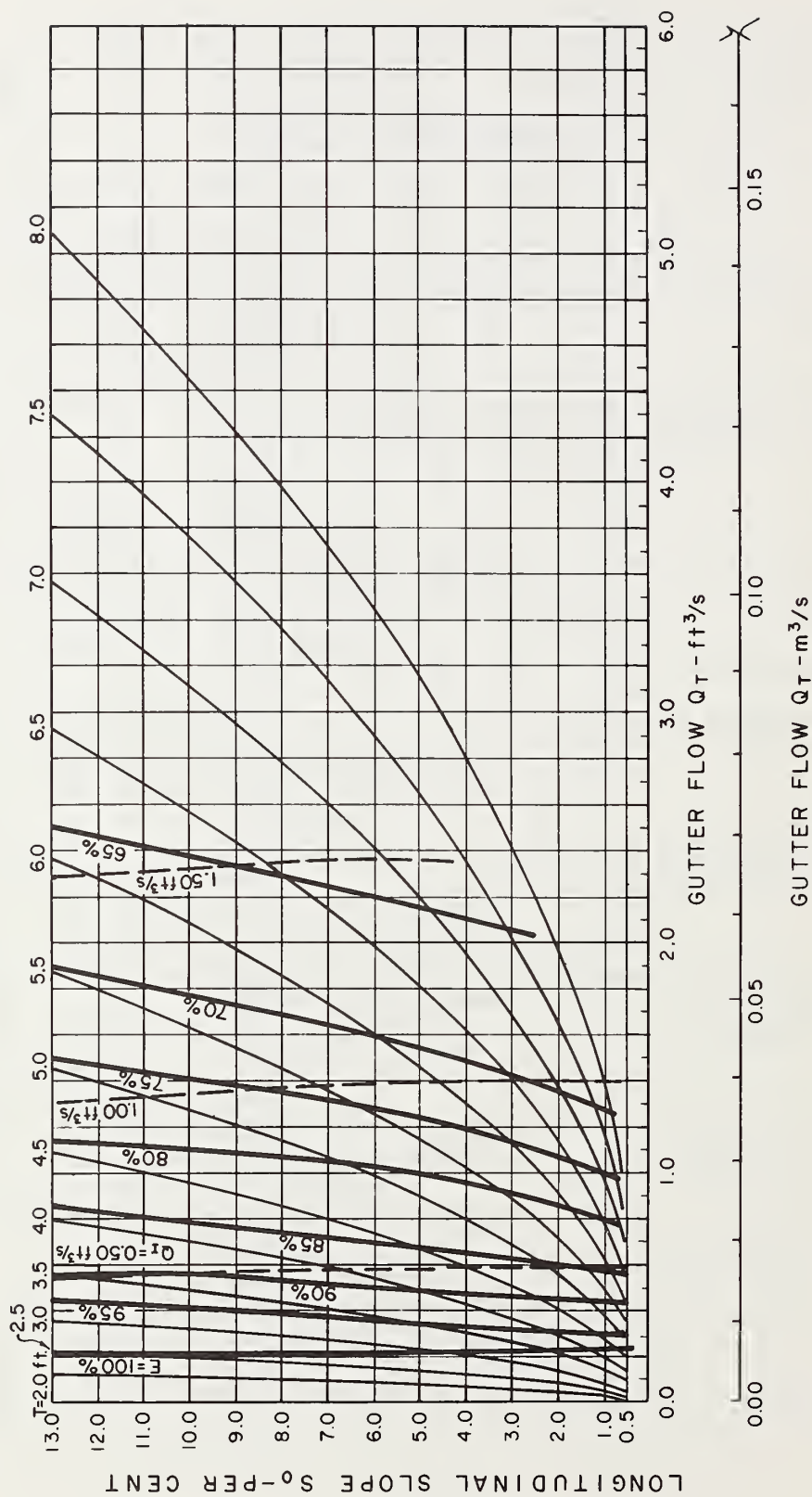


Figure 9-10. - Grate inlet capacity curves, 2 ft by 4 ft (0.61 m by 1.22 m) 30° tilt-bar grate, $Z = 48$ (Note: $1 \text{ ft}^3/\text{s} = 0.028 \text{ m}^3/\text{s}$, $1 \text{ ft} = 0.305 \text{ m}$).

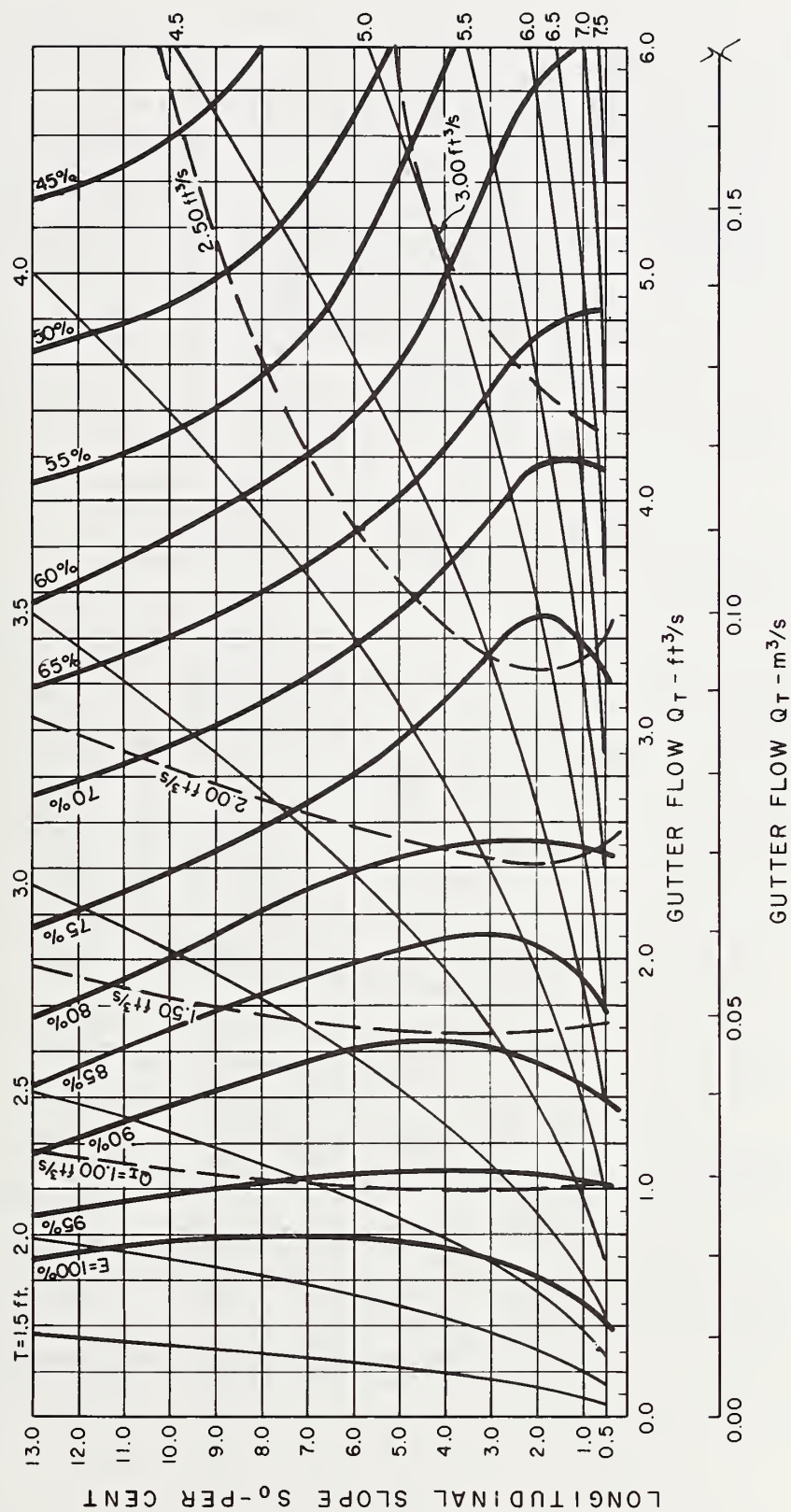


Figure 9-11. - Grate inlet capacity curves, 2 ft by 2 ft (0.61 m by 0.61 m) 30° tilt-bar grate,
 $Z = 16$ (Note: 1 $\text{ft}^3/\text{s} = 0.028 \text{ m}^3/\text{s}$, 1 ft = 0.305 m).

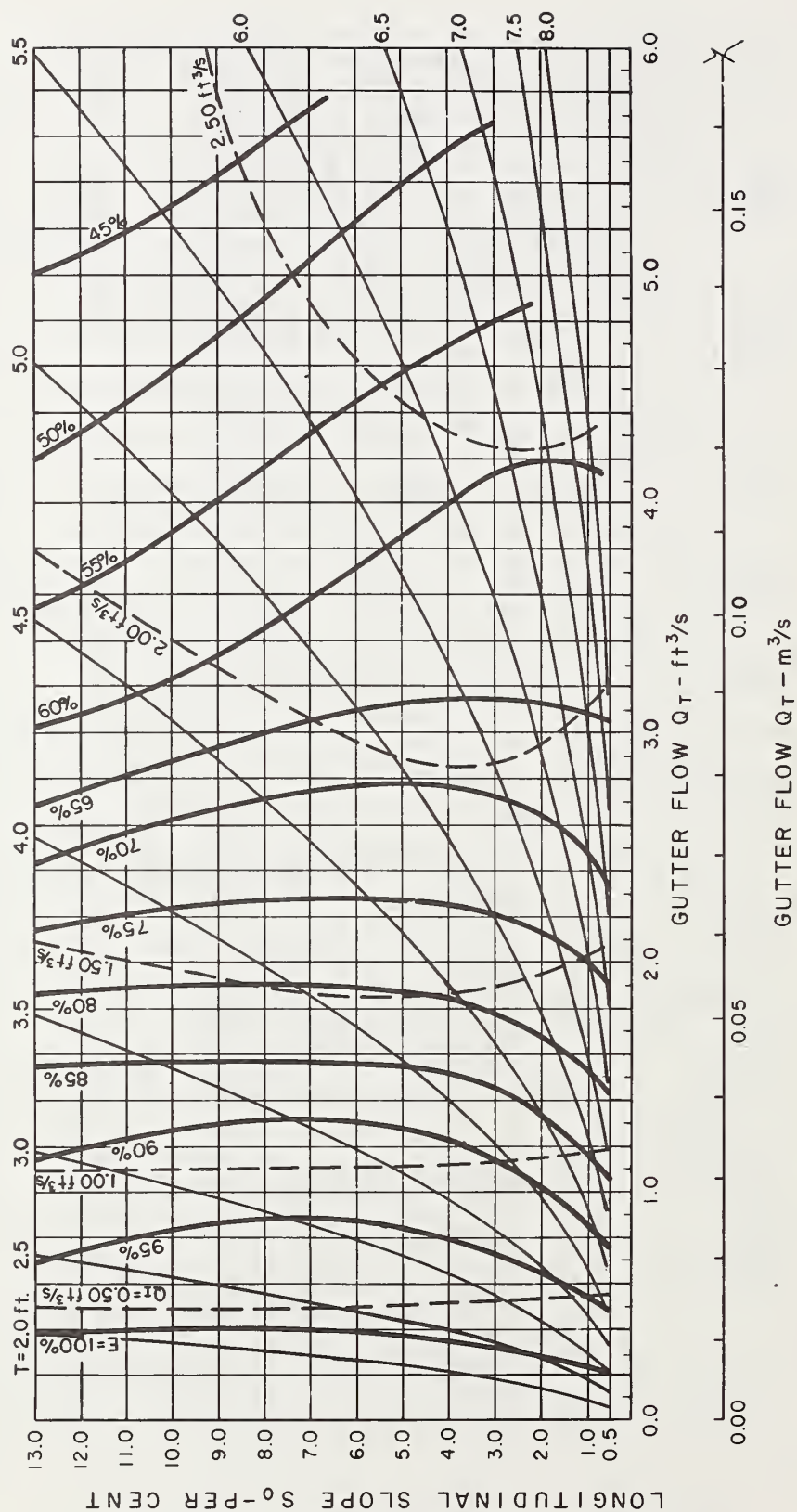


Figure 9-12. - Grate inlet capacity curves, 2 ft by 2 ft (0.61 m by 0.61 m) 30° tilt-bar grate, $Z = 24$ (Note: $1 \text{ ft}^3/\text{s} = 0.028 \text{ m}^3/\text{s}$, $1 \text{ ft} = 0.305 \text{ m}$).

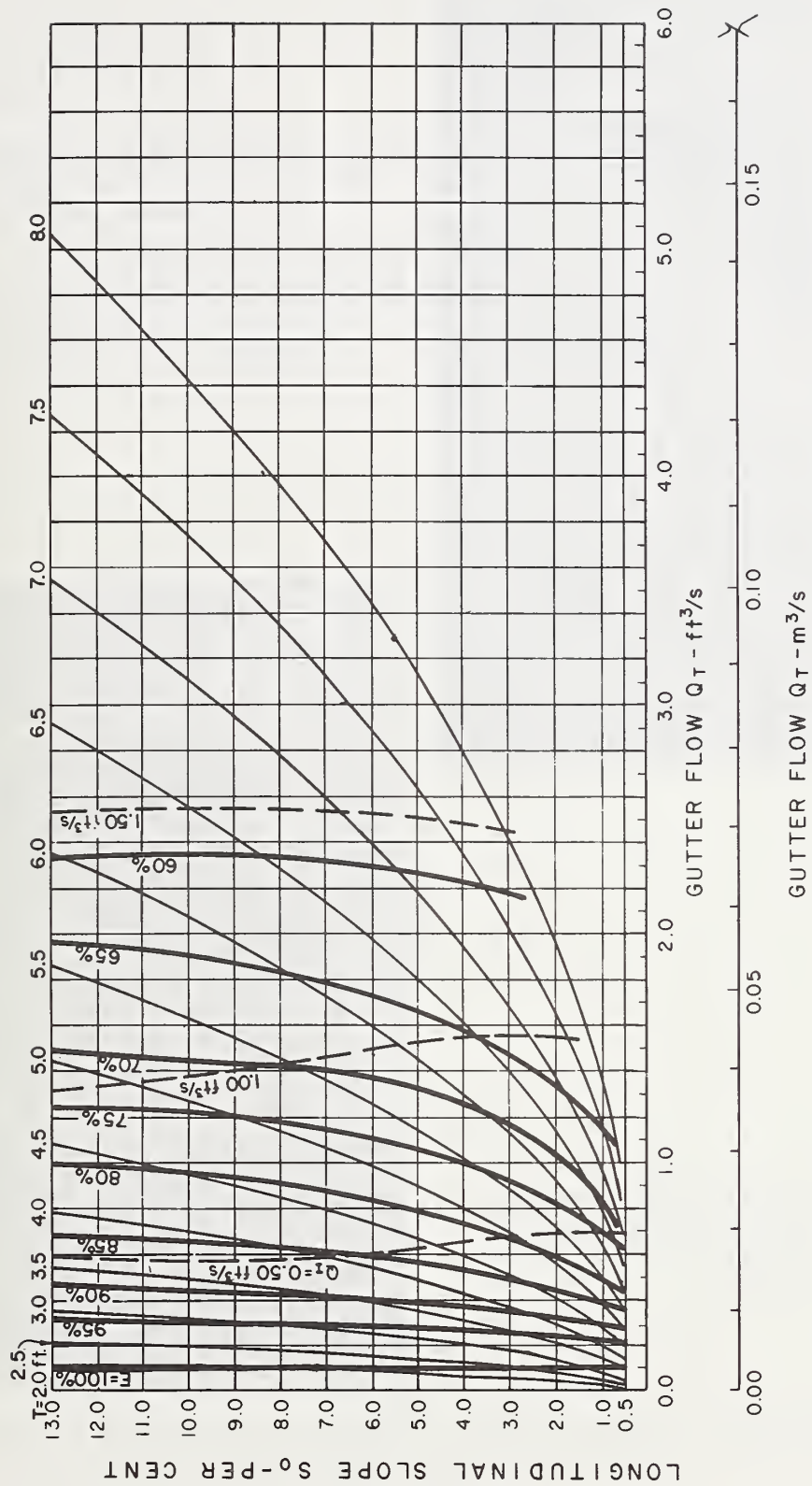


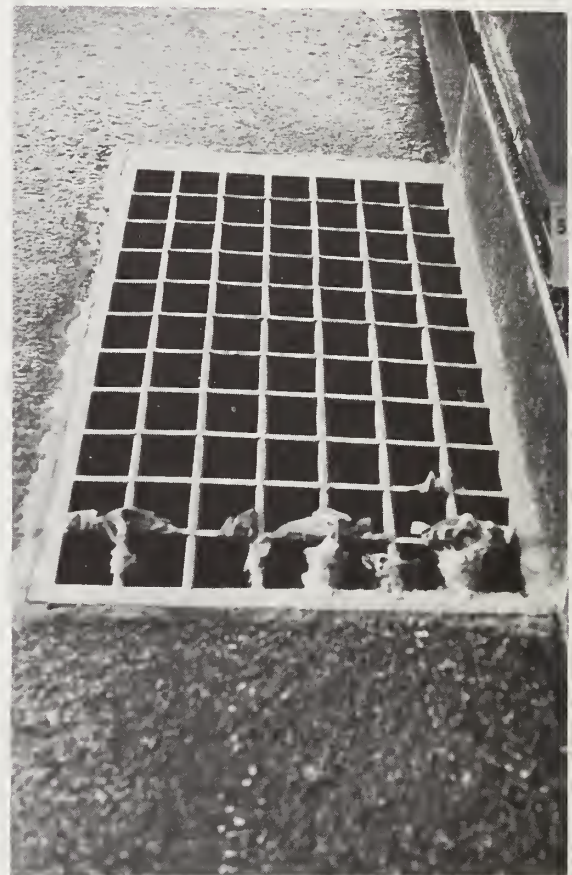
Figure 9-13. - Grate inlet capacity curves, 2 ft by 2 ft (0.61 m by 0.61 m) 30° tilt-bar grate, $Z = 48$ (Note: $1 \text{ ft}^3/\text{s} = 0.028 \text{ m}^3/\text{s}$, $1 \text{ ft} = 0.305 \text{ m}$).



a. $Q_T = 2.7 \text{ ft}^3/\text{s}$ ($0.076 \text{ m}^3/\text{s}$)

$T' = 5.4 \text{ ft}$ (1.65 m)

Photo 98-6A



b. View looking downstream at
67 pieces of debris caught
on the grate.

Photo 98-8A

Figure 9-14. - Debris tests, 2 ft by 4 ft (0.61 m by 1.22 m)
 30° tilt-bar grate, $S_0 = 4\%$, $Z = 24$.

the final distribution of debris after the test. The results of the debris test are presented in table 9-2. The 30° tilt-bar grate is relatively efficient at passing the tested debris.

Summary

The large and small sizes of the 30° tilt-bar grate have relatively good hydraulic characteristics for longitudinal slopes up to 6 percent and 2 percent, respectively.

Results of the debris test for the 30° tilt-bar grate indicated the grate to be efficient in passing debris. On the average, the two sizes of grate passed 42 percent of the leaves in the first 5 minutes and 50 percent in 15 minutes.

Table 9-2

DEBRIS TEST RESULTS - 30° TILT BAR GRATES

Test No.	Number of "leaves" lodged on grate*			
	$S_0 = 0.5\%$		$S_0 = 4.0\%$	
	5 minutes	15 minutes	5 minutes	15 minutes
<u>2 ft by 2 ft (0.61 m by 0.61 m) grate</u>				
1	87	79		
2	82	68		
3	87	82		
4			69	60
5			56	51
6			89	70
Debris handling efficiency* (%)	43	49	52	60
<u>2 ft by 4 ft (0.61 m by 1.22 m) grate</u>				
1	107	94		
2	97	83		
3	107	92		
4			88	76
5			81	67
6			91	78
Debris handling efficiency* (%)	31	40	42	51

* Based on 150 "leaves" arriving at the grate.

CHAPTER 10

HYDRAULIC EFFICIENCY AND DEBRIS TESTS - CURVED VANE GRATES

Introduction

This chapter describes the results of hydraulic and debris tests conducted on two sizes of the curved vane grate shown in figure 10-1. As was the case with the 30° tilt-bar grate, the bar spacings for the curved vane grates were chosen based on the bicycle safety tests of the 45° tilt-bar grate. The center-to-center spacings of the longitudinal and transverse members are 3-7/32 in (82.0 mm) and 4-1/2 in (114.0 mm), respectively.

Structural analysis showed that the maximum compressive and tensile stresses for the curved vane bar described in figure 10-1 meet the allowable stresses for ductile cast iron (Chapter 2).

Experimental Results and Observations

Hydraulics. - Figures 10-2 and 10-3 present the experimental results for the 2 ft by 4 ft (0.61 m by 1.22 m) and 2 ft by 2 ft (0.61 m by 0.61 m) curved vane grates. The results compare favorably with the curves generated for the parallel bar grates in Chapter 6. The hydraulic efficiency, E , continues to increase for a constant gutter flow, Q_T , as the longitudinal slope, S_0 , increases to 13 percent. In general, the curved vane grate, like the parallel bar grate, does not have the limiting longitudinal slope characteristic experienced by the other grates. The exception is the smaller curved vane grate (2 ft by 2 ft (0.61 m by 0.61 m)) when the cross slope, $1/Z = 1/16$, and the longitudinal slope S_0 is greater than 9 percent. This is evident in figure 10-3 where the $S_0 = 13$ percent curve is plotted below the $S_0 = 9$ percent curve for a $Z = 16$ cross slope.

Figure 10-4 illustrates the flow performance for the two sizes of the curved vane grate at the maximum longitudinal slope, $S_0 = 13$ percent. The 2 ft by 4 ft (0.61 m by 1.22 m) curved vane grate performs in a manner similar to the same size parallel bar grate shown in figure 6-4b in volume 6. The effective width of the curved vane grate is approximately 1-1/2 inches (38.1 mm) less than the width of the parallel bar grate which may cause the minor drop in efficiency of the curved vane grate in comparison with the parallel bar grate. The 2 ft by 2 ft (0.61 m by 0.61 m) curved vane grate (figure 10-4a) does not perform as well as the same size parallel bar grate (figure 6-4a, volume 6).

The sequence of photographs in figure 10-5 shows the development of the spray pattern on the 2 ft by 2 ft (0.61 m by 0.61 m) curved vane



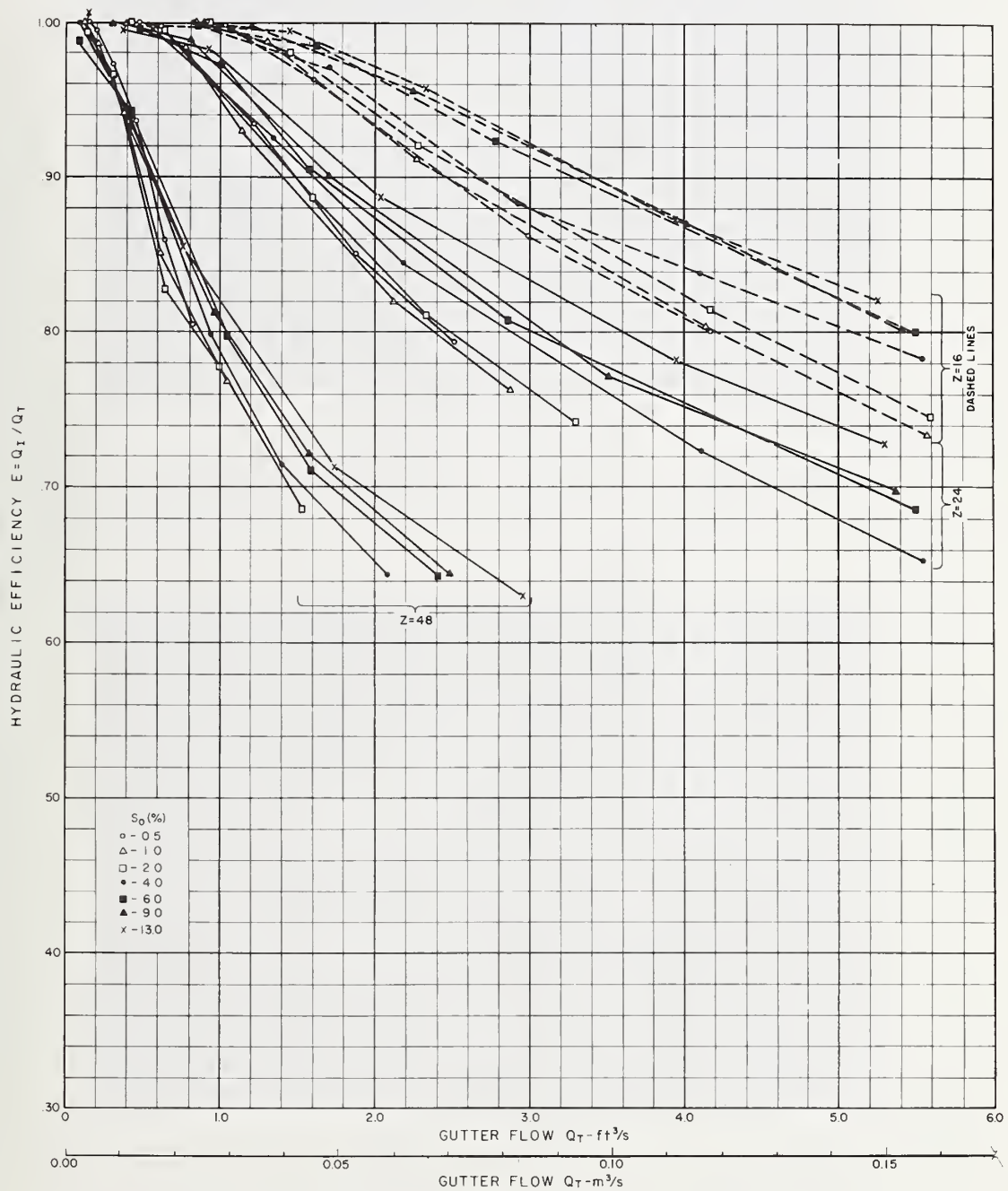


Figure 10-2. - Hydraulic efficiency vs. gutter flow, 2 ft by 4 ft (0.61 m by 1.22 m) curved vane grate.

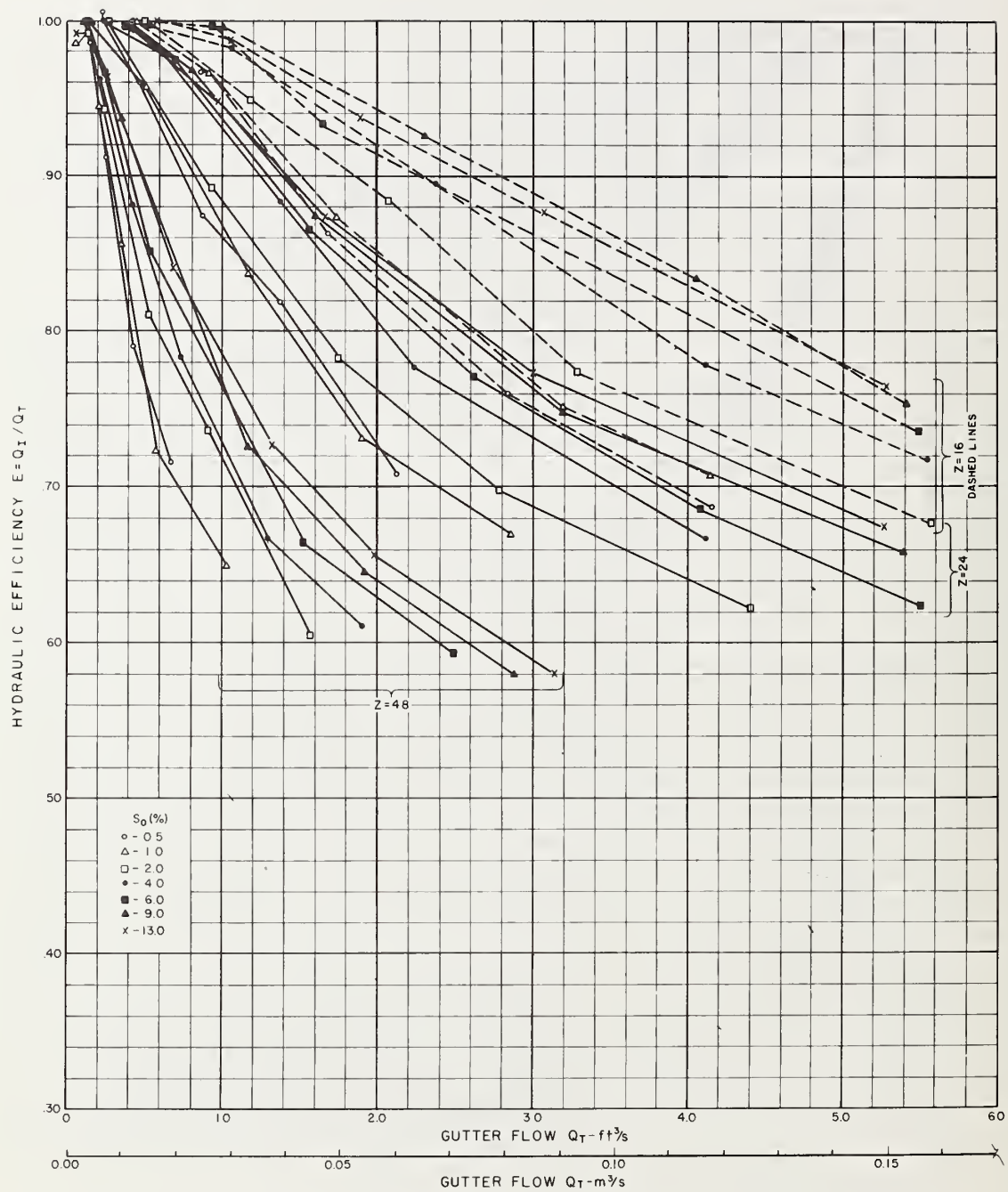


Figure 10-3. - Hydraulic efficiency vs. gutter flow, 2 ft by 2 ft (0.61 m by 0.61 m) curved vane grate.



a. 2 ft by 2 ft (0.61 m by 0.61 m) grate

$$Q_T = 5.26 \text{ ft}^3/\text{s} \quad (0.149 \text{ m}^3/\text{s})$$

Photo 108-20A

$$T' = 5.6 \text{ ft} \quad (1.71 \text{ m})$$

$$E = 67.5\%$$



b. 2 ft by 4 ft (0.61 m by 1.22 m) grate

$$Q_T = 5.29 \text{ ft}^3/\text{s} \quad (0.150 \text{ m}^3/\text{s})$$

Photo 109-20A

$$T' = 5.8 \text{ ft} \quad (1.77 \text{ m})$$

$$E = 72.8\%$$

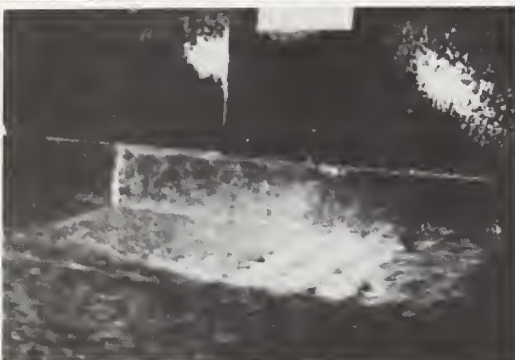
Figure 10-4. - Flow performance of the curved vane grate at $S_0 = 13\%$,
 $Z = 24$.



- a. $S_0 = 4\%$
 $Q_T = 4.11 \text{ ft}^3/\text{s} \text{ (} 0.116 \text{ m}^3/\text{s)}$
 $T' = 6.2 \text{ ft (} 1.89 \text{ m)}$
 $E = 66.7\%$



- b. $S_0 = 6\%$
 $Q_T = 5.50 \text{ ft}^3/\text{s} \text{ (} 0.156 \text{ m}^3/\text{s)}$
 $T' = 6.4 \text{ ft (} 1.95 \text{ m)}$
 $E = 62.5\%$



- c. $S_0 = 9\%$
 $Q_T = 5.39 \text{ ft}^3/\text{s} \text{ (} 0.153 \text{ m}^3/\text{s)}$
 $T' = 6.0 \text{ ft (} 1.83 \text{ m)}$
 $E = 65.9\%$



- d. $S_0 = 13\%$
 $Q_T = 5.26 \text{ ft}^3/\text{s} \text{ (} 0.149 \text{ m}^3/\text{s)}$
 $T' = 5.6 \text{ ft (} 1.71 \text{ m)}$
 $E = 67.5\%$

Figure 10-5. - Development of spray pattern on the 2 ft by 2 ft
 (0.61 m by 0.61 m) curved vane grate, $Z = 24$.
 Photo H-1765-381

grate at $Z = 24$ as the longitudinal slope is increased from 4 percent to 13 percent.

Figures 10-6 and 10-7 illustrate the hydraulic efficiency, E , for the two curved vane grate sizes as a function of measured width of spread, T' .

The grate inlet capacity curves in figures 10-8 through 10-13 relate gutter flow, Q_T , and longitudinal slope, S_0 , to hydraulic efficiency, E , intercepted flow, Q_I , and calculated width of spread, T . There is one figure for each grate size and cross slope, $1/Z$.

For both grate sizes at the lower cross slopes of $Z = 24$ and 48, the hydraulic efficiency, E , continues to increase with increase in the longitudinal slope, S_0 , for a constant gutter flow, Q_T . The 2 ft by 4 ft (0.61 m by 1.22 m) grate for the $1/16$ cross slope produces an increase in efficiency as the longitudinal slope increases up to, $S_0 = 7$ percent to 13 percent (depending on gutter flow) beyond which the efficiency remains constant. For the 2 ft by 2 ft (0.61 m by 0.61 m) grate on the $1/16$ cross slope, there is a limiting longitudinal slope, $S_0 = 9$ percent, where the hydraulic efficiency of the grate begins to decrease with continued increase in slope, S_0 . The grate inlet capacity curves show slightly lower hydraulic efficiencies for all sizes and cross slopes of the curved vane grate than the efficiencies for the parallel bar grate, volume 6.

Debris Tests. - Debris tests were conducted on the two sizes of curved vane grate according to the test procedure described in Chapter 5. Figure 10-14a shows the 2 ft by 4 ft (0.61 m by 1.22 m), curved vane grate during a debris test at $S_0 = 4$ percent. Figure 10-14b shows the final distribution of debris after the test. The results of the debris test are presented in table 10-1. The curved vane grate is quite efficient at passing the tested debris.

Summary

The 2 ft by 4 ft (0.61 m by 1.22 m) and 2 ft by 2 ft (0.61 m by 0.61 m) curved vane grates have excellent hydraulic characteristics. The debris test results for the curved vane grate prove the grate to be efficient at passing debris. On the average, the two sizes of the curved vane grate passed 46 percent of the leaves in the first 5 minutes and 54 percent in 15 minutes.

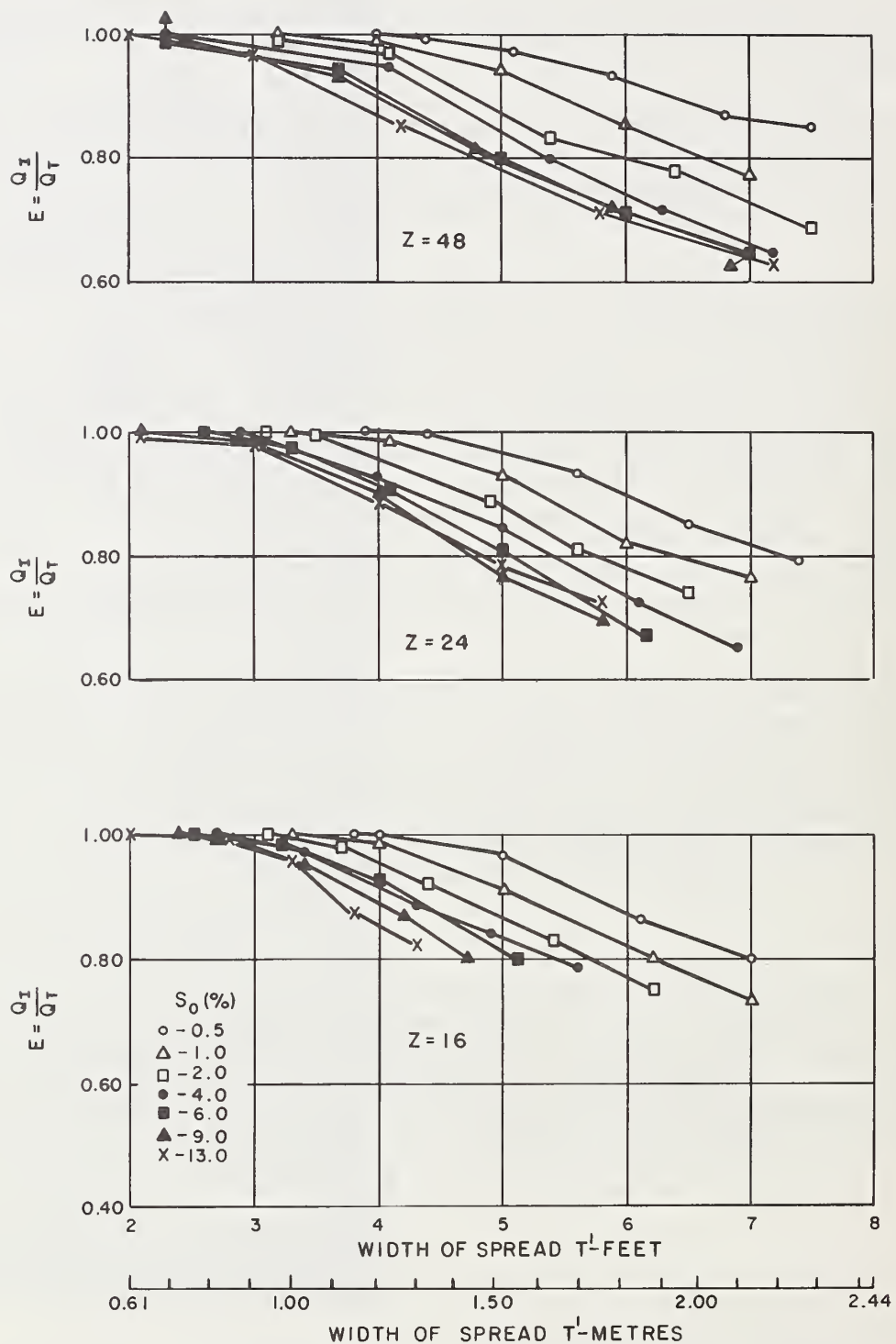


Figure 10-6. - Hydraulic efficiency vs. width of spread, 2 ft by 4 ft (0.61 m by 1.22 m) curved vane gate.

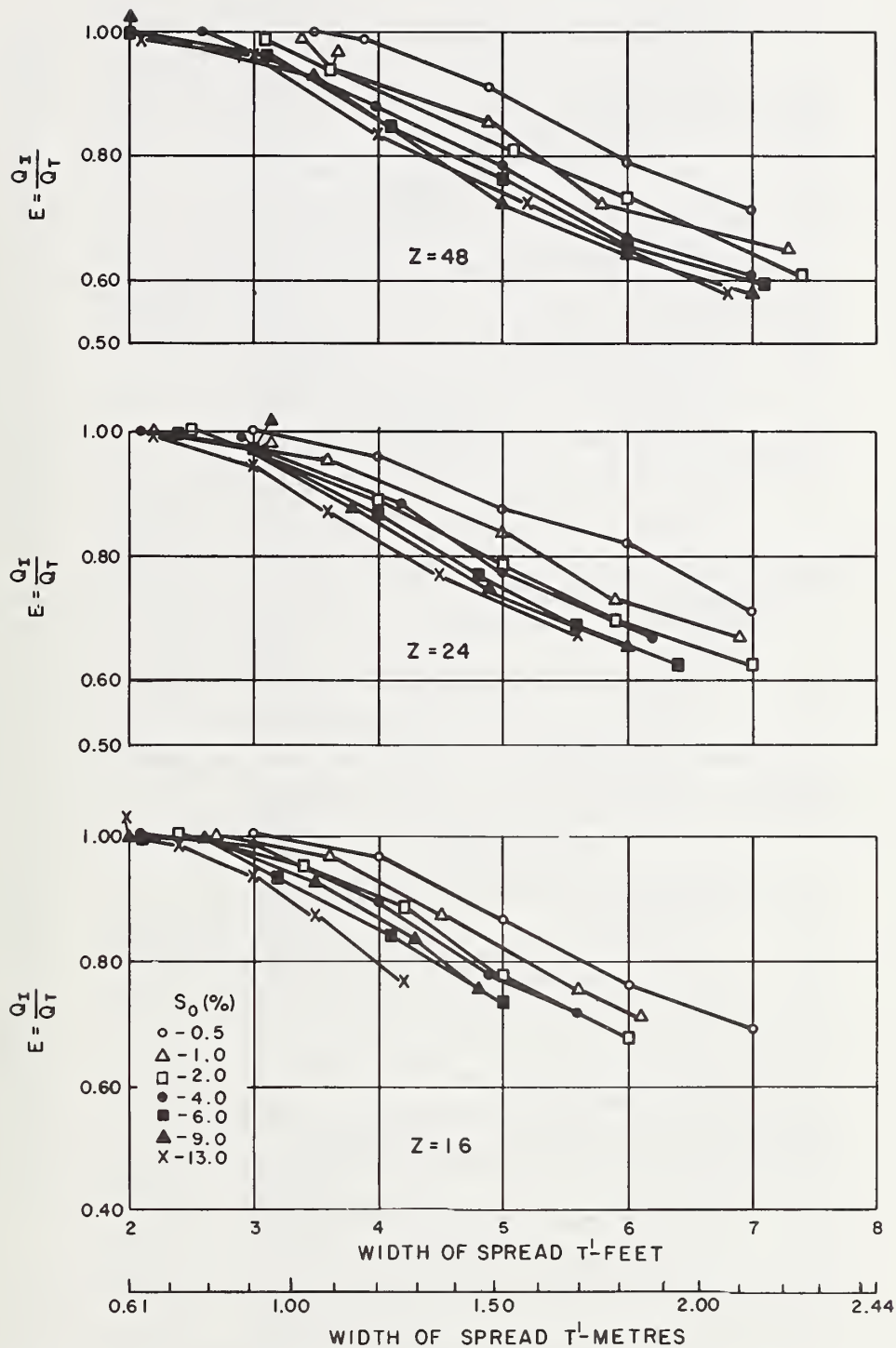


Figure 10-7. - Hydraulic efficiency vs. width of spread, 2 ft by 2 ft (0.61 m by 0.61 m) curved vane grate.

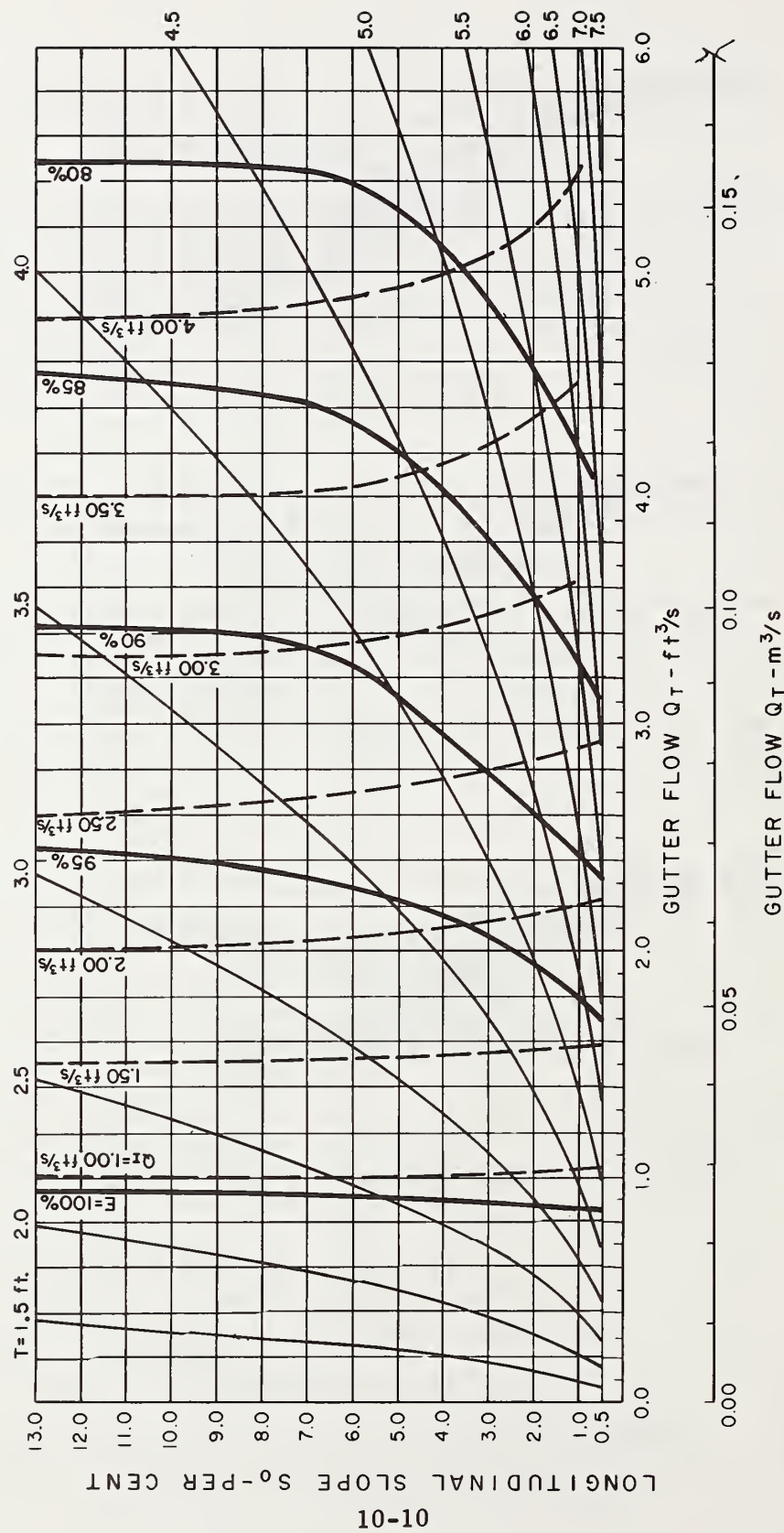


Figure 10-8. - Grate inlet capacity curves, 2 ft by 4 ft (0.61 m by 1.22 m) curved vane grate, $Z = 16$ (Note: $1 \text{ ft}^3/\text{s} = 0.028 \text{ m}^3/\text{s}$, $1 \text{ ft} = 0.305 \text{ m}$).

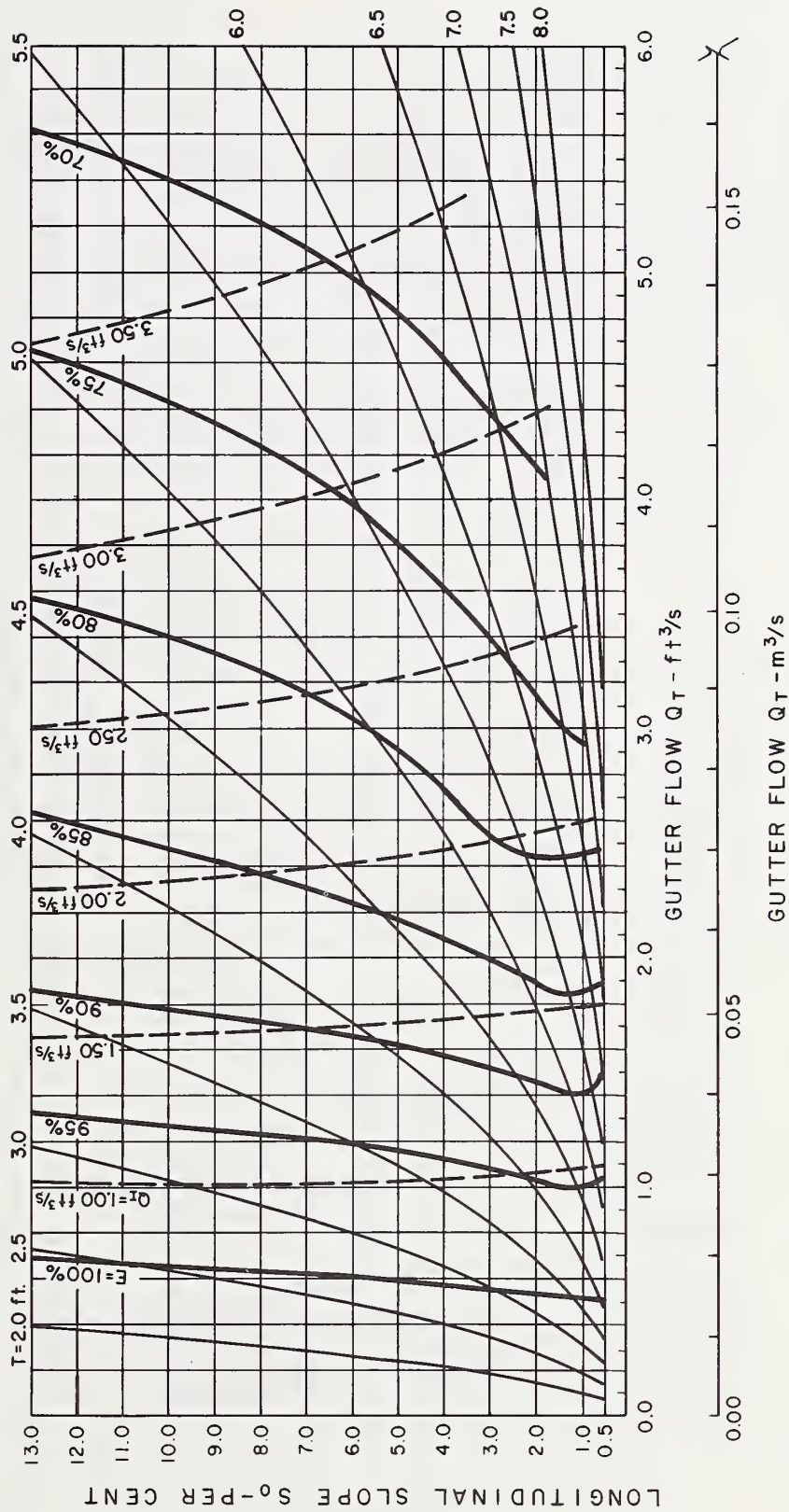


Figure 10-9. - Grate inlet capacity curves, 2 ft by 4 ft (0.61 m by 1.22 m) curved vane grate, Z = 24 (Note: 1 ft³/s = 0.028 m³/s, 1 ft = 0.305 m).

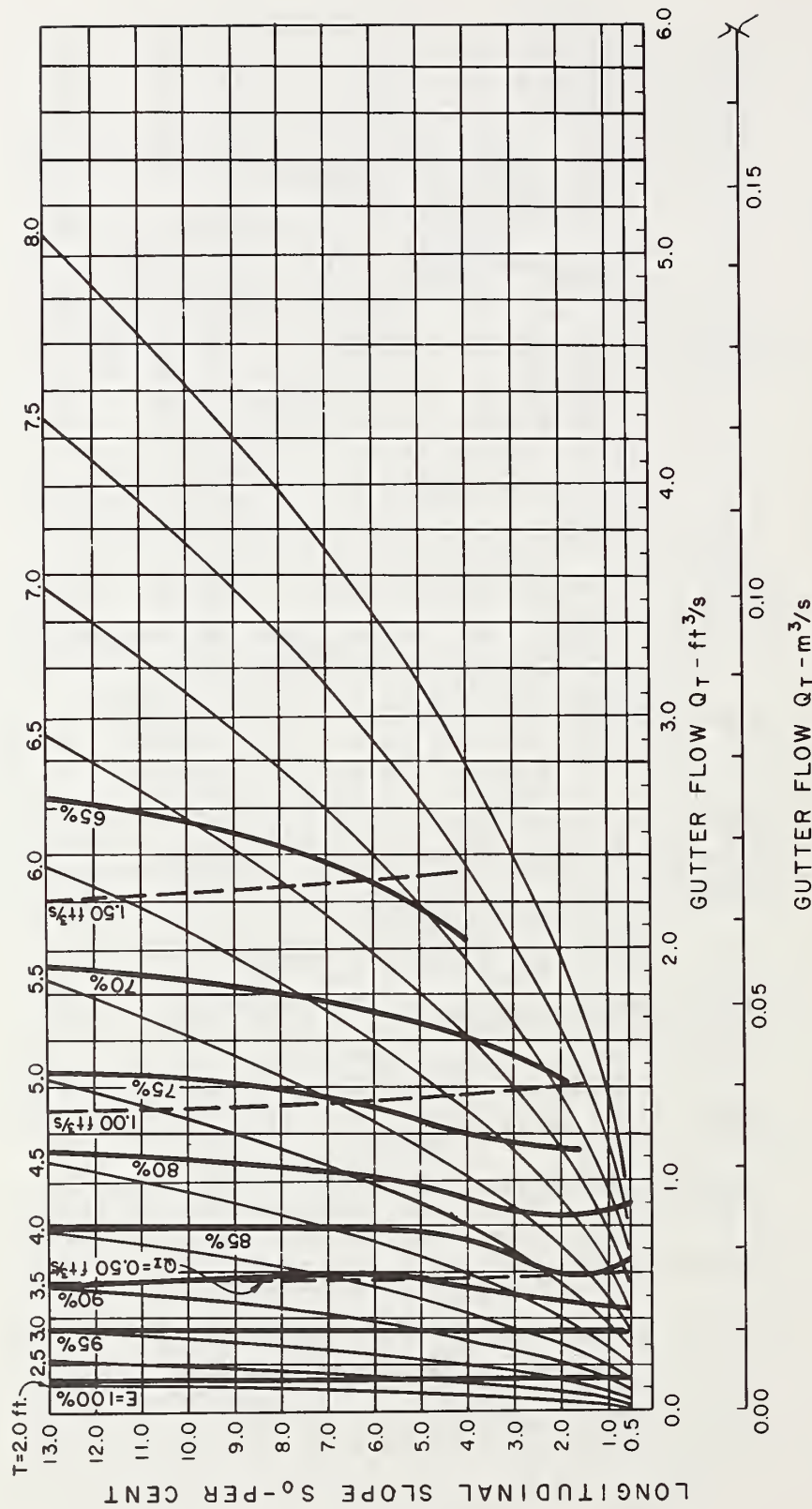


Figure 10-10. - Grate inlet capacity curves, 2 ft by 4 ft (0.61 m by 1.22 m) curved vane grate, $Z = 48$ (Note: $1 \text{ ft}^3/\text{s} = 0.028 \text{ m}^3/\text{s}$, $1 \text{ ft} = 0.305 \text{ m}$).

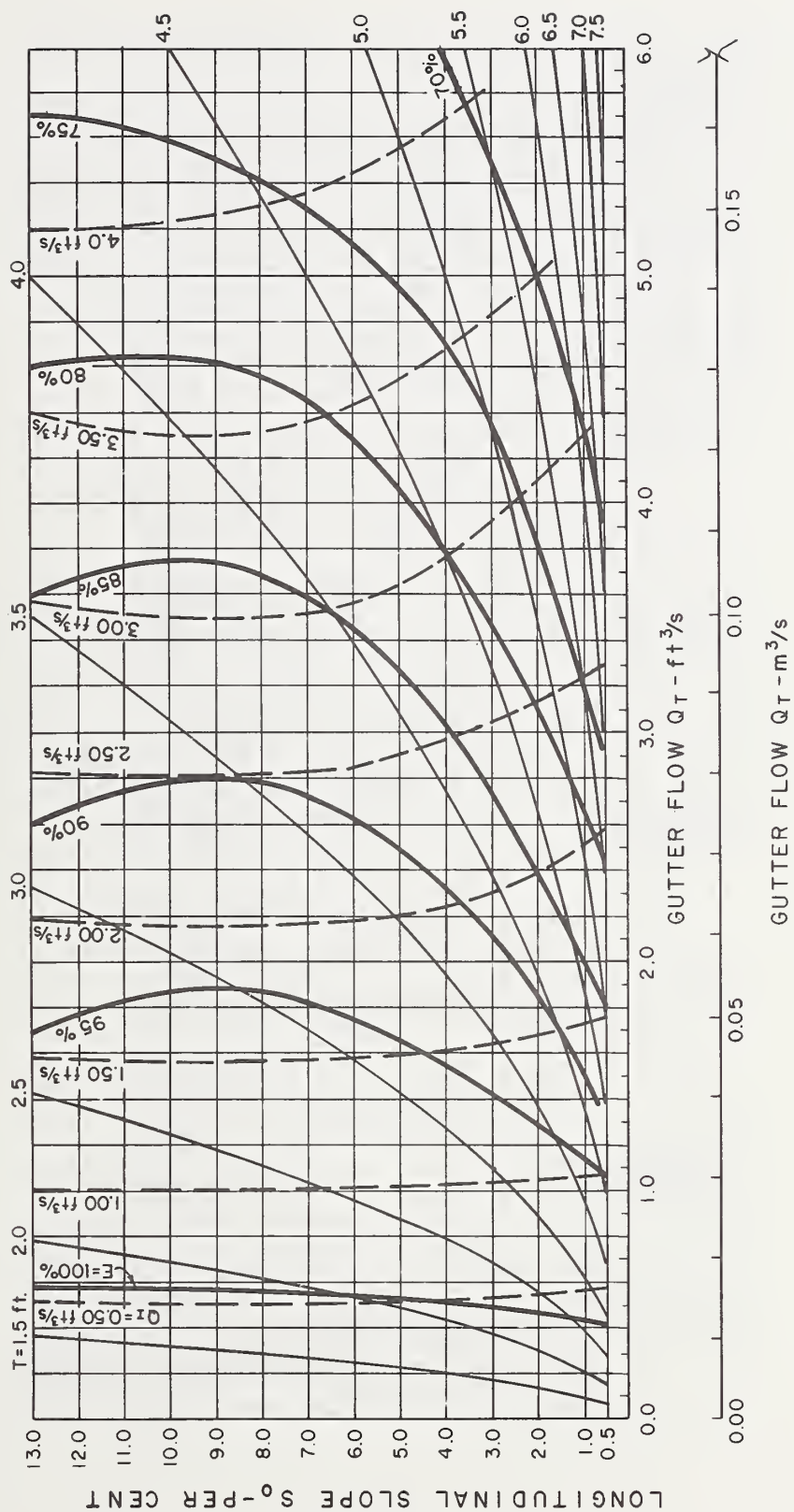


Figure 10-11. - Grate inlet capacity curves, 2 ft by 2 ft (0.61 m by 0.61 m) curved vane grate, $Z = 16$ (Note: 1 $\text{ft}^3/\text{s} = 0.028 \text{ m}^3/\text{s}$, 1 ft = 0.305 m).

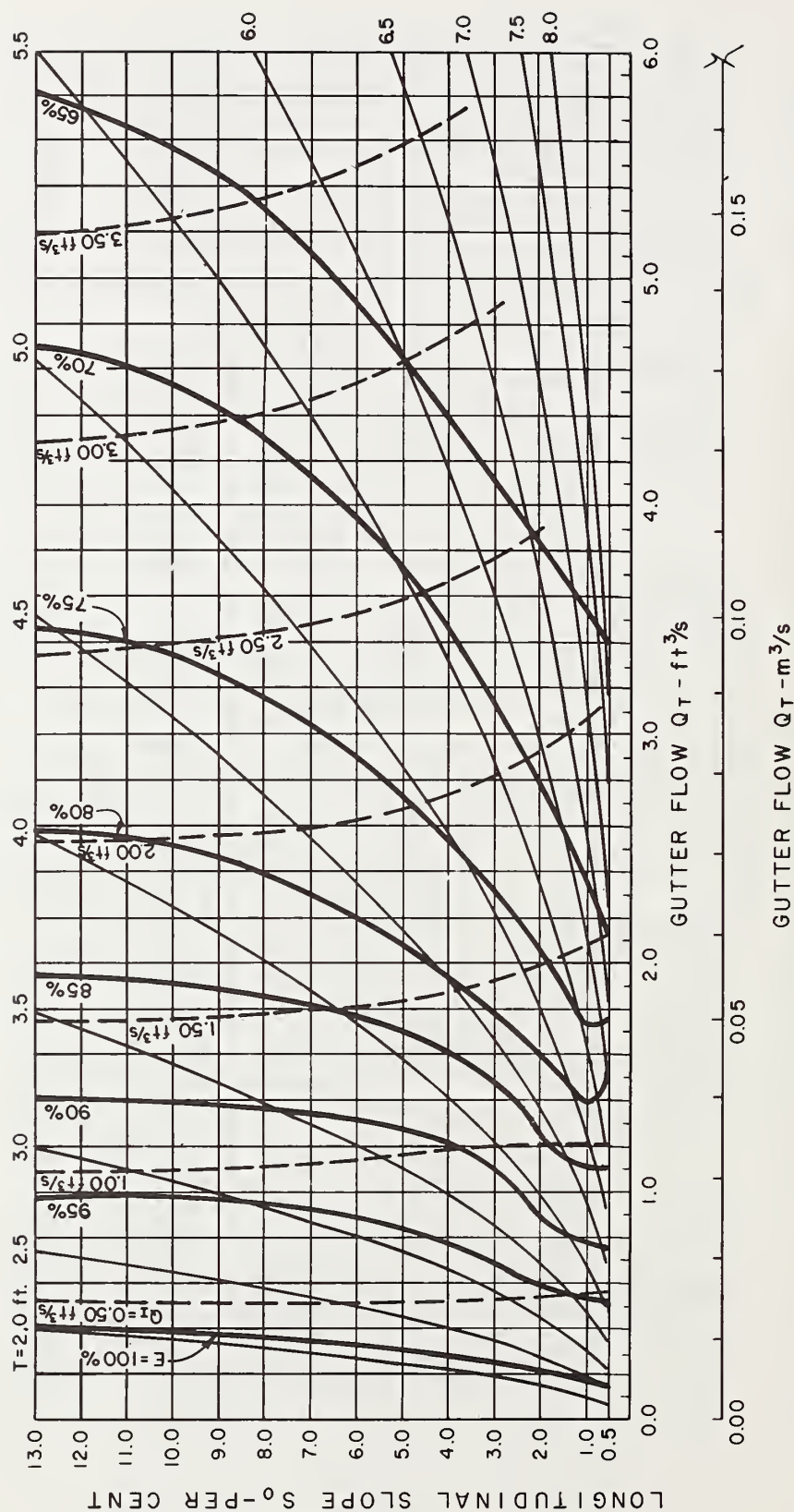


Figure 10-12. - Grate inlet capacity curves, 2 ft by 2 ft (0.61 m by 0.61 m) curved vane grate, $Z = 24$ (Note: $1 \text{ ft}^3/\text{s} = 0.028 \text{ m}^3/\text{s}$, $1 \text{ ft} = 0.305 \text{ m}$).

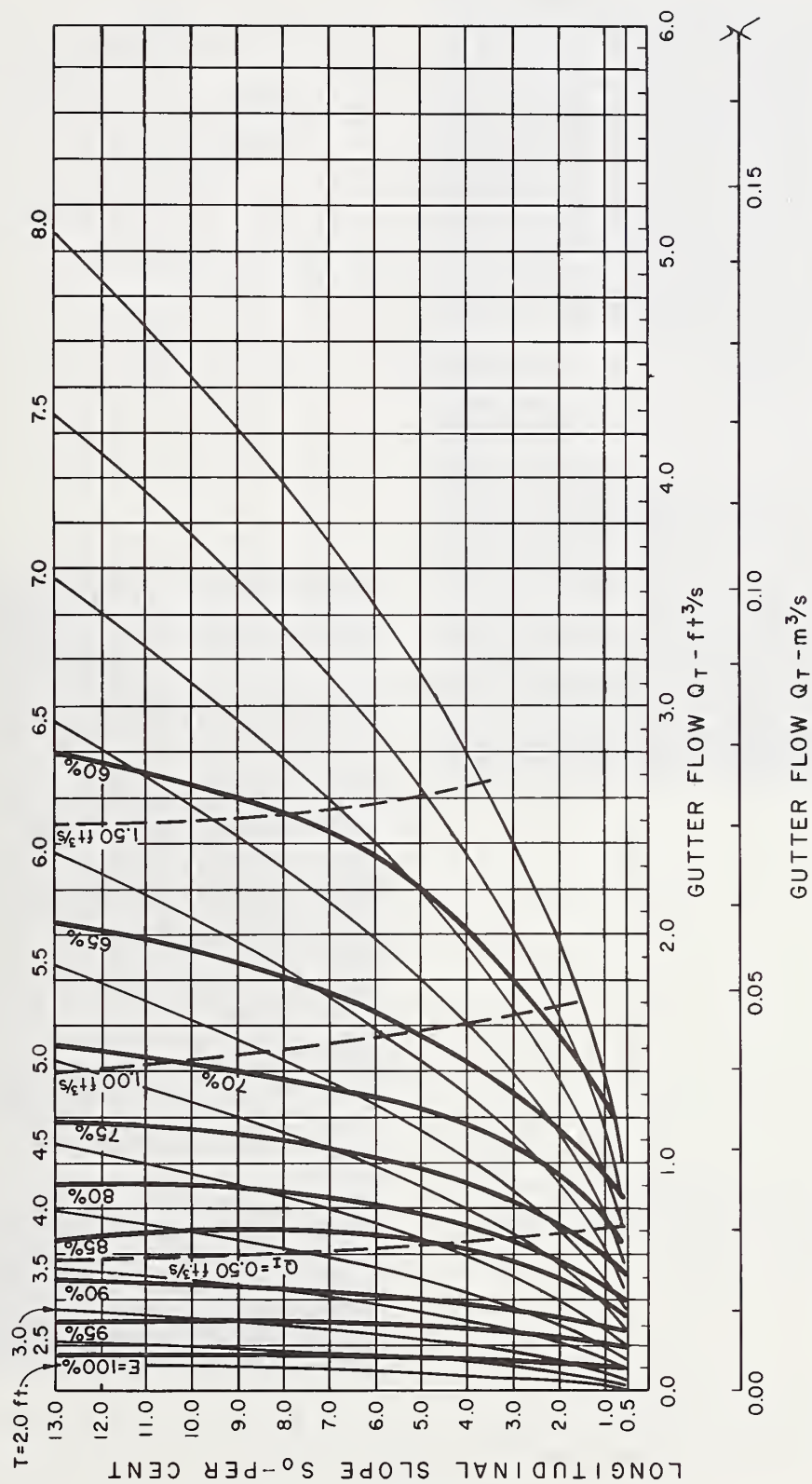


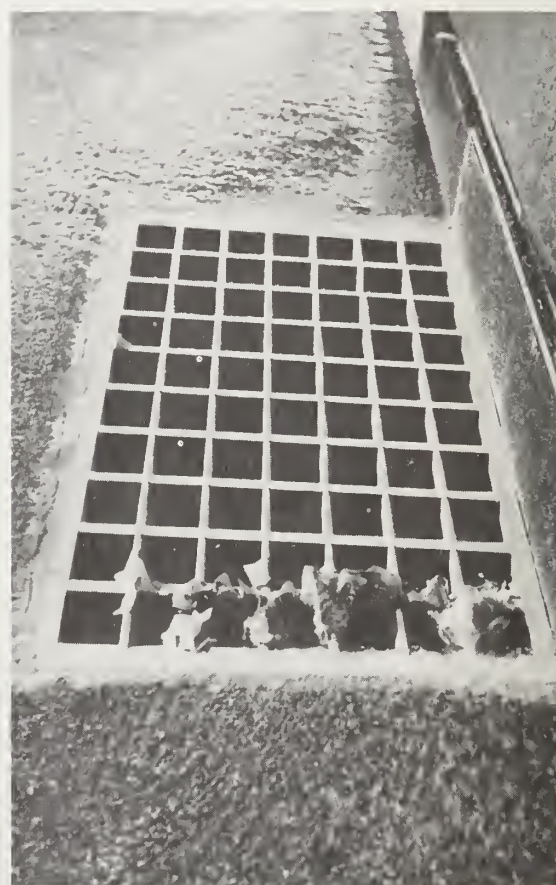
Figure 10-13. - Grate inlet capacity curves, 2 ft by 2 ft (0.61 m by 0.61 m) curved vane grate, $Z = 48$ (Note: $1 \text{ ft}^3/\text{s} = 0.028 \text{ m}^3/\text{s}$, $1 \text{ ft} = 0.305 \text{ m}$).



a. $Q_T = 2.7 \text{ ft}^3/\text{s}$ ($0.076 \text{ m}^3/\text{s}$)

$T' = 5.4 \text{ ft}$ (1.65 m)

Photo 104-1A



b. View looking downstream at
48 pieces of debris caught
on the grate.

Photo 104-3

Figure 10-14. - Debris tests, 2 ft by 4 ft (0.61 m by 1.22 m) curved
vane grate, $S_0 = 4\%$, $Z = 24$.

Table 10-1

DEBRIS TEST RESULTS - CURVED VANE GRATES

Test No.	Number of "leaves" lodged on grate*			
	$S_0 = 0.5\%$		$S_0 = 4.0\%$	
	5 minutes	15 minutes	5 minutes	15 minutes
<u>2 ft by 2 ft (0.61 m by 0.61 m) grate</u>				
1	106	96		
2	108	86		
3	94	83		
4			60	53
5			60	53
6			78	67
Debris handling efficiency* (%)	32	41	56	62
<u>2 ft by 4 ft (0.61 m by 1.22 m) grate</u>				
1	83	65		
2	98	71		
3	99	84		
4			87	75
5			58	51
6			52	48
Debris handling efficiency* (%)	38	51	56	61

* Based on 150 "leaves" arriving at the grate.

CHAPTER 11

HYDRAULIC EFFICIENCY AND DEBRIS TESTS - PARALLEL BAR WITH TRANSVERSE ROD GRATES

Introduction

This chapter describes the results of hydraulic tests conducted on parallel bar with transverse rod grates. To select a grate for detailed hydraulic study, tests were conducted on three promising designs which were identified in the bicycle safety analysis (Chapter 3). The grates tested were the 1-7/8 in (48 mm) longitudinal bar spacing by 4 in (102 mm) transverse rod spacing (P - 1-7/8 - 4), the 2-3/8 in (60 mm) longitudinal bar spacing by 4 in (102 mm) transverse rod spacing (P - 2-3/8 - 4), and the 1-7/8 in (48 mm) longitudinal bar spacing by 6 in (152 mm) transverse rod spacing (P - 1-7/8 - 6). The structural analysis indicated that for 1/4 in (6.4 mm) wide longitudinal bearing bars 24 in (0.61 m) long, a depth of 3.9 in (99 mm) would be needed for a longitudinal bar spacing of 1-7/8 in (48 mm) (table 2-2). To standardize the test grates a longitudinal bar size of 4 in (102 mm) deep and 1/4 in (6.4 mm) wide was used for all three test grates. It is evident from the structural analysis in Chapter 2 that a larger width or depth of bar will be required for a 4 ft (1.22 m) span or the 2-3/8 in (60 mm) longitudinal bar spacing. Hydraulic efficiency will not be affected by the bar depth and studies comparing hydraulic efficiency for the 1-7/8 in (48 mm) and 2-3/8 in (60 mm) longitudinal bar spacing indicate that a bar width greater than 1/4 in (6.4 mm) will not materially affect the grate efficiency.

The preliminary tests were limited to testing a 2 ft by 4 ft (0.61 m by 1.22 m) size of the three grates at 4, 6, 9, and 13 percent longitudinal slopes and 1:48 and 1:24 cross slopes. The 1:48 cross slope tests and the 4 percent longitudinal slope tests resulted in identical hydraulic efficiencies for the three grates. The two grates with the 4 in (102 mm) transverse spacing had nearly identical efficiencies for all tests with the 2-3/8 in (60 mm) longitudinal bar spacing slightly (less than 1 percent) more efficient than the 1-7/8 in (48 mm) spacing. The hydraulic efficiencies for the P - 1-7/8 - 6 grate were greater than those for the grates with the 4 in (102 mm) transverse rod spacing. The differences were small for low gutter flows and increased, as the flow, Q_T , and longitudinal slopes, S_0 , were increased, to a maximum difference of 4 percent for $Q_T = 5.00 \text{ ft}^3/\text{s}$ ($0.14 \text{ m}^3/\text{s}$) and $S_0 = 13$ percent.

The minor hydraulic and self-cleaning advantages of the P - 1-7/8 - 6 and P - 2-3/8 - 4 were not great enough to offset the safety advantages of the P - 1-7/8 - 4. The P - 1-7/8 - 4 grate illustrated in figure 11-1 was therefore selected for further tests. The grate consists of 1/4 in (6.4 mm) wide by 4 in (102 mm) deep bearing bars placed on

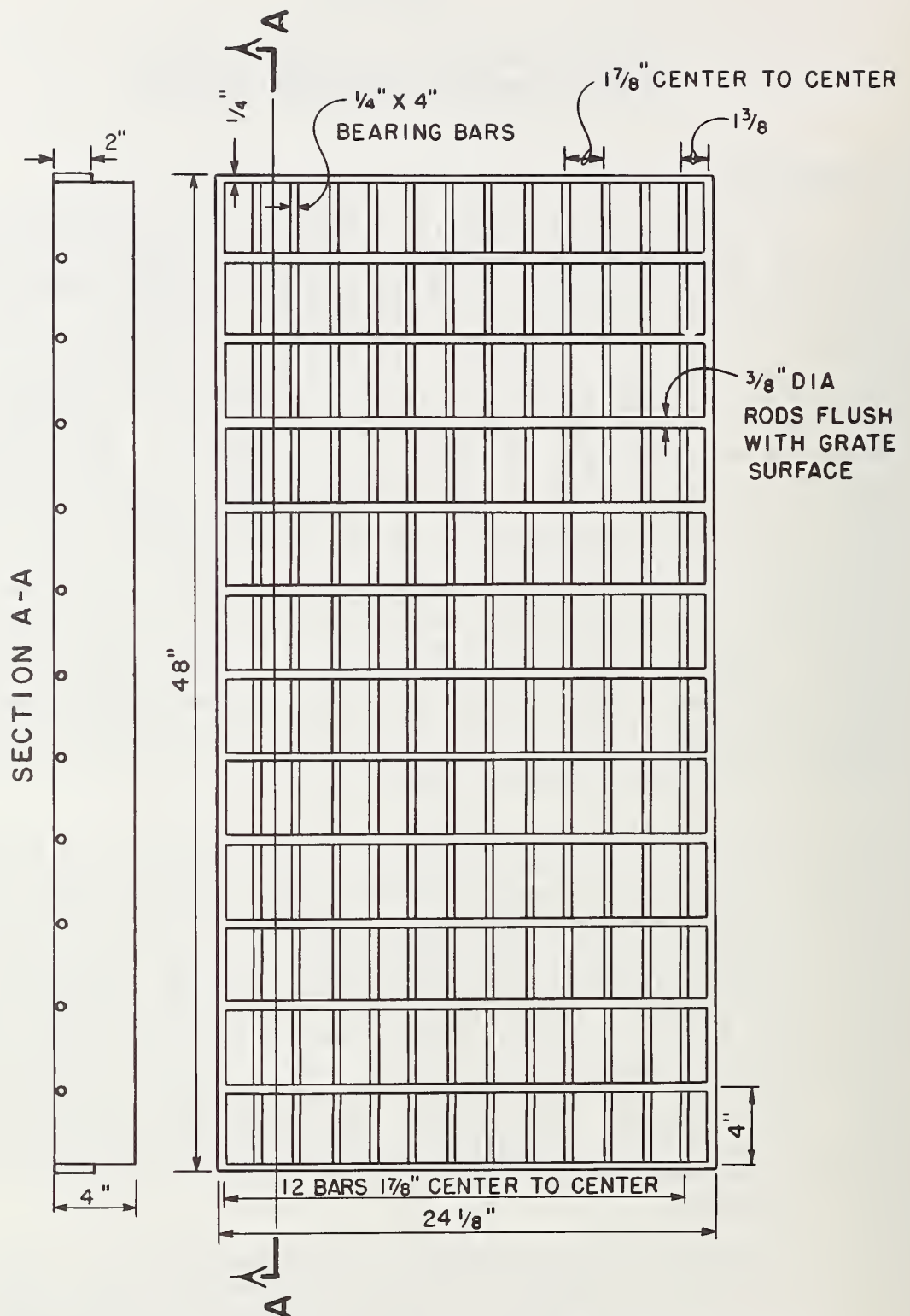


Figure 11-1. - 2 ft by 4 ft (0.61 m by 1.22 m) fabricated steel
P - 1-7/8 - 4 grate.

1-7/8 in (48 mm) centers. Although the bar sizes shown in figure 11-1 were used for the hydraulic tests, they are not large enough to insure structural adequacy for a 4 ft (1.22 m) long grate as shown in table 2-2. The 3/8 in (9.5 mm) transverse rods are placed on 4 in (102 mm) centers. In the report, we will refer to the grates by their nominal sizes of 2 ft by 4 ft (0.61 m by 1.22 m) and 2 ft by 2 ft (0.61 m by 0.61 m).

Experimental Results and Observations

Hydraulics. - Figures 11-2 and 11-3 present the experimental results for the 2 ft by 4 ft (0.61 m by 1.22 m) and 2 ft by 2 ft (0.61 m by 0.61 m) P - 1-7/8 - 4 grate. The drop in hydraulic efficiency is considerably more for the P - 1-7/8 - 4 grate than it was for the parallel bar grate when comparing the 4 ft (1.22 m) to the 2 ft (0.61 m) long grate. The P - 1-7/8 - 4 grate produces a "flow layer" which passes along the surface of the bars instead of penetrating the grate. This can best be illustrated by comparing figures 11-4a and 11-4b with figures 6-5a and 6-4b of the parallel bar report (volume 6). The test flow conditions are practically the same for both grates but the flow patterns over the grates and hydraulic efficiencies are considerably different.

Figures 11-2 and 11-3 reveal an interesting pattern that occurs at the 1:24 and 1:16 cross slopes for both sizes of the P - 1-7/8 - 4 grate. In general, for a given gutter flow, Q_T , the hydraulic efficiency, E , increases as the longitudinal slope, S_0 , increases to approximately 4 percent. As the longitudinal slope increases beyond 4 percent, the hydraulic efficiencies become progressively lower. This results from the inability of the high-velocity gutter flow to penetrate the grate. The sequence of photographs in figure 11-5 shows the development of the flow layer on the 2 ft by 2 ft (0.61 m by 0.61 m) grate at $Z = 48$ as the longitudinal slope is increased from 4 percent to 13 percent. The flow conditions pictured are similar to those in figure 7-5 of the reticulate grate report (volume 7). Although a weak flow layer develops on the P - 1-7/8 - 4 grate for the 1:48 cross slope there is no noticeable decrease in hydraulic efficiencies for steeper ($S_0 > 6$ percent) longitudinal slopes (note figures 11-2 and 11-3). This is due to the fact that a larger portion of the flow is closer to the curb and passes over the grate inlet at steeper longitudinal slopes and therefore offsets the minor flow layer effect developed on the 1:48 cross slope.

Figures 11-6 and 11-7 illustrate the hydraulic efficiencies, E , for the two P - 1-7/8 - 4 grates as a function of measured width of spread, T' . For the same width of spread, hydraulic efficiencies increase as the longitudinal slope is decreased.

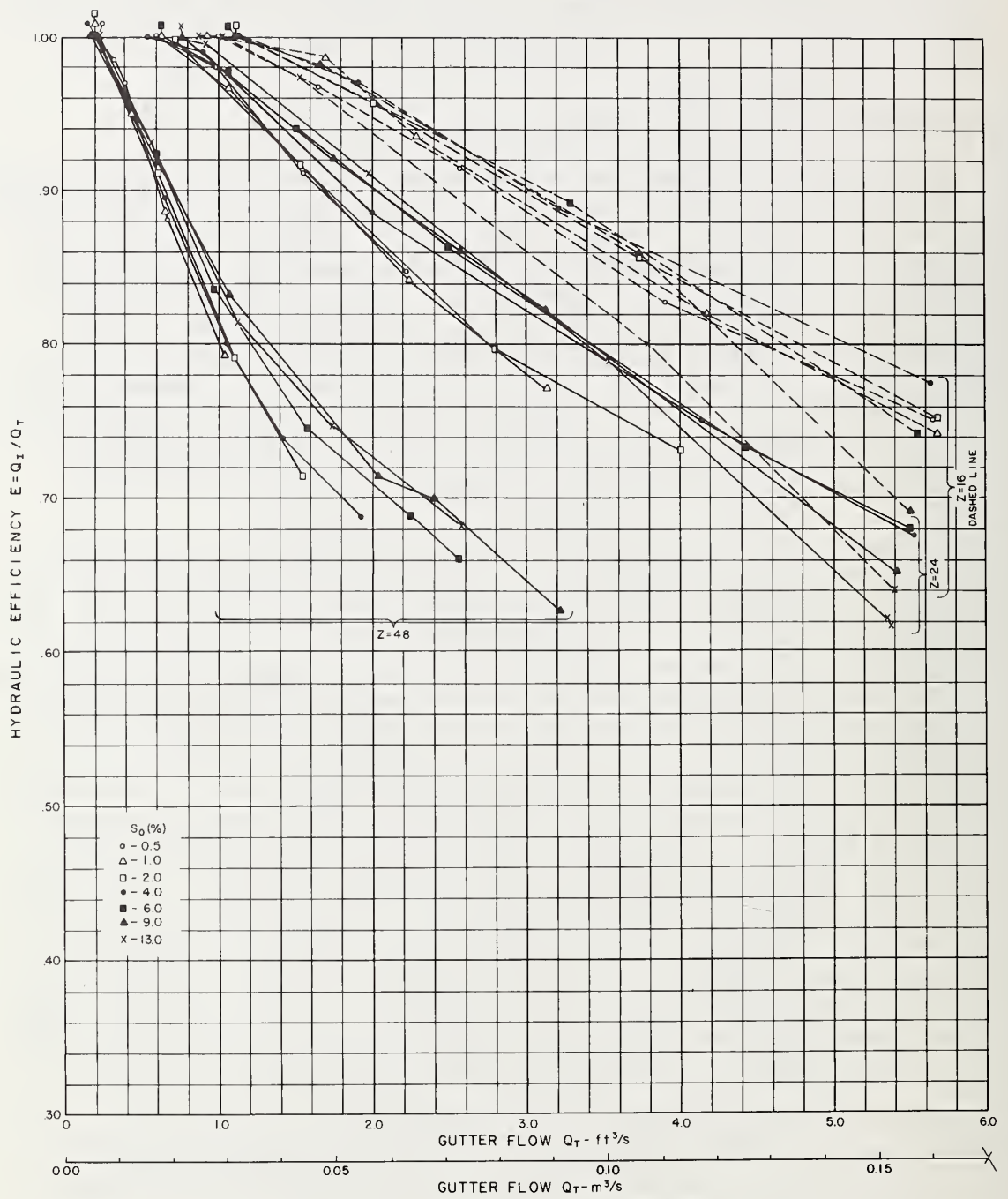


Figure 11-2. - Hydraulic efficiency vs. gutter flow, 2 ft by 4 ft (0.61 m by 1.22 m) P - 1-7/8 - 4 grate.

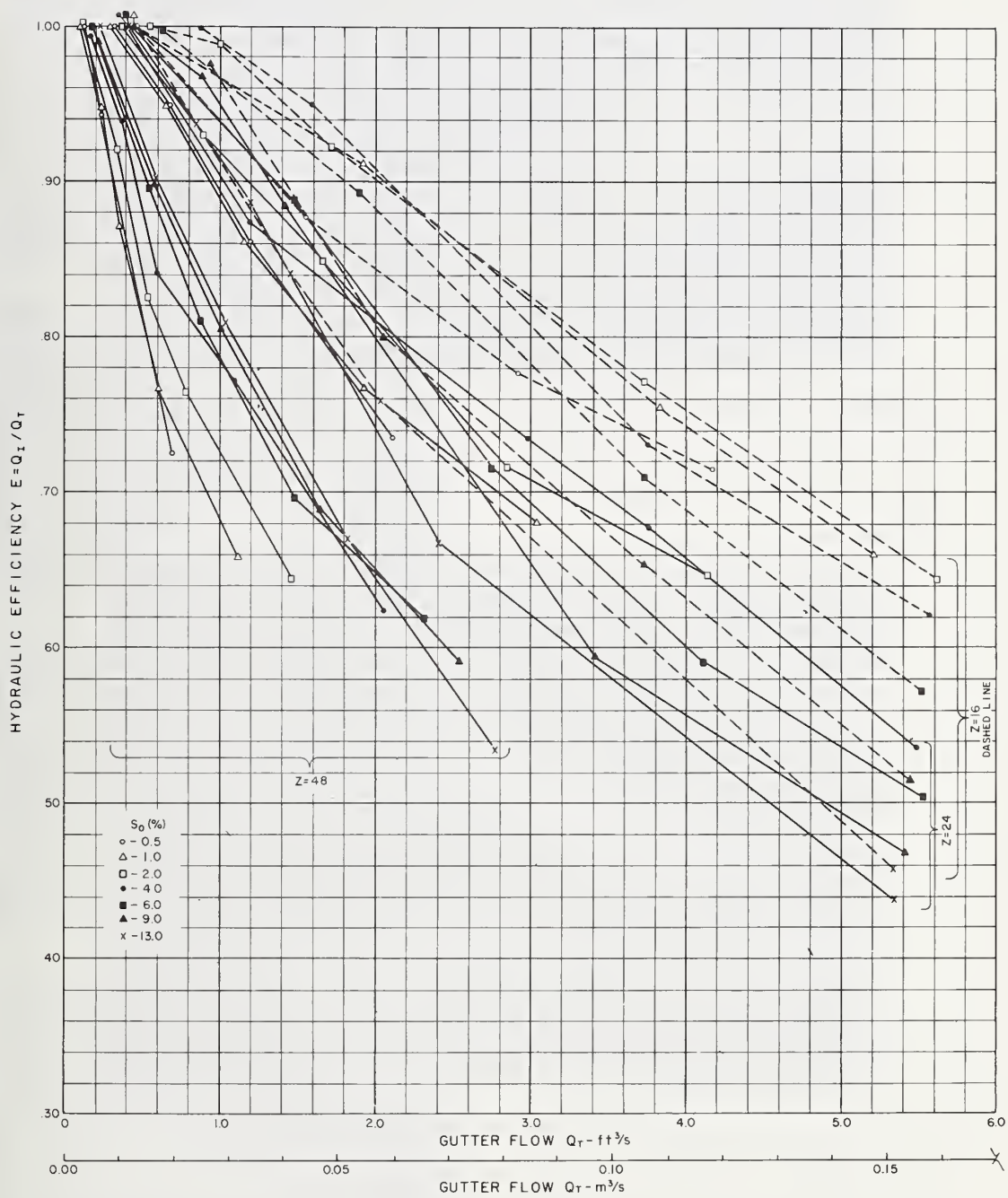


Figure 11-3. - Hydraulic efficiency vs. gutter flow, 2 ft by 2 ft (0.61 m by 0.61 m) P - 1-7/8 - 4 grate.



a. 2 ft by 2 ft (0.61 m by 0.61 m) grate

$$S_0 = 6\%$$

$$T' = 6.3 \text{ ft (1.92 m)}$$

$$Q_T = 5.52 \text{ ft}^3/\text{s (0.156 m}^3/\text{s)}$$

$$E = 50.4\%$$

Photo 89-17A



b. 2 ft by 4 ft (0.61 m by 1.22 m) grate

$$S_0 = 13\%$$

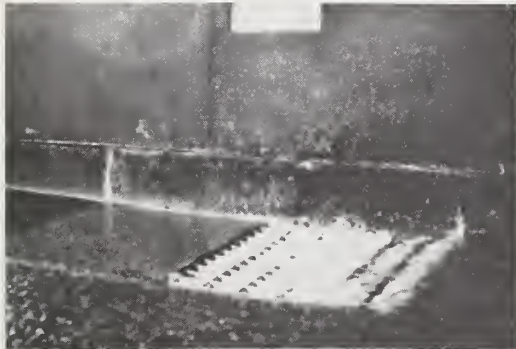
$$T' = 6.0 \text{ ft (1.83 m)}$$

$$Q_T = 5.36 \text{ ft}^3/\text{s (0.152 m}^3/\text{s)}$$

$$E = 61.6\%$$

Photo 50-10

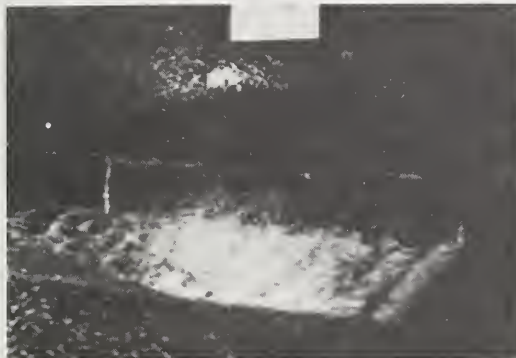
Figure 11-4. - Flow layer effect, P - 1-7/8 - 4 grate, Z = 24.



- a. $S_0 = 4\%$
 $Q_T = 2.05 \text{ ft}^3/\text{s} \text{ (} 0.058 \text{ m}^3/\text{s)}$
 $T' = 7.0 \text{ ft (} 2.13 \text{ m)}$
 $E = 62.4\%$



- b. $S_0 = 6\%$
 $Q_T = 2.31 \text{ ft}^3/\text{s} \text{ (} 0.065 \text{ m}^3/\text{s)}$
 $T' = 7.0 \text{ ft (} 2.13 \text{ m)}$
 $E = 61.9 \%$



- c. $S_0 = 9\%$
 $Q_T = 2.54 \text{ ft}^3/\text{s} \text{ (} 0.072 \text{ m}^3/\text{s)}$
 $T' = 7.1 \text{ ft (} 2.16 \text{ m)}$
 $E = 59.1 \%$



- d. $S_0 = 13\%$
 $Q_T = 2.77 \text{ ft}^3/\text{s} \text{ (} 0.078 \text{ m}^3/\text{s)}$
 $T' = 7.0 \text{ ft (} 2.13 \text{ m)}$
 $E = 53.4\%$

Figure 11-5. - Development of "flow layer" on 2 ft by 2 ft (0.61 m by 0.61 m) P - 1-7/8 - 4 grate, Z = 48. Photo H-1765-364

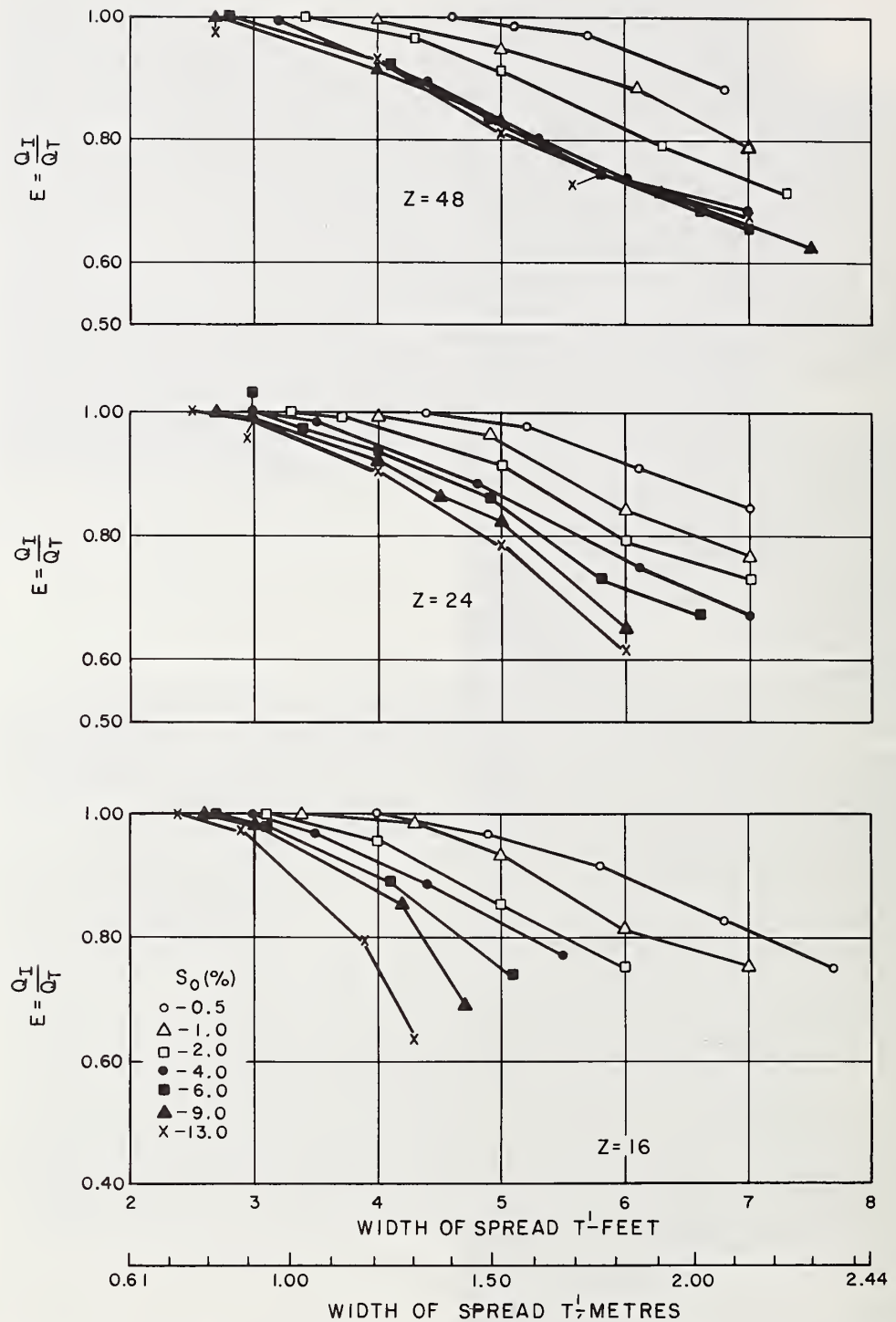


Figure 11-6. - Hydraulic efficiency vs. width of spread, 2 ft by 4 ft (0.61 m by 1.22 m) P - 1-7/8 - 4 grate.

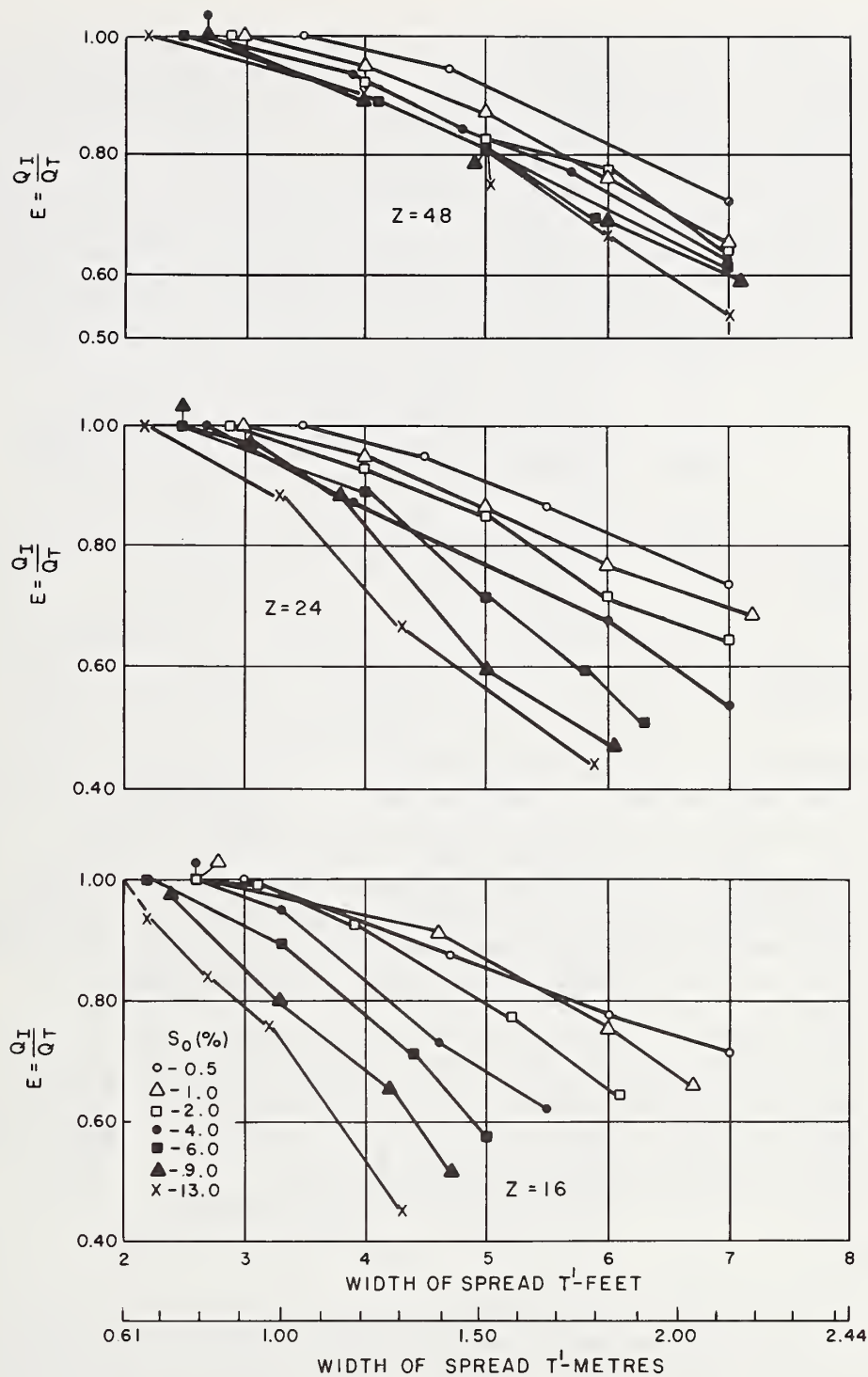


Figure 11-7. - Hydraulic efficiency vs. width of spread, 2 ft by 2 ft (0.61 m by 0.61m) P - 1-7/8 - 4 grate.

The grate inlet capacity curves in figures 11-8 through 11-13 relate gutter flow, Q_T , and longitudinal slope, S_0 , to hydraulic efficiency, E , intercepted flow, Q_T , and calculated width of spread, T . There is one figure for each grate size and cross slope, $1/Z$. In studying figures 11-8 through 11-13, it is evident that for a constant gutter flow, as the longitudinal slope, S_0 , is increased, the hydraulic efficiency increases up to a point. An optimum range of maximum efficiency slopes, S_0 , can be identified which maximize or limit the continued increase in hydraulic efficiency for a given grate size, cross slope, $1/Z$, and gutter flow, Q_T . These maximum efficiency slopes are given in table 11-1.

Table 11-1

MAXIMUM EFFICIENCY SLOPES - P - 1-7/8 - 4 GRATES

Grate size	Z = 48	Z = 24	Z = 16
2 ft by 2 ft (0.61 m by 0.61 m)	8% to 13%	3% to 6%	0% to 2%
2 ft by 4 ft (0.61 m by 1.22 m)	10% to 13%	6% to 13%	3% to 8%

The hydraulic efficiencies decrease quite rapidly for the 1:16 cross slope, once the maximum efficiency slope is exceeded. The hydraulic efficiencies decrease at a slower rate above the maximum efficiency slopes for the flatter cross slopes (1/24 and 1/48).

Debris Tests. - Debris tests were conducted on the P - 1-7/8 - 4 grates according to the test procedure described in Chapter 5. Figure 11-14a shows the 2 ft by 4 ft (0.61 m by 1.22 m) P - 1-7/8 - 4 grate during a debris test at $S_0 = 4$ percent. Figure 11-14b shows the final distribution of debris after the test. The results of the debris tests are presented in table 11-2.

Summary

The 2 ft by 4 ft (0.61 m by 1.22 m) and 2 ft by 2 ft (0.61 m by 0.61 m) P - 1-7/8 - 4 grates have reasonably good hydraulic characteristics for longitudinal slopes up to 8 percent and 3 percent, respectively. Both grate sizes show improved hydraulic efficiency as the longitudinal slope, S_0 , is increased for the same gutter flow, Q_T , up to these limiting slopes. As the longitudinal slope increases further, the rate of decrease in hydraulic efficiency is proportional to the increase in cross slope, $1/Z$ and gutter flow Q_T .

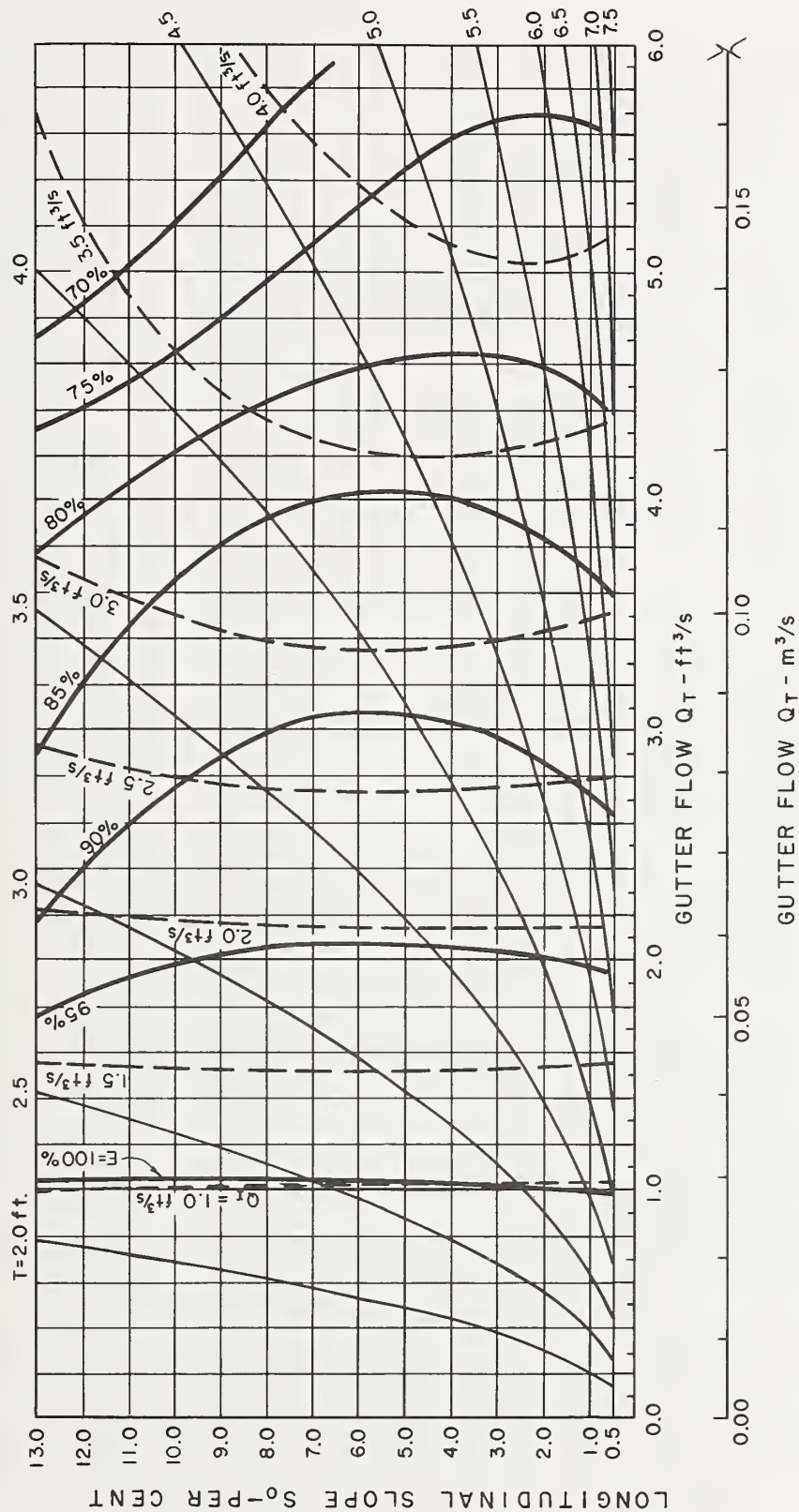


Figure 11-8. - Grate inlet capacity curves, 2 ft by 4 ft (0.61 m by 1.22 m) P - 1-7/8 - 4 grate, Z = 16 (Note: 1 $\text{ft}^3/\text{s} = 0.028 \text{ m}^3/\text{s}$, 1 ft = 0.305 m).

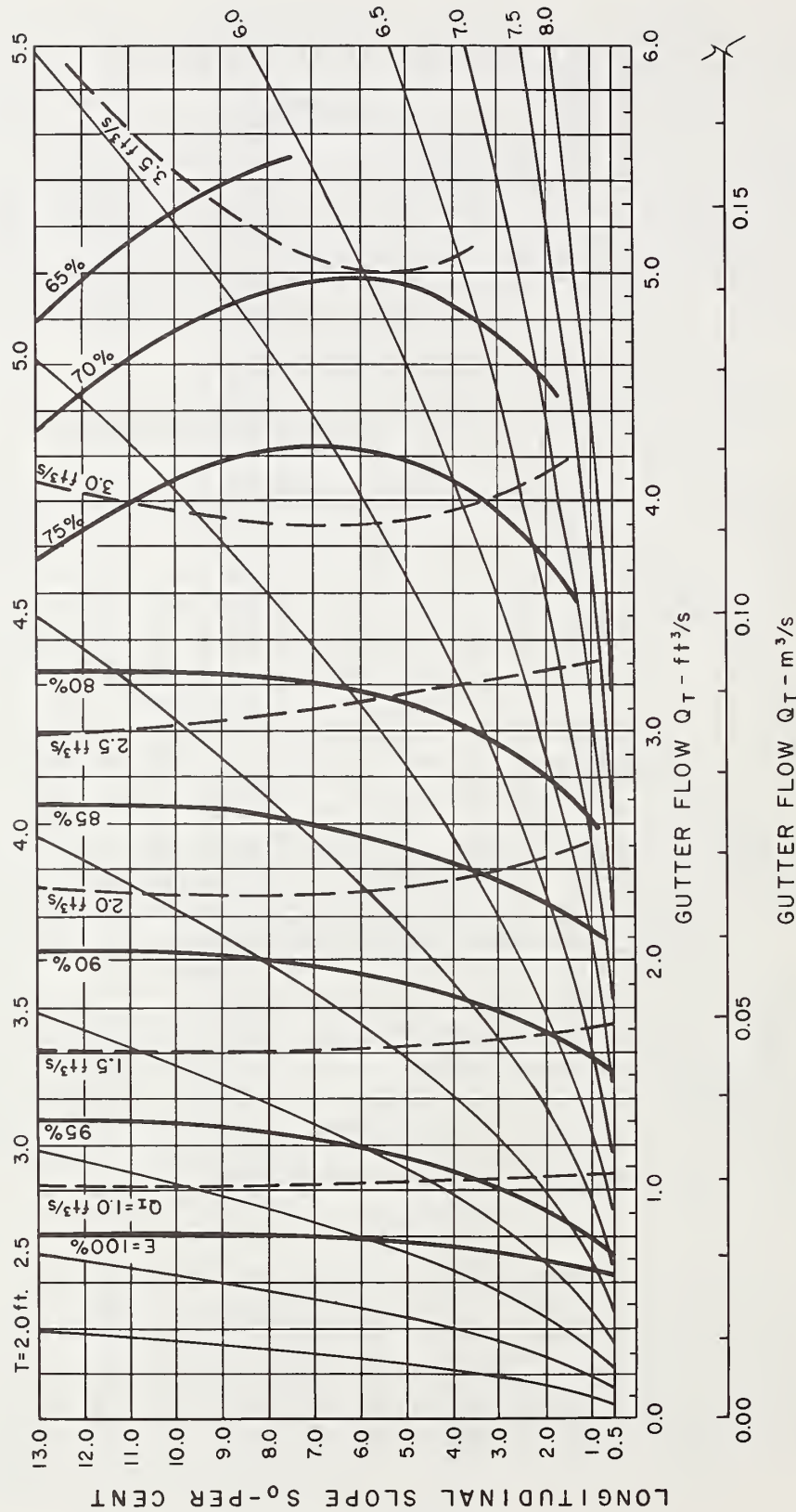


Figure 11-9. - Grate inlet capacity curves, 2 ft by 4 ft (0.61 m by 1.22 m) P - 1-7/8 - 4 grate, Z = 24 (Note: 1 $\text{ft}^3/\text{s} = 0.028 \text{ m}^3/\text{s}$, 1 ft = 0.305 m).

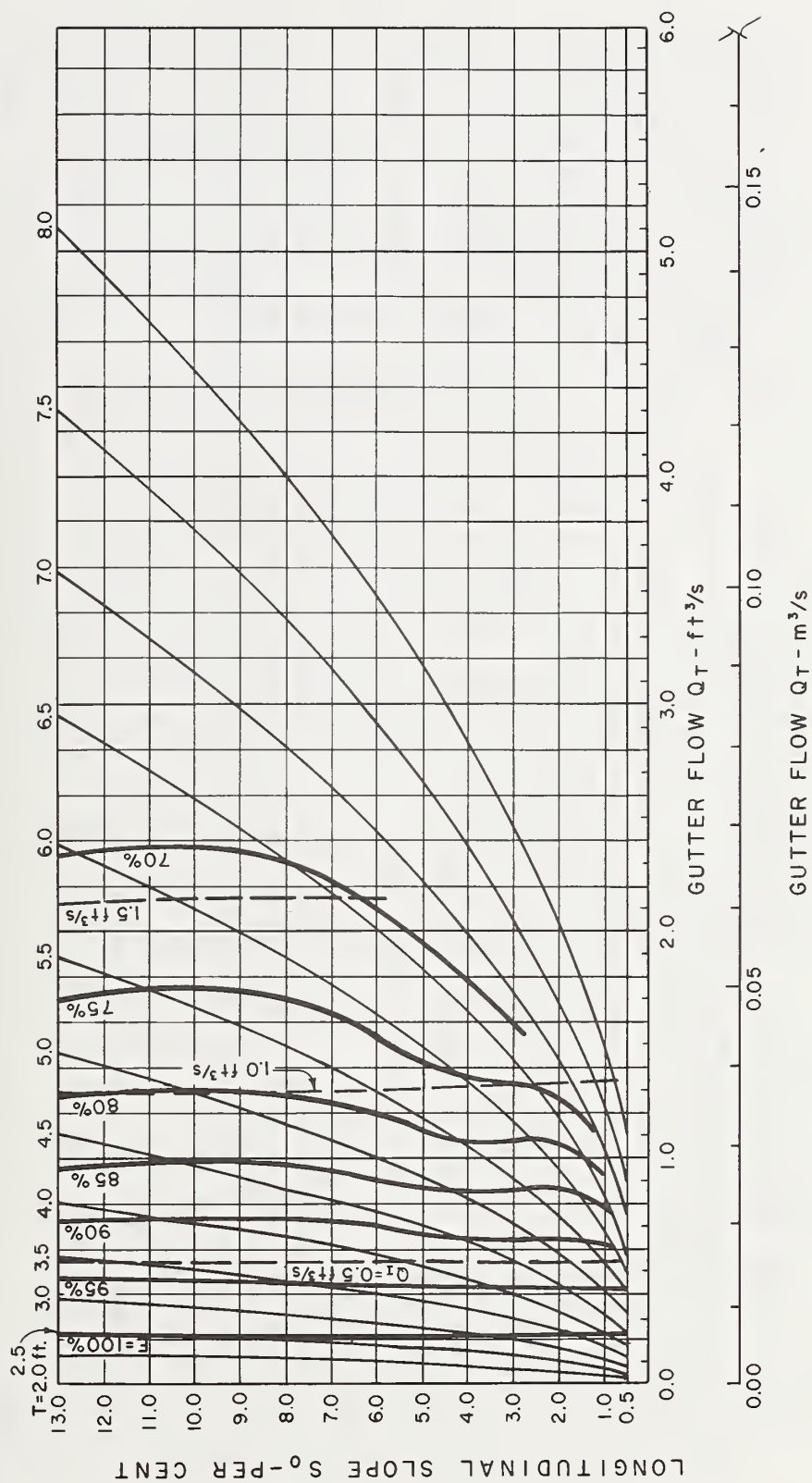


Figure 11-10. - Grate inlet capacity curves, 2 ft by 4 ft (0.61 m by 1.22 m) P - 1-7/8 - 4 grate, $Z = 48$ (Note: $1 \text{ ft}^3/\text{s} = 0.028 \text{ m}^3/\text{s}$, $1 \text{ ft} = 0.305 \text{ m}$).

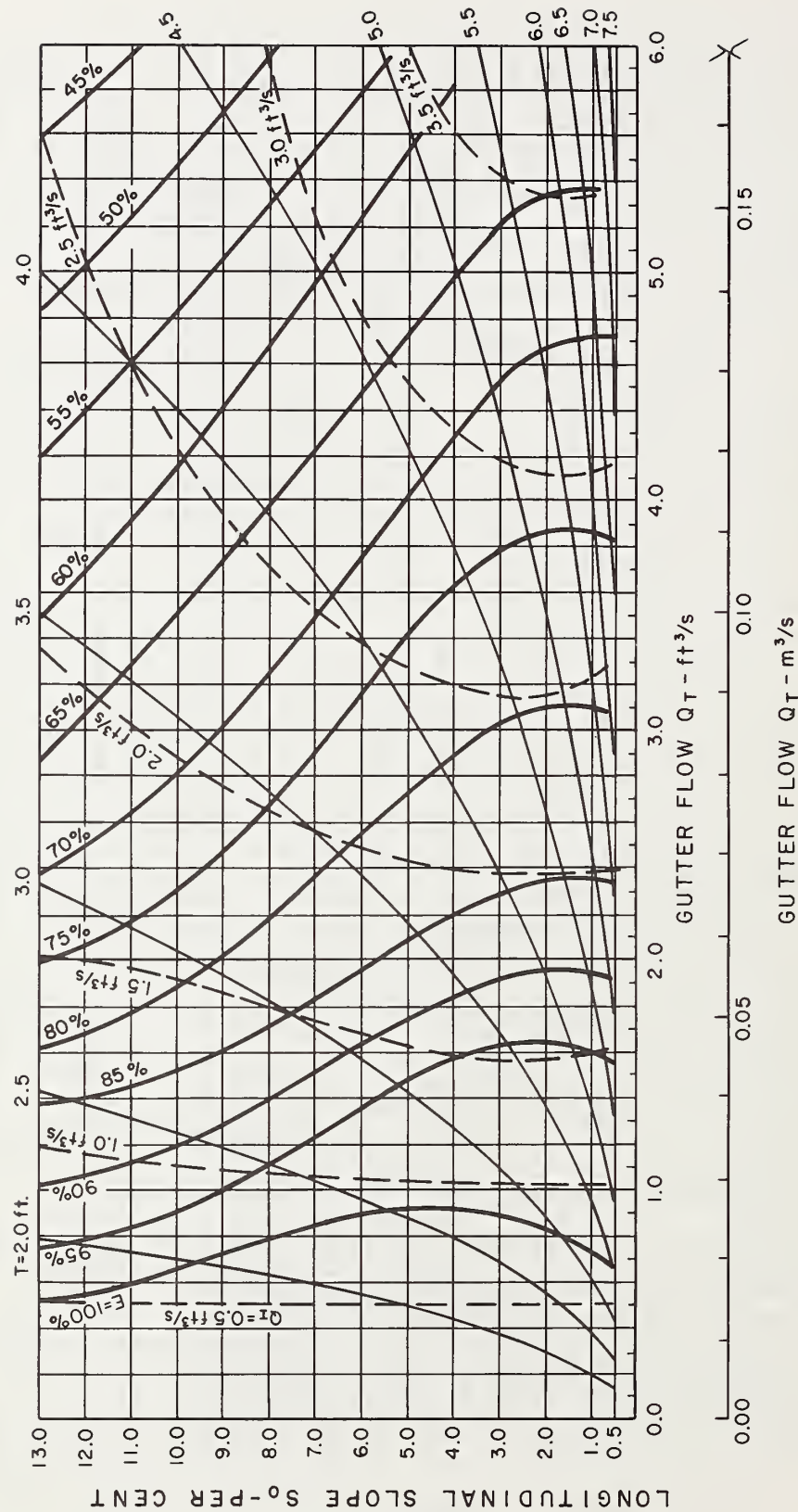


Figure 11-11. - Grate inlet capacity curves, 2 ft by 2 ft (0.61 m by 0.61 m) P - 1-7/8 - 4 grate, Z = 16 (Note: 1 $\text{ft}^3/\text{s} = 0.028 \text{ m}^3/\text{s}$, 1 ft = 0.305 m).

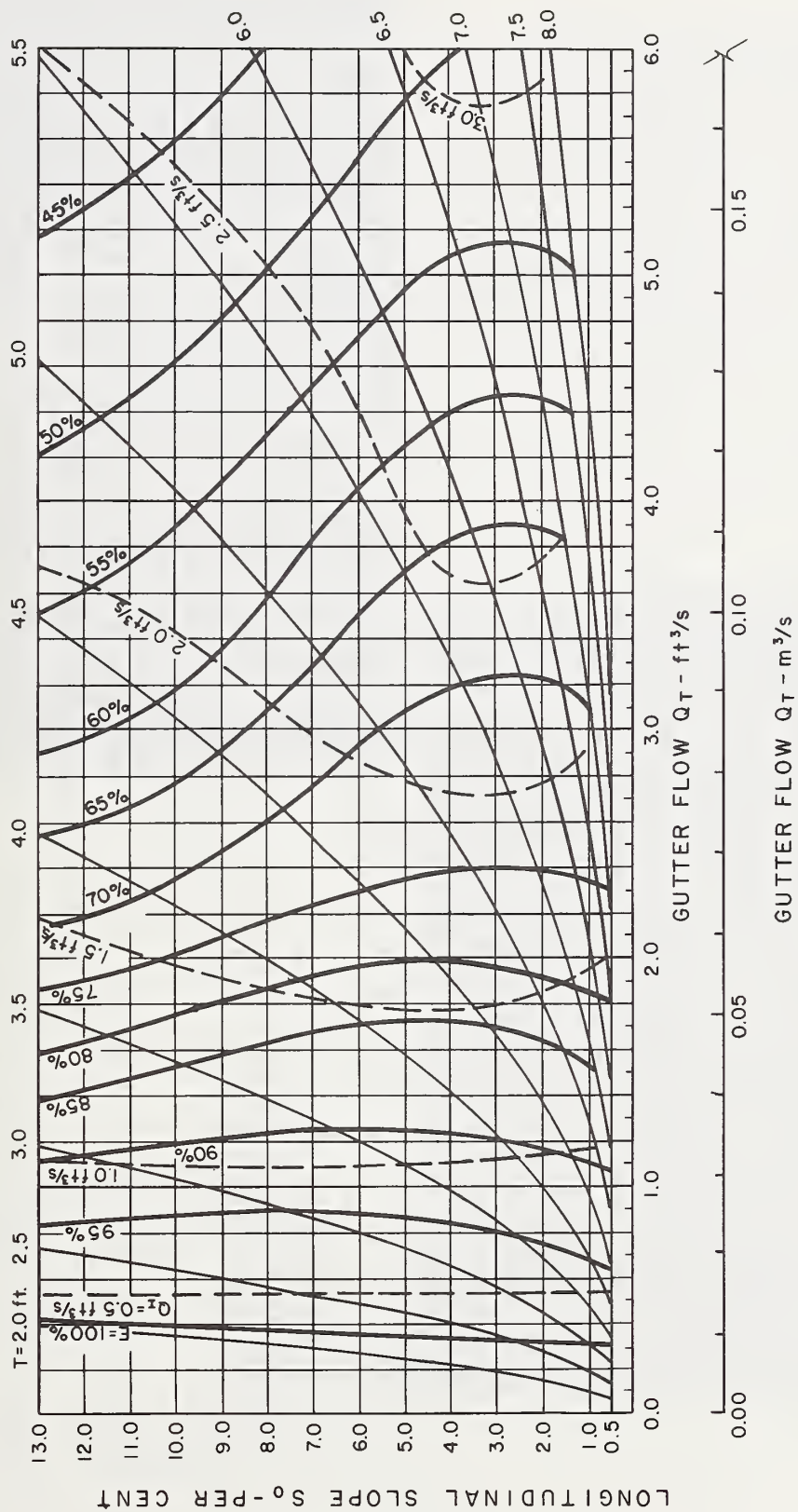


Figure 11-12. - Grate inlet capacity curves, 2 ft by 2 ft (0.61 m by 0.61 m) P - 1-7/8 - 4 grate, $Z = 24$ (Note: $1 \text{ ft}^3/\text{s} = 0.028 \text{ m}^3/\text{s}$, $1 \text{ ft} = 0.305 \text{ m}$).

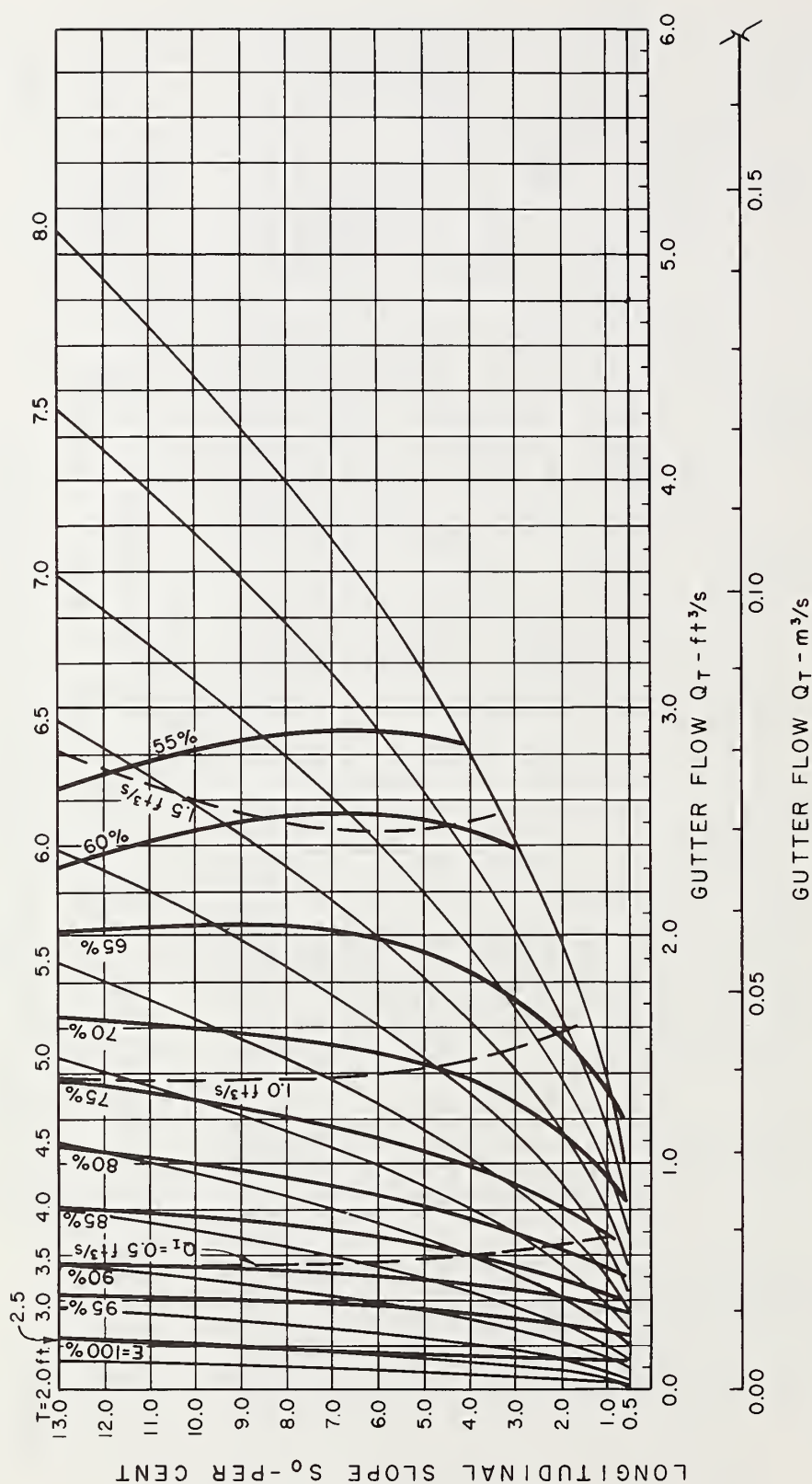


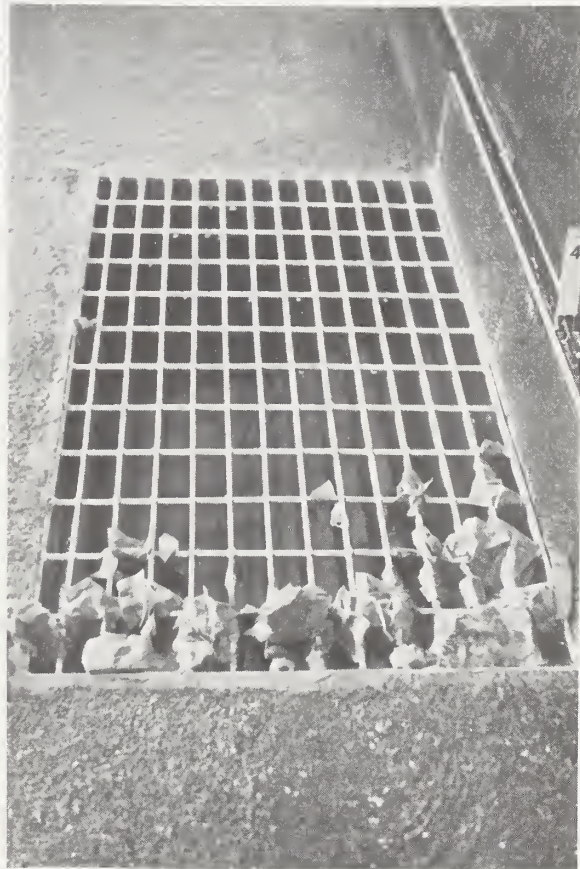
Figure 11-13. - Grate inlet capacity curves, 2 ft by 2 ft (0.61 m by 0.61 m) P - 1-7/8 - 4 grate, $Z = 48$ (Note: 1 $\text{ft}^3/\text{s} = 0.028 \text{ m}^3/\text{s}$, 1 $\text{ft} = 0.305 \text{ m}$).



a. $Q_T = 2.7 \text{ ft}^3/\text{s}$ ($0.076 \text{ m}^3/\text{s}$)

$T' = 5.4 \text{ ft}$ (1.65 m)

Photo 77-17



b. View looking downstream at
104 pieces of debris caught
on the grate.

Photo 77-18

Figure 11-14. - Debris tests, 2 ft by 4 ft (0.61 m by 1.22 m) P - 1-7/8 - 4
grate, $S_0 = 4\%$, $Z = 24$.

Table 11-2

DEBRIS TEST RESULTS - P - 1-7/8 - 4 GRATES

Test No.	Number of "leaves" lodged on grate*			
	$S_0 = 0.5\%$		$S_0 = 4.0\%$	
	5 minutes	15 minutes	5 minutes	15 minutes
<u>2 ft by 2 ft (0.61 m by 0.61 m) grate</u>				
1	141	135		
2	125	111		
3	132	121		
4			132	122
5			131	114
6			121	113
Debris handling efficiency* (%)	12	18	15	32
<u>2 ft by 4 ft (0.61 m by 1.22 m) grate</u>				
1	132	117		
2	139	126		
3	128	121		
4			113	104
5			130	123
6			123	117
Debris handling efficiency* (%)	11	19	19	24

* Based on 150 "leaves" arriving at the grate.

The debris tests showed that the P - 1-7/8 - 4 grates are not very efficient in passing debris. On the average, they passed 14 percent of the leaves in the first 5 minutes and 21 percent in 15 minutes.

CHAPTER 12

HYDRAULIC EFFICIENCY AND DEBRIS TESTS - PARALLEL BAR GRATES WITH SPACERS

Introduction

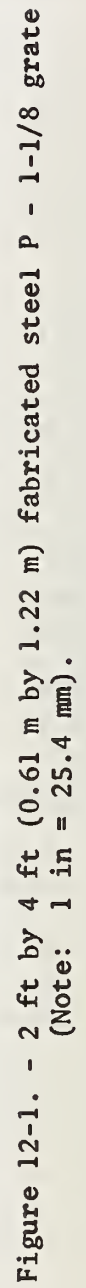
This chapter contains the results of hydraulic and debris tests conducted on parallel bar grates with a very narrow longitudinal bar spacing. The grates tested are similar to those now used by the City of Los Angeles. This type grate has proven to be safe for bicycle and pedestrian traffic in tests conducted by the Wheelmen's Bicycle Club working in cooperation with the City of Los Angeles and the Los Angeles County Flood Control District (1).*

The 2 ft by 4 ft (0.61 m by 1.22 m) grate tested is illustrated in figure 12-1. The grate is constructed of 3/8 in (9 mm) wide by 3-1/2 in (89 mm) deep longitudinal bars spaced on 1-1/8 in (29 mm) centers (table 2-3). The 3/4 in (19 mm) spacing between these bars is maintained by cast steel spacers near each end of the grate and by spacers of 1/2 in (13 mm) standard pipe at intervals along the length of the grate. This 3/4 in (19 mm) spacing must be maintained to prevent bicycle tires from being pinched between the longitudinal bars of the grate. The grate is held together by 1/2 in (13 mm) diameter bolts which pass through the pipe spacers as shown in the figure. This grate style will be referred to throughout the report as the P - 1-1/8 grate. This code name indicates a parallel bar-type grate with a 1-1/8 in (29 mm) center-to-center longitudinal bar spacing.

Experimental Results and Observations

Hydraulics. - Hydraulic test results for the P - 1-1/8 grates are shown in figures 12-2 and 12-3. Hydraulic efficiencies for the 2 ft (0.61 m) long grate are always lower than those for the 4 ft (1.22 m) long grate for the same test conditions. At the flatter longitudinal slopes the shorter grate does not capture as much flow along its side as the 4 ft (1.22 m) grate does. At steeper slopes, side flow becomes less important and the 4 ft (1.22 m) grate is more efficient because of its greater area. At the steepest longitudinal slopes the flow velocity is great enough to carry some flow all the way across the 2 ft (0.61 m) grate. This flow velocity is not great enough to carry across the 4 ft (1.22 m) grate, however. Flow rates and velocities on the Z = 48 cross slope were not high enough to carry across even the 2 ft

* Number in parentheses identifies the references at the end of the chapter.



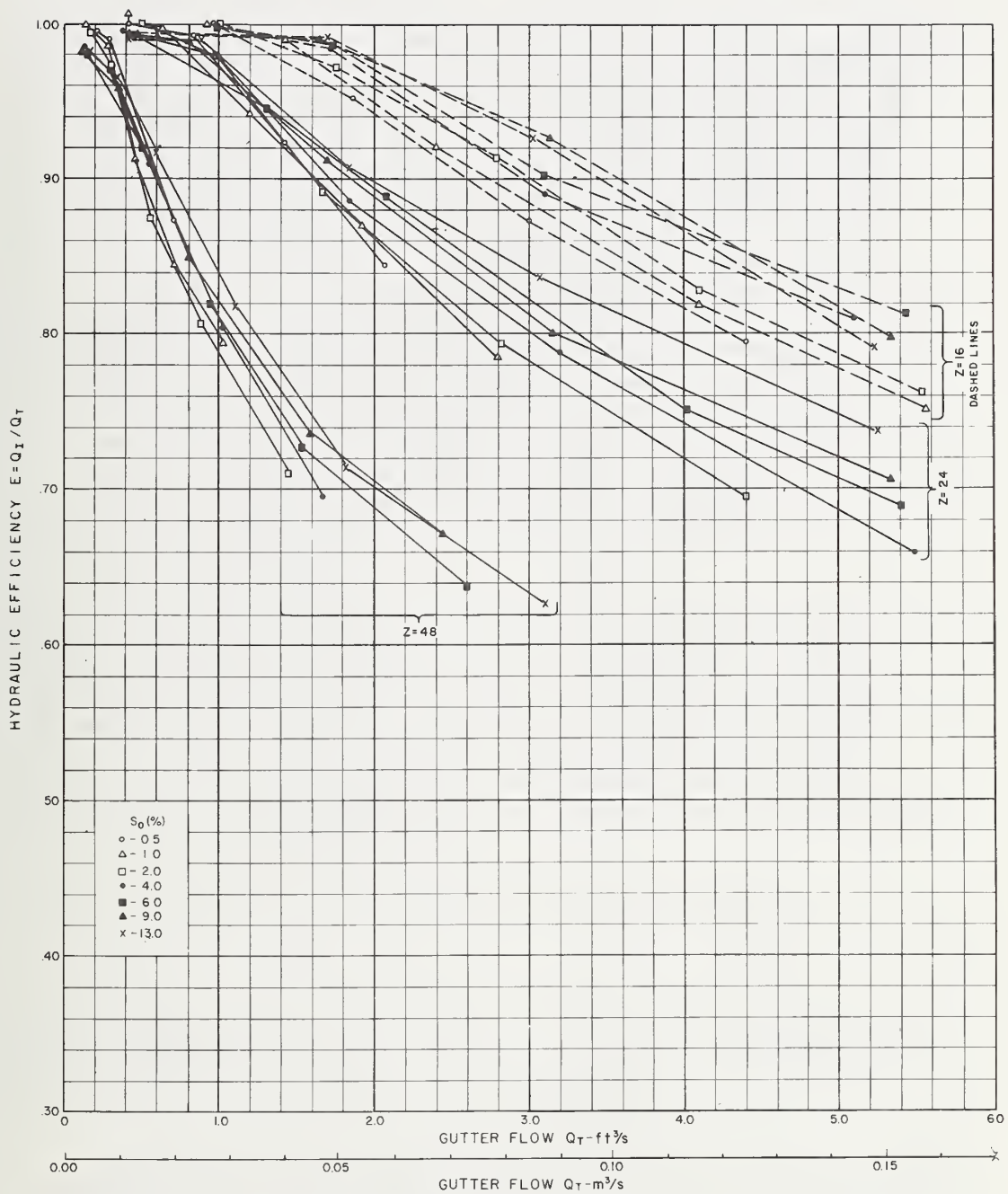


Figure 12-2. - Hydraulic efficiency vs. gutter flow, 2 ft by 4 ft (0.61 m by 1.22 m) P - 1-1/8 grate.

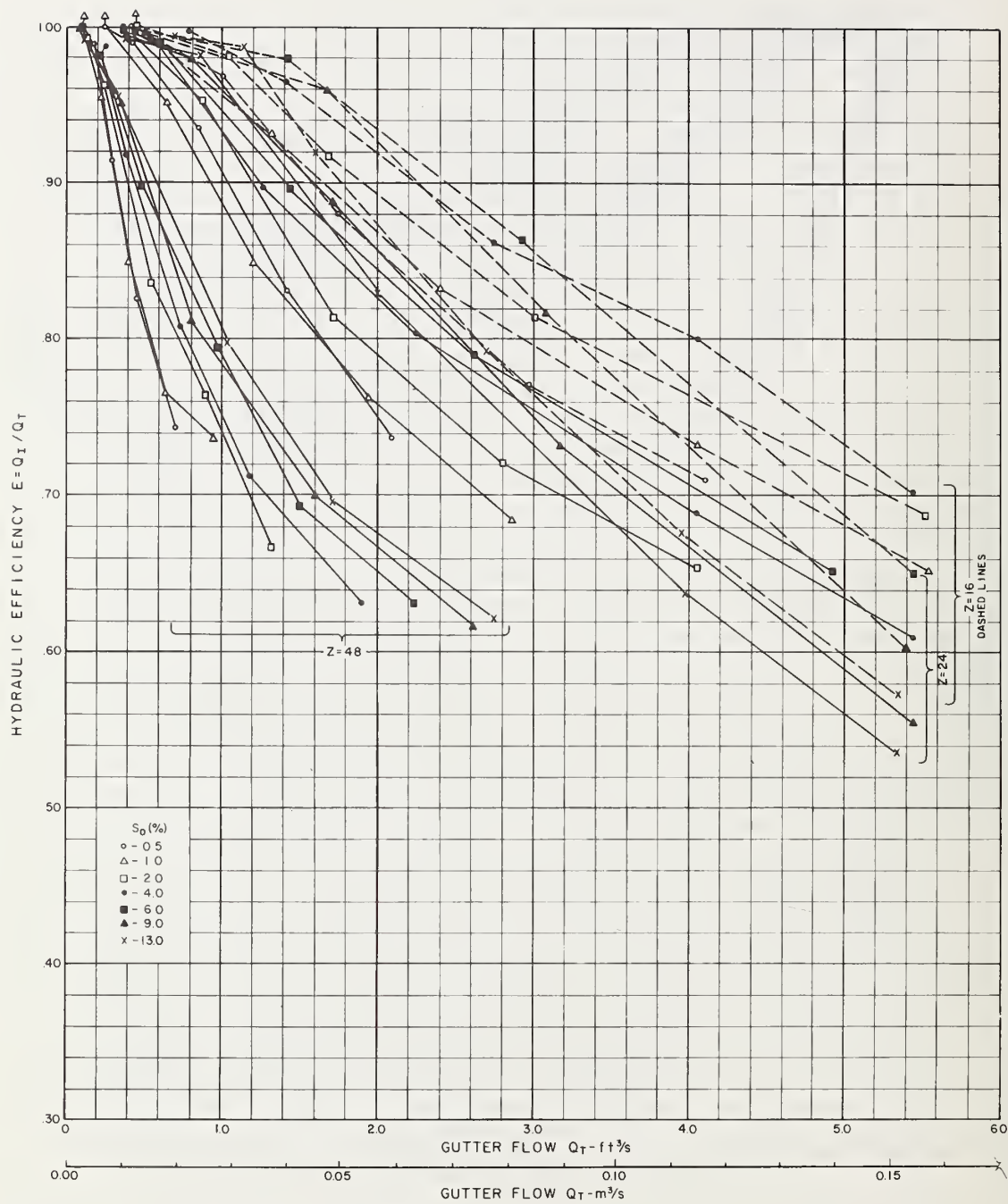


Figure 12-3. - Hydraulic efficiency vs. gutter flow, 2 ft by 2 ft (0.61 m by 0.61 m) P - 1-1/8 grate.

(0.61 m) grate and for this reason, the hydraulic efficiency differences between the two grate sizes for $Z = 48$ are dependent only on the loss of 2 ft (0.61 m) of side flow on the shorter grate.

Splash patterns which are common to grates with transverse members do not occur on the P - 1-1/8 grates. The 1/2 in (13 mm) bolts and pipe spacers are about 1.3 in (33 mm) below the surface of the grate. This location minimizes the effects of the spacer or transverse bar on the flow over the grate. The subsurface spacers do cause some disturbance in the flow pattern as is evident in the sequence of photographs in figure 12-4. Very little splash carries across the 4 ft (1.22 m) long grate even at the steepest longitudinal slope (13 percent) and cross slope ($Z = 16$). The 2 ft (0.61 m) long grate begins to experience splash problems at slopes of 4 percent for $Z = 16$ and 6 percent for $Z = 24$. At these slopes, velocity carries the flow far enough to strike the vertical face of the downstream cast steel spacers. Flow which hits the spacer is deflected up and out of the inlet in a "roostertail" splash pattern. Steeper slopes result in higher velocities; the splash problem gets worse as more and more of the flow strikes the downstream cast spacers. Figure 12-5 shows this splash pattern beginning at a longitudinal slope of 4 percent and traces its development through the 13 percent slope for $Z = 16$. Splash patterns are similar for the $Z = 24$ cross slope.

Figures 12-6 and 12-7 show the relationship between the widths of spread measured on the test facility, T' , and the hydraulic efficiency, E , for the two grates. For the same width of spread, hydraulic efficiencies are highest at the flattest longitudinal and cross slopes and lowest at the steepest longitudinal and cross slopes. In other words, hydraulic efficiencies (for the same width of spread) decrease as flow velocities increase. High flow velocities cause more splash and less contribution from side flow to the total intercepted flow, Q_I .

Figures 12-8 through 12-13 are grate inlet capacity curves for the P - 1-1/8 grates. There is one figure per cross slope for each of the grate sizes tested.

The variation in hydraulic efficiency with changing longitudinal slope is apparent in the inlet capacity curves. Following a line of constant gutter flow, Q_T , from 0.5 percent slope through 13 percent slope in each of the figures shows that:

1. Hydraulic efficiencies increase steadily (or decrease only slightly) with increasing longitudinal slope for both grate sizes on the $Z = 48$ cross slope and for the 4 ft (1.22 m) long grate on the $Z = 24$ cross slope.



- a. $S_0 = 4\%$
 $Q_T = 5.49 \text{ ft}^3/\text{s} \text{ (} 0.155 \text{ m}^3/\text{s)}$
 $T' = 7.0 \text{ ft (} 2.13 \text{ m)}$
 $E = 66\%$



- b. $S_0 = 6\%$
 $Q_T = 5.41 \text{ ft}^3/\text{s} \text{ (} 0.153 \text{ m}^3/\text{s)}$
 $T' = 6.4 \text{ ft (} 1.95 \text{ m)}$
 $E = 69\%$



- c. $S_0 = 9\%$
 $Q_T = 5.34 \text{ ft}^3/\text{s} \text{ (} 0.151 \text{ m}^3/\text{s)}$
 $T' = 6.0 \text{ ft (} 1.83 \text{ m)}$
 $E = 71\%$

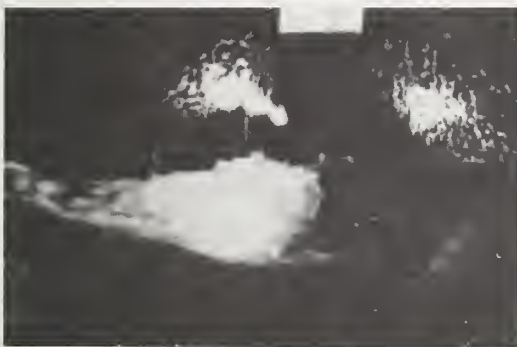


- d. $S_0 = 13\%$
 $Q_T = 5.25 \text{ ft}^3/\text{s} \text{ (} 0.149 \text{ m}^3/\text{s)}$
 $T' = 6.1 \text{ ft (} 1.86 \text{ m)}$
 $E = 74\%$

Figure 12-4. - Development of splash from pipe spacers on 2 ft by 4 ft (0.61 m by 1.22 m) P - 1-1/8 grate, Z = 24.
 Photo H-1765-385



- a. $S_0 = 4\%$
 $Q_T = 5.44 \text{ ft}^3/\text{s} \text{ (} 0.154 \text{ m}^3/\text{s)}$
 $T' = 5.5 \text{ ft (} 1.68 \text{ m)}$
 $E = 70\%$



- b. $S_0 = 6\%$
 $Q_T = 5.44 \text{ ft}^3/\text{s} \text{ (} 0.154 \text{ m}^3/\text{s)}$
 $T' = 5.0 \text{ ft (} 1.52 \text{ m)}$
 $E = 65\%$



- c. $S_0 = 9\%$
 $Q_T = 5.39 \text{ ft}^3/\text{s} \text{ (} 0.153 \text{ m}^3/\text{s)}$
 $T' = 4.7 \text{ ft (} 1.43 \text{ m)}$
 $E = 60\%$



- d. $S_0 = 13\%$
 $Q_T = 5.34 \text{ ft}^3/\text{s} \text{ (} 0.151 \text{ m}^3/\text{s)}$
 $T' = 4.4 \text{ ft (} 1.34 \text{ m)}$
 $E = 57\%$

Figure 12-5. - Flow deflected out of the inlet by the cast steel spacer, 2 ft by 2 ft (0.61 m by 0.61 m) P - 1-1/8 grate, Z = 16. Photo H-1765-386

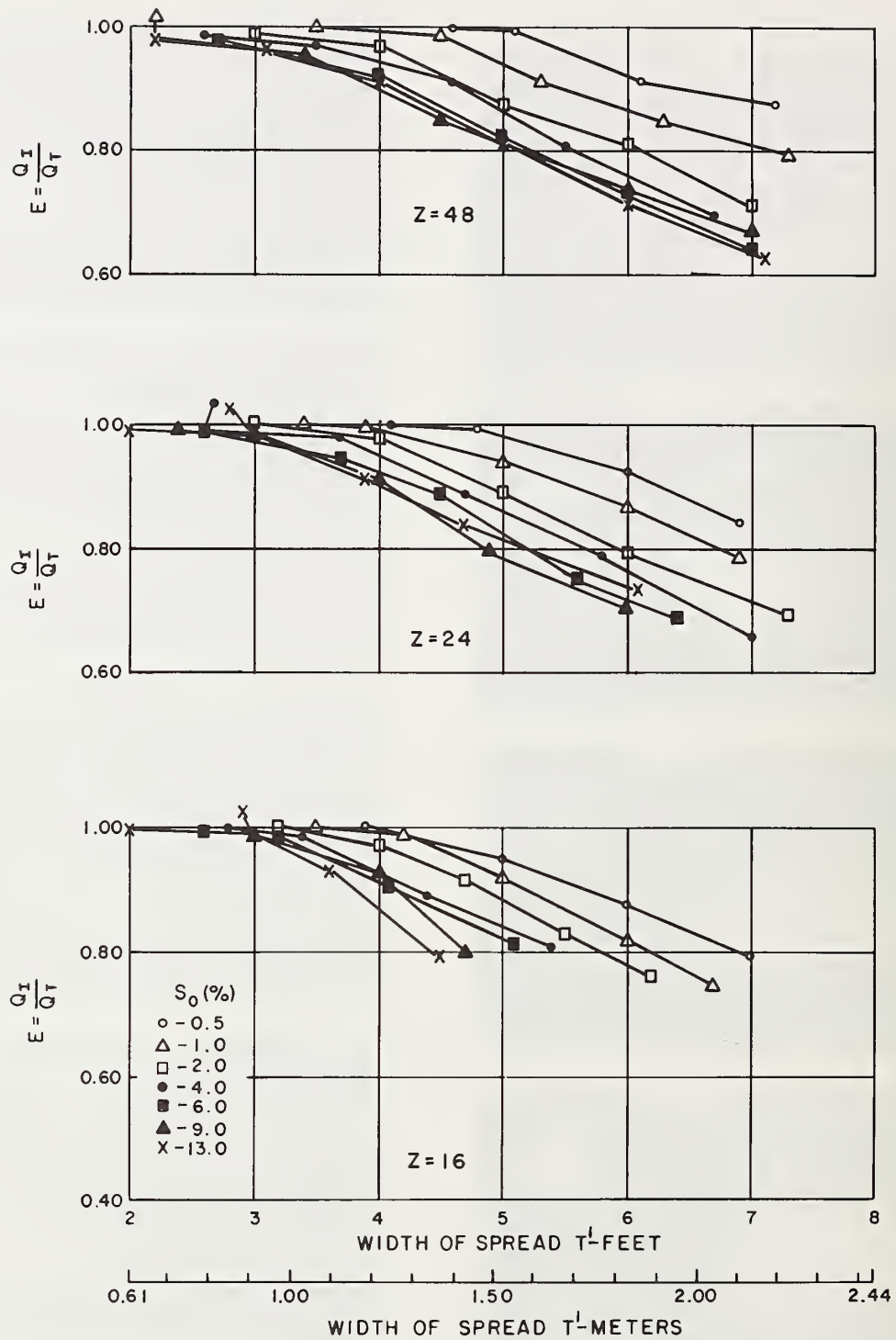


Figure 12-6. - Hydraulic efficiency vs. width of spread, 2 ft by 4 ft (0.61 m by 1.22 m) P - 1-1/8 grate.

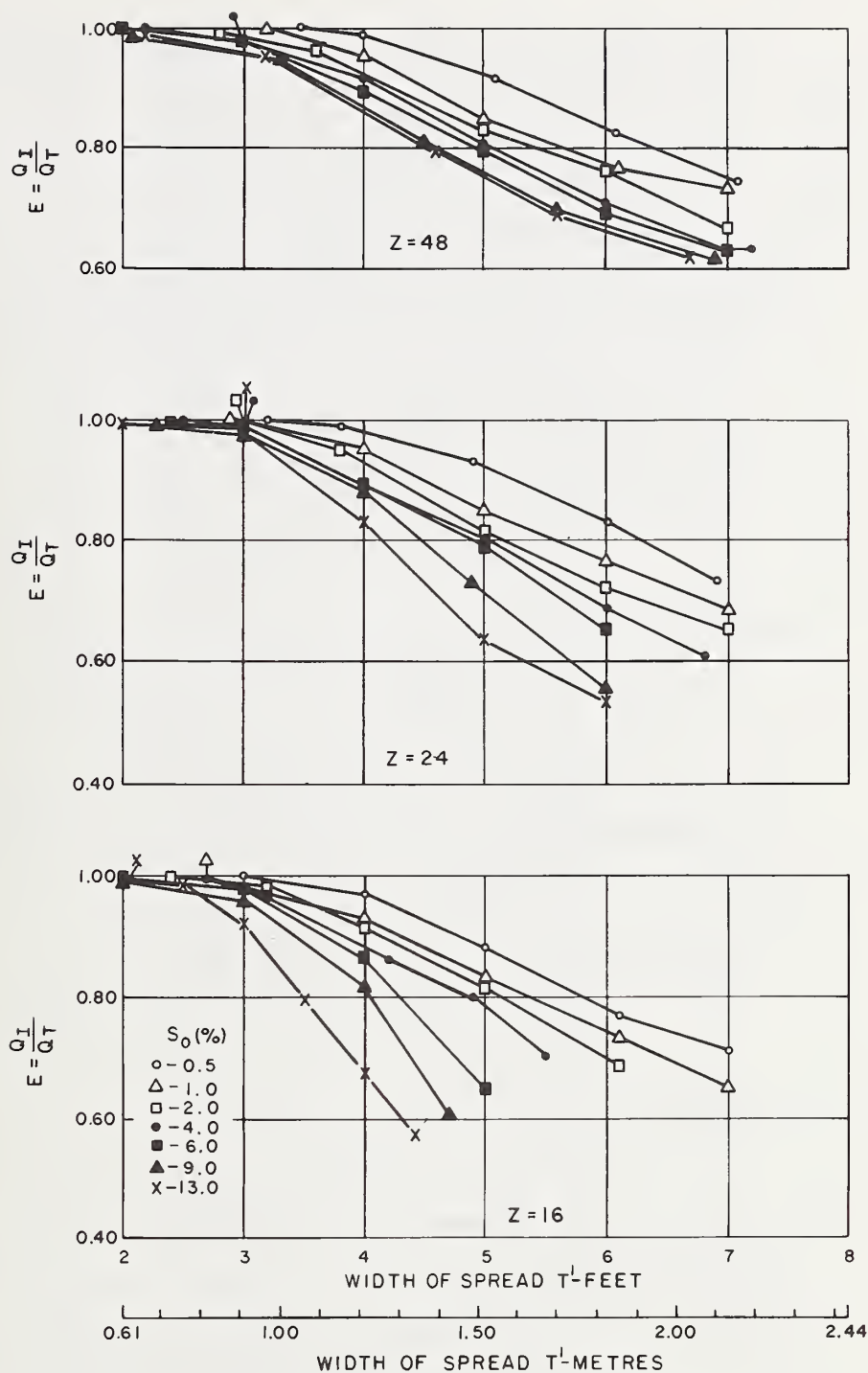


Figure 12-7. - Hydraulic efficiency vs. width of spread, 2 ft by 2 ft (0.61 m by 0.61 m) P - 1-1/8 grate.

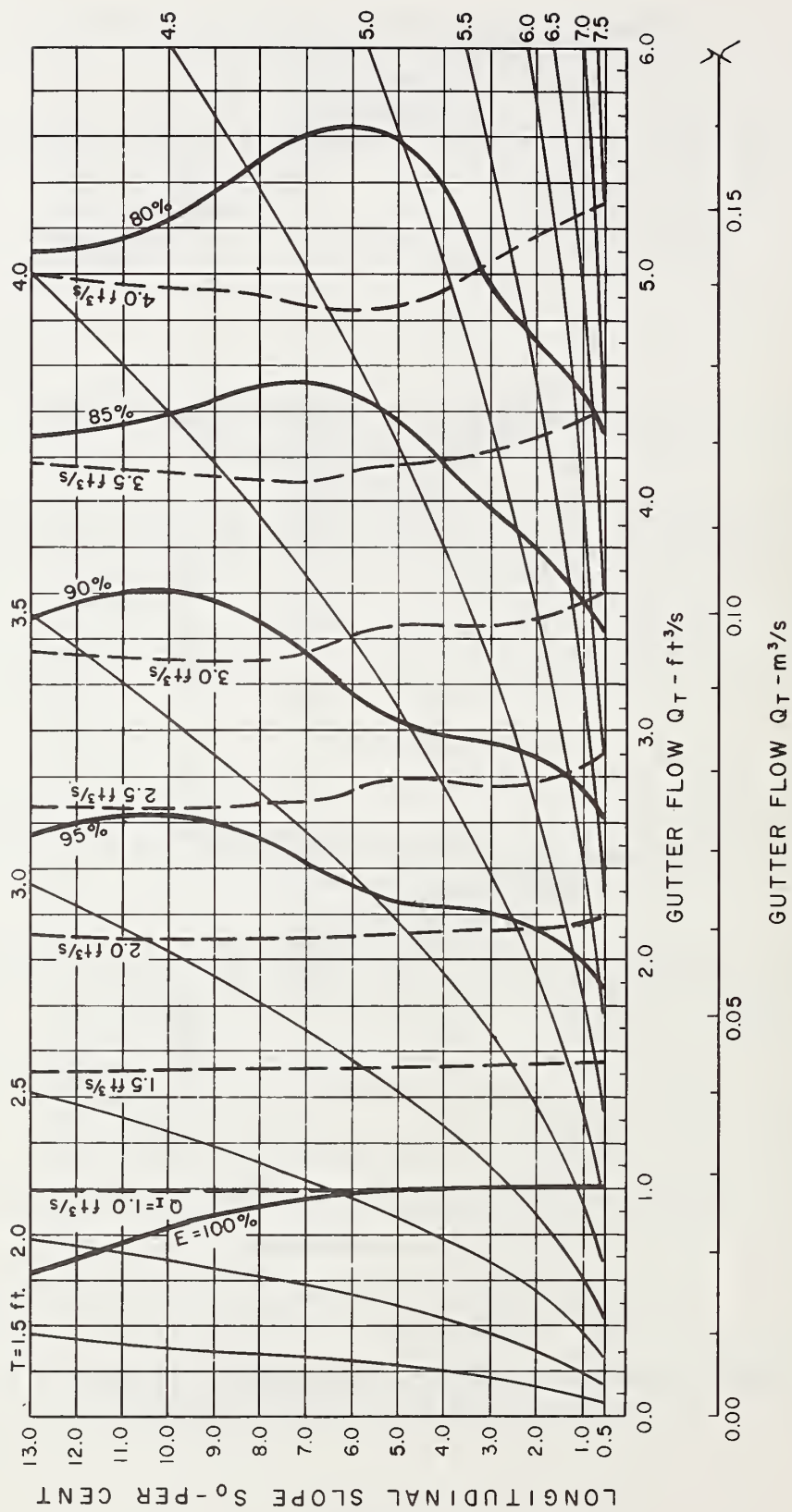


Figure 12-8. - Grate inlet capacity curves, 2 ft by 4 ft (0.61 m by 1.22 m) P - 1-1/8 grate, $Z = 16$ (Note: 1 ft = 0.305 m, 1 $\text{ft}^3/\text{s} = 0.028 \text{ m}^3/\text{s}$).

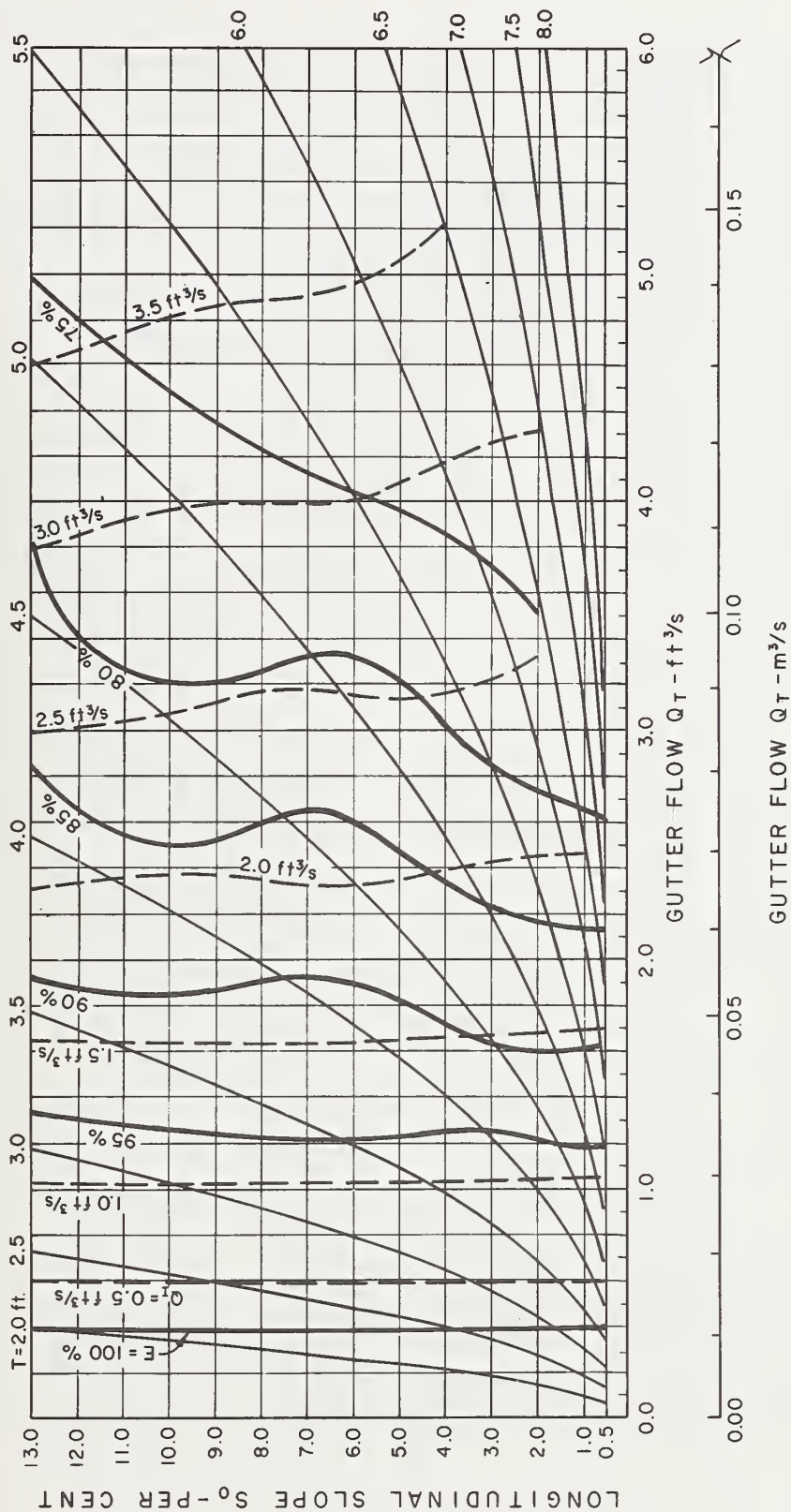


Figure 12-9. - Grate inlet capacity curves, 2 ft by 4 ft (0.61 m by 1.22 m) P - 1-1/8 grate, $Z = 24$ (Note: 1 ft = 0.305 m, 1 ft³/s = 0.028 m³/s).

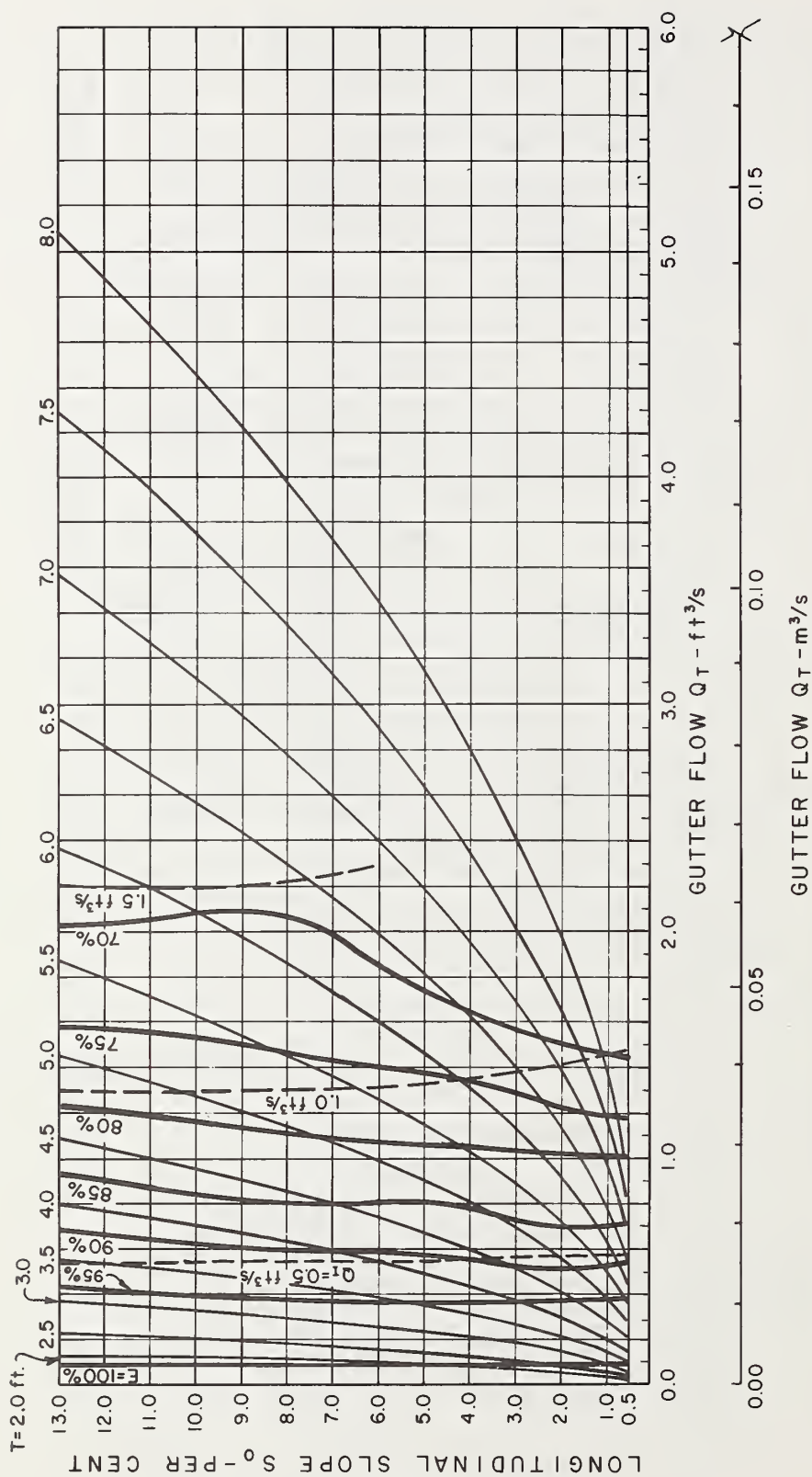


Figure 12-10. - Grate inlet capacity curves, 2 ft by 4 ft (0.61 m by 1.22 m) P - 1-1/8 grate, $Z = 48$ (Note: 1 ft = 0.305 m, 1 $\text{ft}^3/\text{s} = 0.028 \text{ m}^3/\text{s}$).

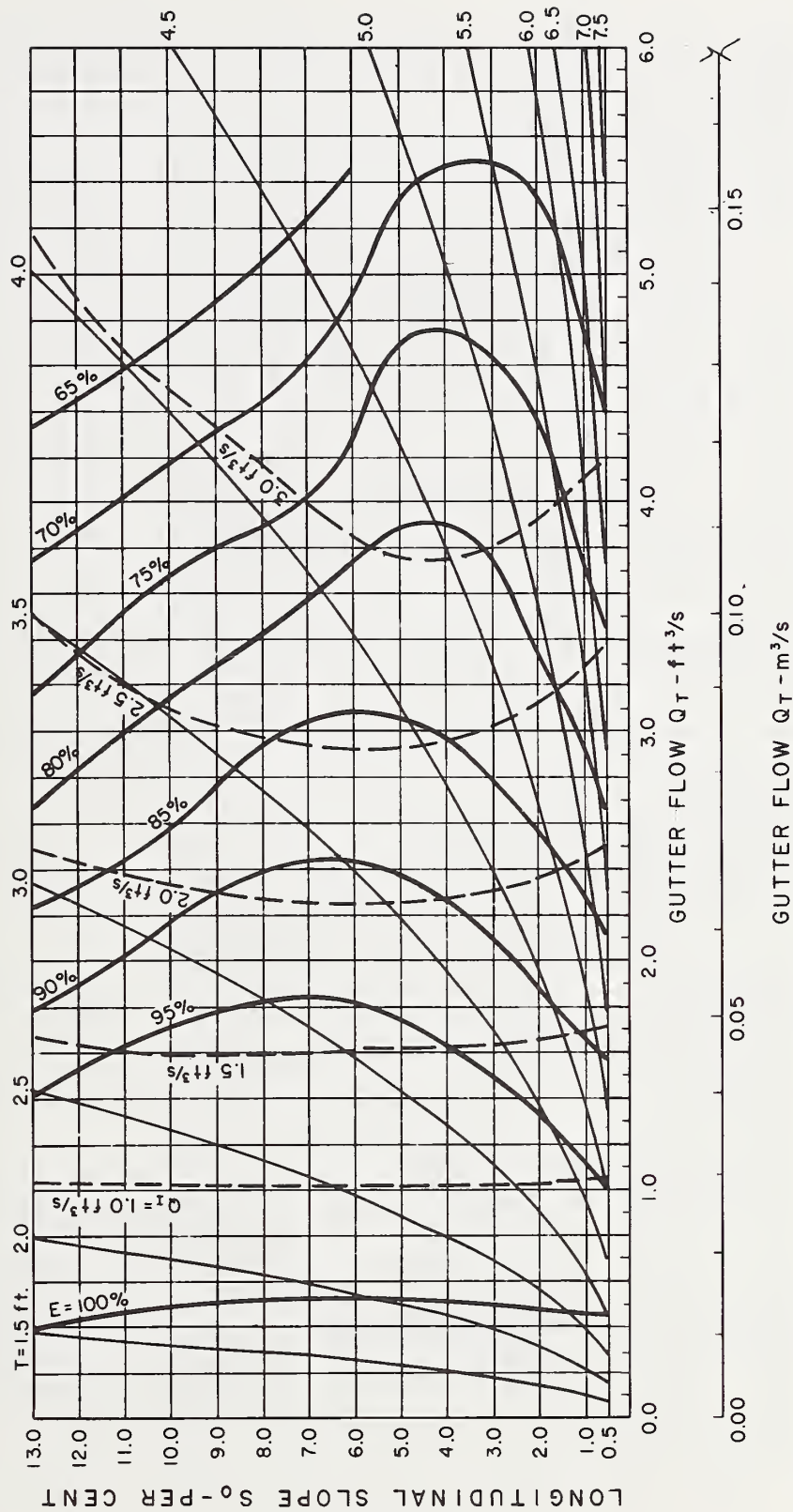


Figure 12-11. - Grate inlet capacity curves, 2 ft by 2 ft (0.61 m by 0.61 m) P - 1-1/8 grate, $Z = 16$ (Note: 1 ft = 0.305 m, 1 ft³/s = 0.028 m³/s).

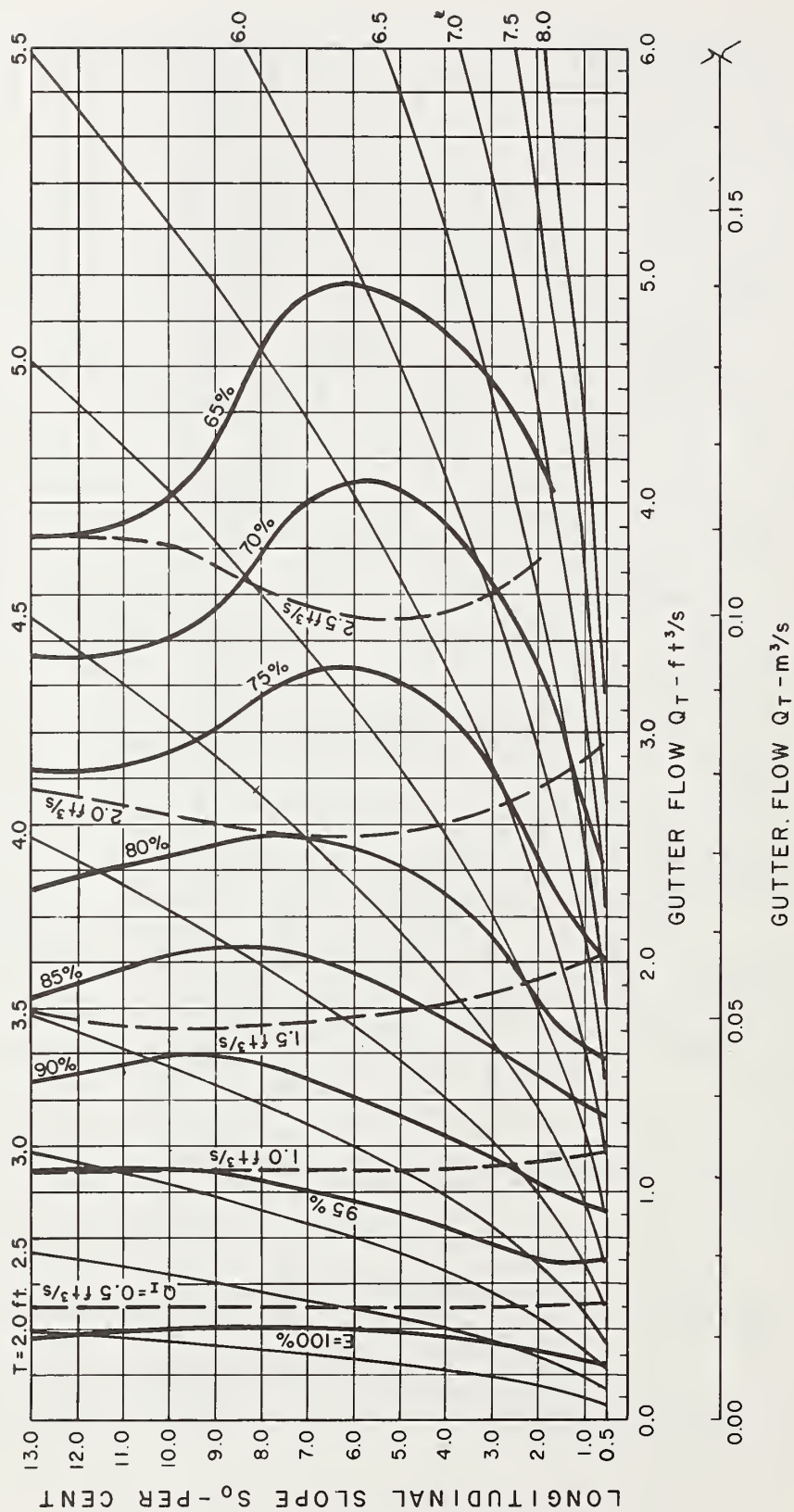


Figure 12-12. - Grate inlet capacity curves, 2 ft by 2 ft (0.61 m by 0.61 m) P - 1-1/8 grate, Z = 24 (Note: 1 ft = 0.305 m, 1 ft^3/s = 0.028 m^3/s).

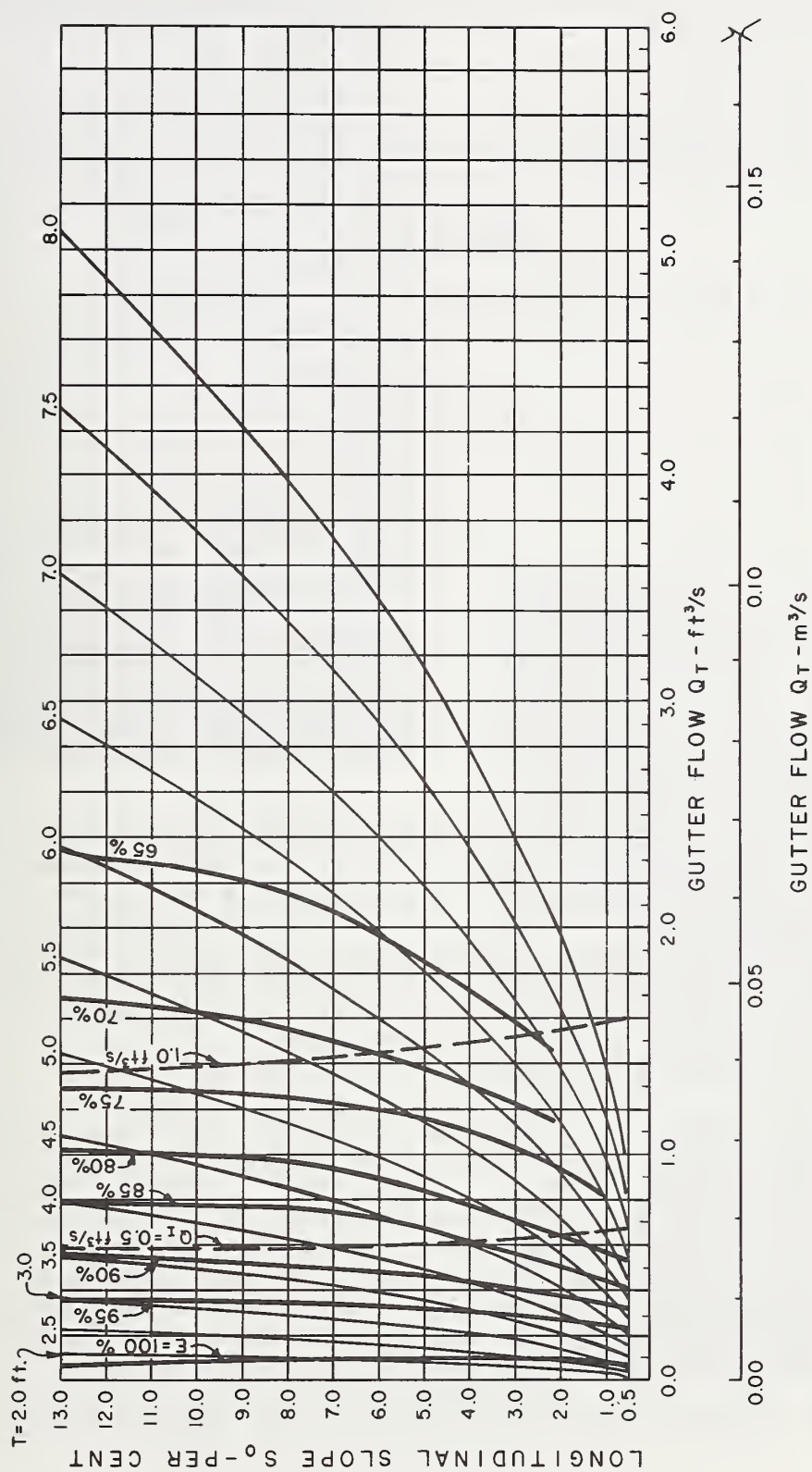


Figure 12-13. - Grate inlet capacity curves, 2 ft by 2 ft (0.61 m by 0.61 m) P - 1-1/8 grate, Z = 48 (Note: 1 ft = 0.305 m, 1 ft^3/s = 0.028 m^3/s).

2. Hydraulic efficiencies increase with increasing longitudinal slope, reach a maximum efficiency at some slope and decrease for steeper slopes for the 2 ft grate at $Z = 24$ and for both grate sizes at $Z = 16$.

The slope where the grate's efficiency is highest depends on the gutter flow, cross slope, and the length of the grate. The maximum efficiency slopes for the P - 1-1/8 grates are shown in table 12-1.

Table 12-1

MAXIMUM EFFICIENCY SLOPES - P - 1-1/8 GRATES

Grate Size	Z = 48	Z = 24	Z = 16
2 ft by 2 ft (0.61 m by 0.61 m)	>13%	6% to 9%	3% to 6%
2 ft by 4 ft (0.61 m by 1.22 m)	>13%	>13%	6% to 10%

The maximum efficiency slopes are apparent in the inlet capacity curves (figures 12-8 through 12-13) as the slope where the efficiency lines reverse direction.

The efficiency of both P - 1-1/8 grates could be improved slightly (particularly where flow velocities are high) if the cast steel spacers were located so that their edges are flush with the ends of the longitudinal bars instead of recessed 11/16 in (17 mm) as they were on the test grates (figure 12-1). Relocating the cast spacers flush with the ends of the grate would increase the effective hydraulic length of the grates by 1-3/8 in (35 mm) as very little flow now passes through the 11/16 in (17 mm) openings on the upstream and downstream ends of the test grates.

Debris Tests. - The P - 1-1/8 grates were tested for debris handling ability using the standard test procedure described in Chapter 5. Figure 12-14a shows the 2 ft by 4 ft (0.61 by 1.22 m) grate during a debris test on a slope of 0.5 percent with a gutter discharge of 2.67 ft³/s (0.076 m³/s). Figure 12-14b shows the final distribution of debris on the grate after the test. Figures 12-15a and b shows the 2 ft by 2 ft (0.61 m by 0.61 m) grate under similar flow conditions but at a longitudinal slope of 4 percent. The debris test results are essentially the same for both grate sizes at the 0.5 percent slope. Both grates handle debris better at the 4 percent slope than at the 0.5 percent slope. At the end of the tests



a. $Q_T = 2.67 \text{ ft}^3/\text{s}$ ($0.076 \text{ m}^3/\text{s}$)

$T' = 7.8 \text{ ft}$ (2.38 m)

Photo 121-4



b. 138 "leaves" lodged on the grate at end of test.

Photo 121-5

Figure 12-14. - Debris test of 2 ft by 4 ft (0.61 m by 1.22 m) P - $1\frac{1}{8}$ grate, $S_0 = 0.5\%$, $Z = 24$.



a. $Q_T = 2.67 \text{ ft}^3/\text{s}$ ($0.076 \text{ m}^3/\text{s}$)

$T' = 5.3 \text{ ft}$ (1.62 m)

Photo 130 12A-13



b. 104 "leaves" lodged on the grate at end of test.

Photo 130 13A-14

Figure 12-15. - Debris test of 2 ft by 2 ft (0.61 m by 0.61 m) P - $1\text{-}1/8$ grate, $S_0 = 4\%$, $Z = 24$.

on the 4 percent slope, an average of 87 percent of the leaves were caught on the 4 ft (1.22 m) long grate and only 73 percent were caught on the 2 ft (0.61 m) long grate. Saying it another way, twice as much debris was removed from the 2 ft (0.61 m) long grate as from the 4 ft (1.22 m) long grate. At the 4 percent slope, the gutter flow has sufficient velocity to carry the flow just over 2 ft (0.61 m) past the front of the grate. Debris was washed off the 2 ft (0.61 m) long grate but was only pushed farther down along the bars of the 4 ft (1.22 m) long grate, where it remained at the end of the test.

The 4 ft (1.22 m) grate seems to be less efficient at handling debris at a slope of 4 percent based on the test results in table 12-2 but in reality both grate sizes behave in the same manner.

Summary

The P - 1-1/8 grates have very good hydraulic characteristics. The hydraulic efficiency of the 2 ft (0.61 m) long grate suffers in high velocity areas when the flow strikes the vertical faces of the downstream cast spacers and splashes out of the inlet. Both grate sizes could be improved hydraulically by relocating the cast spacers so that they are flush with the ends of the grate.

For a given gutter flow, Q_T , both P - 1-1/8 grates show an increase in hydraulic efficiency with increasing longitudinal slope until some maximum efficiency is reached. The slopes where efficiency is maximized depend on gutter flow, cross slope, and grate length (figures 12-8 through 12-13 and table 12-1).

For any given width of spread, T , hydraulic efficiencies are higher in low-velocity situations (flat longitudinal and/or cross slopes) than they are in high-velocity situations (steep longitudinal and/or cross slopes).

Tests showed that the P - 1-1/8 grates are not very efficient at handling debris. On the average they cleared 5 percent of the "leaves" in the first 5 minutes and 9 percent at the end of 15 minutes at a 0.5 percent slope or 20 percent at the end of 15 minutes at a 4 percent slope.

Table 12-2

DEBRIS TEST RESULTS - P - 1-1/8 GRATES

Test No.	Number of "leaves" lodged on grate*			
	$S_0 = 0.5\%$		$S_0 = 4.0\%$	
	5 minutes	15 minutes	5 minutes	15 minutes
<u>2 ft by 2 ft (0.61 m by 0.61 m) grate</u>				
1			142	101
2			143	104
3			142	122
4	147	141		
5	144	139		
6	136	130		
Debris handling efficiency* (%)	5	9	5	27
<u>2 ft by 4 ft (0.61 m by 1.22 m) grate</u>				
1	143	138		
2	137	135		
3	143	137		
4			145	141
5			146	131
6			143	118
Debris handling efficiency* (%)	6	9	4	13

* Based on 150 "leaves" arriving at the grate.

REFERENCES

1. Los Angeles County Flood Control District, "Evaluation of Three Types of Catch Basin Grates for Streets with Bicycle Traffic," Systems and Standards Group, Design Division, January 18, 1973.

CHAPTER 13

DISCUSSION OF RESULTS

Hydraulic Tests

Hydraulic testing of the eight grate designs in two sizes each has shown that all the grates tested behave similarly. The flow into and around each of the grate styles is similar in many respects to the flow conditions at an open hole. These flow conditions are determined by the longitudinal slope, cross slope, and gutter flow.

For a constant gutter flow, all the grates show some increase in hydraulic efficiency if the cross slope is held constant and the longitudinal slope is increased. At a steeper longitudinal slope the same gutter flow occupies a smaller cross sectional area since its velocity has increased. With a smaller flow area, a greater percentage of the gutter flow passes over the grate inlet. If no flow is splashed fully across the grate, intercepted flow is greater and hence hydraulic efficiency is higher. The open hole and P - 1-7/8 grates have no transverse members to cause splash. For any given gutter flow, the P - 1-7/8 grates are most efficient at the steepest slopes. The other grates show similar patterns of increasing efficiency until a point is reached when the increased velocity causes some of the flow to carry completely across the grate without being captured.

The six grate designs other than the P - 1-7/8 and CV - 3-1/4 - 4-1/4 all have problems with splash under some conditions. Each of these grates performs at its maximum efficiency over some range of longitudinal slopes which will be referred to as the maximum efficiency slope or range of slopes. Chapters 7, 8, 9, 11 and 12 contain tables showing the maximum efficiency range for each of the grates tested. Since flow velocity causes smaller cross sectional flow areas and also causes splash, velocity is the factor which determines the maximum efficiency slope. Velocity, of course, is dependent on the cross slope as well as the longitudinal slope. The tables in each chapter show a maximum efficiency slope for each of the cross slopes tested. For a given longitudinal slope, velocities are higher at steeper cross slopes. More grate area is required to intercept high gutter flows, Q_T , and obviously more splash occurs at higher gutter flows than at lower flows. Since the maximum efficiency slope also depends on the flow rate, a range of slopes is shown to cover the gutter flows tested. The lower value shown is for the highest gutter flow, Q_T , tested, and the higher value is for some lower gutter flow. The longer grates reach their maximum efficiencies at steeper longitudinal slopes than the shorter grates for obvious reasons. The long grates capture gutter flows which would splash completely across the shorter grates.

Throughout the test program, the 4 ft (1.22 m) long grates were more efficient than the 2 ft (0.61 m) grates for the same test conditions. At the lower longitudinal slopes, gutter flows and velocities were low and most of the grate area was not utilized.

Since both grate sizes have the same width, the longer grate is more efficient because it collects flow along its side for 4 ft (1.22 m) as opposed to 2 ft (0.61 m) for the short grate. When the combination of longitudinal and cross slope produces gutter flows and velocities sufficient to splash completely across the grates, the longer grate is more efficient since it has a much greater area to intercept the flow passing over it.

For a given width of spread, all the grates are most efficient at the flatter longitudinal and cross slopes. As discussed in Chapter 4, if width of spread is held constant, approximately the same percentage of gutter flow passes over the grate regardless of slope conditions. Flatter cross slopes produce lower gutter flows and velocities and therefore higher efficiencies even though the ratio of frontal flow to gutter flow remains the same for a constant width of spread (figure 4-3). For steep longitudinal slopes and flat cross slopes there is less splash. For mild longitudinal slopes and flat cross slopes, a greater percentage of the flow passing outside the 2 ft (0.61 m) grate width is captured along the length of the grate than at steeper cross slopes.

Figure 13-1 shows a comparison of three different hydraulic efficiencies for a 2 ft by 4 ft (0.61 m by 1.22 m) open hole where the width of spread T' and cross slope, $1/Z$ were held constant and the longitudinal slope S_0 varied from 0.5 percent to 13 percent. The E (total) line shows the performance of the open hole. The E (frontal flow) line shows the performance of the same hole with flow into the front of the hole only. The remaining sides of the hole were blocked off as described in Chapter 4. The E (side flow) line shows the efficiency of the inlet based only on flow entering from the side and the downstream end. Apparently, E (side) is about 22 percent at the 0.5 percent slope and only around 7 percent at the 13 percent slope. This shows the effect of velocity on the amount of flow which enters the side of a grate inlet.

This discussion should not be interpreted as meaning that grates are more efficient at flat cross slopes. The concept of a constant width of spread, T' , is useful for the purposes of comparison, but can be misleading. For the same longitudinal slope the gutter flow required to produce the same width of spread, T' , at $Z = 16$ would be six or seven times the flow needed for $Z = 48$. Based on gutter flow, the grates are more efficient at the steeper cross slopes. For the same gutter flow a steep cross slope will have a smaller width of spread than a flatter cross slope. Therefore, more of the flow is close to

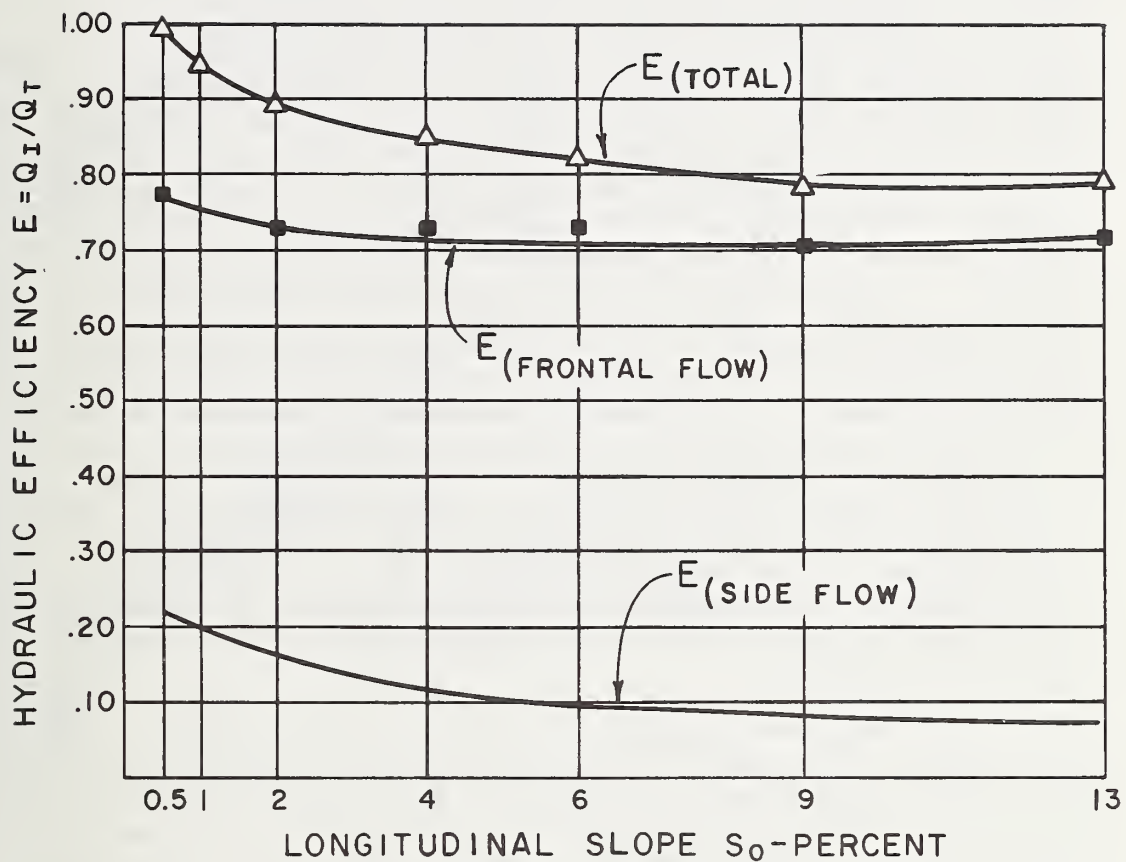


Figure 13-1. - Hydraulic efficiency vs. longitudinal slope for a 2 ft by 4 ft (0.61 m by 1.22 m) open hole. $T = 5.0$ ft (1.52 m), $Z = 24$.

the curb and passes over the inlet. The result is a higher intercepted flow and a greater hydraulic efficiency.

As noted in the previous discussions, the eight grate designs all behave similarly at slope conditions where no flow splashes completely across any of the grates. This is apparent in figures 13-2 through 13-17. The figures show the relationship between gutter flow, Q_T , and hydraulic efficiency, E , for the eight grate designs tested. Figures 13-2 through 13-8 are for the 2 ft by 4 ft (0.61 m by 1.22 m) grates and figures 13-9 through 13-15 are for the 2 ft by 2 ft (0.61 m by 0.61 m) grates. Figures 13-16, and 13-17 show the relationship between gutter flow, Q_T , and hydraulic efficiency, E , for the grates tested on the $Z = 96$ cross slope. At longitudinal and cross slope conditions where no splash occurs, the lines for the various grate designs are close together. The maximum efficiency difference between the grate designs for any gutter flow, Q_T , is only around 6 percent. If no splash carries across any of the grate designs for a particular test condition, differences in efficiency can only be attributed to small differences in the grate widths and lengths. While all the grates tested have the same nominal dimensions, there are variations in actual as well as effective lengths and widths. These differences are easily noted in the detailed grate drawings in Chapters 6 through 12. For example, the outside dimensions of the cast grates are very close to the nominal sizes of 2 ft by 2 ft (0.61 m by 0.61 m) and 2 ft by 4 ft (0.61 m by 1.22 m). However, the cast grates have much wider outside longitudinal bars and wider transverse end bars than the fabricated grates. Their effective widths and lengths, for hydraulic purposes, are slightly smaller. Under conditions where no significant splash occurs, the cast grates have lower efficiencies because they are effectively smaller than the fabricated grates.

At test conditions where splash carries across one or more of the grate designs, differences in efficiency are caused mostly by the type of grate. The effects of small size differences are minimal. Table 13-1 was compiled from figures 13-2 through 13-17 to show the minimum test (Q_T , S_0 , $1/Z$) conditions where splash occurs across at least one of the grate designs.

For slope conditions flatter than those listed in the table, efficiency differences are most dependent on small size variations among the test grates. For steeper slope conditions, efficiency differences between the grates become larger and show which grates are better hydraulically.

Gutter flows and velocities for the $Z = 96$ cross slope were very low and did not produce any carryover splash in tests of several 2 ft by 2 ft (0.61 m by 0.61 m) grate styles. For this reason, the $Z = 96$ cross slope was dropped from the test program. It is apparent in the table that at steeper cross slopes, carryover splash begins at lower

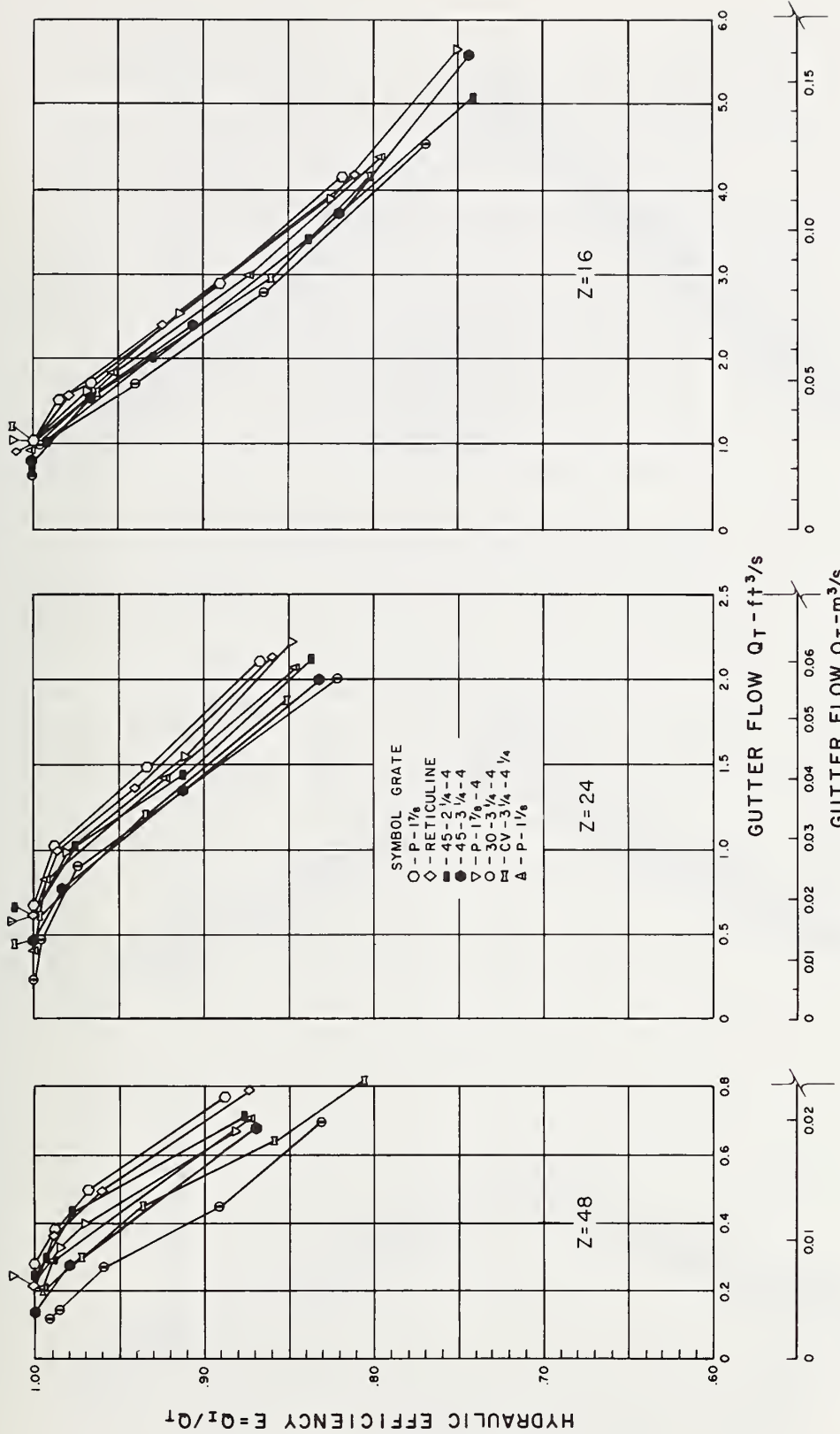


Figure 13-2. - Hydraulic efficiency vs. gutter flow for the 2 ft by 4 ft (0.61 m by 1.22 m) grates. $S_0 = 0.5\%$, $Z = 48, 24,$ and 16 .

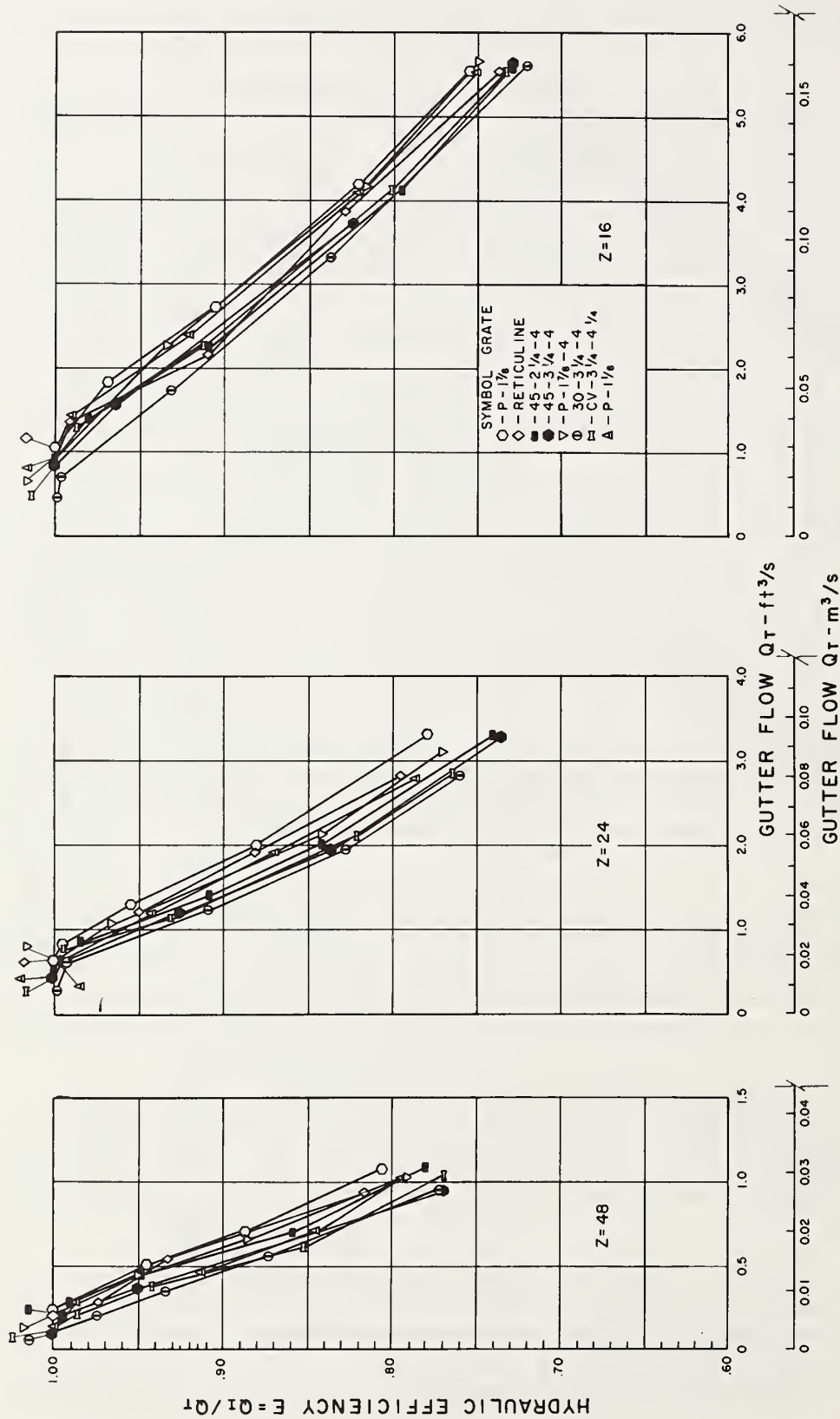


Figure 13-3. - Hydraulic efficiency vs. gutter flow for the 2 ft by 4 ft (0.61 m by 1.22 m) grates. $S_0 = 1.0\%$, $Z = 48, 24$, and 16.

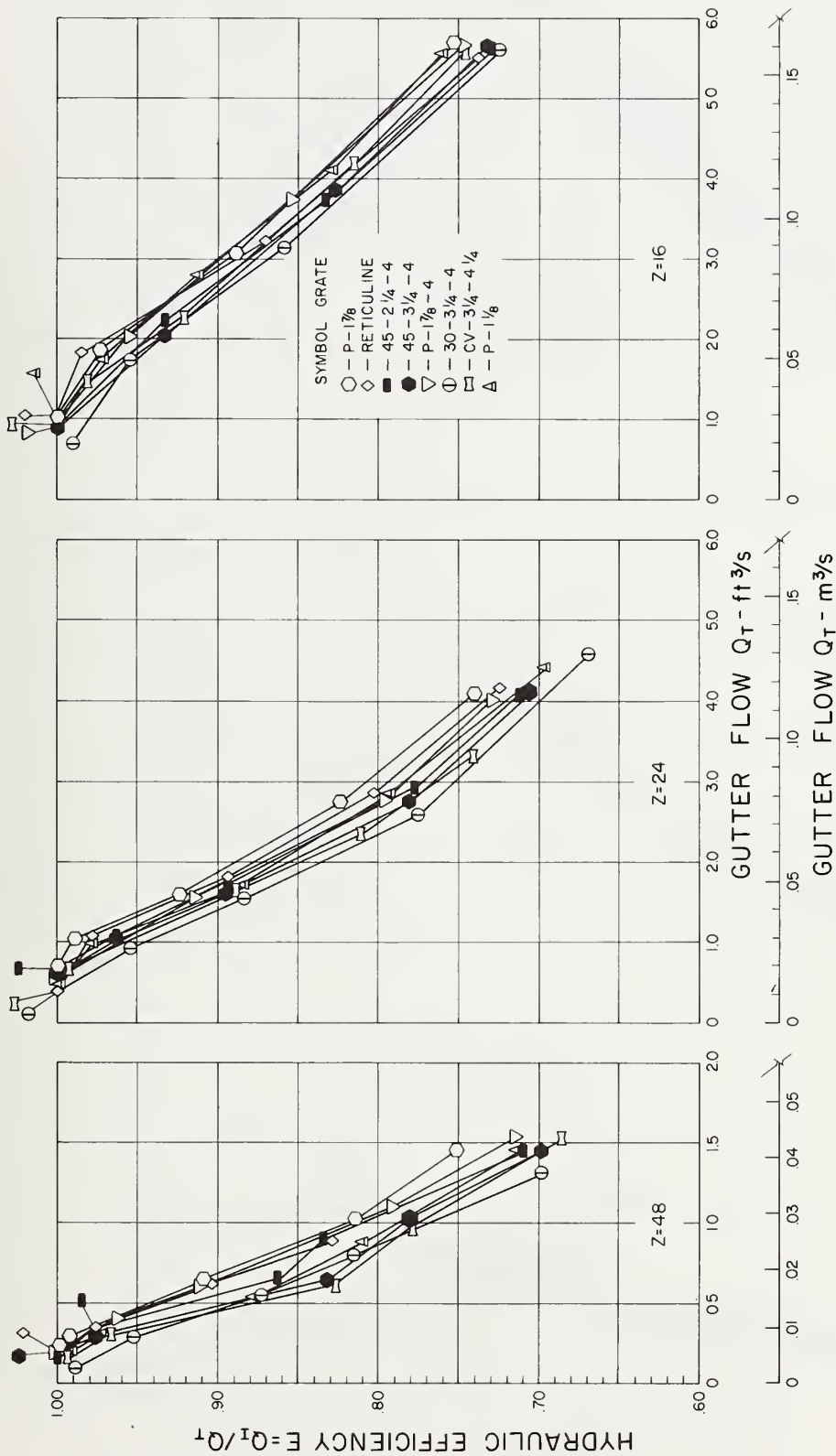


Figure 13-4. - Hydraulic efficiency vs. gutter flow for the 2 ft by 4 ft (0.61 m by 1.22 m) grates. $S_0 = 2.0\%$, $Z = 48, 24,$ and 16.

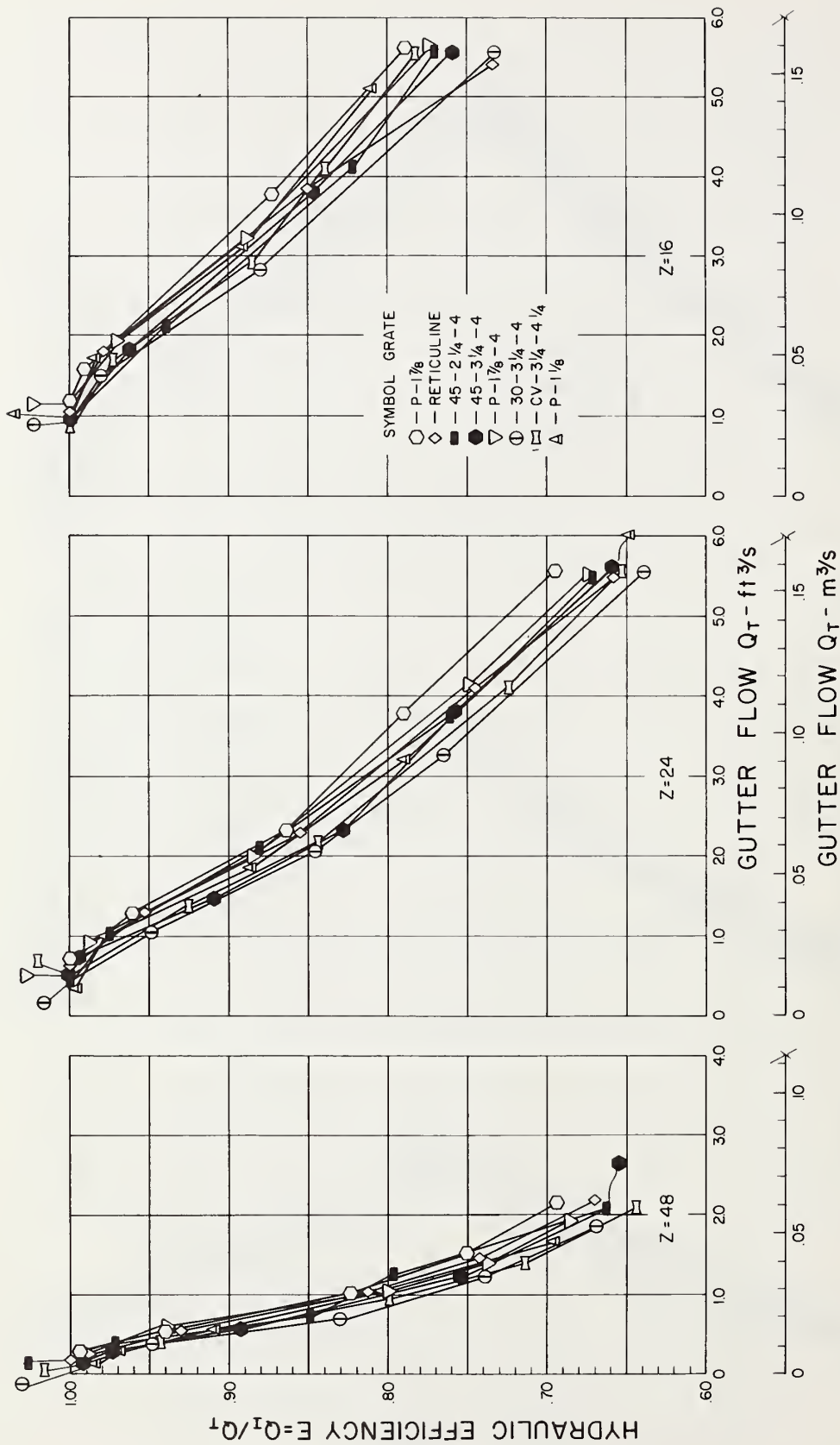


Figure 13-5. - Hydraulic efficiency vs. gutter flow for the 2 ft by 4 ft (0.61 m by 1.22 m) grates. $S_0 = 4.0\%$, $Z = 48, 24,$ and 16.

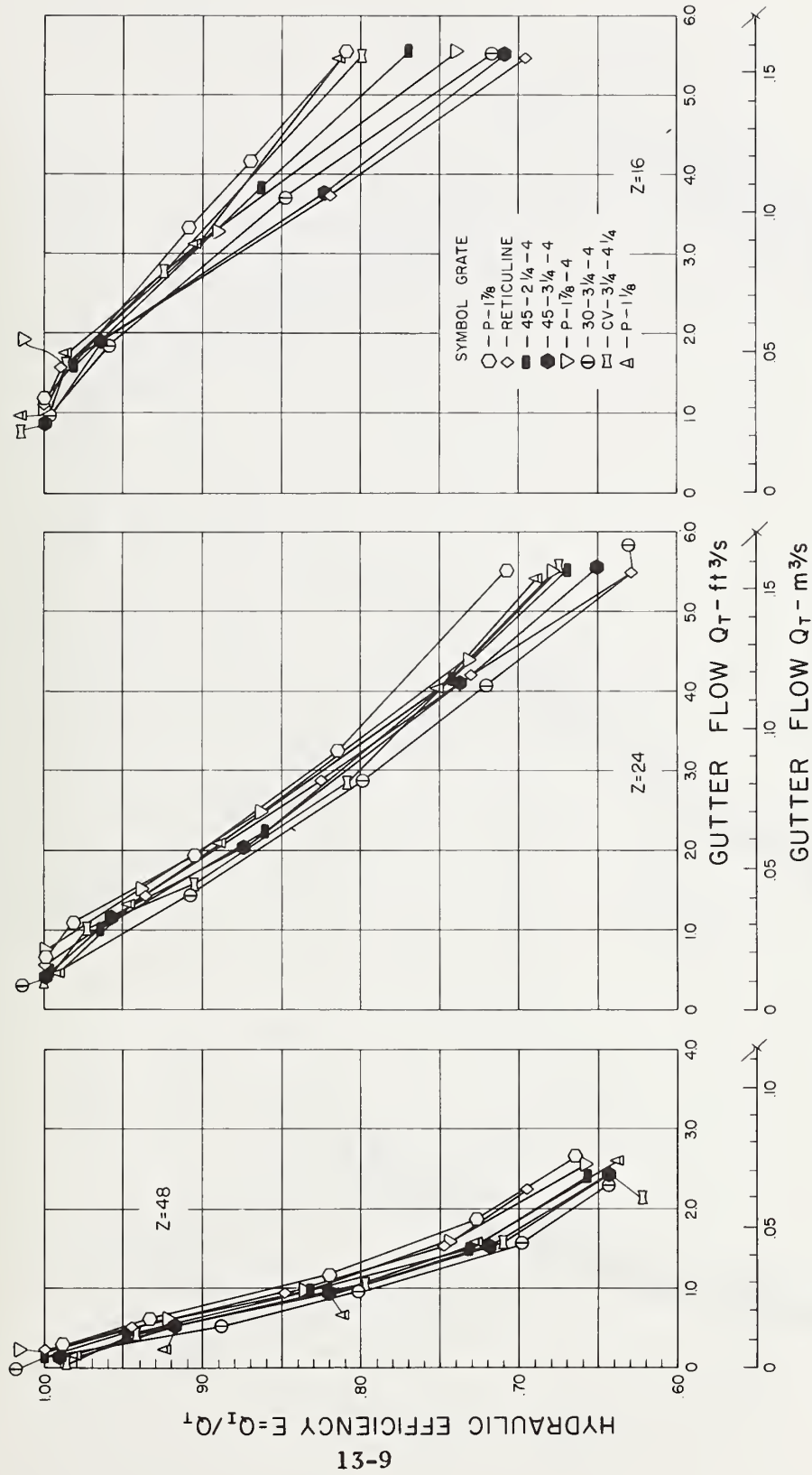


Figure 13-6. - Hydraulic efficiency vs. gutter flow for the 2 ft by 4 ft (0.61 m by 1.22 m) grates. $S_0 = 6.0\%$, $Z = 48, 24,$ and 16.

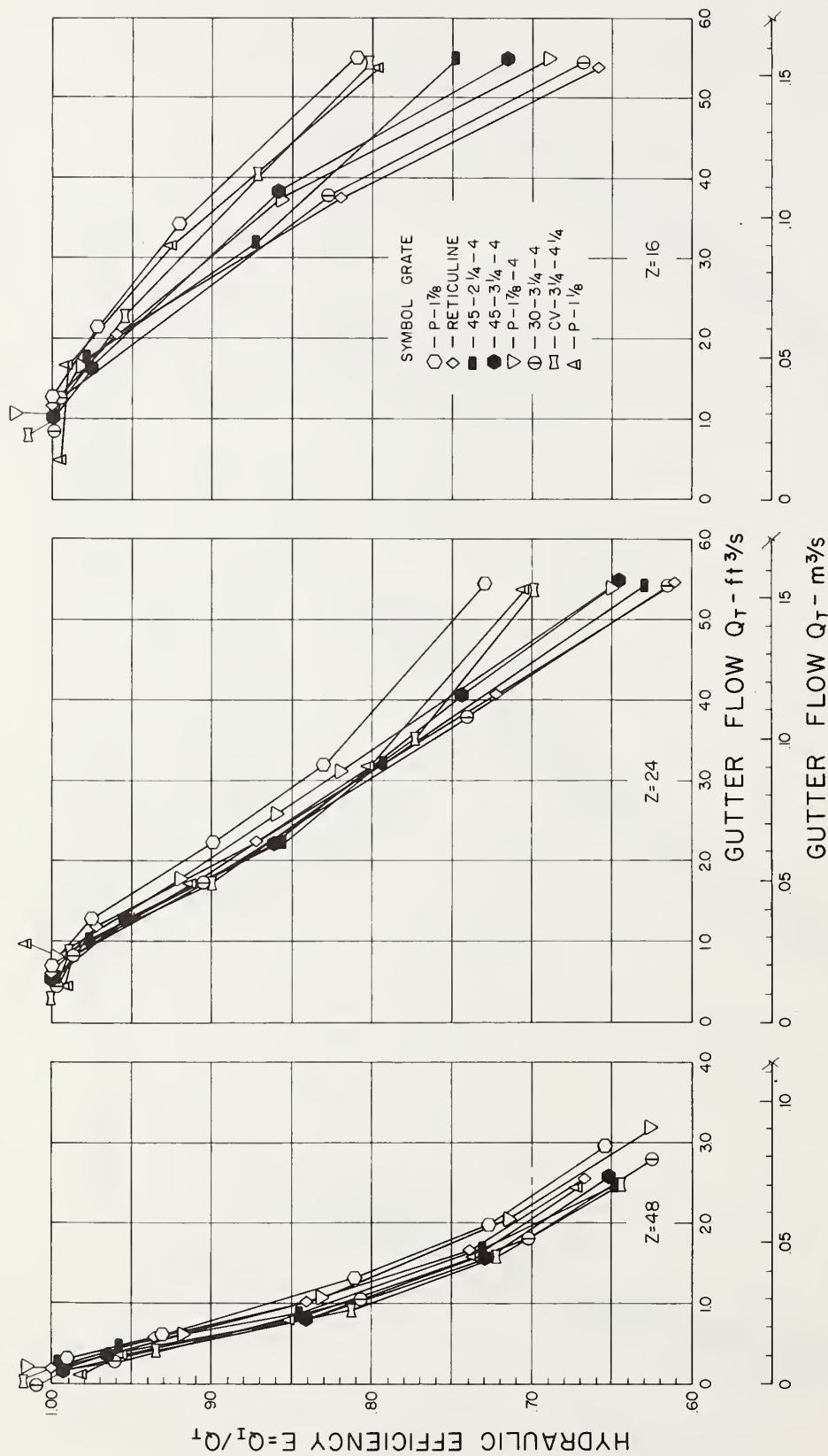


Figure 13-7. - Hydraulic efficiency vs. gutter flow for the 2 ft by 4 ft (0.61 m by 1.22 m) grates. $S_0 = 9.0\%$, $Z = 48, 24,$ and 16.

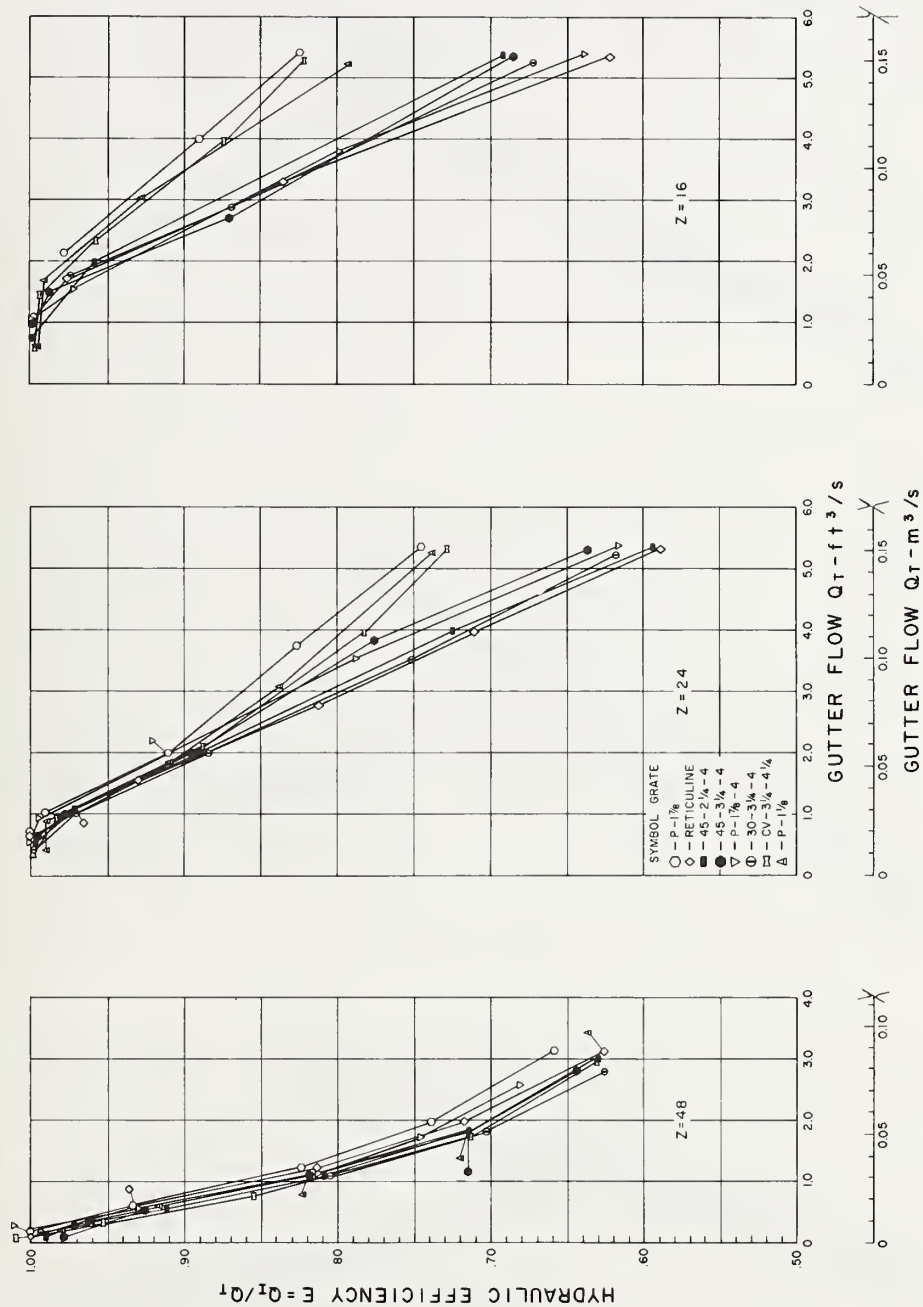


Figure 13-8. - Hydraulic efficiency vs. gutter flow for the 2 ft by 4 ft (0.61 m by 1.22 m) grates. $S_0 = 13.0\%$, $Z = 48, 24,$ and 16.

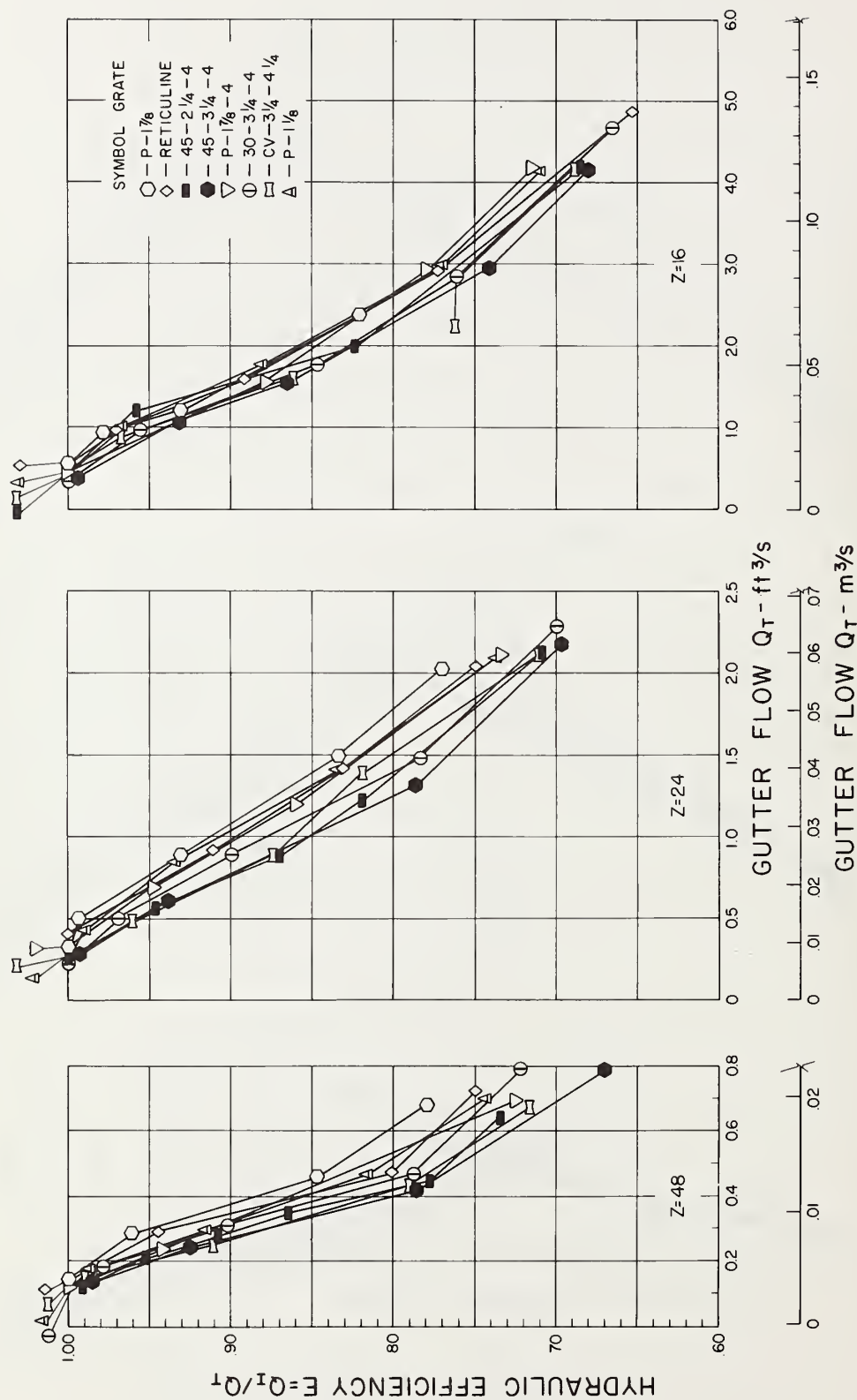


Figure 13-9. - Hydraulic efficiency vs. gutter flow for the 2 ft by 2 ft (0.61 m by 0.61 m) grates. $S_0 = 0.5\%$, $Z = 48, 24$, and 16.

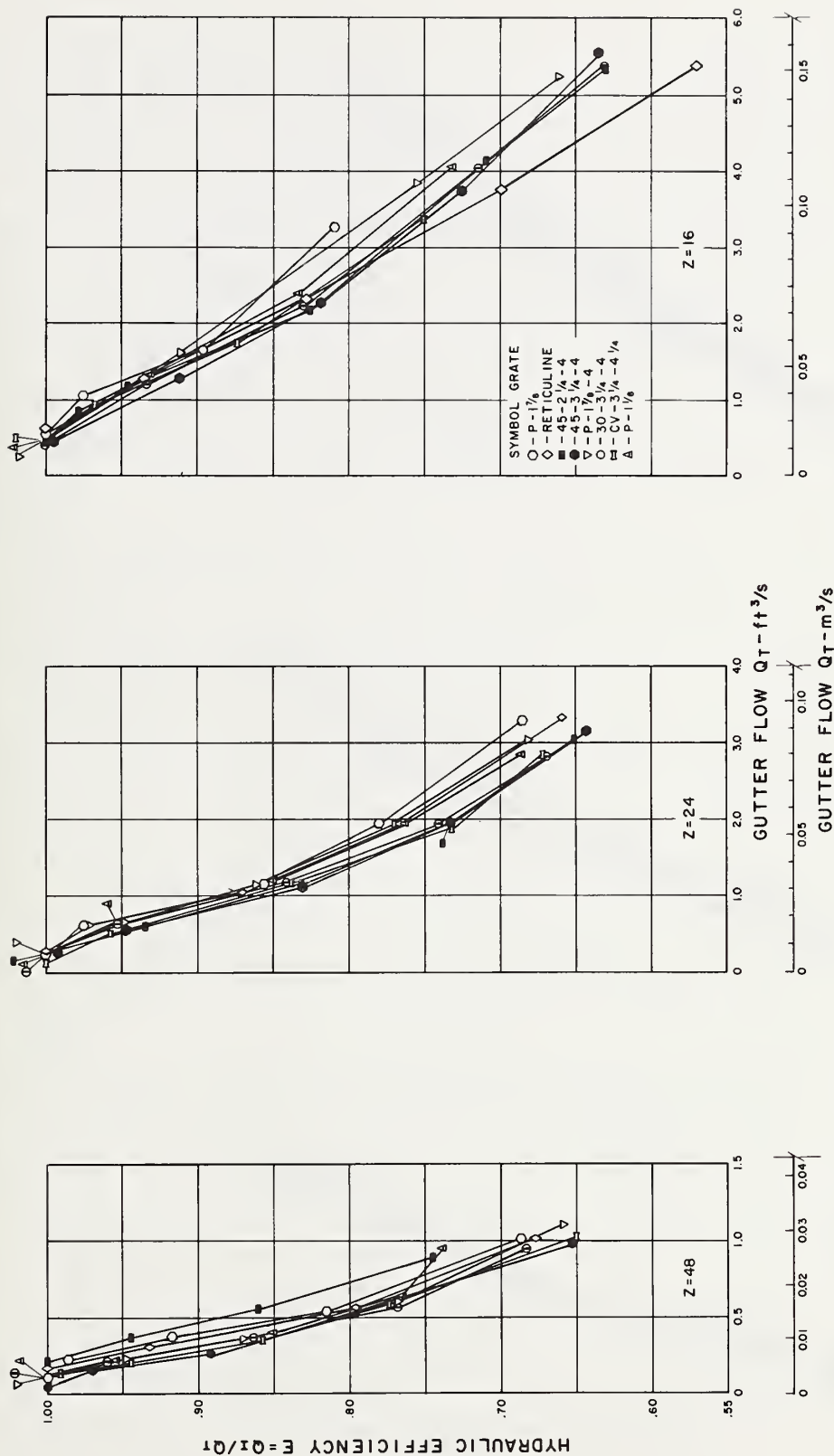


Figure 13-10. - Hydraulic efficiency vs. gutter flow for the 2 ft by 2 ft (0.61 m by 0.61 m) grates. $S_0 = 1.0\%$, $Z = 48, 24,$ and 16.

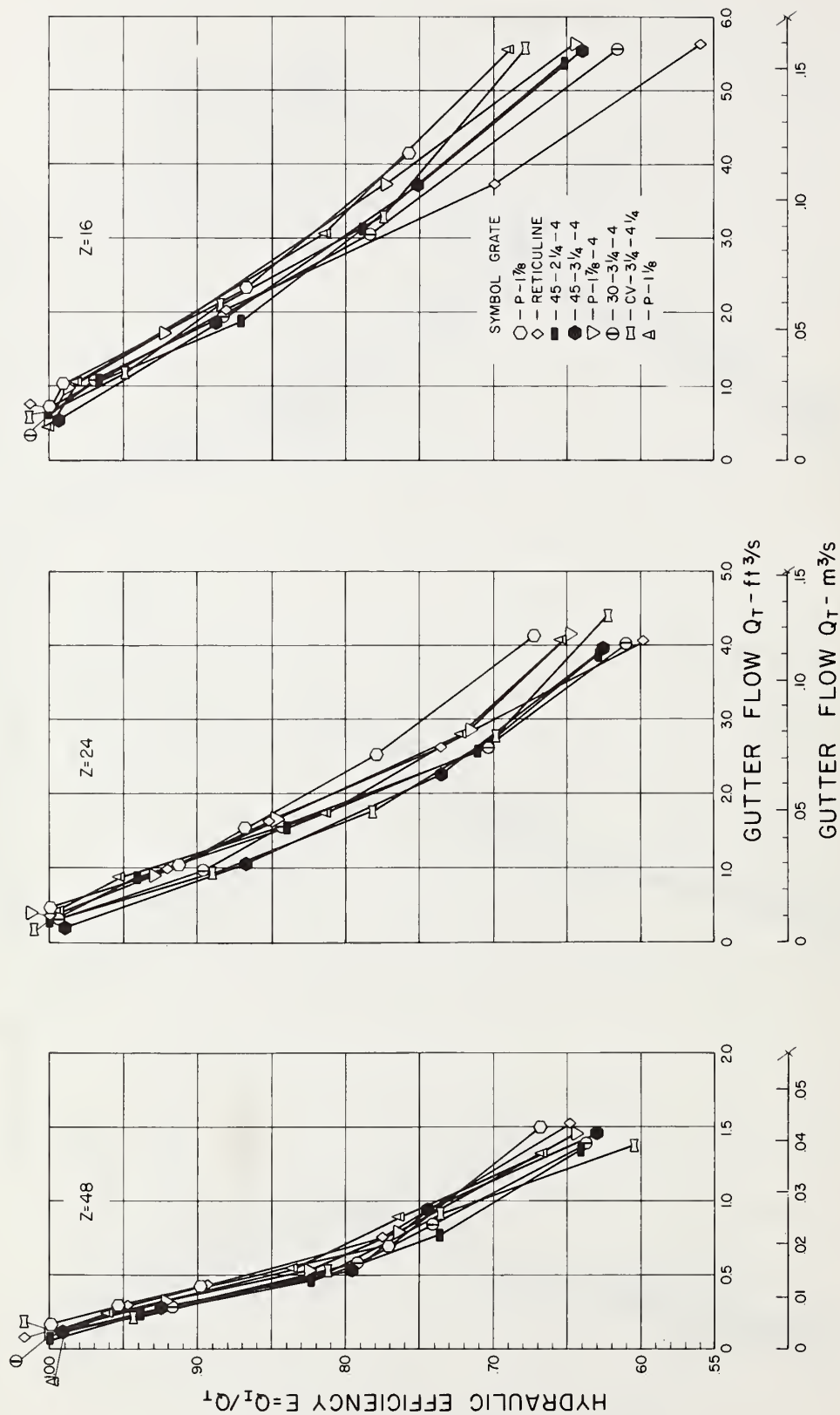


Figure 13-11. - Hydraulic efficiency vs. gutter flow for the 2 ft by 2 ft (0.61 m by 0.61 m) grates. $S_0 = 2.0\%$, $Z = 48, 24,$ and 16.

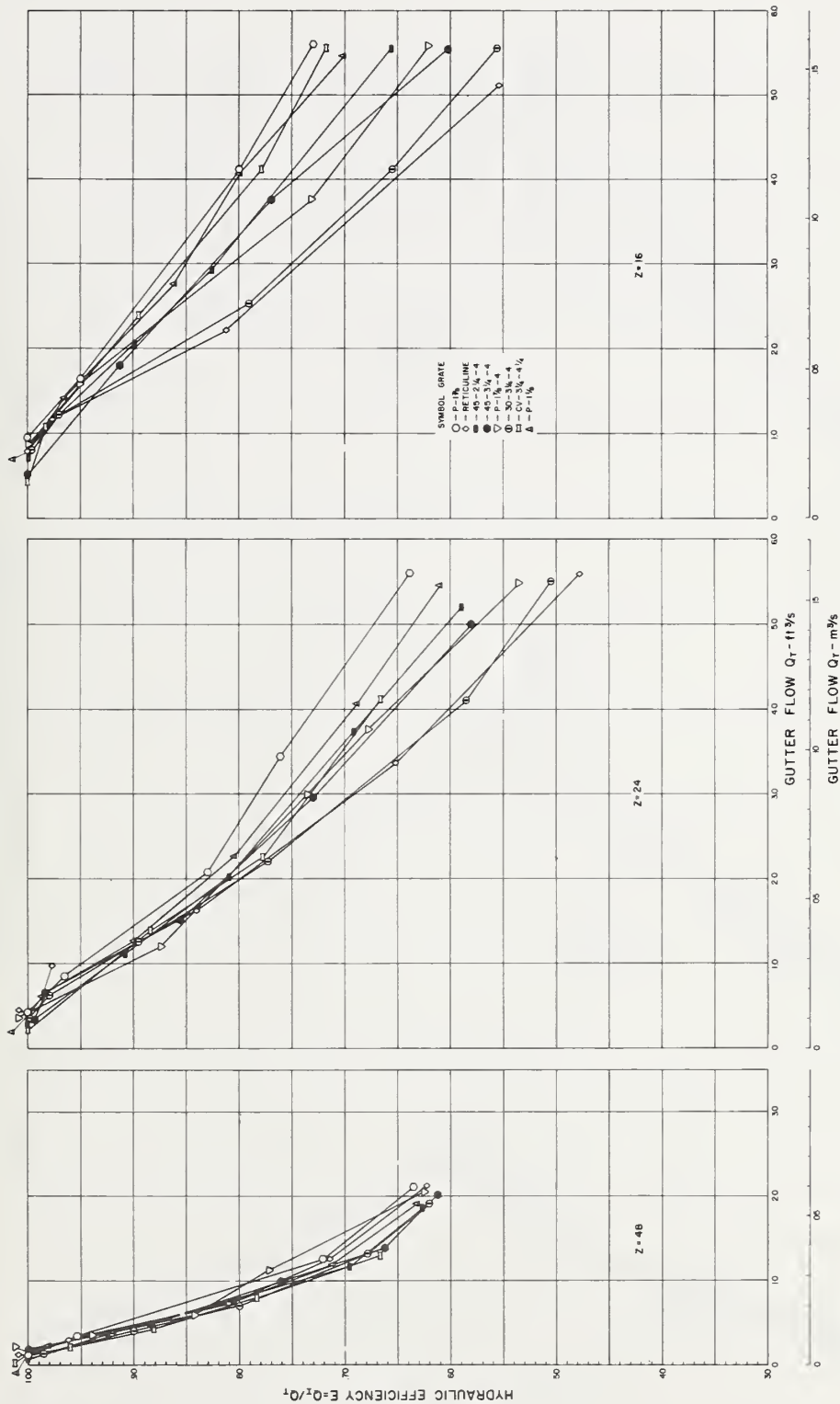


Figure 13-12. - Hydraulic efficiency vs. gutter flow for the 2 ft by 2 ft (0.61 m by 0.61 m) grates. $S_0 = 4.0\%$, $Z = 48, 24$, and 16.

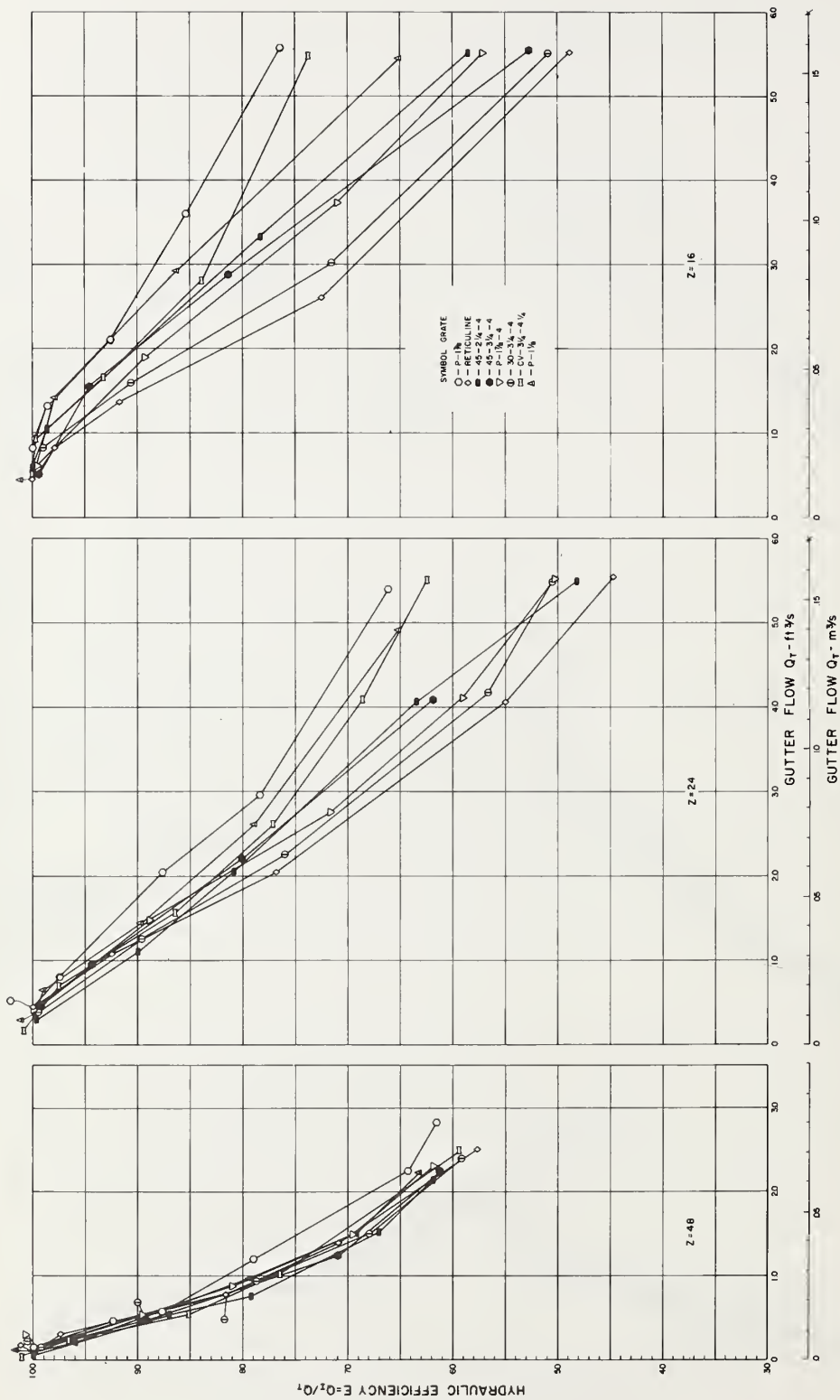


Figure 13-13. - Hydraulic efficiency vs. gutter flow for the 2 ft by 2 ft (0.61 m by 0.61 m) grates. $S_0 = 6.0\%$, $Z = 48, 24$, and 16.

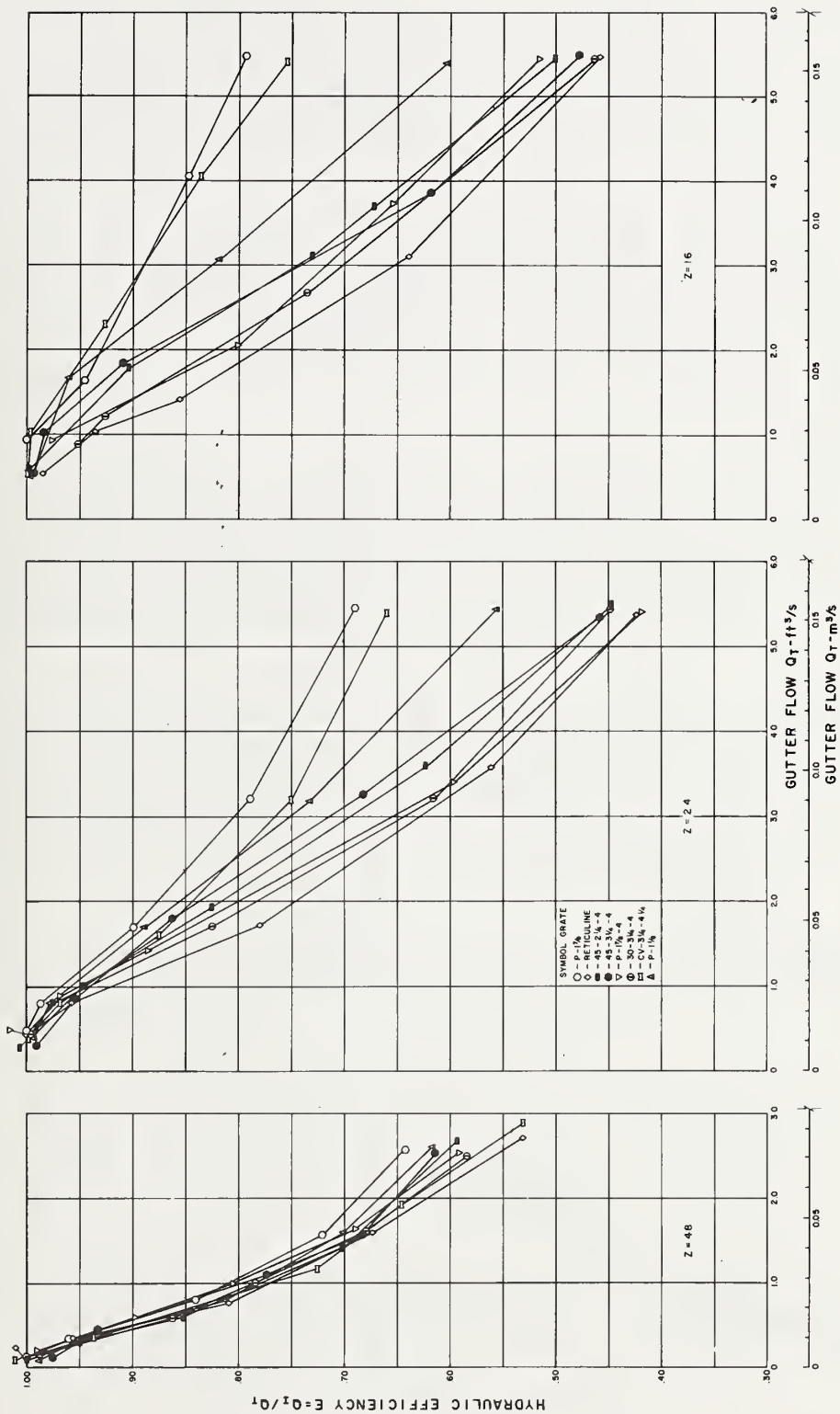


Figure 13-14. - Hydraulic efficiency vs. gutter flow for the 2 ft by 2 ft (0.61 m by 0.61 m) grates. $S_0 = 9.0\%$, $Z = 48, 24$, and 16.

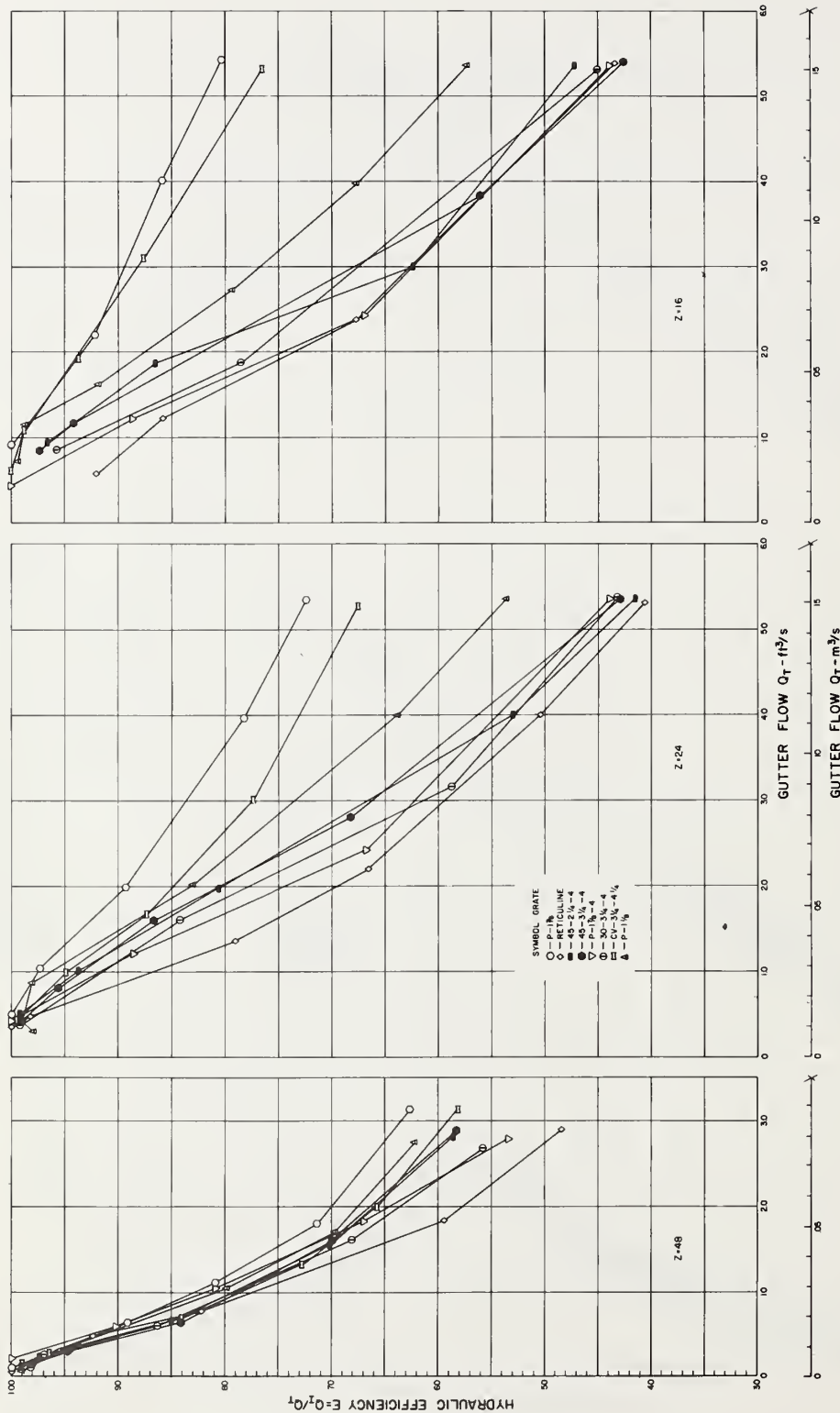


Figure 13-15. - Hydraulic efficiency vs. gutter flow for the 2 ft by 2 ft (0.61 m by 0.61 m) grates. $S_0 = 13.0\%$, $Z = 48, 24,$ and 16.

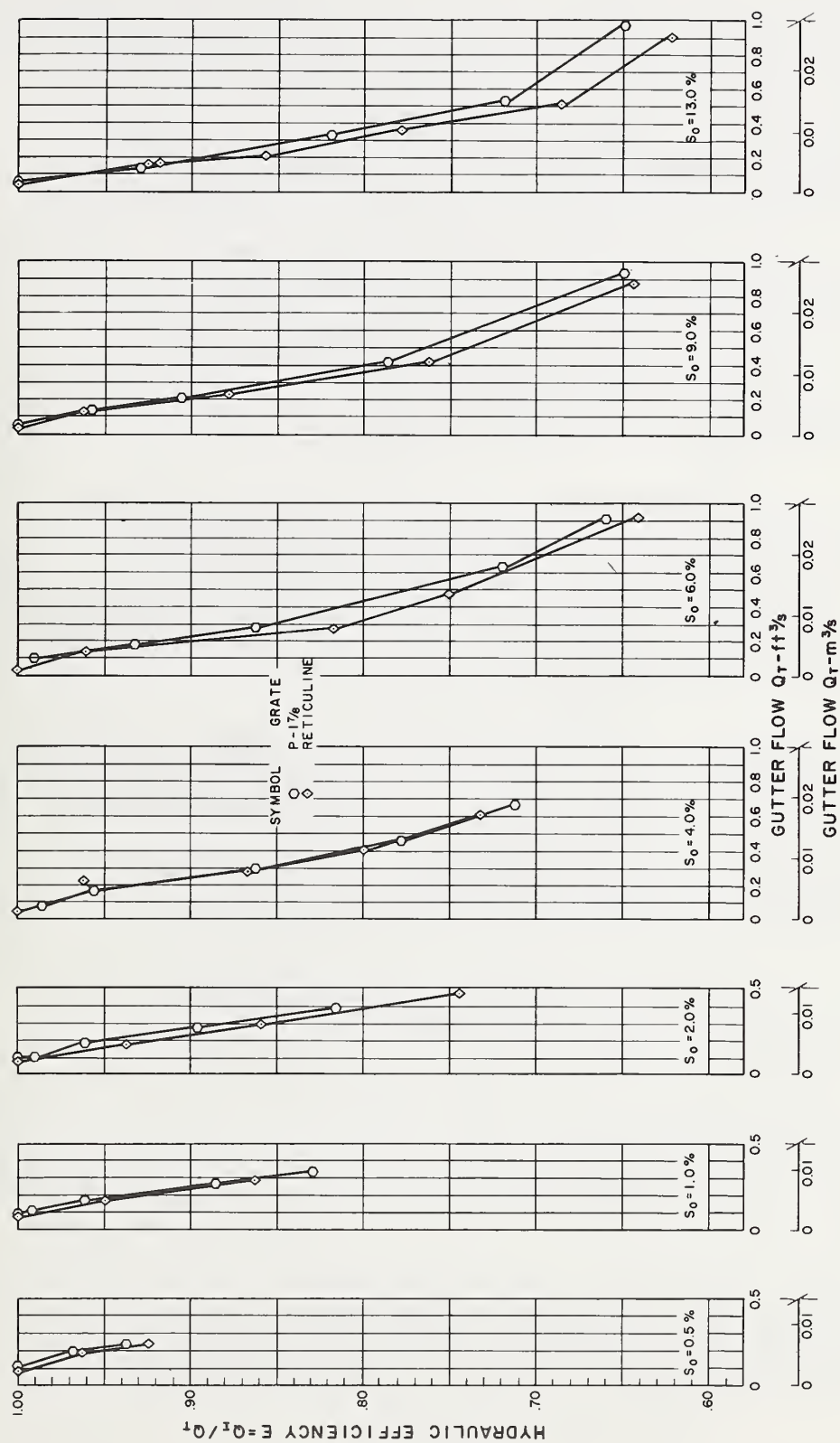


Figure 13-16. - Hydraulic efficiency vs. gutter flow for the 2 ft by 4 ft (0.61 m by 1.22 m) grates. $Z = 96$.

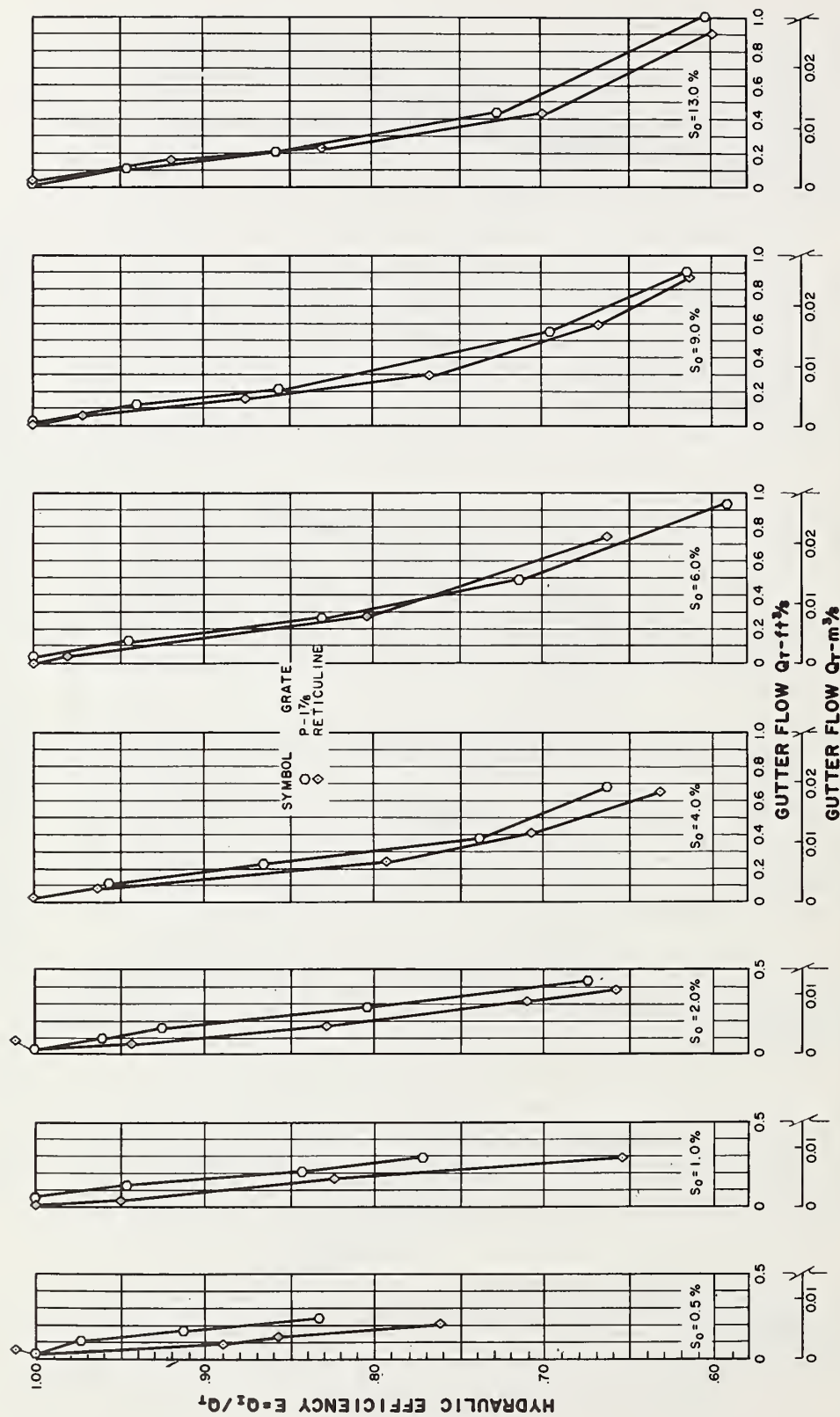


Figure 13-17. - Hydraulic efficiency vs. gutter flow for the 2 ft by 2 ft (0.61 m by 0.61 m) grates. $Z = 96$.

longitudinal slopes. Also, splash carries across the 2 ft (0.61 m) long grates at lower longitudinal slopes than the 4 ft (1.22 m) long grates. The tests conditions at or above those shown in table 13-1 will be referred to as the splash slopes or the splash range.

Table 13-1

MINIMUM LONGITUDINAL SLOPE CONDITIONS FOR CARRYOVER
SPLASH ON AT LEAST ONE GRATE DESIGN

Z	4 ft (1.22 m) grates	2 ft (0.61 m) grates
96	>13%	>13%
48	13%	9%
24	6%	4%
16	6%	2%

At splash slopes, there are several trends evident in figures 13-2 through 13-17. The parallel bar grate (P - 1-7/8) which has no transverse members ranks consistently first in hydraulic efficiency. Though it is not bicycle-safe, this grate is the best hydraulic grate and is the standard to which the bicycle-safe grates are compared.

The seven bicycle-safe grate designs tested fall into three performance groups at the splash slopes. The CV - 3-1/4 - 4-1/4 and P - 1-1/8 grates are consistently superior to the other bicycle-safe grates tested. In fact, the 2 ft by 2 ft (0.61 m by 0.61 m) CV - 3-1/4 - 4-1/4 and both the CV - 3-1/4 - 4-1/4 and P - 1-1/8 grates in the 2 ft by 4 ft (0.61 m by 1.22 m) size are within 3 percent to 4 percent of the P - 1-7/8 grates for the same test conditions in the splash range. The efficiencies for the 2 ft by 2 ft (0.61 m by 0.61 m) P - 1-1/8 grate fall off considerably because of the flow trajectory which hits the downstream vertical spaces and is deflected out of the inlet. The problem is described in Chapter 12.

At the other extreme, the reticuline grates generally rank last. At high gutter flows in the splash range, the reticuline grates usually have the lowest efficiency of the grates tested and often have efficiencies 20 percent to 30 percent less than those for the P - 1-7/8 grates.

The remaining grates, the 45 - 2-1/4 - 4, 45 - 3-1/4 - 4, P - 1-7/8 - 4, and the 30 - 3-1/4 - 4, tend to have efficiencies very close to each other. They rank somewhat better than the reticuline grates but far below the CV - 3-1/4 - 4/14 and P - 1-1/8 grates. These four grates do not rank in any consistent order. The grates that are best

at one particular test condition in the splash range are not necessarily best at another test condition. Their rank in the 2 ft by 2 ft (0.61 m by 0.61 m) size is often different than their rank in the 2 ft by 4 ft (0.61 m by 1.22 m) size for the same test condition. Table 13-2 shows the rank and efficiency of each grate size and design for $Z = 24$ and 16 at a longitudinal slope of 9 percent with a gutter flow of $5 \text{ ft}^3/\text{s}$ ($0.14 \text{ m}^3/\text{s}$). The table does not show the results for $Z = 48$ and 96 since these cross slopes are not in the splash range. The maximum difference in hydraulic efficiency between any two designs in the middle performance group is only around 6 percent. The reticuline grate is only slightly less efficient but has been discussed separately because it is consistently last.

Figures 13-18 through 13-23 show the performance of the test grates in a different format. Each figure is plotted for one width of spread, T' , measured on the test facility. Since T' is held constant for different longitudinal slopes, comparisons of actual efficiency between one slope and another are not meaningful because the gutter flows are different. The figures are useful for comparing the efficiencies of the test grates at any slope and for showing how the various grates perform as the longitudinal slope is increased. These figures show the same performance patterns as the graphs in figures 13-2 through 13-15. The fabricated grates which are effectively wider and longer than the cast grates look superior up to the point where flow rates and velocities are great enough to make the design of the grate the most important factor. The parallel bar grate (P - 1-7/8) is consistently first, followed by the CV - 3-1/4 - 4-1/4 and the P - 1-1/8. Figures 13-22 and 13-23 dramatically show the point where flow hits the downstream spacer of the 2 ft by 2 ft (0.61 m by 0.61 m) P - 1-1/8 grate. This first occurs at the 6 percent slope and the grate loses efficiency rapidly at steeper longitudinal slopes. The middle performance group of grates is the same and the reticuline grates are generally the least efficient grates tested.

Debris Tests

Table 13-3 shows the ranking of the various grate designs based on the debris tests conducted according to the procedure described in Chapter 5. The results presented are the debris handling efficiencies at the end of 15 minutes. The efficiencies for the 2 ft by 4 ft (0.61 m by 1.22 m) and 2 ft by 2 ft (0.61 m by 0.61 m) grates have been averaged to get results and ranks for each grate design. The table shows a clear difference in efficiency between the grates with the 3-1/4 in (83 mm) longitudinal bar spacing and those with smaller spacings. In general, the increased flow velocity at the 4 percent slope results in a higher debris handling efficiency. The efficiencies shown in the table are suitable for comparisons between the grate designs tested. Since the debris testing procedure used in the laboratory was a qualitative attempt to simulate field conditions, the

COMPARISON OF TEST GRATES AT 9% LONGITUDINAL SLOPE

[illegible]

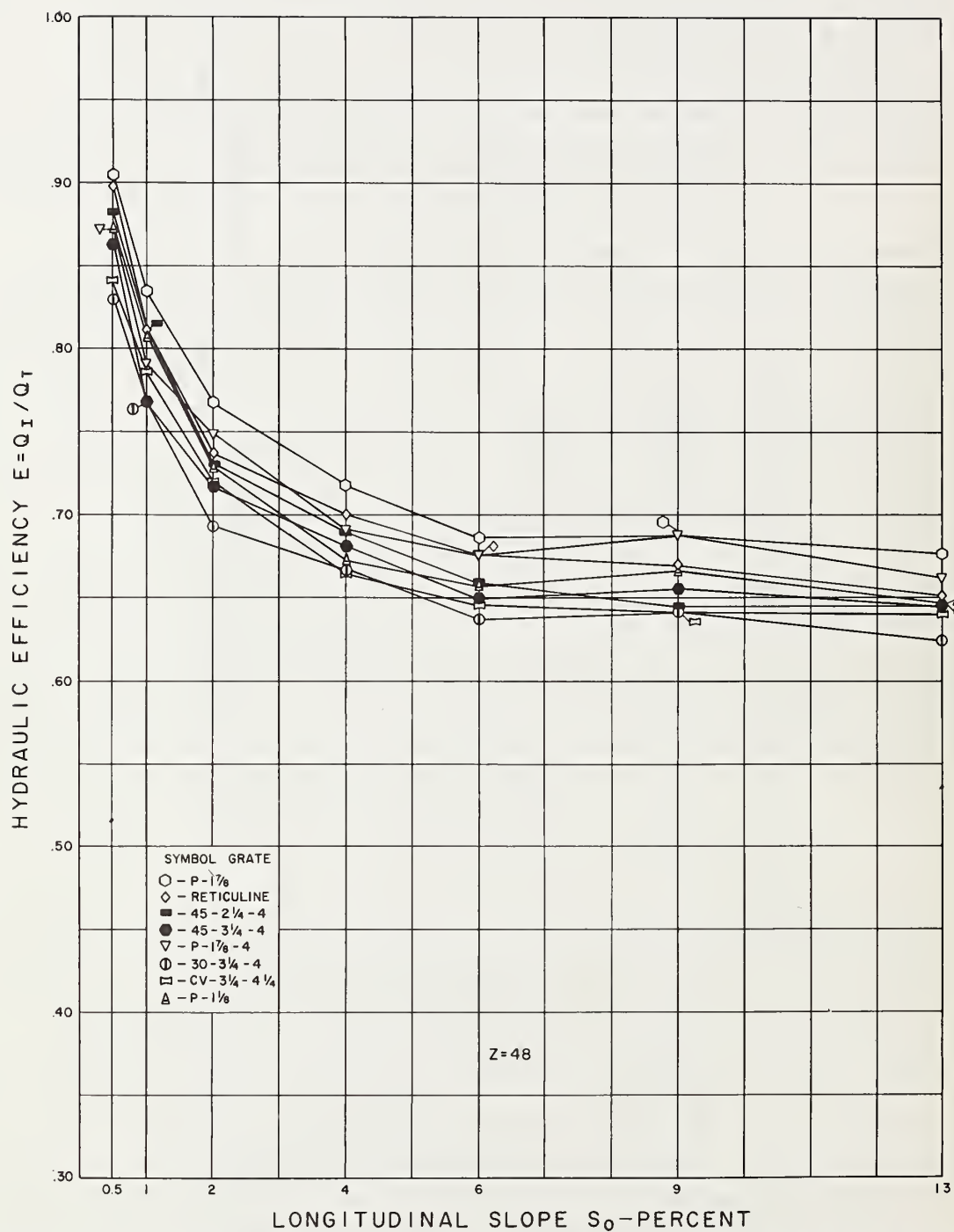


Figure 13-18. - Hydraulic efficiency vs. longitudinal slope for a constant width of spread, $T' = 7.0$ ft (2.13 m), 2 ft by 4 ft (0.61 m by 1.22 m) grates. $Z = 48$.

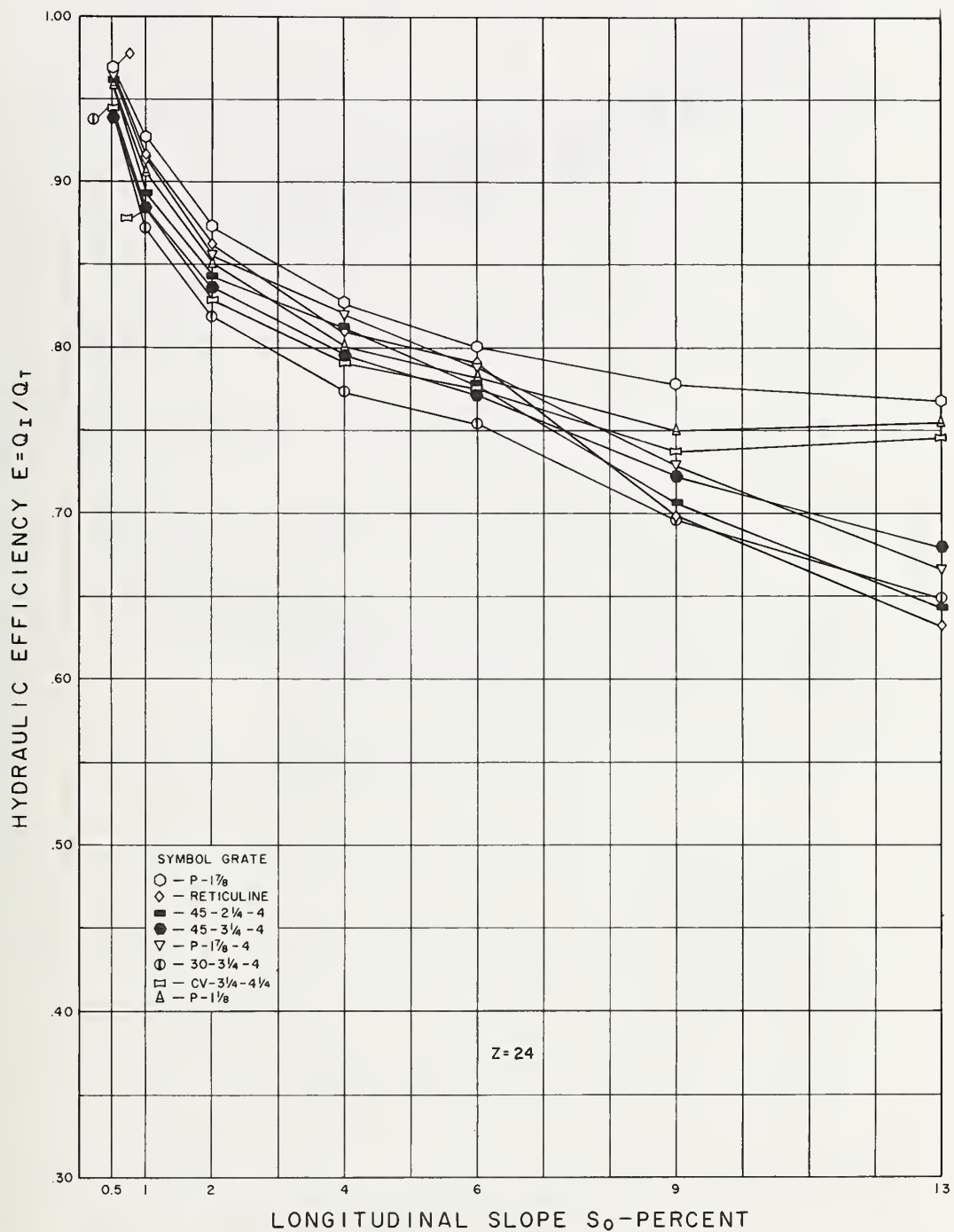


Figure 13-19. - Hydraulic efficiency vs. longitudinal slope for a constant width of spread, $T' = 5.5$ ft (1.68 m), 2 ft by 4 ft (0.61 m by 1.22 m) grates. $Z = 24$.

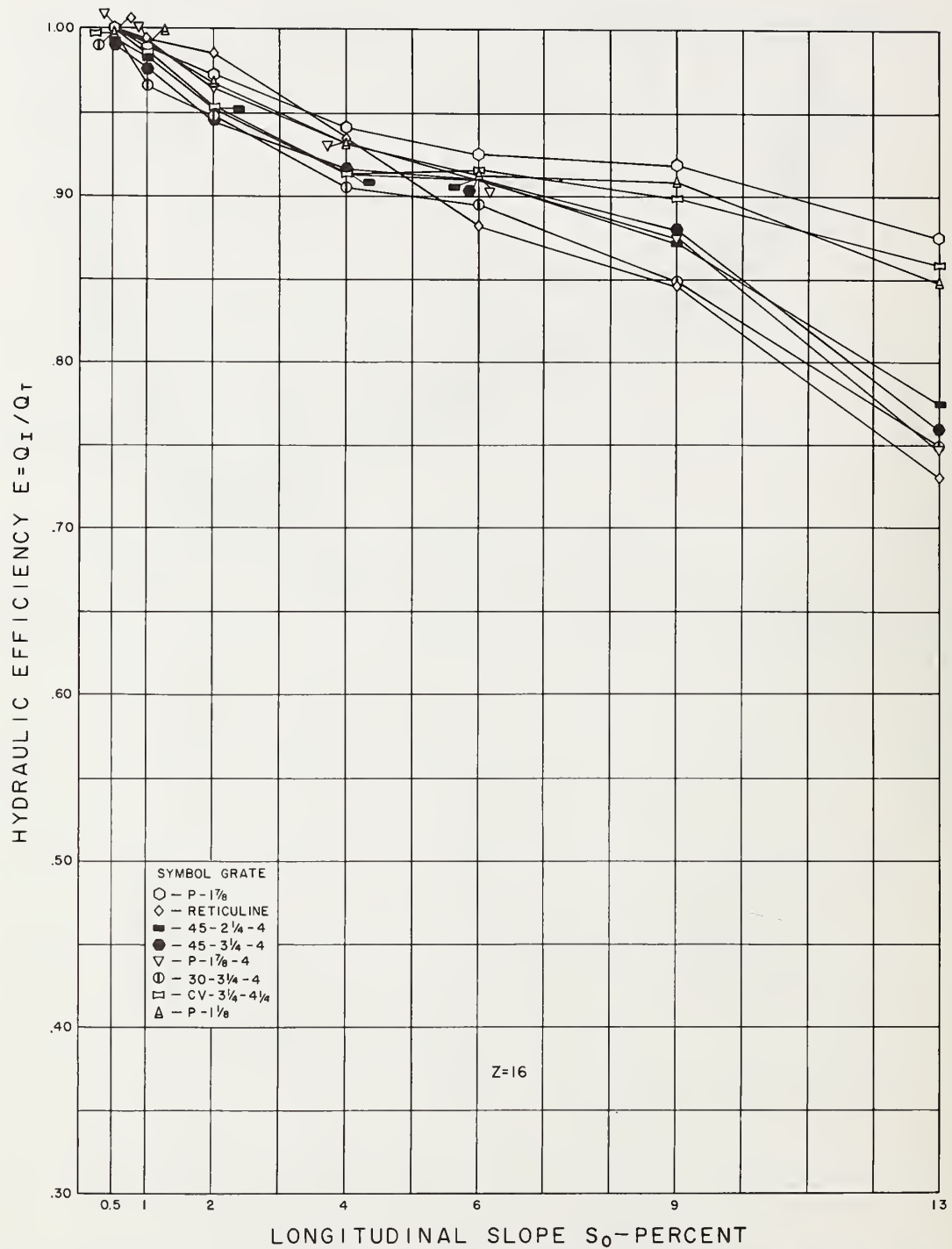


Figure 13-20. - Hydraulic efficiency vs. longitudinal slope for a constant width of spread, $T' = 4.0$ ft (1.22 m), 2 ft by 4 ft (0.61 m by 1.22 m) grates. $Z = 16$.

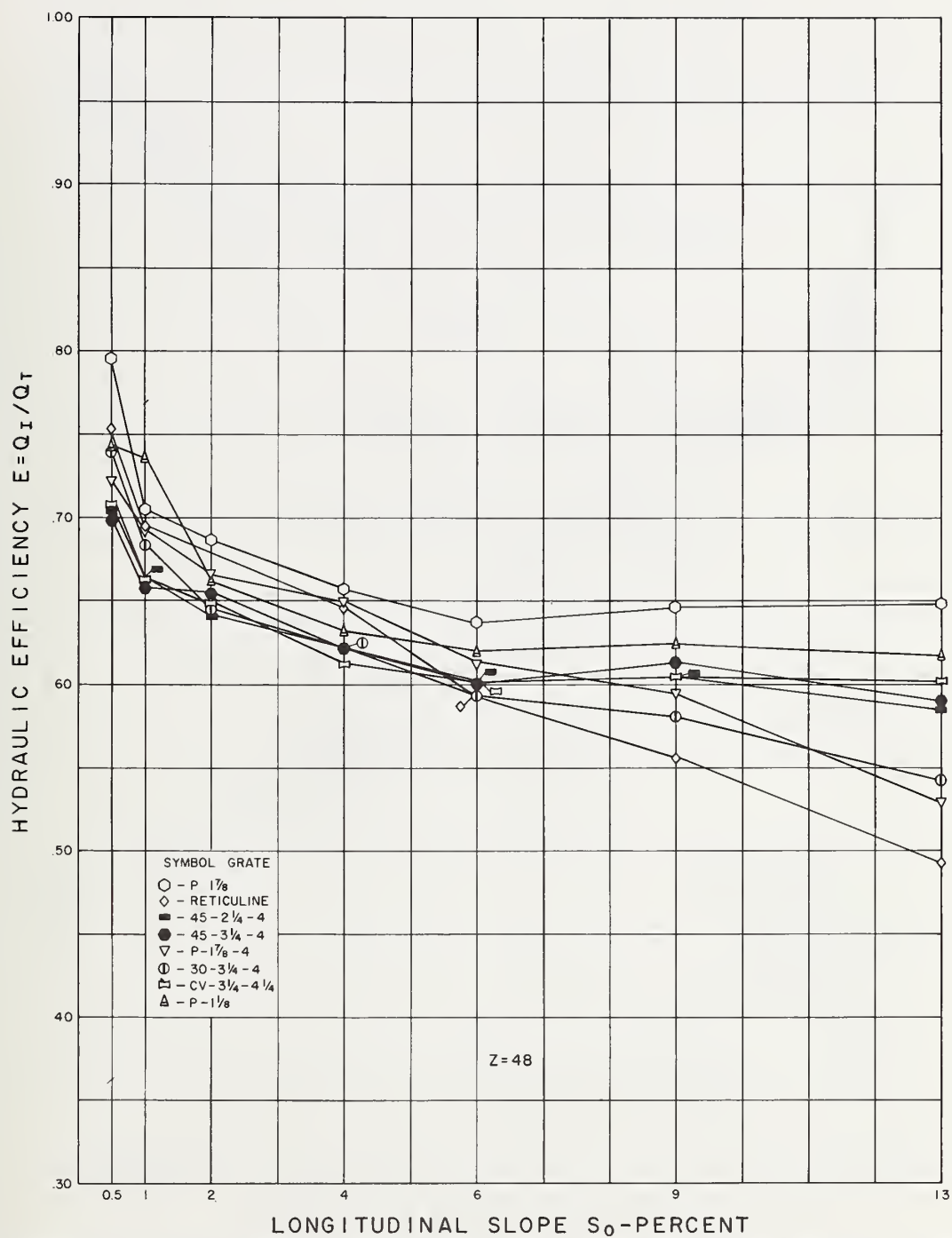


Figure 13-21. - Hydraulic efficiency vs. longitudinal slope for a constant width of spread, $T' = 7.0$ ft (2.13 m), 2 ft by 2 ft (0.61 m by 0.61 m) grates. $Z = 48$.

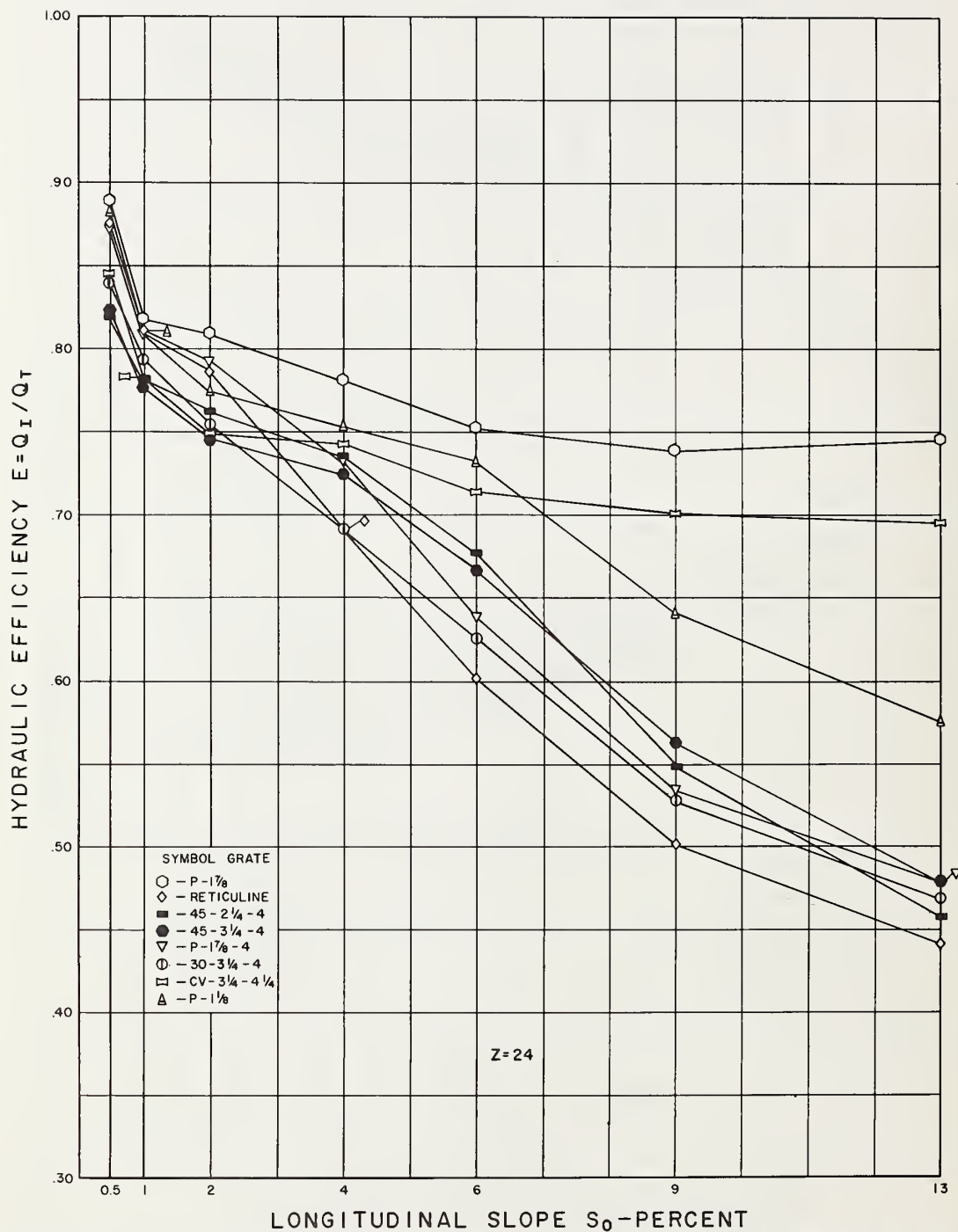


Figure 13-22. - Hydraulic efficiency vs. longitudinal slopes for a constant width of spread, $T' = 5.5$ ft (1.68 m), 2 ft by 2 ft (0.61 m by 0.61 m) grates. $Z = 24$.

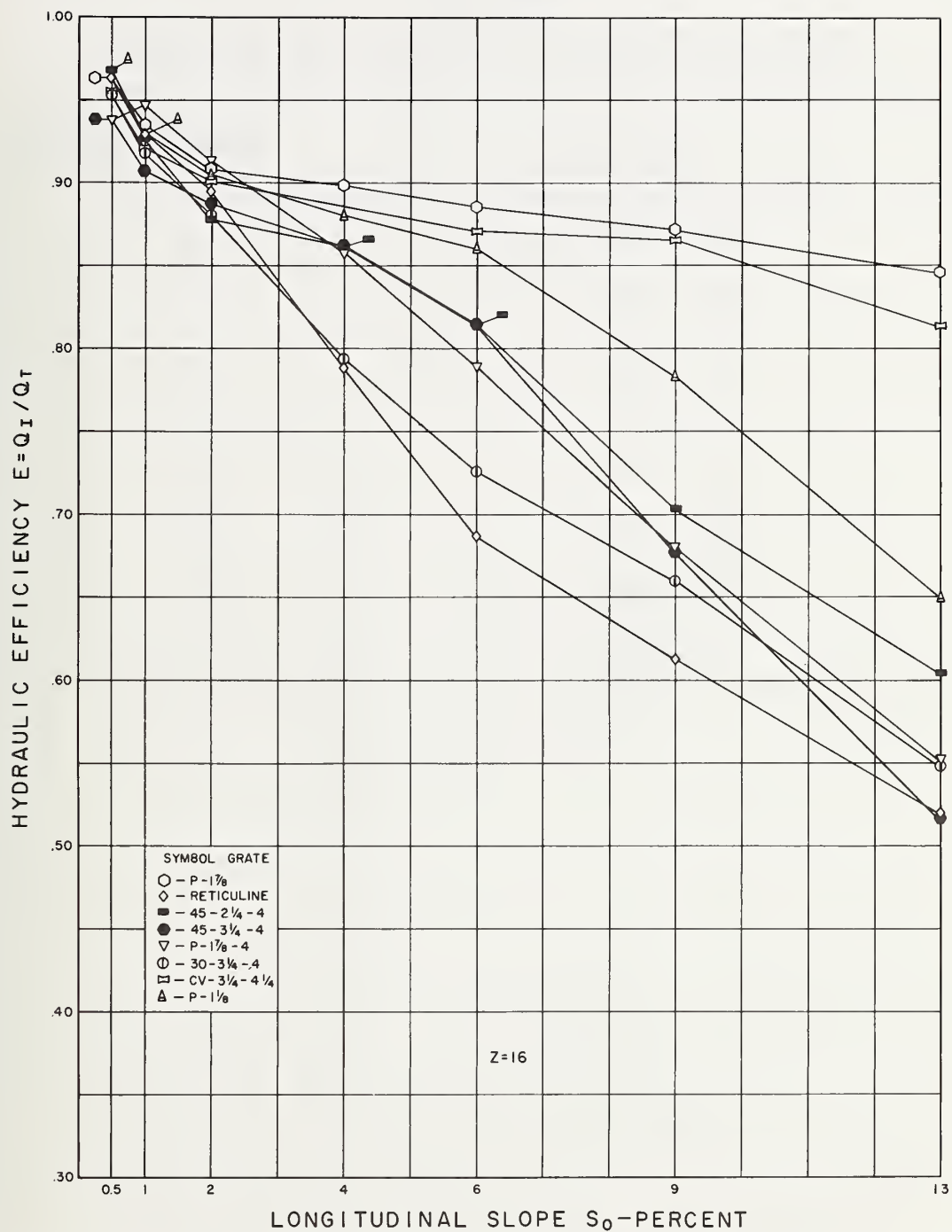


Figure 13-23. - Hydraulic efficiency vs. longitudinal slopes for a constant width of spread, $T' = 4.0$ ft (1.22 m), 2 ft by 2 ft (0.61 m by 0.61 m) grates. $Z = 16$.

Table 13-3

AVERAGE DEBRIS HANDLING EFFICIENCIES FOR TEST GRATES

Rank	Grate style	<u>Longitudinal slope</u>	
		.5%	4%
1	CV - 3-1/4 - 4-1/4	46	61
2	30 - 3-1/4 - 4	44	55
3	45 - 3-1/4 - 4	43	48
4	P - 1-7/8	32	32
5	P - 1-7/8 - 4	18	28
6	45 - 2-1/4 - 4	16	23
7	Reticuline	12	16
8	P - 1-1/8	9	20

individual efficiencies noted are no indication of actual field performance. However, the grates which performed best in the laboratory tests would be expected to perform best under field conditions also.

CHAPTER 14

SUMMARY AND RECOMMENDATIONS

This project consisted of an in-depth investigation of the safety, hydraulic efficiency, and debris handling characteristics of eight grate inlets. A structural analysis for all of the grates selected except the reticuline is presented in Chapter 2. Since the manufacturers of the reticuline grate applied AASHTO's specifications to the development of their load tables, an independent analysis was not necessary.

Over 500 bicycle and pedestrian safety tests were conducted on eleven test grates. The test results of this study and those conducted by other independent organizations* were used to select seven grate inlets for hydraulic tests. The hydraulic characteristics of the highly efficient parallel bar grate inlet are well known and, although it is not a safe grate, its performance offered a high standard with which to compare the other seven grates hydraulically.

Results of the debris tests indicate that the wider the longitudinal bar spacing, the better the debris handling ability of a grate inlet.

In studying the three major test criteria for grate inlets; hydraulic efficiency, safety, and debris handling capability, it is clear that the safety and debris handling characteristics of a grate inlet are not as dependent on longitudinal slope, S_0 , as the hydraulic characteristics. The hydraulic test results indicate that above specific longitudinal slopes, the hydraulic efficiency, E , of several grate inlets is adversely affected by the high velocity flow striking the transverse bar members and splashing over the inlet. The specific longitudinal slopes depend on such variables as cross slope, $1/Z$, gutter flow, Q_T , and grate length, L , but can be identified in two generalized categories as favorable and unfavorable gutter flow conditions for near maximum flow conditions on the test facility ($Q_T = 5.0 \text{ ft}^3/\text{s}$ ($0.142 \text{ m}^3/\text{s}$)) or $T = 7.0 \text{ ft}$ (2.13 m). Looking at figure 13-17 for the 2 ft by 4 ft (0.61 m by 1.22 m) grates at $Z = 24$, several grate inlets show a change in the rate of hydraulic efficiency with increase in longitudinal slope, S_0 , above $S_0 = 6$ percent. For the 2 ft by 4 ft (0.61 m by 1.22 m) grates on a cross slope, $Z = 24$, gutter flow conditions are unfavorable above a longitudinal slope, S_0 , of 6 percent. For the 2 ft by 2 ft (0.61 m by 0.61 m) grates on a cross slope, $Z = 24$, gutter flow conditions are unfavorable above a longitudinal slope of 2 percent (figure 13-20). Similar zones can be identified

* Note references in Chapter 1.

for the cross slopes, $Z = 16$ and $Z = 48$. These zones of favorable and unfavorable gutter flow conditions are shown in figure 14-1.

Table 14-1 is a summary presentation of the test results for debris, safety, and hydraulic considerations. An attempt has been made to classify the selected grates into high and low performance groups for the three major areas of consideration. The high performance (class I) grates for bicycle safety are low performers (class II) with respect to debris handling capabilities. For favorable gutter flow conditions, the class I grates are slightly more efficient than the class II grates. However, the hydraulic efficiencies for grates in class I and class II do not vary by more than 6 percent. For the unfavorable gutter flow conditions, hydraulic efficiencies vary by as much as 34 percent between class I and class II grates for a 2 ft (0.61 m) grate length (figure 13-21) and 15 percent for a 4 ft (1.22 m) grate length (figure 13-18). The composite selections in the table are the authors' overall classification of the selected grates tested.

Recommendations

To broaden the available design data for grate inlet widths other than the 24 in (0.61 m) width used in this study, we recommend three grates be selected for further tests, the curved vane (CV), the parallel bar with transverse spacers (P - 1-1/8), and the parallel bar with transverse rods (P - 1-7/8 - 4). The additional tests would include grate widths of 15 in (0.38 m) and 36 in (0.91 m).

The following recommendations related to specific grate designs are also noted:

1. Relocate the cast spacers used in the parallel bar with transverse spacers (P - 1-1/8) to set flush with the ends of the grate as compared to the 11/16 in (17 mm) offset used in the tested grate (figure 12-1).
2. Roughen the surface of longitudinal bearing bars used in fabricated steel grates when the bar thickness exceeds 1/4 in (6.4 mm). This will help alleviate bicycle tire slippage when the grate is wet.
3. Improve the design of the curved vane grates by placing a radius, possibly 1/4 in (6.4 mm), on the inside surface corners of the end and side members of the grates.

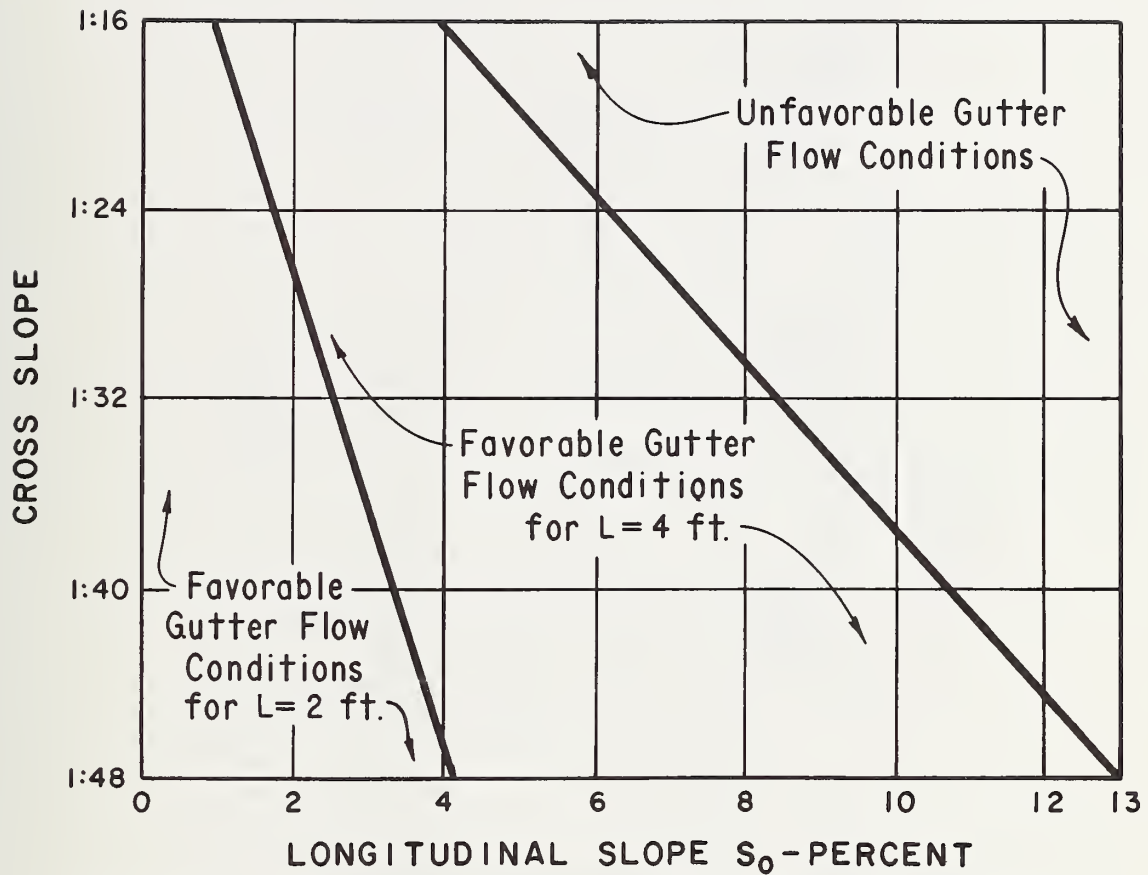


Figure 14-1. - Favorable and unfavorable gutter flow conditions.

Table 14-1

GRATE INLET CLASSIFICATION

Debris	Safety	Hydraulics		Composite selection	
		Favorable gutter flow conditions	Unfavorable gutter flow conditions	Favorable gutter flow conditions	Unfavorable gutter flow conditions
Class I (high performance)					
CV - 3-1/4 - 4-1/4	P - 1-7/8 - 4	P - 1-7/8 - 4	CV - 3-1/4 - 4-1/4	P - 1-7/8 - 4	CV - 3-1/4 - 4-1/4
30° - 3-1/4 - 4	Reticuline	P - 1-1/8	P - 1-1/8	P - 1-1/8 Reticuline	P - 1-1/8
45° - 3-1/4 - 4	P - 1-1/8*	Reticuline		45° - 3-1/4 - 4	
Class II (low performance)					
P - 1-7/8 - 4	45° - 3-1/4 - 4	CV - 3-1/4 - 4-1/4	45° - 3-1/4 - 4	CV - 3-1/4 - 4-1/4	45° - 3-1/4 - 4
45° - 2-1/4 - 4	45° - 2-1/4 - 4	45° - 3-1/4 - 4	P - 1-7/8 - 4	45° - 2-1/4 - 4	P - 1-7/8 - 4
Reticuline	CV - 3-1/4 - 4-1/4	45° - 2-1/4 - 4	45° - 2-1/4 - 4	30° - 3-1/4 - 4	45° - 2-1/4 - 4
P - 1-1/8	30° - 3-1/4 - 4	30° - 3-1/4 - 4	30° - 3-1/4 - 4 Reticuline		Reticuline 30° - 3-1/4 - 4

* Note reference 2, chapter 1.

TE 662 .A3
no. FHWA-RD-
77-24

U.

BORROWER

Form DOT F 1720.2 (8-70)
FORMERLY FORM DOT F 1700.1,1

DOT LIBRARY



00055839

